

# **Informing Heat Network Design: A Study of Demand Diversity and Domestic Hot Water Storage Using High Resolution Measured Data**

Niki Sahabandu

A dissertation submitted in partial fulfilment of the requirements for the degree of  
**Doctor of Philosophy**  
of  
**University College London**

Bartlett School of Environment, Energy and Resources  
University College London

2025

## *Declaration*

I, Chameli Niklesha Sahabandu, confirm that the work presented in my thesis is my own. Where information has been derived from other sources, I confirm that this has been indicated in the thesis.

## *Abstract*

Heat networks (HN) have a key role in strategies proposed by the UK's Committee on Climate Change, in support of which they recognise the requirement of proper standards. Collaboration across industry has culminated in technical standards, however, evidence has cast doubt on some of these. The diversity methods in the DS439, widely used in the UK, has been shown to overestimate peak capacities. Moreover, HN storage and its impact on peak demands and sizing, in which diversity plays a key role, is contested within industry. Thus, further study of the impact of storage and of the diversity methodology is required to inform the development of HNs.

Considering this, the thesis aims to use real demand data to quantify the effect of domestic storage on HN demand. To do this, domestic hot water storage models and a distribution system model were built. The models were used to produce residual consumer demands for a sample of dwellings in a case study HN in the UK and to evaluate the impact of two storage scenarios, representing high and low diversity charging strategies, on the distribution pipe sizing and thermal loss from the stores as well as from the distribution network.

The results in this work can directly inform the district heat industry technical guidance and bring clarification to long standing industry debates. They include the recommendation of a sampling time for measuring demand for sizing HNs and an assessment of the overestimation of peak capacities in a real case study HN. Additionally, results show that although introducing storage reduces the thermal losses in the distribution network as expected, it doesn't outweigh the increase in thermal losses from the stores themselves. Comparing storage scenarios showed the extent of the role that diversity plays in reducing peak demands across various points in the distribution network.

## *Impact Statement*

The research presented in this thesis supports the development of robust technical design guidance for heat networks in the UK where it relates to the sizing of distribution systems and the case for domestic hot water storage. The work presented in this thesis is the first to use measured data from a real case study heat network in the UK. This is in contrast to the existing industry and academic research that uses either only modelled heat network demand or measured data from a sample of dwellings not being served by a heat network as their basis. The empirical demand curves produced in this thesis can be presented alongside the Danish demand curves in the technical guidance either to serve as its replacement or to demonstrate the variability inherent between the two thereby encouraging designers to take more care, and perhaps make their own measurements of demand when sizing their network.

The findings regarding domestic storage brings much needed clarity to the ongoing contention within the industry and academia regarding the case for storage in the presence of diversity. Whilst practitioners are commonly either highly opposed to or strongly in favour of domestic storage, the results suggest a different perspective altogether. Although domestic storage is shown not to bring about an overall savings of heat loss in the network, the difference is so small that it is entirely possible that savings may come about given a different topology or arrangement of storage. Thus, neither of the ‘for’ and ‘against’ camps can be said to be unequivocally correct. What can be said is that whatever the case may be, the difference in savings/costs in thermal loss is likely to be so small that the contention in industry would be a wasted effort if it were to carry on and industry practitioners are therefore free to make decisions around storage on other grounds.

The findings regarding the oversizing of the case study heat network provide evidence to support the chorus of industry practitioners warning the industry about the impact of the use of design guidance not intended for use in the UK. The results, proving the existence of oversizing of heat networks distribution systems and documenting the impact on heat loss, are the first of its kind and should act as clear evidence for the need to revise the sizing methodologies found in technical design guidance.

The key role that the UK HN industry has in the UK’s climate strategies means that work such as this is timely and important. To increase the visibility and impact of the work, the author aims to strategically publish in high impact journals, present at major conferences and industry events, join relevant professional societies and working groups, partake in standards committees and submit evidence to government consultations.

## *Acknowledgements*

I had the privilege of working with an exceptional supervisory team, Bob Lowe, Jenny Crawley and George Bennett, without whom this thesis would not have been possible. Their knowledge, expertise and healthy scepticism helped me shape loose ideas into strong scientific arguments. They have transformed my outlook on research in ways that I will continue to draw inspiration from throughout my professional life. Thank you also to Cliff Elwell whose input and guidance has been valuable throughout. This work would not have been possible without the data that Richard Hanson-Graville was generous enough to share and discuss with me at length.

Thank you to the staff and students of the CDT, a wonderful community that I am grateful to have called myself a part of. Especially to Zack Wang and Minnie Ashdown for their mentorship and friendship, and for helping me weather some challenging times. To my PhD cohort for their support and academic insights. To the friendly government and industry figures who were generous with their time and advice, helping me situate my work in the real world.

Thank you to friends, old and new, whose support and good humour lightened the load and kept me moving. To Aiya, Kumi and baby Kairon for punctuating my life with joy. Finally, to my beloved parents, without whom this thesis and much of anything in life would not be possible.

## Table of Contents

<b>Abstract.....</b>	<b>3</b>
<b>1 Introduction.....</b>	<b>19</b>
1.1 Motivation for the Thesis .....	19
1.2 Research Gap .....	19
1.3 Aims.....	20
1.4 Thesis Layout.....	20
<b>2 Literature Review.....</b>	<b>21</b>
2.1 Introduction.....	21
2.1.1 The Role of HNs in Decarbonisation .....	21
2.1.2 A Brief History of the HN Market in the EU and UK.....	21
2.1.3 The Need for Robust Technical Standards .....	22
2.2 HN Physical Structure.....	23
2.3 Energy Demand.....	24
2.3.1 DHW Demand.....	24
2.3.2 Variation in Domestic Demand .....	27
2.3.3 HN Demand and Drivers.....	27
2.4 Demand Diversity.....	28
2.4.1 Review of Diversity Metrics .....	28
2.4.2 Diversity in Electricity Networks .....	28
2.4.3 Drivers of HN Demand Diversity .....	29
2.4.4 The Need for Empirical Diversity Studies.....	31
2.4.5 The Impact of Sampling Time on Individual and Aggregate Demand.....	32
2.5 Guidance and Standards for Diversity in HNs .....	33
2.5.1 SH Diversity Factor .....	33
2.5.2 DS439: Pipe Sizing Method .....	34
2.5.3 DS439: Heat Exchanger Sizing Method .....	36
2.5.4 DHW Technical Standards .....	38
2.5.5 Real Demand vs. Aggregate Demand in the Distribution System.....	40
2.6 Pipe Sizing and Guidance .....	41
2.6.1 Primary Network Guidance.....	42
2.6.2 Secondary Network Guidance.....	43
2.7 Further Secondary Network Design Guidance .....	44
2.8 Thermal Energy Storage and Diversity.....	46
2.8.1 Thermal Energy Storage in HNs .....	46
2.8.2 The Impact of Distributed Thermal Energy Storage on HNs.....	47
2.8.3 Domestic Demand Storage .....	47
2.8.4 Instantaneous DHW Delivery vs. Stored DHW.....	48
2.9 Summary and Research Gaps .....	48
<b>3 Research Questions and Methodology .....</b>	<b>50</b>
3.1 Research Aims, Questions and Objectives .....	50
3.2 Methodology.....	50
3.3 Overview of Methods.....	51
3.3.1 Research Design .....	51

3.4	<i>Case Study HN</i> .....	52
3.5	<i>Demand Aggregation</i> .....	53
3.6	<i>Heat Store Model</i> .....	54
3.6.1	Storage Scenarios.....	55
3.6.2	TES Model Principles.....	57
3.7	<i>Distribution System Model</i> .....	63
3.7.1	Pipe Sizing Methodology.....	64
3.7.2	Network Topology.....	66
3.7.3	Distribution System Thermal Mass.....	67
3.7.4	Distribution System Heat Loss.....	68
3.8	<i>Applicability of Results and Limitations</i> .....	71
<b>4</b>	<b>Data Collection</b> .....	<b>73</b>
4.1	<i>Node-Red Software</i> .....	74
4.2	<i>Data Hardware</i> .....	74
4.2.1	Located in the HIUs.....	74
4.2.2	Located Externally to the HIUs.....	75
4.2.3	Software and Servers.....	77
4.2.4	Summary of the Data Collection System.....	77
4.3	<i>Node-HIU System</i> .....	79
4.4	<i>M-Bus System</i> .....	79
4.5	<i>The M-Bus Master</i> .....	79
4.6	<i>The Elvaco Interface</i> .....	80
4.7	<i>Master Data Collection Impact on Timestamping of Meter Data</i> .....	82
4.8	<i>Data Collection Locations</i> .....	83
4.9	<i>Timestamping</i> .....	84
4.9.1	Heat Meter Data.....	84
4.9.2	HIU Sensor Data.....	84
4.10	<i>Data Quality Maintenance</i> .....	84
4.11	<i>File Format of Collected Readings</i> .....	87
4.12	<i>Measured Variables and Measurement Errors</i> .....	87
4.13	<i>Uncertainty in Meter Variables</i> .....	89
<b>5</b>	<b>Results 1 – Generating Demand Profiles</b> .....	<b>91</b>
5.1	<i>Introduction and Relevant Objectives</i> .....	91
5.2	<i>Methods</i> .....	91
5.2.1	Data Quality and Cleaning.....	91
5.2.2	Determining DHW Demand.....	96
5.2.3	DHW Demand.....	102
5.2.4	Determining Total Demand.....	103
5.2.5	Total Demand.....	104
5.3	<i>Data Quality for the Selected Set of Variables</i> .....	107
5.4	<i>DHW Demand and Total Demand</i> .....	109
5.4.1	Power Temperature Gradient.....	116
<b>6</b>	<b>Results 2 – Demand and Diversity</b> .....	<b>119</b>

6.1	<i>Introduction and Relevant Objectives</i> .....	119
6.2	<i>Demand Distribution</i> .....	119
6.2.1	Individual Demand Distributions .....	119
6.2.2	Recommended Sampling Time .....	125
6.3	<i>Total Demand Distribution Characteristics</i> .....	127
6.4	<i>DHW Demand Distribution Characteristic</i> .....	129
6.5	<i>Real Peak Demand</i> .....	135
<b>7</b>	<b>Results 3 – DHW Storage Impact on HN Design and Demand</b> .....	<b>139</b>
7.1	<i>Introduction and Relevant Objectives</i> .....	139
7.2	<i>Thermal Store Model Results</i> .....	139
7.2.1	Mixed Thermal Store Results .....	139
7.2.2	Stratified Thermal Store Results .....	141
7.3	<i>Thermal Store Model Validation</i> .....	144
7.3.1	Mixed Thermal Store Model Validation .....	144
7.3.2	Stratified Thermal Store Model Validation .....	147
7.4	<i>Aggregate Demand</i> .....	150
7.5	<i>ADMD and Diversity</i> .....	151
7.6	<i>Distribution System Sizing Results</i> .....	153
7.7	<i>Design Day Thermal Loss</i> .....	158
7.7.1	Sensitivity Analyses .....	160
7.8	<i>Oversizing of the Case Study HN Distribution System</i> .....	164
<b>8</b>	<b>Discussion</b> .....	<b>166</b>
8.1	<i>Results 1 Summary and Discussion</i> .....	166
8.2	<i>Results 2 Summary and Discussion</i> .....	167
8.2.1	Applicability.....	169
8.2.2	Sampling Time .....	169
8.2.3	Validity of Technical Guidance .....	171
8.2.4	Distribution System Sizing.....	172
8.3	<i>Results 3 Summary and Discussion</i> .....	172
8.3.1	Implications for Design Guidance and Industry Practice .....	173
8.3.2	Limitations .....	175
8.3.3	Applicability of Results .....	178
<b>9</b>	<b>Conclusions</b> .....	<b>181</b>
9.1.1	Future Research .....	182
<b>10</b>	<b>References</b> .....	<b>184</b>
<b>11</b>	<b>Appendix A</b> .....	<b>196</b>
11.1	<i>Internal Flow Rate Estimates</i> .....	196
11.2	<i>Heat Store Model Validation</i> .....	198
11.3	<i>Convective Heat Transfer Coefficient of the Insulation Layer</i> .....	198
11.4	<i>Validating the Network Thermal Loss Model</i> .....	199
<b>12</b>	<b>Appendix B</b> .....	<b>200</b>

12.1	<i>Total Demand Distributions at Aggregate Levels .....</i>	200
12.2	<i>DHW Demand Distributions at Aggregate Levels .....</i>	203
<b>13</b>	<b>Appendix C .....</b>	<b>213</b>
13.1	<i>DHW and Total Demand Capacity Calculation .....</i>	213
<b>14</b>	<b>Appendix D .....</b>	<b>215</b>
14.1	<i>Pipe Sizing .....</i>	215
14.2	<i>Distribution System Sizing for all Scenarios .....</i>	215

## *List of Figures*

- Figure 2.1: Shows the component parts of a HN connected to a residential building (CIBSE, 2020)
- Figure 2.2: The cold-water temperature distribution for a sample of dwellings (Energy Savings Trust, 2008)
- Figure 2.3: Annual volumetric hot water consumption (Energy Savings Trust, 2008)
- Figure 2.4: Mean monthly DHW consumption in sample of 49 dwellings (Ivanko et al, 2020)
- Figure 2.5: Annual hot water delivery and cold-water inlet temperatures (Energy Savings Trust, 2008)
- Figure 2.6: The diversity factor as taken from the DS439 (pipe sizing method) (CIBSE, 2020)
- Figure 2.7: a, b, and c are flow contributions that sum to give the design flow  $q$ . The function  $f(x)$  is the frequency function of the normal distribution (Holmberg, 1987)
- Figure 2.8: The formulation of design flow that was in use at the time (Holmberg, 1987)
- Figure 2.9: Guru diversity curve for SH and DHW demand as compared with the DS439 curve (based on the heat exchanger sizing method) for DHW demand only (Open Data Institute, 2017; Smith, 2016)
- Figure 2.10: Comparison of measured flow rates and design standards (Tindall and Pendle, 2018)
- Figure 2.11: Comparison of a range of design standards relating to design flow rates (Jack et al, 2017)
- Figure 2.12: General structure of a HN
- Figure 2.13: Optimisation of pipe diameter on a lifecycle costs basis (CIBSE, 2020)
- Figure 2.14: Illustration of the benefit of shared risers over horizontal runs for a typical flat layout (CIBSE, 2020)
- Figure 3.1: The design occupancy ( $P$ ) and number of bedrooms ( $B$ ) for the sample of HIUs
- Figure 3.2: The floor area of dwellings in the case study HN
- Figure 3.3: Conceptual diagram of the differences in diversity in the real DHW demand, the practicable storage scenarios, and the algorithmically optimised scenarios
- Figure 3.4: Individual DHW heat store sizes
- Figure 3.5: Cylindrical heat store dimensioned to have height equal to its diameter
- Figure 3.6: Flow chart describing the operation of the store. The chart is given in two parts (1/2).
- Figure 3.7: Flow chart describing the operation of the store. The chart is given in two parts (2/2).
- Figure 3.8: Stratified heat store connection to the DHW HEX in the HIU
- Figure 3.9: Heat store diagram illustrating the movement of the thermocline boundary
- Figure 3.10: Mixed heat store connection to the DHW HEX in the HIU
- Figure 3.11: Floor plan showing dwellings, riser cupboard and stairs on one floor. This plan applies to all floors.
- Figure 3.12: Network connection between dwellings within a floor and across floor. Black and red circles indicate where pipe cross floors
- Figure 3.13: Real distribution system and dwelling plan of the case study CHN, showing all 6 floors and the type of dwellings within each floor
- Figure 3.14: Schematic of pipe layers
- Figure 4.1: Shows connected key hardware and interconnections within the HIU (Heatweb Ltd., no date b)

Figure 4.2: Basic structure of the key hardware and interconnections across the communal network (Heatweb Ltd., no date b)

Figure 4.3: The home of Plant Pi and other pieces of hardware- this kit is housed in the plant room (Heatweb Ltd., no date b)

Figure 4.4: Depicts the flow of data from the sensors and the heat meters in an HIU to the data receivers

Figure 4.5: The M-bus physical layer (M-bus, no date)

Figure 4.6: M-Bus Master (Meter Market, no date)

Figure 4.7: Elvaco interface showing the readout schedule

Figure 4.8: Elvaco interface showing push report settings

Figure 5.1: Reading count map for all variables and dwellings across both HNs. Note that x-axis markers are dwelling IDs and are provided only as an indication of the number of dwellings and are not meant to be legible. The y-axis gives the variables in their original tags.

Figure 5.2: Reading count map for all variables and the subset of dwellings from Site W. Note that x-axis markers are dwelling IDs and are provided only as an indication of the number of dwellings and are not meant to be legible.

Figure 5.3: Reading count map of cleaned variables and dwellings across both HNs. Note that x-axis markers are dwelling IDs and are provided only as an indication of the number of dwellings and are not meant to be legible.

Figure 5.4: Reading count map of cleaned variables and the subset of dwellings in Site W. Note that x-axis markers are dwelling IDs and are provided only as an indication of the number of dwellings and are not meant to be legible.

Figure 5.5: Reading count map of subset variables and subset of dwellings. Note that x-axis markers are dwelling IDs and are provided only as an indication of the number of dwellings and are not meant to be legible.

Figure 5.6: The design occupancy (P) and number of bedrooms (B) for the sample of HIUs

Figure 5.7: The floor area of dwellings in the case study HN

Figure 5.8: Schematic of an HIU where the key measured variables considered in determining DHW demand are denoted (Heatweb Ltd., no date c)

Figure 5.9: A timeseries for an individual dwelling showing the raw data for the flow rate of cold inlet water in the DHW circuit and how it is forward filled to produce a fuller timeseries

Figure 5.10: Close-up of cold flow rate for one DHW event occurring after 19:30

Figure 5.11: A timeseries of an individual dwelling showing the raw data for the flow temperature of the DHW and how it is forward filled to produce a fuller timeseries

Figure 5.12: Close-up of DHW flow temperature for event occurring soon after 19:30 in Figure 5.11

Figure 5.13: Hot water delivery temperatures for the sample of dwellings

Figure 5.14: Mean daily volumetric DHW demand for the sample of dwellings

Figure 5.15: Set of three examples of DHW demand profiles on a selected day between 17:00 and 21:00

Figure 5.16: Set of three examples of DHW demand profiles over the course of a selected day

Figure 5.17: Demand profiles of three example dwellings starting at midnight and extending past 21:00 on a chosen day, showing the total demand and the DHW demands

Figure 5.18: Multiple-day profile of cumulative demand (kWh) and instantaneous demand (kW) for an example dwelling

Figure 5.19: Relationship between daily demand using instantaneous data and daily demand using cumulative data; one day, all dwellings

Figure 5.20: Reading count map of each variable used in determining DHW and total demands for the month of October 2021. Note that x-axis markers are dwelling IDs and are provided only as an indication of the number of dwellings and are not meant to be legible.

Figure 5.21: Reading count map of each variables used in determining DHW and total demand for the day of 25<sup>th</sup> of January 2022 which was the coldest day in the monitored period, chosen to represent design day conditions. Note that x-axis markers are dwelling IDs and are provided only as an indication of the number of dwellings and are not meant to be legible.

Figure 5.22: Mean daily external temperatures over the course of the selected cold period

Figure 5.23: Aggregate DHW demand and total demand for the cold period at a sampling time of 5 seconds and 5 minutes respectively

Figure 5.24: Aggregate DHW and total demand for the cold period, both at a sampling time of 5 minutes

Figure 5.25: Aggregate DHW and total demand for the cold period, both at a sampling time of 30 minutes

Figure 5.26: Aggregate DHW and total demand for the coldest day in the cold period

Figure 5.27: Aggregate DHW and total demand for the warmest day of the cold period

Figure 5.28: Mean hourly 24-hour profile for the sample of dwellings for DHW demand and total demand for the cold period

Figure 5.29: Mean hourly 24-hour profile of the total demand for the sample of dwellings for the weekend days and weekday days of the cold period

Figure 5.30: Mean hourly 24-hour profile of the DHW demand for the sample of dwellings for the weekend days and weekday days of the cold period

Figure 5.31: Mean daily total demand per m<sup>2</sup> of floor area

Figure 5.32: Mean daily DHW demand per m<sup>2</sup> of floor area

Figure 5.33: Box and whisker plot of the daily DHW demand for different dwelling occupancies where green triangles mark the mean.

Figure 5.34: Box and whisker plot of the daily total demand for different dwelling occupancies where green triangles mark the mean.

Figure 5.35: Regression of the daily demand of dwellings and external temperature in the case study HN where  $R^2 = 0.51$  and  $PTG = 40W/K$

Figure 6.1: Demand distribution for the total demand at an individual demand ( $k=1$ ) level showing the impact of increasing sampling times. Top-left: 5-minute; top-right: 10-minute; bottom-left: 30-minute; bottom-right: 1-hour.

Figure 6.2: Demand distribution for the DHW demand at an individual demand ( $k=1$ ) level showing the impact of increasing sampling times. Top-left: 1-second; top-right: 5-second; bottom-left: 10-second; bottom-right: 30-second.

Figure 6.3: Demand distribution for the DHW demand at an individual demand ( $k=1$ ) level showing the impact of increasing sampling times. Top-left: 60-second; top-right: 5-minute; bottom-left: 10-minute; bottom-right: 30-minute.

Figure 6.4: Demand distribution for the DHW demand at an individual demand ( $k=1$ ) level at a sampling time of 1 hour

Figure 6.5: The effect that sampling time has on the 95th percentile DHW demand for varying levels of aggregation over dwellings,  $k$

Figure 6.6: Example day-long profiles showing what could be SH, DHW and ambiguous demands which could be DHW or SH demands

Figure 6.7: Distribution of total demand at an individual dwelling level ( $k=1$ ) and a sampling time of 5 minutes where sections of predominant SH demand and predominant DHW demands are highlighted

Figure 6.8: A shower DHW event, often starting with a spike and then levelling off to a constant power. More examples of this kind of event can be found in the appendix

Figure 6.9: DHW demand profile spanning a number of days, showing the range of DHW events that could occur

Figure 6.10: Profile showing two DHW demand events where “peak and plateau” is evident

Figure 6.11: Examples of DHW events where the first in which a transient peak is present is closely followed by a second event in which the peak is less extreme

Figure 6.12: Series of plots showing the behaviour of DHW flow temperature and flow rate behaviour during a peak demand. The series increasingly zooms into the DHW peak event occurring around 17:29

Figure 6.13: DHW flow rate and primary flow rate behaviour during peak events- showing primary flow rate reaching 16 l/s

Figure 6.14: DHW demand distribution where red arrow denotes the large peak centred at 15 kW. Individual demands at a sampling time of one second.

Figure 6.15: Two small demand events which often take the shape of a short, sharp spikey demand that tends to last less than 5 seconds

Figure 6.16: DHW demand distribution showing where the real occupant demands and transient demands are likely to be. Individual demands at a sampling time of one second.

Figure 6.17: The demand per dwelling for the DHW demand and the total demand at a sampling time of 10 and 30 minutes

Figure 6.18: Guru diversity curve for space and DHW demand as compared with the DS439 curve (heat exchanger sizing) for DHW demand only (Smith, 2016)

Figure 6.19: Design total demand and DHW demand capacities with the measured DHW demand and total demand peaks (10- minute sampling time)

Figure 7.1: Residual demand and store temperature example profile for the mixed store model

Figure 7.2: Example multiple day profile resulting from CC-mixed model

Figure 7.3: Histogram of the fraction of the real DHW demand met in individual dwellings in the CC scenario using the mixed store model

Figure 7.4: Histogram of the fraction of the real DHW demand met in individual dwellings in the SC scenario using the mixed store model

Figure 7.5: Residual and thermocline position profile of an example dwelling, obtained using the stratified store model. The height of the store is just above 0.4m. The thermocline at above 0.4 m indicates that the store is empty.

Figure 7.6: A multi-day profile for the residual demand, thermocline position and heat loss profile outputs of the stratified model. A high thermocline position indicates that the store is empty, while a thermocline position at 0.0m indicates that the store is full.

Figure 7.7: Histogram of the fraction of the real DHW demand met in individual dwellings in the CC scenario using the stratified store model

Figure 7.8: Histogram of the fraction of the real DHW demand met in individual dwellings in the SC using the stratified store model

Figure 7.9: Example demand profile for a store where the heat loss factor is equal to 1 W/m<sup>2</sup>K and ambient temperature is set to 18°C

Figure 7.10: Example demand profile for a store where the heat loss factor is equal to 0 W/m<sup>2</sup>K and ambient temperature is set to 18°C

Figure 7.11: Example demand profile for a store where the heat loss factor is equal to 1 W/m<sup>2</sup>K and the ambient temperature is set to 50°C

Figure 7.12: Example demand profile for a store where the heat loss factor is equal to 1 W/m<sup>2</sup>K and ambient temperature is set to 18°C

Figure 7.13: Example demand profile for a store where the heat loss factor is equal to 0 W/m<sup>2</sup>K and ambient temperature is set to 18°C

Figure 7.14: Example demand profile for a store where the heat loss factor is equal to 1 W/m<sup>2</sup>K and ambient temperature is set to 50°C

Figure 7.15: Daily demand profile of the aggregate DHW demand in the SC scenario and the real (raw) DHW demand, comprising 96 dwellings.

Figure 7.16: Daily demand profile of the aggregate DHW demand in the CC scenario and the real (raw) DHW demand, comprising 96 dwellings.

Figure 7.17: The ADMD curves for aggregate demand for both CC and SC scenarios, and for the original DHW demand

Figure 7.18: The diversity curves for the aggregate demand of both CC and SC scenarios, and for the original DHW demand

Figure 7.19: Total length of pipe in the distribution system by the number of dwellings they serve

Figure 7.20: Peak demand of the aggregate demand of each scenario given as a function of number of dwellings. Blue vertical lines mark the distinct number of dwellings served by any pipe in the distribution system

Figure 7.21: Shows the proportion of pipes of a given diameter which all together make up the whole network for each scenario

Figure 7.22: Daily heat loss per meter for each size of pipe in the distribution system

Figure 7.23: Thermal loss of pipes of a given size as a percentage of the thermal loss in the real design

Figure 7.24: Daily thermal loss from the total length of pipes of a given size in the distribution system

Figure 7.25: Delivered DHW demand, store losses and distribution system losses in each storage scenario

Figure 7.26: Impact of varying building temperature parameter on thermal losses

Figure 7.27: Impact of varying the thermal conductivity of the pipe insulation on thermal losses

Figure 7.28: Impact of varying dwelling temperature parameter on thermal losses, where the red line demarks network losses (design day)

Figure 7.29: Impact of varying the heat loss factor of the thermal store on overall thermal loss, where the red line demarks network losses (design day)

Figure 7.30: Variation in heat loss factor with increasing thickness of insulation material for a thermal conductivity of high performing Phenolic foam ( $k = 0.018 \text{ W/mK}$ )

Figure 7.31: Daily heat loss from the total length of pipes of a kind (i.e., serving a given number of dwellings) in the distribution system for the real design and the real demand scenarios

Figure 7.32: Shows the proportion of pipes of a given diameter which all together make up the whole distribution system for each scenario

Figure 8.1: Demand distribution for the aggregate demand of 5 homes at a sampling time of 5 seconds (Cosic, 2017)

Figure 11.1: Key parameters used in determining the DHW flow rate

Figure 12.1: Demand distribution for the total demand showing the impact that sampling times has on demand at an aggregation level of  $k = 10$  dwellings. Top left: 5-minutes; top-right: 10-minutes; bottom-left: 30 minutes; bottom-right: 1 hour.

Figure 12.2: Demand distribution for the total demand showing the impact that sampling times has on demand at an aggregation level of  $k = 35$  dwellings. Top left: 5-minutes; top-right: 10-minutes; bottom-left: 30 minutes; bottom-right: 1 hour.

Figure 12.3: Demand distribution for the total demand showing the impact that sampling times has on demand at an aggregation level of  $k = 60$  dwellings. Top left: 5-minutes; top-right: 10-minutes; bottom-left: 30 minutes; bottom-right: 1 hour.

Figure 12.4: Demand distribution for the DHW demand showing the impact of increasing sampling times at an aggregation level of  $k = 5$  dwellings. Top-left: 1-second; top-right: 5-second; bottom-left: 10-second; bottom-right: 30-second.

Figure 12.5: Demand distribution for the DHW demand showing the impact of increasing sampling times at an aggregation level of  $k = 5$  dwellings. Top-left: 60-second; top-right: 5-minute; bottom-left: 10-minute; bottom-right: 30-minute.

Figure 12.6: Demand distribution for the DHW demand at an aggregation level of  $k = 5$  dwellings and a sampling time of 1 hour.

Figure 12.7: Demand distribution for the DHW demand showing the impact of increasing sampling times at an aggregation level of  $k = 10$  dwellings. Top-left: 1-second; top-right: 5-second; bottom-left: 10-second; bottom-right: 30-second.

Figure 12.8: Demand distribution for the DHW demand showing the impact of increasing sampling times at an aggregation level of  $k = 10$  dwellings. Top-left: 60-second; top-right: 5-minute; bottom-left: 10-minute; bottom-right: 30-minute.

Figure 12.9: Demand distribution for the DHW demand at an aggregation level of  $k = 10$  dwellings and a sampling time of 1 hour.

Figure 12.10: Demand distribution for the DHW demand showing the impact of increasing sampling times at an aggregation level of  $k = 35$  dwellings. Top-left: 1-second; top-right: 5-second; bottom-left: 10-second; bottom-right: 30-second.

Figure 12.11: Demand distribution for the DHW demand showing the impact of increasing sampling times at an aggregation level of  $k = 35$  dwellings. Top-left: 60-second; top-right: 5-minute; bottom-left: 10-minute; bottom-right: 30-minute.

Figure 12.12: Demand distribution for the DHW demand at an aggregation level of  $k = 35$  dwellings and a sampling time of 1 hour.

Figure 12.13: Demand distribution for the DHW demand showing the impact of increasing sampling times at an aggregation level of  $k = 60$  dwellings. Top-left: 1-second; top-right: 5-second; bottom-left: 10-second; bottom-right: 30-second.

Figure 12.14: Demand distribution for the DHW demand showing the impact of increasing sampling times at an aggregation level of  $k = 60$  dwellings. Top-left: 60-second; top-right: 5-minute; bottom-left: 10-minute; bottom-right: 30-minute.

Figure 12.15: Demand distribution for the DHW demand at an aggregation level of  $k = 60$  dwellings and a sampling time of 1 hour.

Figure 13.1: Measured DHW flow rates for the dwelling sample

## *List of Tables*

Table 2.1: Percentile values for the demand distribution of the aggregate demand of 40 dwellings (Cosic, 2017)
Table 2.2: Percentile values for the demand distribution of the aggregate demand of 10 dwellings (Cosic, 2017)
Table 2.3: Percentile values for the demand distribution of individual demand (Cosic, 2017)
Table 2.4: Typical flow velocities for steel pipes to BS EN 253, for use in feasibility-stage pipe sizing of primary network (CIBSE, 2020)
Table 2.5: Typical flow velocities for PEX pipes to BS EN 15632 for feasibility-stage pipe sizing of primary network (CIBSE, 2020)
Table 2.6: Velocity constraints for medium grade steel (CIBSE, 2020)
Table 2.7: Minimum insulation thickness to be used in the secondary network (CIBSE, 2020)
Table 3.1: The total number of demand profiles used in evaluating the aggregate distributions for varying levels of aggregation and sampling times
Table 3.2: Summary of the modelled storage scenarios
Table 3.3: Parameters of the heat store model
Table 3.4: Key parameters of the distribution system model
Table 3.5: Flow velocity constraints for the range of pipe diameters used in the sizing methods
Table 3.6: Selecting the smallest practicable pipe for an example pipe section
Table 3.7: Pipe insulation thickness is dependent on the pipe diameters
Table 4.1: Variables measured directly from sensors and heat meters in the HIU
Table 4.2: Table showing the key events and processes relating to the data collection
Table 4.3: Key measured variables, their identifier tags and sampling times
Table 4.4: Measurement errors of the key measured variables
Table 6.1: Summary of total demand distribution percentiles for k=1 expressed as demand per dwelling (kW)
Table 6.2: Summary of DHW demand distribution percentiles for k=1 expressed as demand per dwelling (kW)
Table 6.3: Summary of total demand distribution percentiles for k=5 expressed as demand per dwelling (kW)
Table 6.4: Summary of DHW demand distribution percentiles for k=5 expressed as demand per dwelling (kW)
Table 6.5: Summary of total demand distribution percentiles for k=10 expressed as demand per dwelling (kW)
Table 6.6: Summary of DHW demand distribution percentiles for k=10 expressed as demand per dwelling (kW)
Table 6.7: Summary of total demand distribution percentiles for k=35 expressed as demand per dwelling (kW)
Table 6.8: Summary of DHW demand distribution percentiles for k=35 expressed as demand per dwelling (kW)
Table 6.9: Summary of total demand distribution percentiles for k=60 expressed as demand per dwelling (kW)
Table 6.10: Summary of DHW demand distribution percentiles for k=60 expressed as demand per dwelling (kW)

Table 6.11: Comparison of design capacities compared with measured values for DHW and total demand

Table 7.1: Examples of the pipe diameters required to adequately deliver where pipes are serving 4, 30 and 48 dwellings

Table 7.2: Store and distribution system thermal losses given as a percentage of the DHW demand. Total losses for the coincident and spaced charging scenarios are given with the percentage difference from the real design scenario

Table 11.1: Thermal store model validation results

Table 11.2: Determining parameters for the convective heat transfer coefficient used in determining thermal loss from the network

Table 11.3: Network thermal model validation results

Table 12.1: Demand distribution for the total demand showing the impact that sampling times has on demand at an aggregation level of  $k=5$  dwellings. Top left: 5-minute; top-right: 10-minute; bottom-left: 30-minute; bottom-right: 1-hour.

Table 12.2: Summary of the demand distribution percentiles for the total demand at an aggregation level of  $k=5$  dwellings expressed as demand per dwelling (kW)

Table 12.3: Summary of the demand distribution percentiles for the total demand at an aggregation level of  $k=10$  dwellings expressed as demand per dwelling (kW)

Table 12.4: Summary of the demand distribution percentiles for the total demand at an aggregation level of  $k=35$  dwellings expressed as demand per dwelling (kW)

Table 12.5: Summary of the demand distribution percentiles for the total demand at an aggregation level of  $k=60$  dwellings expressed as demand per dwelling (kW)

Table 12.6: Summary of the demand distribution percentiles for DHW demand at an aggregation level of  $k=5$  dwellings expressed as demand per dwelling (kW)

Table 12.7: Summary of the demand distribution percentiles for DHW demand at an aggregation level of  $k=10$  dwellings expressed as demand per dwelling (kW)

Table 12.8: Summary of the demand distribution percentiles for DHW demand at an aggregation level of  $k=35$  dwellings expressed as demand per dwelling (kW)

Table 12.9: Summary of the demand distribution percentiles for DHW demand at an aggregation level of  $k=60$  dwellings expressed as demand per dwelling (kW)

Table 13.1: Variables used in determining DHW and total demand capacities (CIBSE, 2020)

Table 14.1: Nominal pipe diameters and thickness (HardHat Engineer, 2023)

Table 14.2: The aggregate peak demands (kW) needed to be met in the distribution system for the storage scenarios and the real demand scenario

Table 14.3: Distribution system sizing of the real design of the case study HN

Table 14.4: Distribution system sizing and related variables for the SC mixed scenario

Table 14.5: Distribution system sizing and related variables for SC stratified scenario

Table 14.6: Distribution system sizing and related variables for the CC mixed scenario

Table 14.7: The distribution system sizing and related variables for CC stratified scenario

Table 14.8: Distribution system sizing and related variables for the real demand scenario

## *List of Abbreviations*

<b>Abbreviation</b>	<b>Description</b>
ADE	Association for Decentralised Energy (previously known as the District Heat Association)
ADMD	After diversity maximum demand
ASHRAE	The American Society of Heating, Refrigerating and Air-Conditioning Engineers
BEIS	Department for Business, Energy and Industrial Strategy
BSRIA	Building Services Research and Information Association
CCC	Committee for Climate Change
CHP	Combined heat and power
CIBSE	Chartered Institution of Building Services Engineers Chartered Institute of Plumbing and Heating Engineering
CIPHE	Engineering
DECC	Department of Energy and Climate Change
DH	District heating
DHS	District heating system
DHW	Domestic hot water
DHWT	Domestic hot water tank
HEX	Heat exchanger
HIU	Heat interface
HN	Heat network
HWA	Hot Water Association
MQTT	Message queuing telemetry transport
SH	Space heat
TES	Thermal energy storage

# 1 Introduction

## 1.1 Motivation for the Thesis

In response to the Paris Agreement, a global agreement that sets temperature goals in light of the challenge of climate change, the UK's Committee on Climate Change (CCC) has developed strategies to enable the UK to reach net zero (CCC, 2020; Paris Agreement, 2015). Primary among the challenges to decarbonising the UK energy system is decarbonising heat to buildings. The CCC published the "Balanced Net Zero Pathway" setting out a detailed scenario through which the UK could reach its climate goals. Part of the package of solutions to address decarbonising heat to buildings is the roll-out of heat networks (HN), in addition to upgrading the supply sources of existing HNs to being low-carbon. HNs and electrifying heat through heat pumps, supported by an increase in energy efficiency in homes describes the general scenario for decarbonising heat to buildings. Low-carbon HNs are set to be built through 2020-2050, where scaling-up occurs through to 2028, at which point 0.5% of the total heat demand per year will be delivered through HNs (CCC, 2020). This will result in around a fifth of heat being distributed through HNs by 2050 (CCC, 2020).

HNs are recognised globally as a technology that can aid the transition to a cleaner energy system, e.g., through the integration of renewable energy sources (RES) because of the potential for HNs to provide operational flexibility which can act to buffer the fluctuating nature of the RES supply (Luc et al., 2020). Countries leading in the use of cleaner heating technologies, such as Sweden, have energy systems that have developed based on HNs (Kavvadias et al., 2019). The UK, on the other hand, which has been historically reliant on natural gas and is heated primarily using gas boilers requires government action to leverage HNs into the market. This is being undertaken, for example, through the HNs Delivery Unit, which was formed to provide funding and support to local authorities, and through the HNs Investment Project, created to provide capital funding for HN projects. The Balanced Net Zero Pathway expects that by 2030, 19% of all low-carbon heat installation sales will be HNs (CCC, 2020).

## 1.2 Research Gap

The CCC recognise the enforcement of robust design standards being critical in enabling HNs to perform effectively in the climate strategies (CCC, 2020). Industry organisations have been working together to create such standards, guidelines and best practices. These efforts have culminated in the Code of Practice, a document that sets out guidelines and best practices for all the stages of HN development (CIBSE, 2014; CIBSE, 2020). Although the information in the document is the result of extensive collaboration across industry experts, there remain some points of contention which, if persisting, could create uncertainty for HN designers and developers.

A key point of contention lies around the effect of diversity, the use of thermal energy storage (TES) and the combined effect of these on the demand of a HN (HWA, 2018; Smith, 2016). Diversity is used to describe the effect on the aggregate demand of a HN that results from the peak demands of individual users being unlikely to occur all at the same time. The peak aggregate demand is smaller than the sum of the individual peak demands, and it is as such to a degree that increases with the number of users connected to the network (Wang et al., 2020; Weissmann et al., 2017). Some studies on the impact of diversity on aggregate HN demand

have been conducted in European countries, however, few UK studies exist and fewer still are studies that use real data (Smith, 2016; Wang et al., 2020; Weissmann et al., 2017). Diversity is sensitive to the presence of DHW TES because it changes the shape of a demand profile. There is a significant amount of literature on storage in HNs, but none that focus on the relationship between diversity and storage (Borri et al., 2021; Guelpa and Verda, 2019; HWA, 2018). The limited understanding of the complex interplay between the effect of diversity and storage has prevented the establishment of best practices in this area. Adding further complexity to the matter is the uncertainty around accurately quantifying the effect of diversity using existing methods, as evidenced by the discrepancy between design values and real values of aggregate demand and peak flow rates, and the question of viability in applying standards outside of the country of origin (CIBSE, 2020, 2016; Jack et al., 2017; Fuentes et al., 2018; Kõiv and Toode, 2006). As it stands, HN designers commonly use the Danish standard of diversity, which is recommended in the Code of Practice (CIBSE, 2020). Being able to quantify the diversity effect is crucial to the design of efficient HNs. Underestimating the effect of diversity can lead to increased capital expenditure, for example through investment in oversized distribution pipes and peak power boilers, as well as resulting in increased thermal losses because of oversized network components (Weissmann et al., 2017). Thus, there is a strong need to understand the basis of the diversity estimation methods provided in existing technical standards and to assess their applicability outside the country of origin. There is a clear need to develop a family of diversity curves using real UK demand data (Open Data Institute, 2017; Smith, 2016).

### 1.3 Aims

Considering the above, the proposed study aims to inform the technical standards, 1. by characterising the real diversity effect of a HN and identifying influencing factors, and 2. by evaluating the impact of domestic hot water (DHW) TES on HN demand and design in the presence of diversity. The study will use real data from a large group of dwellings in a communal HN to determine individual and aggregate demand profiles, and then use the demand profiles to determine the real diversity effect and examine how it behaves across different levels of aggregation (over the number of dwellings and over time). Secondly, the individual demand profiles will be used to produce residual demands, i.e., the demand after storage installation, for each dwelling in the dwelling sample. The set of residual demands will then be used in assessing the impact of storage on demand and relevant aspects of the design of a HN.

### 1.4 Thesis Layout

The chapter that follows the current one is the Literature Review chapter in which a review of relevant research is presented. Following that, the Research Questions and Methodology chapter provides an outline of the research gaps identified in the literature review and summarises them by forming two research questions. The methods used in this work are given in the same chapter. Following that, the Data Collection chapter outlines the systems and methods of collecting the data and describes the data and its limitations. The results of the work are then presented in three results chapters: Results 1 – Generating Demand Profiles, Results 2 – Demand and Diversity, and finally, Results 3 – DHW Storage Impact on HN Design and Demand. The thesis concludes by summarising and discussing the key results and implications for the UK HNs industry in the Discussion and Conclusions chapters.

## 2 Literature Review

### 2.1 Introduction

This section starts by laying out the physical concepts most pertinent to this thesis. Following this, a literature review, conducted with the aim of laying out the existing research and debates that have shaped this study, is presented. The review considers the topics of energy demand in HNs and the physical and social factors that influence it, diversity of demand and relevant guidance and technical standards, and finally, thermal energy storage and its impact on HNs.

The remainder of this section gives the context of the research area, describing the wider implications of the topic. Section 2.2 describes the structure of a HN and outlines the function of key components that make up a typical HN. Section 2.3 details the physical and social factors playing a part in DHW demand, space heat (SH) demand, and HN demand as a whole. Section 2.4 draws on key studies on demand diversity in the context of HNs and electricity networks as well as in stand-alone dwellings, presenting their findings and describing the various metrics used by each to describe diversity in demand. The relevant diversity guidance and technical standards and their origins are investigated and critiqued in their application in UK HNs in Section 2.5. Section 2.6 details the technical guidance and standards relating to pipe sizing. Section 2.7 presents other relevant HN design guidance. Section 2.8 explores thermal storage in HNs, presenting the various potential configurations and their merits and limitations. Finally, Section 2.9 summarises the key take-aways from the literature review and highlights the research gaps made evident.

#### 2.1.1 The Role of HNs in Decarbonisation

The Paris Agreement is a global agreement that sets long-term temperature goals and aims to reduce global emissions to Net Zero by 2050 (Paris Agreement, 2015). In response to the agreement, the CCC have been developing strategies to enable the UK to reach these goals (CCC, 2020). The committee recognises one of the key challenges as being the decarbonisation of heat in buildings. In their recent publication, the "Balance Net Zero Pathway", the CCC propose that decarbonising heat to buildings could be achieved through a combination of electrifying heat through the widespread use of heat pumps, the roll-out of low-carbon HNs in heat-dense areas and shifting existing HNs that have combined heat and power (CHP) as their supply source to having low-carbon or waste heat sources (CCC, 2020). This shift is to be supported by an increase in the energy efficiency of homes, which acts to reduce the energy demand that needs to be met by the heating technologies (CCC, 2020). The CCC refer to HNs that deliver heat to both domestic, non-domestic and mixed areas, however, this thesis focusses on HNs that serve domestic buildings. In the long term, HNs bring other strategic benefits such as the facilitation of the deployment of large-scale thermal storage that contribute to the terawatt hours of energy storage required in future, partially or wholly, renewable energy systems (Cassarino and Barrett, 2022).

#### 2.1.2 A Brief History of the HN Market in the EU and UK

Having had reliable access historically, the UK has grown reliant on natural gas resulting in the gas boiler being the dominant method by which the UK heats its homes. There are around 20,000 HNs in the UK, comprising both communal HNs and district heating, connected to a

total of around half a million consumers (ADE; 2018; BEIS, 2019). Other EU countries, such as Denmark which has historically had limited access to fuel commodities like natural gas, have had to adapt to the limited availability of resources by developing highly efficient HNs that provide heat to consumers at reasonable prices (Kavvadias et al., 2019; Werner, 2017). The Balanced Net Zero Pathway predicts that low-carbon installation in homes will account for 80% of all heat sales, of which 19% will be low-carbon HNs (CCC, 2020). In the UK where the market is dominated by cheap gas, leveraging technologies like HNs into the market needs government support (ADE, 2018; BEIS, 2020a; BEIS, 2020b). As a response to the demand for growth in HNs, the UK government have created the HNs Delivery Unit (HNDU) to provide strategic funding and support to local authorities and the HN Investment Project (HNIP) to provide capital funding to HN projects in the UK (BEIS, 2020a).

### 2.1.3 The Need for Robust Technical Standards

The CCC views the "proper enforcement of standards" as being one of the key requirements needed for HNs to play an effective role in decarbonisation (CCC, 2020). Some industry bodies have already been working together to develop such standards and to set out how they can be met through guidelines and best practices, and other supporting entities, such as a voluntary standards body, have also been established (CIBSE, 2020; Heat Trust, 2021). The Association for Decentralised Energy (ADE) and the Chartered Institute for Buildings Service Engineers (CIBSE) together have published the Code of Practice (CP) which brings together the experience and expertise of a large number of individuals across both organisations (CIBSE, 2014; CIBSE, 2020). The second edition of this document, referred to as CP1.2, was published in 2020 given feedback from industry and researchers (CIBSE, 2020). The document provides guidelines and best practices for all stages of HN development, from the feasibility stages to operation and maintenance stages. Even though significant progress has been made, there are still points of contention within the industry, leading to gaps in knowledge which create uncertainty for network designers and developers and, in turn, increases the risk of the development of poorly performing HNs (Smith, 2016).

For example, it has been shown that the method recommended in CP1.2 for assessing peak aggregate heat demand, based on the Danish DS439 standard for determining design flow rates and therefore for distributing pipe sizing, overestimates values significantly (Open Data Institute, 2017; Dansk Standard, 2009). Studies have shown that using this method could potentially misinform the economic assessment for the construction of a HN because of overestimated capital costs (Smith, 2016). Other studies, focussed on apartment buildings, have shown that the DS439 has overestimated design flow rates and should it be used for this purpose in a HN, a likely outcome will be oversized pipes in the distribution system leading to additional heat losses (Jack et al., 2017; Weismann et al., 2016). Thus, there is concern within industry regarding the recommendation of this method and the implications that it could have for the performance of HNs, and, in light of this concern, there is recognition of the need for empirical studies to inform the standards, making them more robust in their application (Smith, 2016). Such empirical studies would need to be undertaken regularly enough to keep on top of evolving space heating and hot water patterns.

With the advent of the internet-of-things type systems being used in HNs, making high-frequency data collectable and accessible, there is a rich and growing source of data to support such studies (Heatweb Ltd., no date a). Thus, the available guidance information should be viewed as a work in development that stands to benefit significantly from on-going

research using real data, especially at this crucial juncture where HNs are being leveraged into the market.

## 2.2 HN Physical Structure

A HN is a centralised system that delivers heat to multiple buildings or dwellings from a central heat source. There are two main types of HNs. A communal HN (CHN) typically serves a smaller cluster of buildings or a single building. A district heating system (DHS) is a much larger HN often delivering heat to a neighbourhood, a town, or a city. It serves a diverse range of buildings, including residential, commercial and public properties. DHSs are commonly found in countries such as Denmark and Sweden, whereas CHNs are commonly found in the UK (ADE, 2018; BEIS, 2020a; Bøhm, 2013; Gadd, 2013a). This work is based on a CHN, and therefore, much of the material in the literature review focusses on CHNs.

Figure 2.1 shows the typical structure of a HN where the heat plant is located in a different locale to the residential building that is served. The two are connected by distribution system whose secondary and tertiary parts are within the building and whose primary part connects the heat plant to the building.

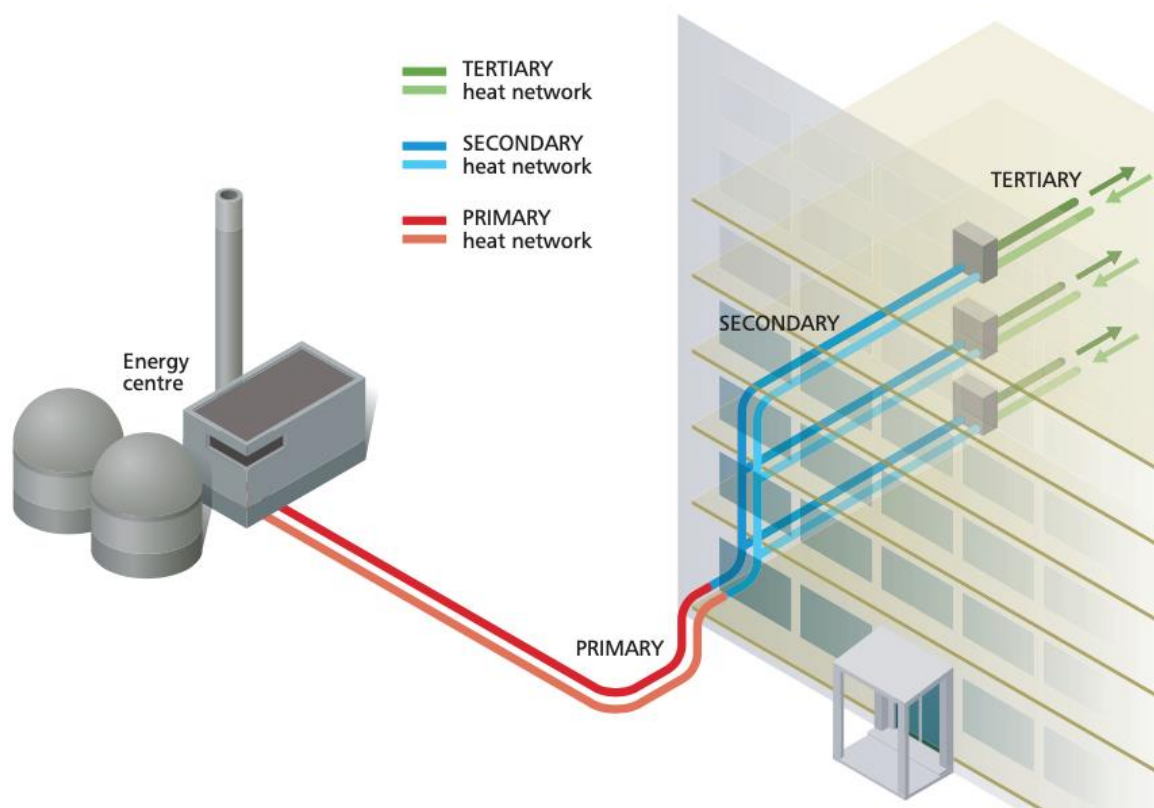


Figure 2.1: Shows the component parts of a HN connected to a residential building (CIBSE, 2020)

The typical structure of a HN will involve the following components.

- Heat source: a central source where heat is generated, e.g., a CHP plant, a biomass boiler or a conventional natural gas boiler. The heat source generates heated fluid which is then transported through pipes in a distribution system.

- Distribution system: this is a network consisting of insulated pipes that transport the heat from the heat source to the building or dwellings. The pipes are often buried underground to reduce heat loss to surroundings.
- Heat substations: substations, consisting of heat exchangers, can be found at points in the distribution system and act as interfaces between different parts of the network. They can be located in the basement of residential buildings for example, where they act as an interface between the primary network and the secondary network<sup>1</sup> which is within the building.
- Heat interface units: these are heat exchangers that act as the interface between the heating systems in individual dwellings and the distribution system (often the secondary or tertiary parts of the distribution network, depending on the network design)

The heat interface unit (HIU) is the interface between the domestic SH and DHW circuits, and typically consists of two heat exchangers, one for each domestic circuit. The distribution pipes of the HN enter the HIU to meet the heat exchangers. Typically, there is one primary flow and return that is diverted either to the SH heat exchanger when there is SH demand or to the DHW heat exchanger when there is DHW demand. If DHW is given priority, the flow will divert to the DHW exchanger at all times of demand, regardless of a coincident demand for SH. A detailed schematic of a typical HIU is given in Section 5.2.2.1.

## 2.3 Energy Demand

Heat demand in dwellings derives either from the need for space heating or hot water, and both are driven by both social and physical factors. Social factors are based on the occupants of the dwelling and their behaviour such as the number of occupants, occupancy patterns, and the socio-economic and cultural backgrounds of the occupants (Marini et al., 2019; van den Brom et al., 2019). Physical factors include factors such as external temperature and climate, building design (e.g., building size, insulation levels, etc.), and heating system characteristics (Aragon et al., 2022). The total resulting demand profile is dependent on the occupant heating behaviour, the properties of the heating system and the building, and the external temperatures. The complete load profile of a dwelling is the result of the interaction between the social and physical factors and how that interaction drives the demand. In this section, the driving factors of DHW demand are described and the role that DHW demand plays in diversity is introduced. Secondly, the key factors that drive variation in domestic demand are also described and finally, the key components of HN demand in totality are laid out.

### 2.3.1 DHW Demand

Instantaneous DHW demand in dwellings is largely dependent on the set point temperature and the incoming cold-water temperature. When designing for the supply of DHW in HNs, DHW tends to be estimated using the factors of demand temperature, volume requirement per person and household size (DECC, 2019; Yao and Steemers, 2005). The Energy Savings Trust conducted a study, consisting of ~120 dwellings, of which one aim was to measure the volumetric consumption of DHW and the associated energy requirement (Energy Savings Trust, 2008). Measurements were taken to describe the hot water consumption, the hot water

---

<sup>1</sup> In this thesis, the terms ‘secondary network’ and ‘primary network’ will be used to refer to a specific section of the connected system of pipes between the heat plant and HIU whereas the terms ‘distribution system’ or ‘network’ are used to refer to the connected system of pipes as a whole.

delivery temperature, and the cold-water inlet temperatures. The cold-water temperature distribution is shown in Figure 2.2. The mean of the cold-water temperatures measured was 15.2°C.

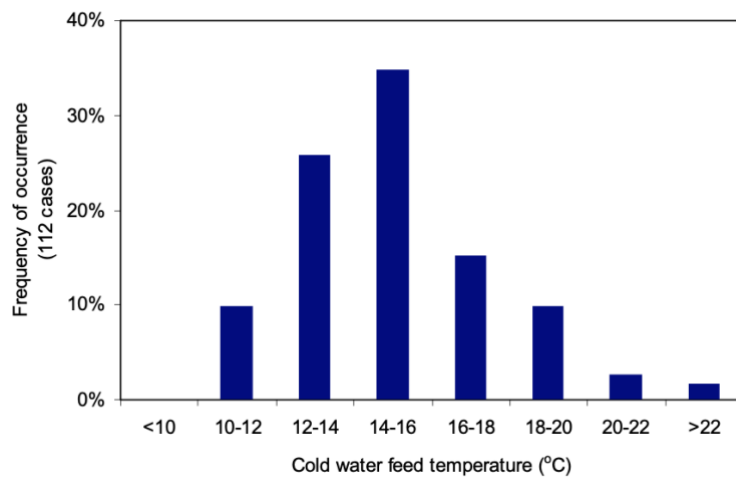


Figure 2.2: The cold-water temperature distribution for a sample of dwellings (Energy Savings Trust, 2008)

There is a small seasonality effect on DHW demand resulting from holiday taking and warmer cold inlet temperatures in the off-heating season. Figure 2.3 shows the volumetric hot water consumption by month for the sample of dwellings, indicating a reduction of consumption in the months of July and August, attributed to the absence of occupants due to holiday-taking (Energy Savings Trust, 2008). A study of apartments in an apartment building in Norway showed a similar pattern, shown in Figure 2.4, again attributed to holiday-taking (Ivanko et al., 2020). Similar findings are also presented in a study of DHW consumption in apartment buildings in other European countries (Grasmanis et al., 2015; Vámos and Horváth, 2022). In Figure 2.5 below, a marked seasonal variation in cold-water inlet temperatures is seen; however, the hot water delivery temperatures are seen to be constant through the year. The above suggests that there is a seasonal variation in DHW demand resulting from the increase in both cold-water inlet temperatures and periods of occupant absence in the off-heating season.

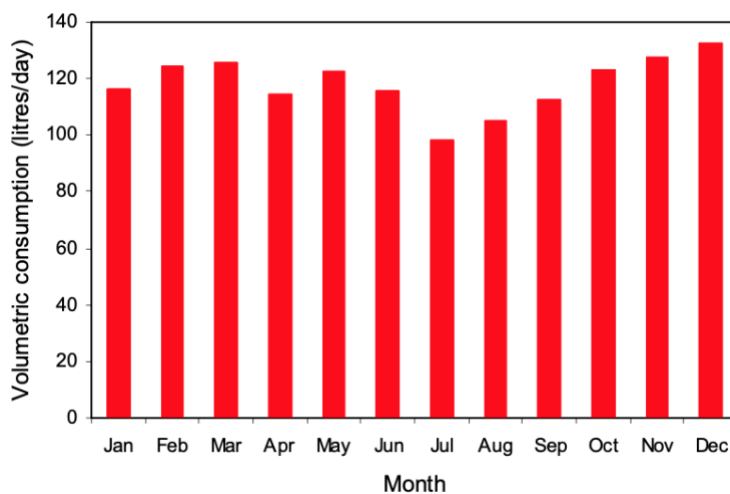


Figure 2.3: Annual volumetric hot water consumption (Energy Savings Trust, 2008)

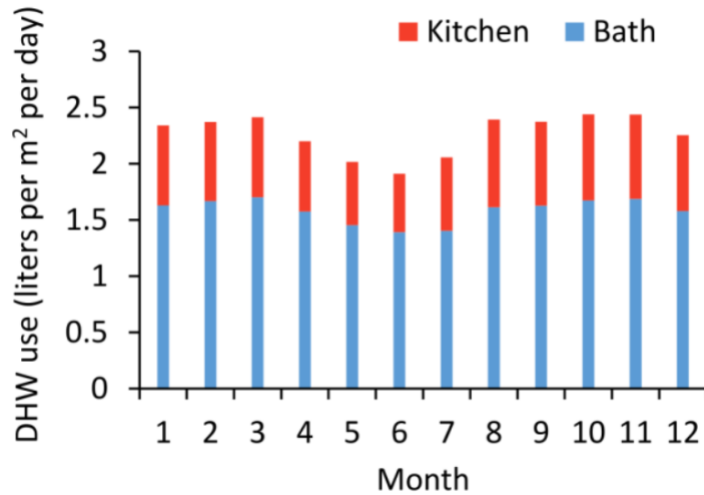


Figure 2.4: Mean monthly DHW consumption in sample of 49 dwellings (Ivanko et al, 2020)

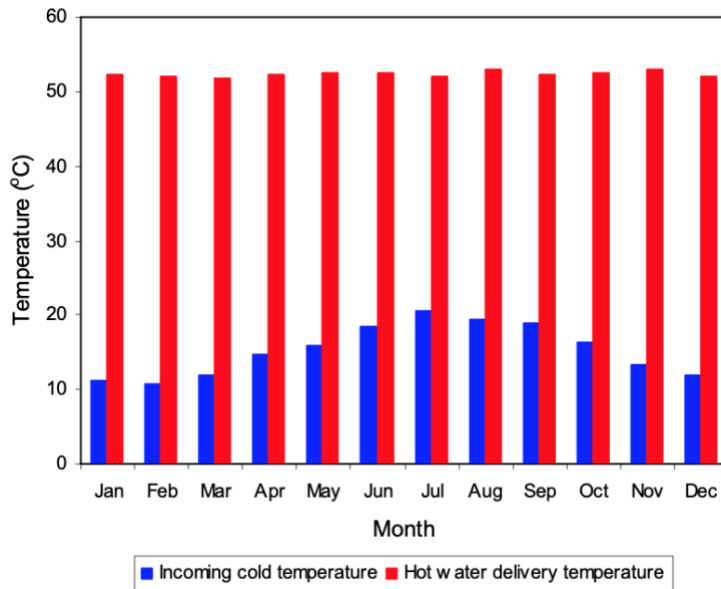


Figure 2.5: Annual hot water delivery and cold-water inlet temperatures (Energy Savings Trust, 2008)

### 2.3.1.1 HN Demand and Diversity

Due to the characteristic differences in SH and DHW demands, the diversity effect is different in each. There is a distinct lack of literature that explore these differences (Huang et al., 2020). Current design standards treat diversity in SH and DHW independently, instructing that diversified flow rates be calculated separately for SH and DHW and combined afterward (CIBSE, 2020). The DS439 is the basis for the DHW diversity, and another Danish curve is used for SH diversity. The curve recommended for the SH calculation was originally intended for calculations concerning SH and DHW together and therefore it is noted that further analyses using existing UK HNs is required (CIBSE, 2020). The diversity methods for DHW and SH are explored further in Section 2.5.

Ultimately, there is little understanding of how the diversity effect is different in DHW demand and SH demand and how this may impact aggregate demands that need to be considered when sizing pipes in the distribution system. Expanding knowledge in these areas

would not only be useful in informing existing technical guidance but also in understanding the implications of evolving DHW and SH demands. For example, increasing building insulation, which reduces the demand for SH, means that DHW demand may become increasingly dominant (Bøhm, 2013; Marini et al., 2015; Marszal-Pomianowska et al., 2019). At present, DHW demand accounts for about 20-25% of the total demand of a dwelling, or 40-45% in energy-efficient homes, however, as occupant demands evolve so too should technical guidance (Bøhm, 2013; Marini et al., 2015; Marszal-Pomianowska et al., 2019). Empirical studies with a focus on understanding the diversity effect in SH and DHW independently will aid such an aim.

### 2.3.2 Variation in Domestic Demand

Van den Brom et al. (2019) in their study of variance in residential heat consumption concluded that approximately half of the variation seen in demand is because of differences in occupant behaviour, the remaining half being because of differences in building characteristics. Furthermore, it was shown that the influence of the occupant is more significant in energy-efficient houses and vice versa (van den Brom et al., 2019). Thus, as dwellings become more energy-efficient in the future, it can be expected that the influence of occupants will become more significant. Patterns can be seen in how occupant behaviour affects heat demand; for example, working outside their homes means that those occupants will be absent for working hours, leading to many domestic demand profiles having a peak in the morning and a peak in the evening, where much of the energy demand occurs (Do Carmo et al., 2016; Summerfield et al., 2015). Although there are common patterns across domestic load profiles, there are also variations that result from the stochastic nature of occupant behaviour and the variation in the heating systems and building properties. These factors drive the diversity effect seen when individual demand aggregates to form network demand (Fischer et al., 2016; Weissmann et al., 2017; Yan et al., 2015).

### 2.3.3 HN Demand and Drivers

Gadd et al. (2013a) describe the heat load of a network as being the sum of the aggregate heat load and the heat losses occurring in the distribution system. They add that the heat load is controlled by four system components; the hot water taps and valves in the radiators, the control valves on the primary side of the substations, which are responsible for maintaining the supply temperatures using variable flow, the differential pressure control on the primary side, which maintains the differential pressure at the periphery of the system at a set point, and the supply temperatures on the primary side (Gadd et al., 2013a). The extent of losses from the distribution length depends on the physical properties of the pipes that make up the system, e.g., insulation levels, pipe surface area, piping length, etc, and on the temperature of the fluid and the external temperature (Guelpa, 2021; Hennessy et al., 2019). The aggregate consumer demand is driven largely by individual and collective heat demands where collective demands refer to the demand that results from collective behaviours such as uniform or harmonised working hours (Gadd et al., 2013a; Gadd et al., 2013b). HN load profiles usually present variation across seasons due to the significant shift in external temperatures and the resulting changes in collective heating behaviour (Gadd et al., 2013a; Gadd et al., 2013b; Pakere et al., 2016). Daily variation is driven by changes in external temperature too, as well as variation in solar radiation that is incident on the dwelling, and the behaviour of occupants (Noussan et al., 2017; Pakere et al., 2016).

## 2.4 Demand Diversity

Diversity of the individual demand profiles that make up the aggregate demand profile means that the maximum aggregate demand will not be higher than the sum of the individual maximum demands; thus, the effect of diversity is a key consideration when designing HNs (Chesser et al., 2020; Ramírez-Mendiola et al., 2017; Weissmann et al., 2017; Wang et al., 2020). In addition to the variation across the individual demand profiles, features of the network itself can add to the diversity effect. For example, the return flow in a larger network will reach the central plant at more varied times compared with a smaller network, thereby adding to the diversity effect (Gadd et al., 2013a; Pakere et al., 2016). Furthermore, larger networks that use parts of the pipeline as temporary storage will also contribute a larger diversity effect (Guelpa, 2021). This effect is present for any HN because any distribution system will act as a store of sorts even though it may not be deliberately utilised as a store. The resulting diversified aggregate peak demand bring benefits such as reduced installed capacity, resulting in lower investment costs and lower operational and maintenance costs (Weissmann et al., 2017; Winter et al., 2001). Smaller peak demands also allow for smaller pipe sizing, thus reducing the heat losses from the distribution system (CIBSE, 2014; CIBSE, 2020).

### 2.4.1 Review of Diversity Metrics

Diversity is referred to in the literature in many ways, and one can find a range of metrics being used to quantify diversity and related parameters. For example, Happle et al. (2020) defines it as being the "fundamental differences between buildings", thus suggesting that diversity is the differences in the physical and social characteristics of the buildings and their components. In some studies, on the subject of energy security, diversity is used to refer to the diversity in energy sources or energy suppliers (Skea, 2010; Stirling, 2010). The Diversity Factor is a metric defined as the ratio between the "sum of the peaks" (i.e., the sum of the peaks of the individual demand) and the "peak of the sum" (i.e., the peak of the aggregate load) (Happle et al., 2020; McKenna et al., 2016; Wang et al., 2020). The inverse of the Diversity Factor, referred to as the Simultaneity Factor or the Coincidence Factor, are also metrics that have been used in studies (Guan et al., 2016). Investigations based on the aggregate peak load have been seen to use the After Diversity Maximum Demand (ADMD) which describes the peak of the aggregate load per number of dwellings (Chesser et al., 2020; Wang et al., 2020). Winter et al. (2001) and Weissmann et al. (2017) refer to the metric of peak load ratio (PLR), which is similar to the Diversity Factor in that they are both calculated using the variables of the "peak of the sum" and the "sum of the peaks."

### 2.4.2 Diversity in Electricity Networks

Understanding diversity and its effects is crucial in designing any energy network, such as electricity grids (Gallo Cassarino et al., 2018; McKenna et al., 2016; Torriti, 2014) or multi-energy systems (Good et al., 2015). Electricity has always been distributed through large networks and so there is a significant amount of literature that has looked at the diversity in electricity systems in the UK (Chesser et al., 2020; McKenna et al., 2016; Torriti, 2014). Since transitioning to cleaner energy systems has become a global priority there have been numerous studies published on the topic of diversity in electricity networks and how they are impacted in light of these new challenges. For instance, McKenna et al. (2016) conducted a study on the impact of electricity demand profiles and their diversity on residential buildings

in the context of low-carbon technology uptake. Chesser et al. (2020) investigated the impact on the ADMD in the context of uptake of Air Source Heat Pumps in residential households. Although diversity studies in the context of electricity demand are common, there is limited literature on the diversity in the context of heat demand in the UK, likely due to the recency of their emergence in the UK market. The impact of diversity is more important for HNs than gas or electricity networks where cost and losses are less of a function of peak demand and pipe/cable size.

### 2.4.3 Drivers of HN Demand Diversity

Weissmann et al. (2017) conducted a study that aims to identify the building and occupant related characteristics that have a significant influence on the demand profile of residential buildings and quantify their influence on the diversity effect, with a view to understanding how the effect of diversity may be leveraged to reduce the installed capacity of the central heat source. The study modelled a large number of diverse load profiles based on varying building properties, user profiles, temperature control, etc. The metric of PLR is used to describe diversity. PLR is defined as the difference between the sum of the individual peak demand and the central supply maximum as a fraction of the sum of the individual peak demand. The sum of the individual peak demands is also referred to as the "sum of the peaks." The central supply maximum demand is a theoretical figure that describes the maximum demand of the aggregate demand. This is sometimes referred to as the "peak of the sum." A higher PLR indicates an increased diversity effect.

The first set of results suggests that certain features can have a larger impact on diversity than other features. For multi-family buildings with a higher occupant density, it was found that the diversity effect was especially sensitive to changes in the user profile. In contrast, in single-family homes with a lower occupant density, it was found that changing the insulation of the building envelope had the most significant impact on the diversity effect. The study also showed that the kinds of individual demand profiles that significantly add to the diversity effect are those of newly built buildings that have higher levels of insulation and thus the influence of hot water demand on the maximum load becomes primary. This suggests that DHW has a stronger influence on diversity than SH demand. This is an important consideration given that DHW demand is likely to become a more dominant part of total dwelling demand in the future. Control features such as temperature set-back can either increase or decrease PLR, depending on the start time of the heating up period. If the start time is different from other buildings in the district, the effect of diversity will increase. Considering the study's aim to maximise the benefits gained from diversity and at the same time reduce the increased losses from the distribution system, the authors recommend that the HN connects as diverse a mix of profiles as possible given the constraint imposed by the supply temperature requirements of buildings in order to increase the benefits gained from the diversity effect. They specifically recommend a combination of buildings with different construction years, different temperature setback controls and different user profiles to increase the PLR.

In the second part of the study the most diverse of the profiles were used as inputs in a district heat (DH) model of four types that vary in their location, in a city or a rural setting, and in the year in which the buildings in the district were built, 1960 or 2016. The study showed that supply temperatures were required to be around a couple of degrees higher in the district supply models in order to overcome the distribution losses. The results showed that the 1960s

scenarios had a diversified demand peak (the peak needed to be met by the central heat generator, thus including distribution losses) that was significantly higher than the aggregate individual supply load because of the higher supply temperatures required for space heating which led to high distribution losses. Moreover, in this scenario, the supply temperature is higher than the required hot water temperature of the buildings, which could lead to inefficiencies that would not present in an individual supply scenario in which the individual boilers can meet the two separate demands using different supply temperatures. Resultantly, in these scenarios, the reduced aggregate peak demand is outweighed by the distribution losses.

The profile shape that is applied by a large number of suppliers in Germany is a synthetic profile that represents the mean demand from a multitude of buildings where the influence of single-building-related characteristics cannot be recognised, thus implying that using such synthetic profiles may lead to errors when estimating the aggregate peak demand of a HN because it fails to account for the effect of diversity. Because of the continued use of such synthetic profiles, the authors recommend that further work be done with the aim of enhancing the synthetic profiles so that they become a more accurate representation of reality, such as by including the use of the PLR-related results for analysing the diversity effect. The authors point out that their models are limited since they used static hot water demand profiles and thus did not capture the effect of stochastic occupant behaviour around hot water use on the diversity effect. They highlight that such inclusion is likely to have produced higher PLR values. Weissmann et al. (2017) also state the next steps for extending the model to be to include thermal storage.

Happle et al. (2020) is a recently published study that investigated the impact of the diversity of occupancy profiles of commercial buildings of the same use-type and its impact on the energy demand in a case study district cooling system. The authors raise concern over the use of Urban Building Occupant Presence Models (UBOP) that are used to generate occupancy profiles for use in Urban Building Energy Modelling for HNs because such occupancy models account only for differences that result from building geometry and construction properties, whilst disregarding the differences that exist within buildings of the same use-type. The authors describe the variability in occupancy profiles of buildings of the same use-type as being a combination of diversity, stochasticity, and seasonality. Diversity, as referred to in this paper, describes the "fundamental difference between buildings of the same use-type." Stochasticity is used to describe the "random variation in daily profiles of a specific building." Seasonality is used to describe "underlying behavioural trends influencing all types of buildings, such as the weather or holidays." Diversity in residential buildings or single dwelling homes could also be said to be contributed by these factors, as they are different buildings of the same use-type.

The above study considers only how diverse occupant behaviour affects district energy demand. It does not account for the diversity that results from building system properties, for example. Similar to conclusions drawn about residential buildings in Weissmann et al. (2017), it was found that diversity effect is more important when occupant density is higher. Another key result of the study showed that using diverse urban occupancy profiles results in a diversity factor below 0.8 for the studied district. This leads the authors to warn that using uniform individual profiles in designing heat or cool networks may result to diversity factors that are above the threshold below which network development can go ahead. The threshold diversity factor of 0.8 is based on the operator experience of the operators of HNs in Hong Kong. The value of 0.8 is also the diversity factor value that is given for a number of district

cooling systems in the surrounding area, suggesting that it might be the accepted threshold value for what is a key parameter that is considered when deciding to develop a district energy system or not. This highlights the significant effect that simplistic UBOP models have on district energy demand estimation and, therefore, also on energy system planning decisions. Further work suggested by the authors is the use of probabilistic demand simulation in the design of heat or cool networks with high occupant densities, thus highlighting the need for the integration of the effect of variability in occupancy profiles and, therefore, also on the diversity effect of a district. Although there is little evidence for instances where HN plans have fallen short of the threshold, it is easy to imagine that such occurrences are going on unnoticed in urban and residential networks alike. The study also brings to light the prevalence of dependence on practitioner experience and the use of 'rules of thumb' when designing and constructing HNs. Applying experience-based techniques in the development of HNs could have unforeseen consequences because their generalisability is seldom studied or confirmed. Thus, there is a need to supplement using rules of thumb in HN design with studies based on real data in order to test and map the limits of the applicability of the rules of thumb.

#### 2.4.4 The Need for Empirical Diversity Studies

The studies in the preceding sections have demonstrated how the use of simplistic models can have an adverse impact on HN development decision making and also potentially on their performance. The above modelling studies can only describe the isolated impact of a given factor on diversity, e.g., occupancy profiles, building properties, etc. These kinds of studies are useful in describing the sensitivity that diversity might have to any of these factors, but the approach of modelling cannot accurately describe the real impact of the combined effect of the factors. Modelling studies are complemented by studies that use real data because measured data have the capacity to capture the idiosyncratic behaviours that are not present in model simulations. This could be especially the case where stochasticity is a key component of the studied phenomena, and where the various factors at play, such as the physical building and network related factors, along with the social behaviour related factors, have a combined and complex impact.

One study using real data from UK dwellings to understand diversity looked specifically at the ADMD, the aggregate load peak, and its dependence on the number of dwellings in order to understand the minimum number of dwellings required to accurately assess ADMD (Wang et al., 2020). Using smart meter data giving gas consumption over a period of a year which included two of the coldest days in recent UK weather history which is pertinent to understanding demand in extreme weather events. The ADMD was calculated for the two cold days and expressed as a function of the number of dwellings, revealing an asymptotic relationship that was used to identify the number of dwellings that are required to accurately assess the ADMD. This work is an important first step in understanding the effect of diversity in UK HNs, and it could be used to inform technical standards. However, limitations include that the findings cannot be generalised to networks with storage and since findings describe extreme cold day events, they may only be part of the picture. Furthermore, the data is not from dwellings on a HN. Thus, one has to consider whether the fact of being connected to a wider system would have an effect on aggregate peak load that would not be present in the analysis of disconnected dwelling demand. Understanding the ADMD is crucial in determining the size of the installed capacities and the distribution pipes. Likewise, understanding the aggregate peak load where the constituent loads are residual loads of

systems with storage will be crucial to sizing capacities and transmission pipes of networks with storage. The use of half-hourly data may have limited the size of the peaks, too.

#### 2.4.5 The Impact of Sampling Time on Individual and Aggregate Demand

When delivering demand through any kind of energy network, it is important to consider the relationship between individual consumer demands and aggregate demands (Carpaneto, 2006; Carpaneto, 2008; Sajjad, 2016). An important consideration when investigating individual and aggregate demands is the sampling time. A study investigating the impact of sampling time on load variation at different levels of aggregation for electricity networks, with the aim of determining the potential flexibility of residential demand, explicated the relationship between sampling time and aggregate demand in the following ways (Sajjad, 2014).

- There is a trend to losing the impact of single customers on the aggregate demand with increasing sampling time.
- As aggregation increases the demand profile becomes more and more similar.
- As sampling time increases, the diverse behaviour of aggregate profiles is increasingly ignored.

Although these results refer to the specific set of customers studied in the paper, the general trends are expected to hold, with slight variations dependent on demographic and topology (Sajjad, 2014). These trends have also been noted in studies using real HN data to study diversity. Cosic (2017) used high-frequency DHW data collected for a group of dwellings by the Energy Savings Trust in order to inform the design standards and practices of UK HNs and thereby improve their performance. A key consideration in this effort was addressing HN oversizing resulting from the use of accepted design standards that overestimate DHW peak loads. The authors state the need for a national UK standard derived from primary data from a relevant sample of dwellings, which can be cited by consultants accepting a design liability. The DHW data were used to create individual load profiles for 40 homes. Demand distributions for the aggregate demand for 1, 5, 10, and 40 dwellings were presented. Table 2.3 summarise the key percentile values for the aggregate demand distribution for 40 dwellings, 10 dwellings, and the demand distribution for individual demand respectively. The authors found that 5-second, 10-second, 30-second and 1-minute data led to nearly identical aggregate demand distribution at an aggregation level of 40 dwellings, and thus, 1-minute data would be acceptable for analysing HN demand at this scale. 5-minute data is said to be likely acceptable for analysing demand at this scale with an appropriate safety factor of 20-30%, or where the demand of residents in the HN is as similar to each other as the sample of suburban dwellings used in the study. Hourly data is said to be indicative of the storage and the heating capacity that would be required to meet demand at the plant room. 1-second or 5-second data at an aggregation level of 10 dwellings is deemed suitable for sizing pipework to individual HIUs where DHW is generated instantaneously. 30-second and 1-minute data could be used for the same with a safety factor of 10-20%. Sampling times higher than this are deemed unsuitable for sizing pipework directly connected to individual HIUs but may be used to size buffer vessels at the “riser” level of the network or for storage at the plant. The summary conclusions of the report are that 5 second or 10-second data is needed to fully capture the peaks of aggregate demands, whilst for fully capturing peaks in individual demands, higher sampling times are required. This conclusion is in alignment with findings

regarding electricity network loads presented above, where longer sampling time intervals are noted as leading to increasing loss of information at aggregate levels (Sajjad, 2014).

Table 2.1: Percentile values for the demand distribution of the aggregate demand of 40 dwellings (Cotic, 2017)

## 40 homes - 1 combination

Power per home (kW) - cumulative distribution analysis						
Sample Time	Zero Power (%)	95%	99%	99.90%	99.95%	100%
5 seconds	56%	1.4	2.1	2.9	3.2	4.6
10 seconds	53%	1.4	2.0	2.9	3.1	4.4
30 seconds	44%	1.3	1.9	2.8	3.0	4.1
1 minute	36%	1.2	1.8	2.7	2.9	3.9
5 minutes	16%	1.1	1.6	2.3	2.6	3.4
10 minutes	10%	1.0	1.4	2.1	2.2	2.9
1 hour	1%	0.9	1.1	1.3	1.5	1.5

Table 2.2: Percentile values for the demand distribution of the aggregate demand of 10 dwellings (Cotic, 2017)

## 10 homes - 1000 combinations

Power per home (kW) - cumulative distribution analysis						
Sample Time	Zero Power (%)	95%	99%	99.90%	99.95%	100%
5 seconds	85%	3.5	5.2	7.0	7.6	14.8
10 seconds	83%	3.5	5.0	7.0	7.4	14.2
30 seconds	78%	3.5	4.6	6.6	7.1	13.4
1 minute	73%	3.2	4.3	6.3	6.3	13.4
5 minutes	49%	2.4	3.5	5.0	5.5	10.2
10 minutes	36%	2.1	3.1	4.2	4.6	7.9
1 hour	10%	1.4	1.9	2.5	2.7	3.9

Table 2.3: Percentile values for the demand distribution of individual demand (Cotic, 2017)

## 1 home - 40 combinations

Power per home (kW) - cumulative distribution analysis						
Sample Time	Zero Power (%)	95%	99%	99.90%	99.95%	100%
5 seconds	98%	35.0	35.0	35.0	35.0	35.0
10 seconds	98%	34.0	35.0	35.0	35.0	35.0
30 seconds	98%	29.0	35.0	35.0	35.0	35.0
1 minute	97%	26.4	35.0	35.0	35.0	35.0
5 minutes	92%	18.0	27.9	35.0	35.0	35.0
10 minutes	88%	13.2	22.9	32.5	34.4	35.0
1 hour	63%	5.3	9.7	15.6	18.9	34.4

## 2.5 Guidance and Standards for Diversity in HNs

### 2.5.1 SH Diversity Factor

For diversity in SH demand alone, CP1.2 calls for the use of operational data from a similar HN, or from modelling, to be used to derive a diversity curve. Failing this, a Danish 'rule of thumb' formula for a diversity factor as a function of the number of dwellings is given, reproduced below in Equation (2-1).

$$SH \text{ diversity factor} = 0.62 + \frac{0.38}{N}$$

(2-1)

The SH diversity curve is intended for district schemes in Denmark with both space and hot water needs; however, its use in determining SH capacities is considered valid provided that peak heating demand is calculated assuming heat losses to adjacent properties. No further clarifications are provided on this point; however, the need for further work analysing data from existing schemes for "more robust diversity calculations" is highlighted (CIBSE, 2020). Moreover, the individual impact of SH demand, separate to that of DHW demand, on diversity and therefore capacity estimations, has not been found to be the subject of any research literature.

## 2.5.2 DS439: Pipe Sizing Method

The most up to date guidance by CIBSE, given in CP1.2, calls for the use of the Danish diversity standards in diversifying peak demands where instantaneous DHW is being delivered. CP1.2 recommends that where data measured at intervals of one minute or less is available for dwellings of a similar type and occupancy it should be used to calculate a more empirical and specific diversity curve. When developing a diversity curve from the monitored data, the designer is instructed to consider the disaggregate demand for SH and DHW, the probability distribution of the measured diversified demand, and the variation in temperature of the cold feed-in water. The Distributing Pipe Sizing section in the DS439 (Section 2.3, DS439) provides the method that is used in CP1.2 for the calculation of the design local flow rate, a requirement for sizing the distributing pipes (any pipe that is connected to multiple outlets downstream of the system),

$$q_d = 2q_m + \theta \left( \sum q_f - 2q_m \right) + A\sqrt{q_m \cdot \theta} \sqrt{\sum q_f - 2q_m}$$

(2-2)

where  $q_m$  is the weighted mean water flow rate of all outlets connected to the distributing pipe,  $q_d$  is the design water flow rate for randomly used outlets connected to the distributing pipe,  $\sum q_f$  is the sum of assumed water flow rates of randomly used connected outlets and where  $A$  is a safety factor, and  $\theta$  is the probability of draining  $q_m$  at times of peak demand. These factors are to be elected by the designer depending on the levels of service that are required. Although the method was developed for centrally generated water systems, CP1.2 justifies its use in sizing the distribution pipe sizes in HNs on the basis that flow rates in a secondary HN system are similar to flow rates where there is instantaneous hot water production (CIBSE, 2020). Figure 2.6 shows the diversity curve that corresponds to this method.

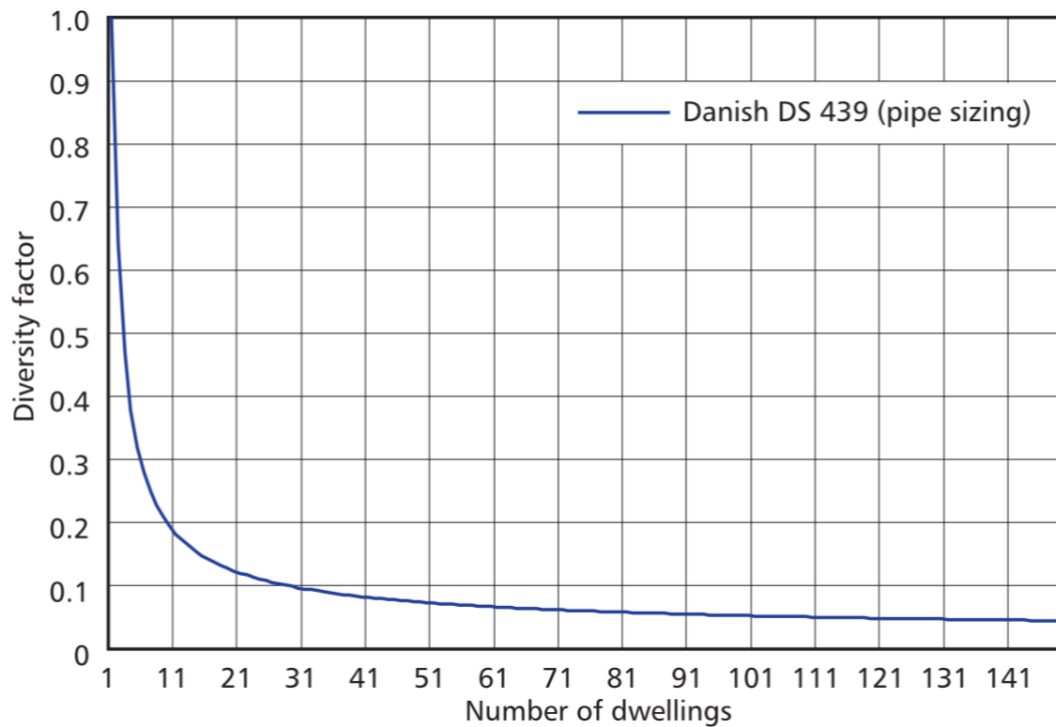


Figure 2.6: The diversity factor as taken from the DS439 (pipe sizing method) (CIBSE, 2020)

### 2.5.2.1 The Origin of the DS439 Pipe Sizing Diversity Standard

The basis for the analytical form of the sizing equation in the DS439 was built on probability arguments first proposed by Jonsson (1933). In its very earliest and most basic form, the formulation of the design flow rate,  $q$ , can be stated as a function of  $a$ ,  $b$  and  $c$ , where  $a$  is the standard flow at a given outlet,  $b$  is the mean of the other outlets, and  $c$  is the risk factor which accounts for the random variation of the flow at the other outlets.

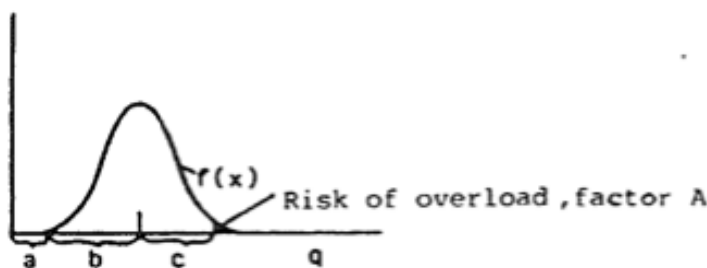


Figure 2.7:  $a$ ,  $b$ , and  $c$  are flow contributions that sum to give the design flow  $q$ . The function  $f(x)$  is the frequency function of the normal distribution (Holmberg, 1987)

The probability arguments were taken by Rydberg (1945) and used to lay the theoretical basis for the analytical formulation that came to be used in Scandinavia (Holmberg, 1987). By 1987, it had developed to be a formulation that is similar to the one used in the DS439 and in CP1.2. At the time, it was being used for dimensioning supply pipes and calculating the power requirement for hot water supplies (Holmberg, 1987). By 1997, the formulation shown in Figure 2.8 was being used for dimensioning DH substations (Wollerstrand, 1997). In

Wollerstrand (1997), it was critiqued, and a new formulation was proposed based on simulation results.

$$q = \underbrace{q_1}_a + \underbrace{\Theta(Q-q_1)}_b + \underbrace{A \sqrt{q_m \Theta} \sqrt{(Q-q_1)}}_c \quad (3.5)$$

- where  $q$  = design flow rate (l/s)
- $q_1$  = standard flow for the largest water outlet (l/s)
- $q_m$  = mean value for water flow from each outlet (l/s)
- $\Theta$  = probability that  $q_m$  is used during a peak load period
- $Q$  = sum of standard flows connected to the line (l/s)
- $A$  = factor which takes account of the number of times the design flow rate  $q$  is exceeded.  $A$  has the following values:

Uncertainty	A
0.01	2,3
0.001	3,1
0.0001	3,7

When calculating for supply pipes in dwellings, offices and similar, the following values are allowed in Sweden.

- $q_1$  = 0.4 l/s (0.2 l/s if there is no bathtub)
- $q_m$  = 0.2 l/s
- $\Theta$  = 0.015
- $A$  = 3.1, i.e.  $A\sqrt{q_m \Theta} = 0.17$

Figure 2.8: The formulation of design flow that was in use at the time (Holmberg, 1987)

Although the development of the formulation can be tracked some of the way, the evolution in its entirety that has led to the present formulation in the DS439 is unknown. Industry practitioners hold the belief that the formulation is based on empirical data from a Danish HN; however, no evidence has been found in support of this. Essentially, the extent to which empirical data has driven the evolution of the formulation seen in the DS439 in the present day, if any at all, is unknown.

### 2.5.3 DS439: Heat Exchanger Sizing Method

To further convolute matters, the DS439 has not one but two sections that have been interpreted by the UK HN industry as being useful in HN systems sizing, one being the sizing section intended for pipes (discussed in the previous section) and the other being the section

intended for sizing heat exchangers which are Sections 2.3 and 2.5 in the DS439 respectively (Dansk Standard, 2009).

An empirical curve, developed by Guru Systems using real data from UK HNs, shown below in Figure 2.9, demonstrates oversizing by comparing the real capacities to the design capacities as determined using the Heat Exchanger Sizing method in the DS439 (Dansk Standard, 2009; Open Data Institute, 2017). The real demand in the graph below is the aggregate of individual demand; however, Guru Systems has done other work to show similar findings using real bulk meter readings (meter readings taken at substations), plant and building entry points (T. Noughton, personal communication, 2022). This shows that the oversizing that is indicated by the aggregate demand is confirmed using the real demand across the distribution network (the difference between aggregate demand and real demand is clarified in Section 2.5.4). The Guru curve shown below shows that for a scheme of 100 customers, the real peak capacity would be 2.5 kW per customer, whereas the Danish curve estimates it to be 3.3 kW per customer. To produce the measured curve, Guru Systems, a HNs hardware and data-analytics company, analysed monitored operational data from a large number HNs. The curve is a result of 40 million real-time data readings from 2,000 dwellings (Open Data Institute, 2017; Smith, 2016). Moreover, the Guru Systems diversity curve considers both DHW and SH demand together, whereas the Danish curve is only for DHW demand, thus resulting in an overestimation that is even more severe (Open Data Institute, 2017; Smith, 2016).

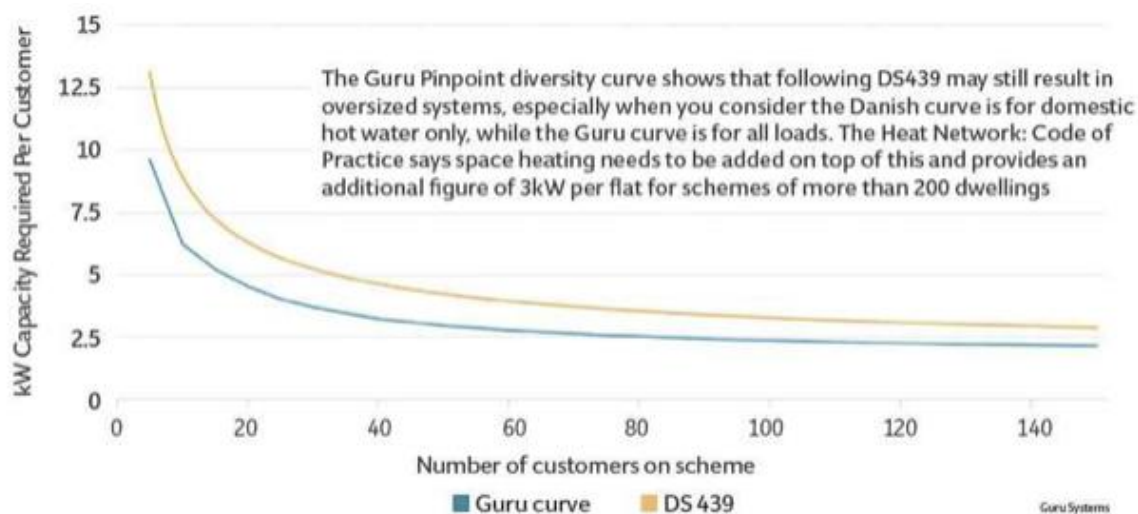


Figure 2.9: Guru diversity curve for SH and DHW demand as compared with the DS439 curve (based on the heat exchanger sizing method) for DHW demand only (Open Data Institute, 2017; Smith, 2016)

The other findings that demonstrate the potential oversizing of HNs resulting from the use of the DS439 standards (discussed in the following section) do not specify which part of the standards is being used. Thus, although it is accepted knowledge within the UK HN industry that the DS439 standards lead to pipe oversizing, limited efforts have been made to distinguish between the two relevant parts of the standard. Generally, there is no single accepted design standard being used for sizing HNs; designers will select what they deem to be suitable out of several different available standards, e.g., DS439 or SAV (as in SAV Systems (2013)). There have been accounts of designers misusing these standards, for example, by inappropriately scaling the diversity curves found in SAV Systems (2013) which are not intended to be scaled (Hanson-Graville, personal communication, January 2021).

The DS439 diversity curves were intended for use in specific settings, but there appears to be limited guidance or caveats in CP1.2 about their application in settings where conditions may vary. For example, the DHW diversity curve is intended for residential buildings, and there is no explicit guidance about determining diversity when designing networks composed of other kinds of buildings, apart from the guidance asking designers to develop their own empirical curves. This suggests that the development of empirical diversity curves for the most common kinds of HNs would be of value in the HN industry.

#### 2.5.4 DHW Technical Standards

Kõiv and Toode (2006) conducted a study that assessed how DHW consumption had evolved over the last 30 years. Importantly, the study looked at how measured values of flow rates and DHW load compare with design values in the Estonian standards and other EU standards. The methodology for calculating design DHW flow rates in the Estonian standards are the same as those in the DS439. They found that measured flow rates are considerably lower than the design flow rates as calculated by methods provided in the standards. The authors also highlight that the discrepancy between measured and design heat load grows with an increasing number of dwellings. The paper contains limited discussion about the reasons why the methods in the technical standards lead to poor estimations; however, it is implied that it's related to the drastic changes in DHW consumption behaviour and systems in the past decades, suggesting that the Estonian standards and the DS439 are outdated (Kõiv and Toode, 2006; Kõiv and Toode, 2005). Methods in a number of other technical standards (e.g., Finland and Swedish) for estimating design DHW heat load were also shown to be considerably divergent from measured values, with the Estonian standards estimating values twice as high as measured values. The increasing extent of this divergence with an increasing number of dwellings suggests that assumptions made about diversity and the way in which it is represented in the technical standards' methodologies play a key role. The authors recommend creating new methodologies for "dimensioning instantaneous heat exchangers in apartment buildings" which include factoring in and being able to accurately represent the effect of diversity for different numbers of apartments. Further investigations could also attempt bringing to light what assumptions are being made in the methods in the technical standards that lead to design values that misrepresent real values.

A similar, more recent study by Jack et al. (2017) aimed at addressing the widespread concern about the overestimation of design flow rates for residential buildings in the UK reviewed and categorised relevant technical standards according to their approaches. The study used the design estimates for a number of case study residential buildings to compare with measured values. Their key findings are shown in Figure 2.11. Resonant with what Kõiv and Toode (2006) implied, the authors state the reasons for overestimation as "the way in which appliance type, design, and usage patterns have changed significantly since the current probability-based method was first developed and adopted" (Jack et al., 2017). The DS439 was among the studied standards, and results showed that it overestimates design flow rates for buildings with less than 100 apartments and significantly overestimates otherwise. The authors conclude that an empirical approach would be the most viable; however, they also point out that with more time, resources and data availability, other approaches, such as probabilistic or stochastic, may perform better (Ilha et al., 2008; Jack et al., 2017; Oliveira et al., 2013). Tindall and Pendle (2018) conducted a similar study, again comparing the measured flow rates with the design flow rates, showing that all investigated standards overestimate the design flow, as shown in Figure 2.10.

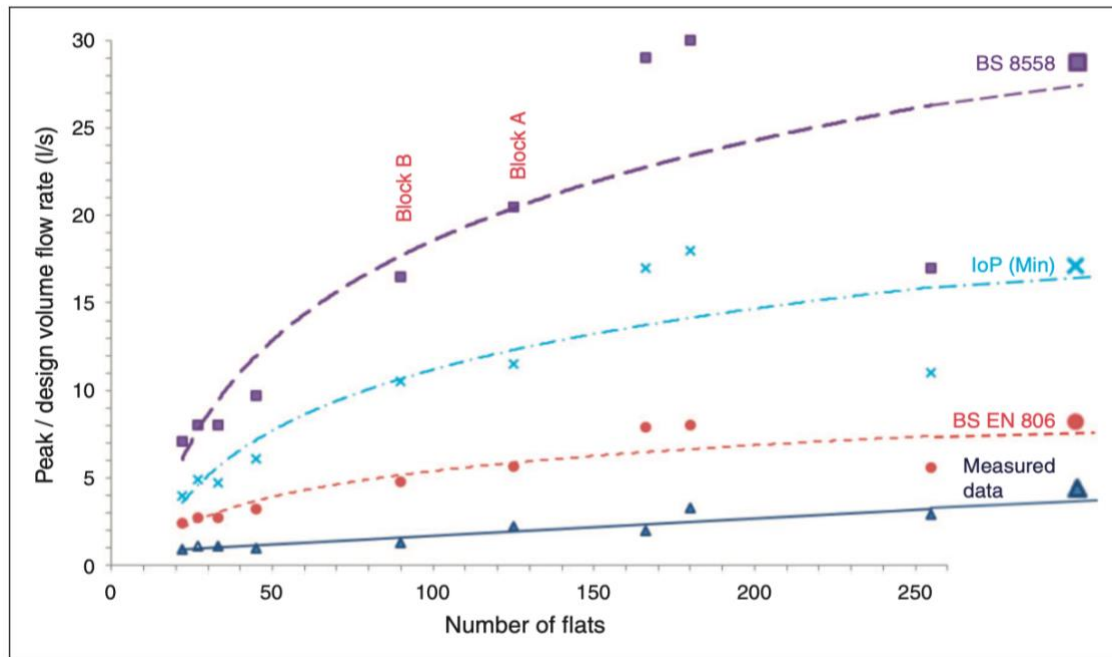


Figure 2.10: Comparison of measured flow rates and design standards (Tindall and Pendle, 2018)

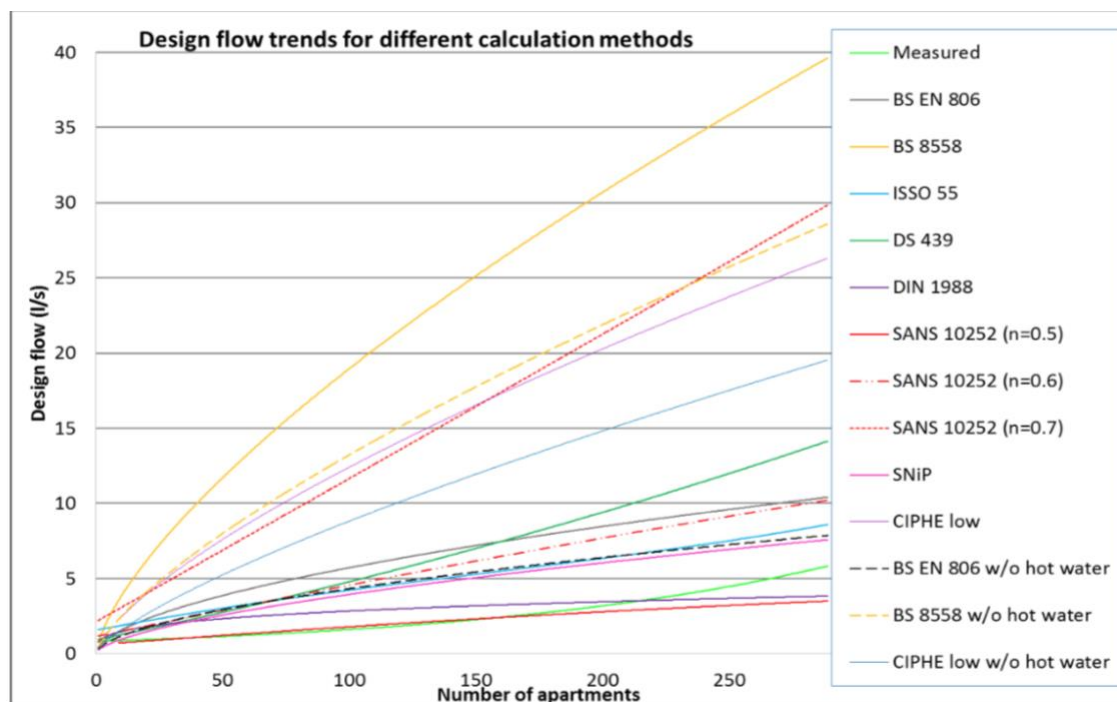


Figure 2.11: Comparison of a range of design standards relating to design flow rates (Jack et al, 2017)

Fuentes et al. (2018) is a review of studies of DHW consumption in different types of buildings with the aim of estimating DHW consumption demand by synthesising the information found. Water consumption patterns in technical standards from a range of countries are also reviewed in order to identify influencing factors (e.g., climatic conditions, building type, seasonality, and socio-economic factors). The study shows variability in design flow rates of end-use devices given in the standards. The authors posit that this is likely due to the technological differences between countries. This raises concerns about the implications of applying national standards in countries outside the country of origin.

Furthermore, it is shown that measured values of delivery temperatures are less than those commonly used in many technical standards (55°C - 60°C) (Fuentes et al., 2018). This reflects findings in other studies; the Energy Savings Trust UK conducted a field study that showed that hot water was delivered at mean temperatures of 52.9°C for boilers and 49.5°C for combi-boilers (Energy Savings Trust, 2008). The use of these temperatures can result in overestimating the energy use for DHW.

Along with several other studies, Fuentes et al. (2018) call for further research to understand and characterise DHW consumption, specifically in terms of their profiles and their variance, and to go beyond metrics that describe mean consumption (Ivanko et al., 2020; Marszal-Pomianowska et al., 2019; Weissmann et al., 2017). Research that produces characterisations of this level of resolution can be done with the use of high-frequency measured temperature and flow rate data, which gives information on profile shape at high resolution from which draw length and timings of draws can be calculated.

### 2.5.5 Real Demand vs. Aggregate Demand in the Distribution System

In this section, clarifications are made between the aggregate demand and the real demand at a given point in the distribution system. Consider a point immediately to the right of the energy centre shown in Figure 2.12, before the first junction in the distribution system. One could install sensors to measure the heat demand at this point and develop a heat demand profile using the measured data. This would be the *real* demand at that point. The aggregate demand, on the other hand, is the aggregate of the individual demands, individual demands being demands measured at each individual dwelling (denoted by the house icons in Figure 2.12). The aggregate demand is not real in the sense that it is not measured directly; however, it is used to represent the real demand at varying points along the distribution system. The real demand will be driven by several physical principles acting in the distribution system and the demand of the individual dwellings; as a first approximation, the real demand at this point is the aggregate demand from the dwellings downstream of that point, with the added effects of the time lag and longitudinal mixing that occurs in the distribution system and the addition of the heat losses that occur in the distribution system. Longitudinal mixing can be described by imagining a cold plug of water in the return pipe that occurs because of a short tap draw at an HIU. This cold plug of water, starting out at a given temperature, through its journey will reduce in temperature. This is partly because of the longitudinal mixing that occurs as the cold plug travels down the pipe. The mixing occurs because fluid closer to the surface of the pipe travels slower due to the surface friction. Over time this leads to the water being mixed longitudinally. Thus, the temperatures are also mixed longitudinally. This would lead to a flatter demand profile higher upstream compared to at the point of demand.

In most UK HN studies, concerning the sizing of the distribution system, the aggregate demand has been used in place of the real demand (Cotic, 2017; Open Data Institute, 2017; Smith, 2016; Wang et al., 2020). Limited work has been found that uses the real demand; only the work by Guru noted in the previous section (T. Noughton, personal communication, 2022). This is likely due to the prohibitive costs required to implement such a study, as it would be heavily invasive and would require the installation of heat measurement equipment in hard-to-access places in the distribution system.

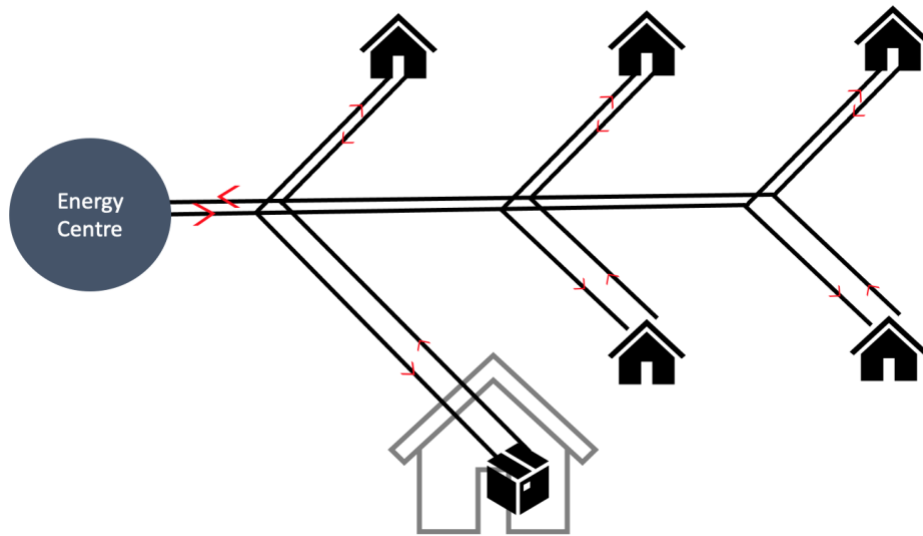


Figure 2.12: General structure of a HN

## 2.6 Pipe Sizing and Guidance

Pipe sizing is an important consideration in minimising heat losses from the distribution systems, and also minimising operational and capital costs. Pipe sizing in HNs needs to account for a number of factors to ensure high performance throughout a HN's lifetime. Several institutes contribute to the body of guidance that exists for pipe sizing, including CIPHE, CIBSE, BSRIA, and ASHRAE, each taking their own individual approaches (ASHRAE, 1997; BSRIA, 2011; CIBSE Guide B1, 2019; CIPHE, 2002). Much like the diversity standards, the pipe sizing methodologies are evolving alongside the growth of HNs in the UK. Research on pipe sizing methodologies have been underway since as early as 2004 (Bøhm and Larsen, 2005). Hlebnikov et al. (2007) published a comparison of heat losses in Danish and Estonian DHS, proposing that the optimisation of pipe diameters in Danish DHS design is required to minimise operational costs. In the UK, with the aim of providing further guidance to HN designers and reducing the risk of oversizing and resultant high heat loss, a study was conducted on optimally sizing pipes to minimise the operational energy required to deliver a given heat flow rate at peak load (Martin-Du Pan et al., 2019). However, the optimised velocities were found to be higher than those suggested in the CIBSE's CP1 which states that it is important for flow velocities through a pipe to be maintained within velocity bounds in order to ensure that pipes are kept clean and performing well (CIBSE, 2014). Flow velocities that are too low may lead to a build-up of debris and air which leads to pipe corrosion and biofouling, and velocities that are too high lead to vibration induced noise and erosion (CIBSE, 2014). The CIBSE CP1 recommends sizing pipes based on typical design velocities for each pipe size, which is an approach influenced by technical standards in the UK, such as Guide B1 (CIBSE, 2016). It is argued that although Guide B1 results in oversizing, it is appropriate for use in communal heating systems on the grounds that the extra heat loss resulting from over sizing are useful heat gains and that pumping energy required for larger pipes is less, thus saving electricity demand for pumping (Martin-Du Pan et al., 2019). When considering the merits of this argument, one must bear in mind the concerning accounts of communal space overheating and warmed cold-water temperatures in communal heating systems (Compton, 2015; Lowe, personal communication, March 11, 2024; McBride, personal communication, December 16, 2022).

The second edition of The Code of Practice (CP1.2) takes into account the set of critiques and feedback received from the industry in response to the first edition. For instance, previous guidance on pipe sizing assumed a constant volume system; however, with the advent of variable volume control and variable speed pumps, the cost of pumping energy has been reduced allowing for higher velocities and smaller pipes to be more economic. Pipe erosion effects are also reduced with variable volume control because peak velocities and flow rates occur less frequently. The up-to-date CP1.2 guidance relevant to the sizing of the primary and secondary networks is summarised in the remainder of this section. Other guidance, relevant to network design but not specifically about sizing, is summarised in the following section.

## 2.6.1 Primary Network Guidance

### 2.6.1.1 Feasibility Stage Guidance

In the guidance given in CP1.2 for the feasibility stage, the velocities outlined in the table below, which are based on Swedish guidelines, are presented for use in initial pipe sizing for the primary network (Svensk Fjärrvärme, 2007).

Table 2.4: Typical flow velocities for steel pipes to BS EN 253, for use in feasibility-stage pipe sizing of primary network (CIBSE, 2020)

Pipe size (mm)	Pipe internal diameter (mm)	Typical velocity (m/s)
DN25	29.1	0.9
DN32	37.2	0.9
DN40	43.1	1.0
DN50	54.5	1.0
DN65	70.3	1.3
DN80	82.5	1.4
DN100	107.1	1.5
DN125	132.5	1.8
DN150	160.3	2.0
DN200	210.1	2.4
DN250	263.0	2.4
DN300	312.7	2.5

Note: Values are not strict velocity limits, higher velocities are allowed.

Table 2.5: Typical flow velocities for PEX pipes to BS EN 15632 for feasibility-stage pipe sizing of primary network (CIBSE, 2020)

Pipe size (mm)	Pipe internal diameter (mm)	Typical velocity (m/s)
25	20.4	1.0
32	26.2	1.0
40	32.6	1.1
50	40.8	1.3
63	51.4	1.4
75	61.4	1.5
90	73.6	1.55
110	90.0	1.6
125	102.2	1.7
140	114.6	1.8
160	130.8	1.9

Note: Values are not strict velocity limits, higher velocities are allowed.

### 2.6.1.2 Design Stage Guidance

Pipe sizing should aim to minimise overall lifetime costs, considering pumping capital costs, capital costs, heat loss costs, and energy costs. Designers should consider a range of pipe materials and systems for each section of the network and assess the optimum based on capital costs, operational costs for the operating temperatures and pressures selected (CIBSE, 2020).

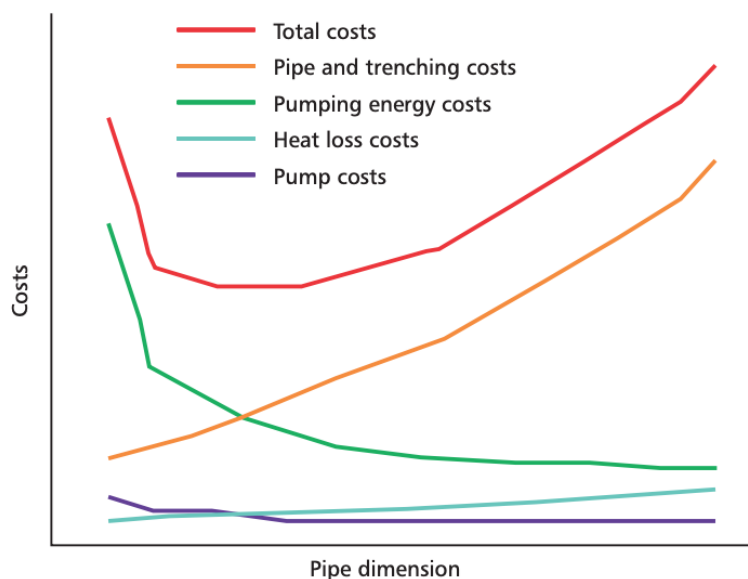


Figure 2.13: Optimisation of pipe diameter on a lifecycle costs basis (CIBSE, 2020)

### 2.6.2 Secondary Network Guidance

CIBSE Guide B1 states that pipe sizing should aim to minimise pumping energy costs; however, this approach has been critiqued for not accounting for the costs of thermal loss, which can be significant (CIBSE Guide B1, 2019; Hanson-Graville, personal communication, September 2020). The methodology used in CP1.2 Appendix D, however, instructs that the smallest pipe that can meet the flow velocity bounds should be selected, prioritising minimising thermal losses by minimising pipe surface area. CP1.2 states that the sizing of

pipes shall be based on realistic diversified demands (as discussed in Section 2.5.2), and an accurate estimation of expected flow and return temperatures expected under peak conditions (CIBSE, 2020).

To keep heat losses to a minimum, care must be taken to avoid oversizing of pipes, taking into account that peak demands in final branches occur for short periods of time. Maximum diameters for final branches are set out: 20mm for steel pipework, 22mm for copper pipework, 25mm for PEX/PB (cross linked polyethylene) pipework, calculated using assumptions of 7kW/dwelling of SH, and 45kW/dwelling for DHW.

CIBSE guidance states that all flow velocities in a HN should be a minimum of 0.5m/s, especially in HN flow pipes within a building (CIBSE Guide B1, 2019; CIBSE, 2020). This is reflected in the flow velocity limits for medium-grade steel given in CP1.2, summarised in the table below (CIBSE, 2020).

*Table 2.6: Velocity constraints for medium grade steel (CIBSE, 2020)*

Pipe size	Lower flow velocity limit (m/s)	Upper flow velocity limit (m/s)
Below and including DN50	0.5	1.5
Above DN50	0.5	3

Velocity limits are instructed for pipes in the following ways.

- The velocity of flow must be kept low enough to prevent noise and erosion; the larger the pipe, the higher this maximum velocity.
- The velocity of flow must be high enough to prevent debris and air bubble settling in pipes; the larger the pipe, the larger this minimum velocity.

Altogether, in guidance related to primary network design, the main point of focus in the approach is minimising costs, whereas for the secondary network, there is an additional focus on minimising heat losses. Guidelines for the secondary network are accordingly focussed on preventing oversizing, discussed above, and the installation of adequate levels of insulation, summarised in the following section. For both primary and secondary networks, routes should be defined such that the total length of the network is minimised.

## 2.7 Further Secondary Network Design Guidance

A separate set of guidelines is provided for the secondary network and the primary network in CP1.2. Secondary networks typically lie inside residential buildings and being in a different environment, they involve a separate set of concerns. The heat losses from the small-diameter branches, those connected directly to HIUs within dwellings, are of primary importance because the total length of these pipes can be significant relative to other parts of the distribution system in CHNs. Overheating due to heat loss from the secondary network is a risk and therefore should be carefully considered from the outset. Although, in the winter, this heat loss can be considered as useful heat gains, it does pose the risk of uncontrolled overheating in the summer and increases costs to the consumer. There are several reasons why heat loss from a secondary network may be higher than an acceptable level as identified in CP1.2:

- Oversized pipes
- Insulation not specified over valves, fitting, and pipe supports
- Insulation thickness insufficient
- HIUs operating in keep-warm modes (keeping flow rates and temperatures high)
- Fixed bypasses that lead to high return temperatures under part-load
- Length of network too large (potentially due to the use of horizontal runs in network design, illustrated in Figure 2.14)

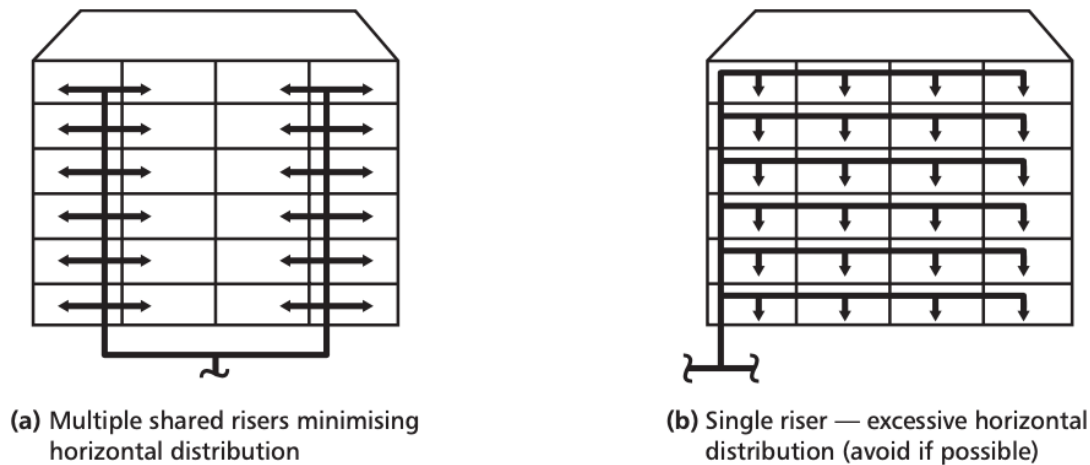


Figure 2.14: Illustration of the benefit of shared risers over horizontal runs for a typical flat layout (CIBSE, 2020)

Minimum insulation thicknesses described in Table 2.7 below are dictated for use for all heating distribution pipes in the secondary network where practical. These thicknesses are greater than typical for other operations because the pipework in the secondary network is in continuous operation.

Table 2.7: Minimum insulation thickness to be used in the secondary network (CIBSE, 2020)

Pipe diameter (steel) (mm)	Phenolic foam (internal space) (mm)	Phenolic foam (external space) (mm)	Mineral fibre (internal space) (mm)	Mineral fibre (external space) (mm)
15	50	50	50	50
20	50	50	50	50
25	50	50	50	50
32	50	50	50	50
40	50	50	50	50
50	50	50	60	60
65	50	50	60	60
80	50	50	60	60

Note: Insulation thicknesses are calculated assuming a conductivity (K-factor or lambda) of 0.035 W/m·K for mineral fibre and 0.025 W/m·K for phenolic foam insulation with a low surface emissivity of 0.05. Hence, for pipe diameters of 32 mm and smaller, the heat loss will be lower for the phenolic foam insulation.

The total annual heat losses from the secondary system within the buildings are to be calculated and divided by the number of dwellings. This value is to be lower than 876kWh/dwelling equivalent to 2.4kWh/dwelling/day. CP1.2 further provides a worked example for pipe sizing for a secondary network, where velocity constraints for each pipe diameter are sourced from the CIBSE Heating Guide B1 (CIBSE, 2016).

## 2.8 Thermal Energy Storage and Diversity

Borri et al. (2021) conducted a thorough review of the subject of thermal energy storage in research. The review showed that publications on thermal energy storage as applied to districts started to rise sharply around the year 2014, and publications were mainly from Canada, Europe (most being from Italy, Germany, and Sweden), the US, and China. The results further showed that thermal energy storage in districts was usually studied at the system level, i.e. to understand incorporation into the wider heating system, rather than being studied to understand the impact of their material composition for example. Research at the system level fell into two main categories: use of solar energy through seasonal thermal energy storage (TES) and cogeneration, and management of energy in districts through demand-side management and artificial intelligence. The authors highlight the abundance of studies based on modelling, artificial intelligence, and numerical analyses and the lack of economic, techno-economic, and environmental studies.

Many studies investigate the impact of storage in HNs (Guelpa et al., 2019; Hennessy et al., 2018; Ma et al., 2020; Romanchenko et al., 2018; Vandermeulen et al., 2018). Using both models and real data from case studies, studies have investigated improving flexibility, system efficiency, cost implications, and environmental impacts in HNs through storage. Some studies investigate buildings integrated thermal storage, or network as storage, and others compare the two (Chen et al., 2014; Guelpa et al., 2017, 2021; Luc et al., 2020; Turski et al., 2018). Studies also focus on different storage materials as well as different periods of storage (Faraj et al., 2020; Rosato et al., 2020). Huang et al. (2020) and others have looked at operational strategies. Cai et al. (2018) studied demand-side management in order to manage the congestion and improve the efficiency of an urban network and evaluated the impact on peak reduction. Other kinds of studies focus on future HNs, focussing on the integration of renewable energy sources and the use of storage (Abokersh et al., 2020; Foteinaki et al., 2020; Kensby et al., 2017; Rämä et al., 2018). The above studies consider the impact of storage on the demand of a HN, but none have been found that focus on the nexus between storage and diversity and how their interaction impacts network demand.

### 2.8.1 Thermal Energy Storage in HNs

Thermal energy storage is likely to be a key feature of future energy systems which are expected to be cleaner and to integrate renewables more readily (Abokersh et al., 2020; CCC, 2020; Luc et al., 2020; Lund et al., 2018). Thermal energy storage incorporation benefits energy systems in a number of ways. Storing heat at times when demand is low and deploying the stored heat when demand is high has the effect of levelling the load and reducing the peak demands that need to be met by the heat generators (Gadd et al., 2013a; Gadd et al., 2013b; Guelpa et al., 2019; Pakere et al., 2016). Load levelling enables heat generators to operate for longer hours to meet the baseload, which reduces fuel consumption and overall production costs because such conditions allow the heat generators to perform at their most efficient mode (Borri et al., 2021; Guelpa et al., 2019). Reducing the peak demand can also remove the need for expensive peak power which reduces investment costs as well as operational costs (CIBSE, 2020). Storage can also enable generator starts and stops to be minimised (CIBSE, 2020). Furthermore, storage can act as a buffer to support intermittent supply from renewable sources and to increase the overall resilience of the supply system against breakdowns (Pakere et al., 2016). Thermal storage also has drawbacks that must be considered when designing it into any system, the primary being the heat losses which are dependent on the surface area and temperature of the store (CIBSE, 2020). Other

considerations, such as pasteurisation requirements that protect against Legionella, should also be considered (CIBSE, 2020). Depending on the location of the storage in the network, be it at the plant, midway in the distribution system, or in the dwellings, there will be a different set of benefits and drawbacks.

### 2.8.2 The Impact of Distributed Thermal Energy Storage on HNs

Storage in HNs can be centralised, meaning connected directly to or close to the main heat generators, or distributed, where stores can be installed midway between the heat plant and the consumer, or installed directly in the heating systems in the consumer buildings (Jebamalai et al., 2020; Schuchardt, 2016)<sup>2</sup>. Installing building-level storage has the effect of levelling the load profile of the building, and therefore reducing the peak demand in the system further upstream of the dwellings. Designing for reduced individual peak load allows the distribution pipes to be sized smaller which is beneficial because of lower heat losses that result from reduced pipe surface area (Hennessy et al., 2018). Having said this, the diversity effect in a network composed of dwellings with storage has not yet been characterised. This is to say that the effect that levelled individual loads, as compared to non-levelled individual loads, has on the aggregate peak demand at all points in the distribution system upstream of more than one dwelling is yet unknown. This means that although pipes directly connected to a consumer can be sized smaller, whether this can be said for pipes elsewhere has not been explicitly investigated. Furthermore, the aggregate peak demand of all dwellings on the network being unknown means that the effect on the required peak plant capacity is also unknown.

The case for building-level storage is highly contested within the industry where practitioners hold contrasting opinions based on their individual experiences. This is reflected in the guidance information; although CP1.2 mentions a few points about why distributed storage would be beneficial, the information is limited and there is no recognition of the uncertainty around the effect of distributed storage on a network (CIBSE, 2020). The effect that distributed storage would have on the diversity and aggregate demand of a network is yet to be the subject of a formal study. Such a study could produce results that contribute to building the case for, or against, distributed storage and ultimately feed into the relevant parts of the guidance and standards information.

### 2.8.3 Domestic Demand Storage

Dwelling-level storage is commonly provided by hot water tanks; however, the advent of combi-boilers reduced the presence of hot water tanks in UK dwellings by enabling instantaneous hot water delivery (Guelpa et al., 2019). Despite their reducing popularity, hot water tanks or any other form of domestic storage is a viable option worth strongly considering when designing HNs because of its impact on pipe sizing and heat losses. The potential for the incorporation of domestic storage raises questions about the impact that it could have on HN design and performance. Huang et al. (2020) is a study on the operation of DHW tanks and its impact on network return temperatures that used real DHW load profiles and is one of the few studies that investigate the impact of domestic storage in peak reduction. The work in this thesis will focus on the impact of DHW storage.

---

<sup>2</sup> Note that the term building can apply to both a residential building (e.g., an apartment block) and a dwelling (e.g., an apartment), and similarly the term individual load can refer to both the demand of a residential building or to the demand of a single dwelling.

#### 2.8.4 Instantaneous DHW Delivery vs. Stored DHW

The benefits of storage are that it can reduce peak demands, allows a buffer against short term interruptions, enables intermittent heat supply and allows for scheduling that can be useful, for example, when the heat is generated using heat pumps. The reduction in peak demands comes with the added benefits of smaller service pipe sizes as well as smaller pipes further upstream (CIBSE, 2020; Gadd et al., 2013a; Hennessy et al., 2018). On the other hand, storage has downsides such as standing losses from the stores which add to the overall demand, temperature restrictions that need to account for Legionella risk, potentially higher return temperatures where an indirect coil is used in the hot water cylinder and space requirements for the stores (CIBSE, 2020; Hennessy et al., 2018). With instantaneous delivery, the benefits are that there is no extra space requirement, no limit to heat supply, lower thermal loss as there is no store and lower return temperatures are more likely to be achieved (CIBSE, 2020; Huang et al., 2020). The downsides are that higher flow rates are necessary, encourages the use of ‘keep hot’ function in network segments near the dwellings which can add to the thermal losses and there is no buffer in the case of short interruptions to supply.

A key benefit of stored DHW is the reduction in peak demands, and although the impact on service pipes is clear, the impact on pipes further upstream is less defined. The key concept that comes into play is the diversity effect. Storage acts to flatten the demand, i.e., a reduced peak but longer acting demand. The effect of diversity is dependent on both the peak and the coincidence of the demands of dwellings. The coincidence describes how much dwelling demands overlap. Thus, storage introduces two effects that compete against each other through the diversity as they act on the aggregate peaks; the reduction in individual peak demands acts to reduce the aggregate peak demand but the increase in coincidence due to longer demands acts to reduce the diversity and therefore reduce the aggregate peak demand. There is a dearth of studies that look to directly compare stored DHW and instantaneous DHW supply and what the role of diversity plays in this as well as how it impacts HN demand and design. This work aims to address this gap.

### 2.9 Summary and Research Gaps

The literature review was introduced by outlining the role of HNs in the decarbonisation of the UK energy system and the HN market in Europe and the UK, highlighting the ability of HNs to enable the use of low-carbon heat sources, especially in population-dense areas. The introduction section then went on to describe the requirement of robust technical standards in developing high-performing HNs whilst bringing forth the issue of uncertainty around distribution system sizing methods that mitigate this aim. The widespread concern in the HN industry on this issue has hitherto not been addressed formally in academia or within industry, and if left overlooked, may have a significant detrimental impact on the growing UK HNs industry. The following section of the literature review described the key components of a HN and the ways in which they are structured together. The third section delved into energy demand, detailing the drivers of SH and DHW demand on a dwelling level and at a HN level. The focus of the fourth section are pertinent findings from the body of literature investigating diversity of demand and its drivers. Additionally, diversity in electricity networks and diversity related metrics are discussed. The concluding subsections of this section provide arguments for the need for empirical diversity studies and discusses findings on the impact of sampling time on aggregate and individual demand. In the fifth

section, widely used technical design guidance is laid out, along with the likely origins of the mathematical formulation of the sizing methods therein. The section goes into detail on existing technical guidance relating to DHW and HN distribution pipe sizing. The sixth section of the literature review discusses heat storage in HNs, highlighting the lack of consideration of the role of diversity when explicating the relationship between storage, demand, and HN sizing.

Overall, the literature review discussed the existing discrepancy between real DHW peak demands and those estimated using accepted technical standards and the resulting impact this has on the cost and performance of HNs. The lack of understanding about what is driving the discrepancy between real and estimated values and the absence of alternative guidance creates uncertainty for HN designers, which will be problematic for the performance of future HNs, especially at this critical juncture where rapid HN growth is expected. The overestimation of peak DHW demands may be caused by the invalid mathematical formulation of diversity and/or the overestimation of individual peak demands used in the estimation. To date, there has only been a handful of studies investigating the extent and impact of oversizing in HNs and the role that diversity plays in this. Of the studies that do, none have used dwellings from a real HN, and therefore may have missed crucial findings that could inform the design of future HNs. Pertinent to the issue of oversizing, is the inclusion of domestic storage in a HN. As the energy system transitions, many anticipate storage becoming a key component because of the increased need for flexibility to integrate an intermittent renewable supply. This transition will be reflected in HNs too, and the prospect of this has been the subject of many studies, including studies about the case for different storage configurations and identifying the unique set of benefits and drawbacks that each bring to a network. However, the existing studies fail to consider the impact that introducing storage would have on the demand diversity and distribution system sizing, and therefore overlook a key consideration affecting the cost and performance of future HNs.

The research gaps that have been made evident are summarised in the following points.

- Although there are accounts from the UK HN industry of the sizing methods in the DS439 leading to HN oversizing and a lack of understanding of the origins and therefore applicability of the methods, its use continues, potentially leading to the development of costly oversized HNs (Open Data Institute, 2017; Smith, 2016; Personal communication, T. Noughton, May 2022).
- There is further uncertainty resulting from a failure in the literature and in industry reports to acknowledge the two different sizing methods in the DS439 that have both been either used or recommended for use in HN design (CIBSE, 2020).
- Although there is an impetus towards the incorporation of heat storage in future HNs, there is no research that investigates the impact that storage has on demand diversity, and the combined impact of these on HN demand and therefore its sizing (Abokersh et al., 2020; CCC, 2020; Luc et al., 2020; Lund et al., 2018).
- There is a dearth of studies investigating demand diversity using real demand, and even fewer using real demand data from dwellings on a real HN (Cosic, 2017; Wang et al., 2020).
- There is a lack of empirical studies on the impact that sampling time has on individual and aggregate demand and therefore on HN sizing despite the clear impact of sampling time on peak demands (Cosic, 2017).

### 3 Research Questions and Methodology

A set of research questions have been formed to address the research gaps identified in the literature review that can have a significant impact on HN development. They are presented in this chapter, along with the objectives that need to be achieved in order to produce findings that can appropriately answer each of the questions. The sections within this chapter describe the methods used in achieving the objectives.

#### 3.1 Research Aims, Questions and Objectives

The aim of this thesis is to inform the development of HN design in the UK by characterising the real diversity effect in UK HNs and assessing the impact that DHW storage has on the demand of a network, and the role that diversity plays therein. To achieve the stated aim, research questions have been formed, and are each given with a corresponding set of objectives below.

- *What is the real diversity effect in UK HNs?*
  - Estimate the individual demand profiles of dwellings on a real HN using measured data.
  - Analyse the impact that aggregation, over number of dwellings and over time, has on the demand.
- *What is the impact of DHW TES on HN demand and design in the presence of diversity?*
  - Estimate the residual DHW demands that would result from DHW TES installation for the sample of dwellings.
  - Assess the impact that DHW TES has on the aggregate demand.
  - Assess the impact that DHW TES has on the distribution system pipe sizing and the resultant impact on thermal loss.

#### 3.2 Methodology

The results of studies that are based on real data capture idiosyncratic phenomena that models, by their nature, are incapable of capturing (Flyvbjerg, 2006). However, there are instances where obtaining the real data required is an unreasonable pursuit given the resource and time constraints. The first of the research questions outlined in the previous section needs to be addressed using measured data; however, answering the second research question requires modelling because it would be too costly and resource-intensive to obtain data concerning the before and after of a real intervention, which in this case would be the installation of DHW TES in a large group of dwellings on a HN. The proposed study is therefore based on the quantitative analysis of real data together with models using the real data. The work in this thesis can be considered to be, in parts, a case study and a modelling study. A typical case study would take a handful of cases and investigate them in detail. This study is similar to a typical case study in that the data used is from dwellings on a single HN but is limited to only one HN, and thus the resultant findings may only provide information about this particular HN and should be generalised with care. Given that case studies where multiple cases are considered are critiqued for their lack of generalisability, it is only natural that this is the case to an even greater extent for a case study of just one case (Flyvbjerg,

2006). What is of value, however, is that the demand data is from dwellings on a real HN, even if it is just from one. This is because, to date, demand studies have only used demand data from a random sample of dwellings which are not on a HN.

### 3.3 Overview of Methods

The first research question concerns the characterisation of the real diversity effect in HN demand. In achieving the first objective, DHW demand profiles and total demand profiles will be estimated for each individual dwelling in the sample. The demand is then analysed with respect to varying levels of aggregation and varying sampling times.

The case for DHW storage represents is contested in the UK HN industry because of the unknown impact on wider network performance and costs. Thus, simulating DHW storage can provide valuable and immediately applicable insights. As such, the second research question pertains to the impact that DHW storage has on pipe sizing and thermal loss in the presence of diversity. Additionally, as DHW demand peaks are substantially greater than SH demand peaks, it stands to have the greatest impact on network sizing. A key part of the method here is modelling domestic thermal stores for DHW. One of the models will be a stratified cylindrical hot water tank, where energy and mass transfers for each layer are considered, and the other a mixed heat store model, both of which are described in full in Section 3.6.2. The models are used to produce residual demand profiles under different storage scenarios outlined in Section 3.6.1. The approach taken in selecting the scenarios is based on the requirement that the storage scenarios that represent what is feasible in existing HNs or what is likely in near-future HNs is balanced against the requirement to explore maximally and minimally diverse demands. To evaluate the thermal losses from the distribution system, a distribution system is modelled, with pipe sizes being determined individually for each storage scenario. The distribution system that is modelled is described in full in Section 3.7.

Finally, Sections 3.4 and 3.8 describe the case study HN from which data was collected, and the limitations of the methods and applicability of the results to the wider UK HN population respectively.

#### 3.3.1 Research Design

The research design in this work is atypical because it was developed and iterated in response to the data as it was collected. The novel nature of the data meant that there was a process of discovery and grappling that had to take place for the author to get familiar with the data. This is different to the usual process of the researcher outlining their data needs and implementing data collection to meet those needs. The methods developed in tandem with the data discovery process and thus informed each other (the processes involved are outlined in Section 4.10, Section 4.13 and Section 5.2), underlined by the aim which was to address the issue of oversizing in UK HNs. Pertinent to this aim were the concepts of diversity and demand, the behaviour of which can be illuminated by investigating how demand evolves with aggregation over time and aggregation over number of dwellings. Objectives were adapted as blockers were encountered through the data collection process. One such instance was the failure to determine SH demand using the available data but instead being able to use total demand data to achieve the same aims. There is value in focussing on the behaviour and effects of DHW demand alone in the question of storage because DHW storage is already accepted in UK households.

Equally important was the concept of storage. Storage is key because it would fundamentally change the diversity effect by changing the shape of the demand resulting in changed aggregate peaks and a requirement to reconsider the design of the distribution system. The storage component of the thesis necessitated the construction of models to estimate residual demands as they were more fitting to the resource constraints than would be a physical intervention in a real case study for example. This part of the work was largely planned out before execution but nevertheless also had some real-time iteration. The storage related methods are explained in detail in Section 3.6. The aim was to determine the boundaries of all possible demand that would result from the installation of DHW TES in the dwellings.

The analysis that followed the data collection, real demand estimation and residual demand estimation was conducted in a free and exploratory manner with the aim of informing the issue of distribution system oversizing and related aspects. The fundamentally exploratory nature of the work is a response to the dearth of relevant studies, which meant that directions for further study were ill-defined, and the novelty of the high-frequency data and a lack of accompanying tried and tested methods for analysing such data.

### 3.4 Case Study HN

The case study HN on which this research is based is a CHN with ~150 dwellings<sup>3</sup> located in the Southeast of England, which was fully developed by 2018. Heat is generated in a series of boilers located in the basement of the building and is delivered through a distribution system with two main branches that feed one half of the dwellings in the building. A small-scale HN is one where the heat source is less than a few hundred meters away from the consumers. In a medium-scale HN the consumers would be 200-300 metres away, and in a large-scale HN, the consumers would be > 300 meters away. The case study HN used in this work has a total network length of ~450 m, and the consumers and plant are in a single building, and thus the case study HN would likely be considered a small-scale HN. The design occupancy of 84 of the dwellings is 2 occupants (1 bed), 52 of the dwellings have a design occupancy of 4 occupants (2 bed), 6 dwellings have an occupancy of 6 people (3 bed) and the final 5 have an occupancy of 3 occupants (2 bed), as summarised in Figure 3.1. The floor area of the dwellings has a range of 40 m<sup>2</sup> to 129 m<sup>2</sup>, with a large proportion of dwellings having a floor area of 40-49 m<sup>2</sup>.

---

<sup>3</sup> To protect the anonymity of the case study HN and its occupants the exact number of dwellings is omitted.

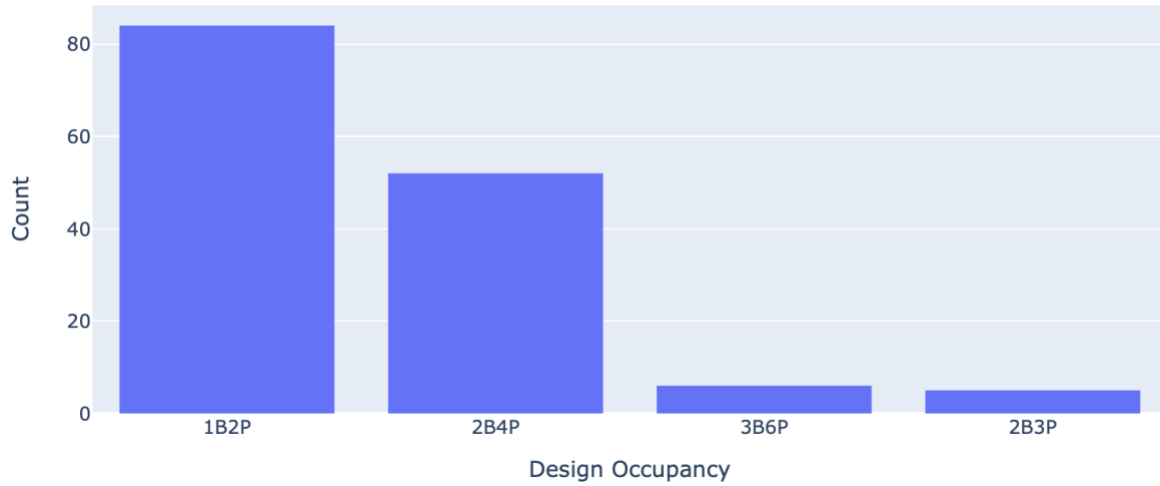


Figure 3.1: The design occupancy (P) and number of bedrooms (B) for the sample of HIUs

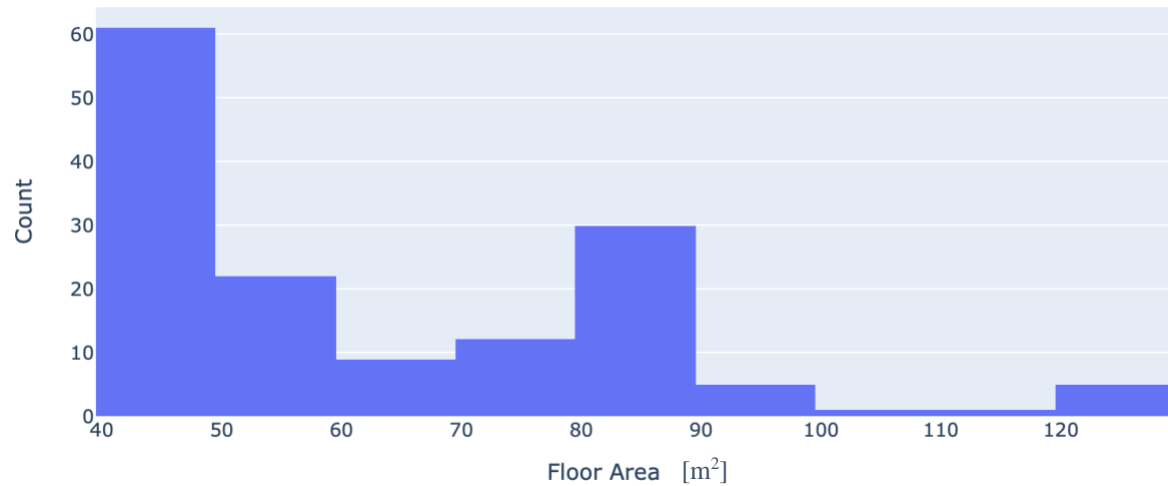


Figure 3.2: The floor area of dwellings in the case study HN

### 3.5 Demand Aggregation

In order to understand how diversity impacts demand, it is important to understand how demand behaves at increasing levels of aggregation over dwellings, as well as how resampling, meaning averaging over larger time intervals, comes into play at each level. This section specifies how the demand distributions were determined for varying levels of aggregation over the number of dwellings and over time.

There are two kinds of aggregation that can be considered: aggregation over the number of dwellings and aggregation over time. When aggregating over the number of dwellings, demand profiles were created for  $k = 1, 5, 10, 35$ , and 60 dwellings. When creating a profile for any level of  $k$ , there are many unique combinations of  $k$  dwellings that can be selected from the total pool of  $N$  dwellings. The total number of unique combinations,  $T$ , for a  $k$  sized pool of  $N$  dwellings is given by the equation below.

$$T = \frac{N!}{k!(N-k)!}$$

(3-1)

Equation (3-1) above shows that T can get extremely large. For example, where N = 81, k = 5 results in T = 2.56e+7 and k = 35 results in T = 1.02e+23. The number of unique combinations of individual profiles for a given k and N used to generate aggregate profiles had to therefore be limited to 1,000 to work within the limits of the computational power that was available. It is important to note that where k is close to N in value, the resulting aggregate profiles are likely to be made up of more of the same individual profiles. The implications of this will be outlined in the results chapters. The second kind of aggregation, aggregation over time, was considered in the following way. The intention is that the raw demand profiles, measured at some sampling time, are averaged over larger time intervals such that the time elapsed between consecutive data points increases. Sampling times were 1, 5, 10, 30 seconds and 1, 5, 10, and 30 minutes, and 1 hour for DHW demand. For the total demand, sampling times below 5 minutes could not be evaluated because the sampling time of the raw data was 5 minutes. Table 3.1 below summarises the total number of profiles created at each sampling time and for each level of aggregation over dwellings.

*Table 3.1: The total number of demand profiles used in evaluating the aggregate distributions for varying levels of aggregation and sampling times*

<b>k</b>	<b>Sampling Times</b>								
	<b>1s</b>	<b>5s</b>	<b>10s</b>	<b>30s</b>	<b>1m</b>	<b>5m</b>	<b>10m</b>	<b>30m</b>	<b>1hr</b>
<b>1</b>	115	115	115	115	115	115	115	115	115
<b>5</b>	1000	1000	1000	1000	1000	1000	1000	1000	1000
<b>10</b>	1000	1000	1000	1000	1000	1000	1000	1000	1000
<b>35</b>	1000	1000	1000	1000	1000	1000	1000	1000	1000
<b>60</b>	1000	1000	1000	1000	1000	1000	1000	1000	1000

Although profiles for all k are generally referred to as aggregate profiles, at k = 1 the profiles are individual profiles. Similarly, all time intervals will be referred to as sampling times despite the distinction between the time intervals at which raw data was measured and the larger time intervals over which the data was averaged. If the latter needs referring to specifically, the term ‘resampling’ will be used.

### 3.6 Heat Store Model

Two heat store models were built to produce the demand profiles of a dwelling with a DHW store installed, i.e., the residual demands, using the real DHW demand. The store model is required to produce residuals for a large number of dwellings with relatively fast computational times such that the time constraints of the project could be met. Coupled with this is the requirement that the outputs of the model give a comprehensive picture of the real behaviour that could be expected. Given these requirements, two models were developed: a mixed thermal store and a stratified thermal store, which reflect two ideal thermal store behaviours and are therefore relatively straightforward to model. A real heat store would not be perfectly stratified, nor would it be perfectly mixed, but would be somewhere in between the two states. The real behaviour of a thermal store is therefore proposed to lie somewhere in between the set of results from the models.

This section describes the physical principles underpinning each model, the logic with which they are controlled, and the variables that they handle. Both models are used to produce demand profiles for all dwellings according to two HN-wide control strategies in which charging times are defined: the ‘Spaced Charging’ (SC) scenario and the ‘Coincident Charging’ (CC) scenario. These scenarios are outlined further in the section below.

### 3.6.1 Storage Scenarios

The main objective of introducing domestic storage here is to reduce the overall demand of a HN by producing a reduction in distribution system losses that outweighs the standing losses introduced by the stores. The distribution system losses are dependent on pipe sizing, which itself is dependent on the aggregate peak demand, which in turn is dependent on the diversity of the demand of the individual dwellings. Introducing domestic storage will reduce the diversity across the dwelling demand to varying degrees, depending on how the storage is implemented.

The objectives of the second research question are designed to outline the bounding limits of the impact that storage can have on network demand. Higher diversity in individual demand profiles will lead to lower aggregate peak demands. Knowing this, one can then assert that taking the diversity to its minimum (or maximum) is likely to produce a maximum (or minimum) in the aggregate peak. Thus, implementing storage in such a way that diversity is maintained as high as possible will lead to the lowest aggregate peak demands, and vice versa. As a result, the full scope of the impact of storage on demand can be drawn out by considering two storage scenarios; one designed to produce residual demands, in which diversity is at a minimum, and the other where it is at a maximum. The third scenario that will be considered is the case study as it is, with no storage. The sizing of the distribution system in this scenario will therefore be based on the real, unbuffered demand of the case study. Results may show that the aggregate peak demands that result from the storage scenarios are not lower than they are for the real demand scenario, in which case the conclusion that storage does not reduce overall HN demand is likely.

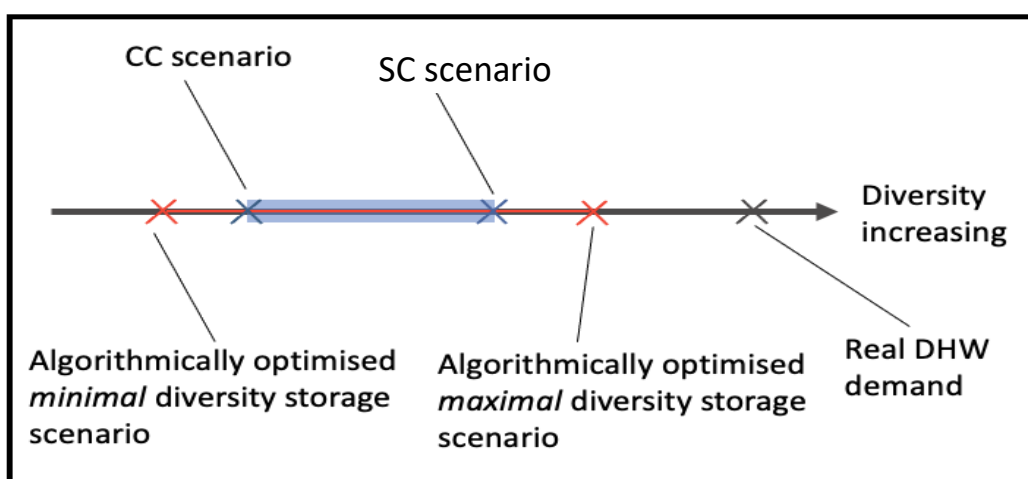


Figure 3.3: Conceptual diagram of the differences in diversity in the real DHW demand, the practicable storage scenarios, and the algorithmically optimised scenarios

Storage control can be optimised algorithmically to deliver maximal and minimal diversity in the scenarios. However, it is significantly computationally demanding and, more importantly,

unnecessary to scope out the impact to this extreme because it is very unlikely to be physically realisable for the reasons given below.

When it comes to control of domestic hot water tanks (DHWT) in occupant dwellings, one must consider the level of control that an occupant would be comfortable with relinquishing to HN operators. It is distinguished from the case of storage within the distribution system or in the plant room, both of which are domains within which occupants do not typically assume or desire control, leaving the operator able to implement control strategies with more freedom. The potential for gaining control of DHWTs in a HN is limited because the occupants are unlikely to value the potential benefits afforded to them above the ability to have full control of an appliance in their home (Cao, 2014). This is, of course, assuming that they understand the proposition being made and that they trust the operators in the first place. The scenario of SC, which seeks to maximise diversity, has therefore been designed based on the following presumptions.

- HN operators are likely only to leverage minimal, if any, control within the occupant's domain.
- If occupants relinquish control, it would likely be on the condition that storage control resembles a control regime that they are likely to implement themselves, and that all dwellings in the network are subject to similar control regimes such that treatment of all occupants is fair.

The SC scenario, which has been designed to balance the above prerequisites with the objective of maximising diversity, dictates that charging times for the dwellings are spread evenly across the duration of the day. The SC scenario groups the dwellings in the HN and assigns each group two blocks of time within which they can charge their DHW stores in order to spread the charging times equally across all hours of the day. This is to say that dwellings in group A can charge their stores for a given window of time at 12 p.m. and 12 a.m. every day, group B can do so at 2 p.m. and 2 a.m. and so on. The CC scenario is where all dwellings charge their stores within the same time blocks during the day, and thus, result in minimal demand diversity. The scenarios have been summarised in the table below.

In summary, two storage scenarios were modelled to outline the bounding limits of the impact of storage on demand of what is physically realisable and practicably implementable by a HN operator given the socio-technical constraints that are likely to exist in HNs with domestic storage. Together the two scenarios will be used to map out the impact that storage can have on the demand and design of a HN and compared to the scenario where there is no storage. In addition to the two scenarios in which storage is present, two other scenarios, without storage, are considered. One of which is the 'Real Design' scenario where the design of the real case study HN as it exists is used. The second is the 'Real Demand' scenario where the distribution system is sized using the real demand of the case study HN. All four scenarios are outlined in Table 3.2 below.

*Table 3.2: Summary of the modelled storage scenarios*

Scenario	Description	Charging Time-Block Length	Total Daily Charging Windows	Daily Charging Times
----------	-------------	----------------------------	------------------------------	----------------------

CC (Coincident charging)	Where all dwellings charge their stores together	2 hours	Twice daily	All dwellings: 5-7 a.m., 3-5 p.m.
SC (Spaced charging)	Where the dwellings stagger the times in which they charge their stores	2 hours	Twice daily	Dwellings grouped into 6 groups of equal size. Group 1: 12-2 a.m., 12-2 p.m. Group 2: 2-4 a.m., 2-4 p.m. Group 3: 4-6 a.m., 4-6 p.m. Group 4: 6-8 a.m., 6-8 p.m. Group 5: 8-10 a.m., 8-10 p.m. Group 6: 10-12 a.m., 10-12 p.m.
Real Design	Where the design of the real case study HN's distribution system is used	No thermal stores present	-	-
Real Demand	Where the distribution system is sized to the real demand of the case study HN	No thermal stores present	-	-

### 3.6.2 TES Model Principles

DHWT sizes were obtained individually for each dwelling and presented in Figure 3.4 below. The capacity of an individual store is sized to accommodate the maximum daily demand present for the dwelling in the monitored period. To elaborate, the total demand of each day in the monitored period is calculated for a given dwelling and the maximum of these is taken to size the store. If dwelling B has a larger maximum daily demand than dwelling A, dwelling B will have a larger store. The dimensions of the heat store for an individual dwelling are calculated on the basis that the store is of a cylindrical shape with equal height and diameter (Figure 3.5). Stores are designed as such to keep surface area to a minimum and reduce heat losses. In reality, DHW storage tanks are sized based on rules of thumb relating to, typically, the number of occupants in a home and tend to have longer heights than diameters. The Hot Water Association recommends an allocation of between 35 L (0.035 m<sup>3</sup>) and 45 L (0.045 m<sup>3</sup>) per occupant with some high demand consumption being up to 70 L per occupant. In the case study's sample of dwellings there is between 2 and 6 occupants in each dwelling. This would equate to a range of store sizes of between 0.07 m<sup>3</sup> and 0.42 m<sup>3</sup> if high demand consumption occupants are included (Hot Water Association, no date). The figure below gives a histogram of all store volumes obtained. Store volumes ranged from 0.05 m<sup>3</sup> to just over 1.0 m<sup>3</sup>, however, many of the store volumes were between 0.05 m<sup>3</sup> and 0.5 m<sup>3</sup>. Although the store size based on daily demand cannot be compared to the recommended sizing based on occupancy because demand data is not linked to occupancy data individually,

the range of demand-based store sizes is here shown to be similar to the range of recommended store sizing for the occupancies in the sample.

The stores are based on external heat exchangers rather than indirect coils for simplicity of modelling. The charging power of the store is dependent on the type of model used. In the mixed store, the charging power is a function of varying temperature difference whereas in the stratified model, by its nature, the charging power will be a fixed constant. This means that the stratified store will tend to charge up quicker and stay at a full or close-to-full state for longer than the mixed store. A store may not use up the entire 2 hour charging window to charge up to full depending on the type of model it is and how full the store was at the start of the charging window. The stratified and mixed stores are explained in more detail in the coming sections.

Generally, the larger the store and the longer the allowed heat up time, the lower the individual peaks can be. However, there is a limit to the sizing benefits this effect brings, especially further upstream of the dwellings, because of the increase in coincidence of the individual demands. As demands aggregate the now long and low individual demands will start to overlap each other (more than short, spikey demands would) which means that the aggregate demands would ‘stack up’ more quickly, reducing the diversity and negating the aggregate peak reduction. Note that although this work focusses on certain technical aspects of storage, practitioners would typically need to consider other factors such as cost, demands on space and occupant preferences when designing storage within a HN.

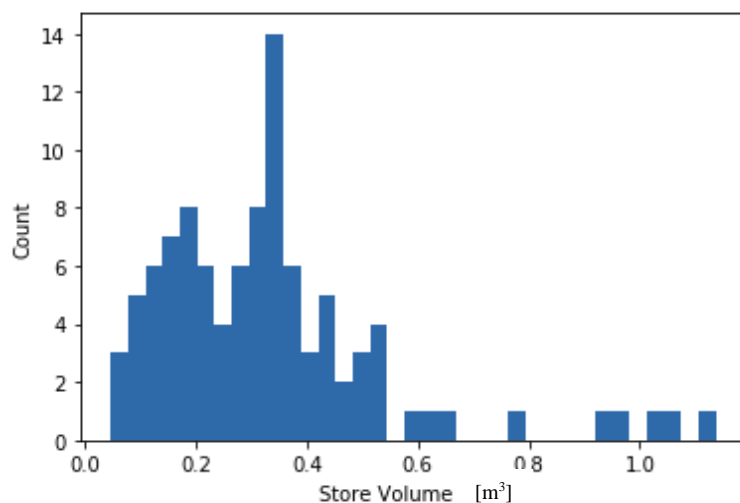


Figure 3.4: Individual DHW heat store sizes

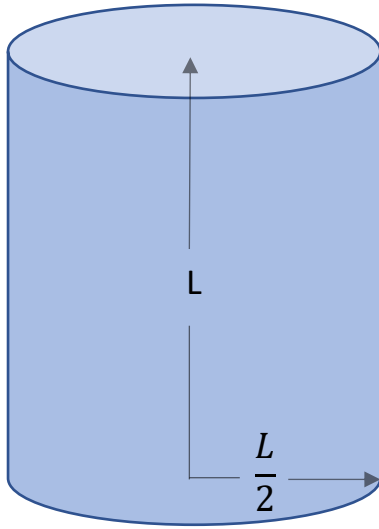


Figure 3.5: Cylindrical heat store dimensioned to have height equal to its diameter

### 3.6.2.1 Key Parameters

The models were built using parameters that described the physical character of the store and the environment within which the store sits. Key parameter values used in the model are given in Table 3.3. The heat loss factor (HLF) for the DHWT is set to 1 W/m<sup>2</sup>K as per field measurements conducted in Cruickshank et al (2010). Although lower HLFs can be achieved with adequate insulation, such as in larger stores, in the case of domestic stores, the extra space requirements and the relative high investment cost per volume mean that insulation is kept minimal (Guadalfajara, 2014). Sensitivity analyses are conducted for key parameters, including the HLF of the store, in order to investigate the impact that it has on the store losses, and therefore, the overall case for storage.

Table 3.3: Parameters of the heat store model

Parameter	Unit	Value	Reference
Heat loss factor	W/m <sup>2</sup> K	1	(Zhang et al, 2021)
Minimum store temperature	°C	20	Assumption based on Huang et al. (2020)
Maximum store temperature	°C	50	Assumption based on Huang et al. (2020)
Specific heat capacity of water	kJ/kg°C	4.182	(Allison et al., 2018; Holman et al, 1992)
Density of Water	kg/m <sup>3</sup>	997	(Holman et al, 1992)
Ambient temperature	°C	18	Assumption
Charge/discharge efficiency	%	100	Assumption based on Huebner et al. (2013)

### 3.6.2.2 Control Logic

Figure 3.6 and Figure 3.7 together describe the deterministic control logic applied to both the stratified and the mixed store models.

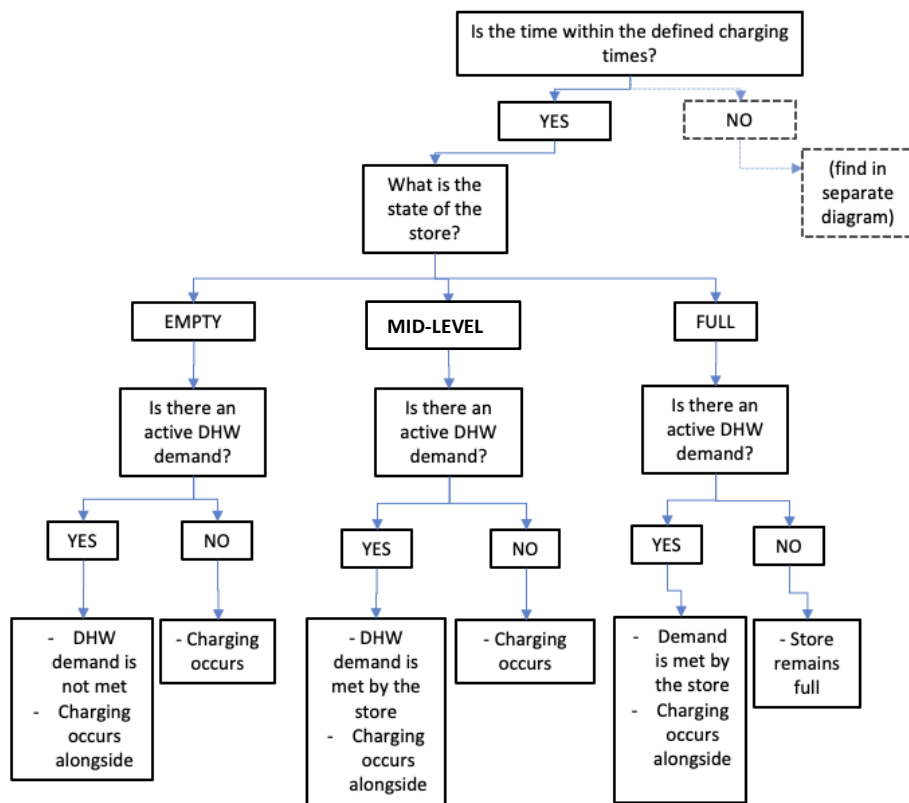


Figure 3.6: Flow chart describing the operation of the store. The chart is given in two parts (1/2).

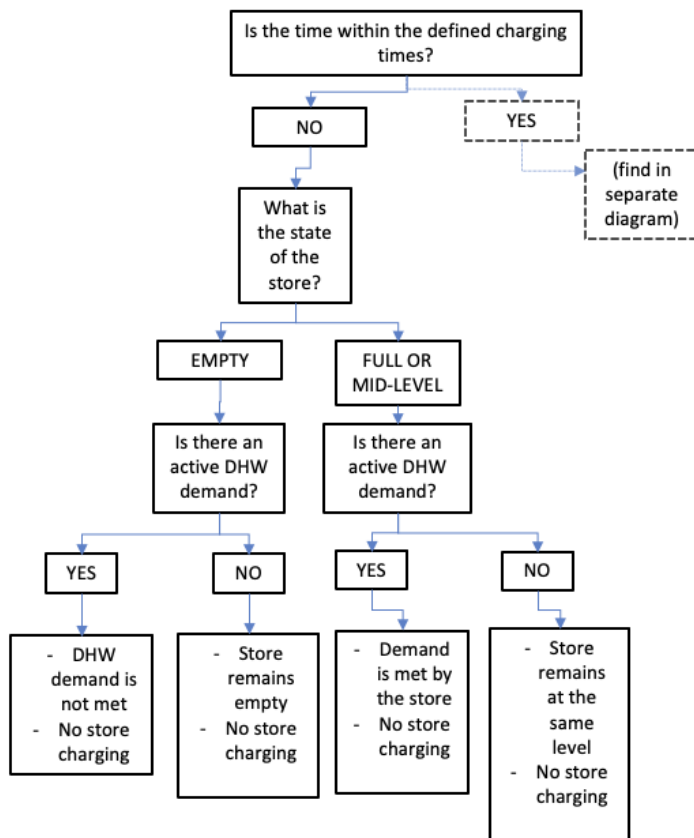


Figure 3.7: Flow chart describing the operation of the store. The chart is given in two parts (2/2).

### 3.6.2.3 Stratified Heat Store Physical Principles

Stratified thermal stores have been previously modelled in studies to varying degrees of complexity (Cruickshank and Harrison, 2010). The modelled heat store is a DHWT consisting of two stratified zones. The zones are two bodies of water that are separated by a sharp thermocline boundary. The temperature of the water in each zone is homogenous; one contains heated water and the other contains cold mains water. The thermocline between the hot and cold water moves vertically down as the heat exchanger transfers heated water into the store and vertically up as the taps in the dwelling are opened and hot water is drawn. The temperature of the hot zone is assumed to be constant and corresponds to the modal supply temperature of the DHW in the case study HN (see Figure 5.13). The temperature of the cold zone is also assumed to be constant and to correspond to the temperature of the cold water from the mains. It is assumed that no heat transfer occurs across the thermocline. Legionella risk is mitigated because the water within the store is regularly changing in temperature. The idealised model does not take into account of conduction heat transfer and conduction through the cylinder wall. The stratified heat store model is illustrated in Figure 3.8 below.

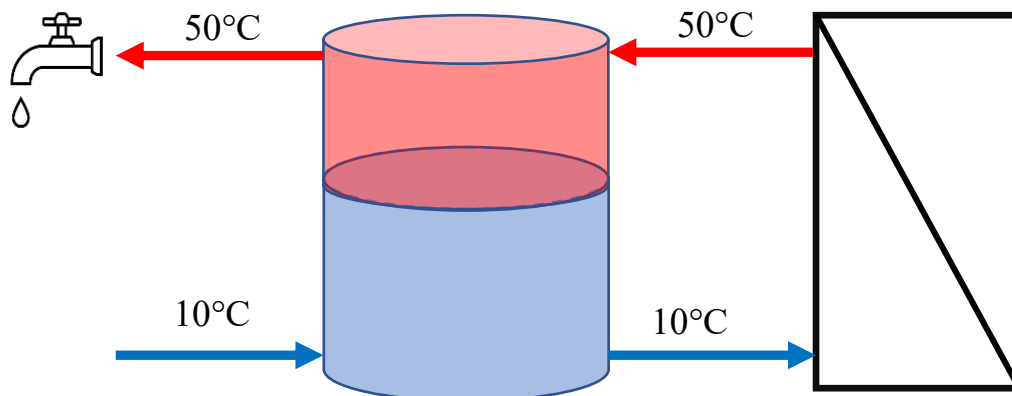


Figure 3.8: Stratified heat store connection to the DHW HEX in the HIU

The status of the store as being ‘full’, ‘empty’ or ‘mid-level’ is based on the change in total energy input relative to the capacity of the store.  $\Delta h$  is the change in height of the boundary that travels vertically up and down the store. If there is a net energy input, the  $\Delta h$  is negative, and the boundary moves down. If there is a net energy output, such as when the demand on the store is higher than the demand being delivered to the store by the HIU, the  $\Delta h$  is positive, and the boundary moves up. This is illustrated in Figure 3.9 below.

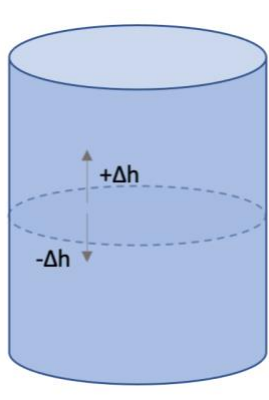


Figure 3.9: Heat store diagram illustrating the movement of the thermocline boundary

The energy balance that drives the model is given below.

$$\dot{m}^{HEX,control} \cdot c \cdot \Delta T^{HEX,design} = \rho \cdot V \cdot c \cdot \Delta T^{Store} - \dot{Q}_t^{DHW} - k^{Store} \cdot A_{ext}^{Store,hot} \quad (3-2)$$

Where volume,  $V$  is a function of the change in  $h$  over time, as described below.

$$V = \pi \cdot r^2 \cdot \left( \frac{h_t - h_{t-1}}{\Delta t} \right) \quad (3-3)$$

The mass flow of fluid into the store from the HEX,  $\dot{m}^{HEX,control}$ , is controlled by the control logic described in Figure 3.6 and Figure 3.7 together. Both the stratified and mixed models connect in parallel to the DHW HEX.

#### 3.6.2.4 Mixed Heat Store Model Physical Principles

In addition to the above model, a perfectly mixed heat store was modelled. The store is modelled as an ideally mixed volume of water with a homogenous temperature. This simplified storage model has been used since the 1980's extensively in studies (Mosbech, 1983; Collazos et al., 2009; Schütz et al, 2015). The mixed store model is illustrated in the schematic shown below, in Figure 3.10. The temperature of the store is dependent on the heat transfer into the store, from the heat exchanger, HEX, and out of the store, through losses and DHW demand. Fluid from the store is passed through the HEX, picking up heat on each pass, gradually charging the store up to its maximum capacity. The store's temperature has the bounds of a lower temperature that is equal to the room temperature, and an upper bound that is equal to the maximum flow temperature of the HEX. The energy balance of the perfectly mixed store is as follows,

$$\dot{m}^{sto} \cdot c \cdot \frac{T_t^{Store} - T_{t-1}}{\Delta t} = \dot{Q}_t^{HEX} - \dot{Q}_t^{DHW} - k^{Store} \cdot A^{Store} \cdot (T_t^{Store} - T^{Env}), \quad (3-4)$$

where,

$$\dot{Q}_t^{HEX} = \dot{m}^{HEX,control} \cdot c \cdot (T_{Max} - T_t^{Store}). \quad (3-5)$$

The mass flow of fluid into the store from the HEX,  $\dot{m}^{HEX,control}$ , is controlled by the control logic described in Figure 3.6 and Figure 3.7 together, in the same way as the stratified model.

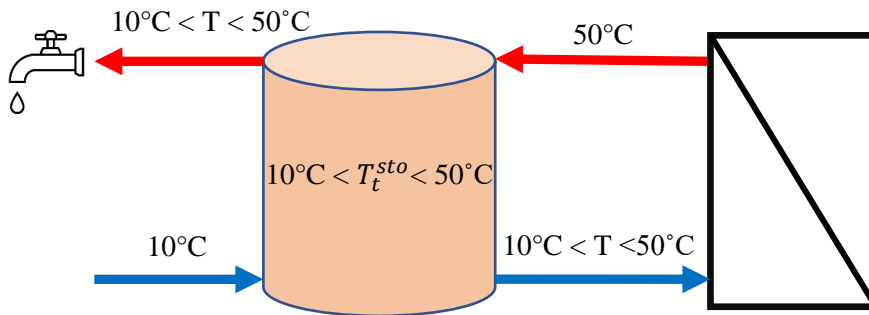


Figure 3.10: Mixed heat store connection to the DHW HEX in the HIU

### 3.7 Distribution System Model

To assess the thermal losses from the distribution system for the storage scenarios, a model of the distribution system was built to represent the real distribution system as closely as possible, which has been sized according to the peak demands in each scenario. The tables below give the parameters, their values, and associated references for the heat store model and the distribution system model.

Table 3.4: Key parameters of the distribution system model

Parameter	Unit	Value	Reference
Flow temperature	°C	62	(Hanson-Graville, personal communication, September 2019)
Return temperature	°C	30	(Hanson-Graville, personal communication, September 2019)
Ambient temperature	°C	18	- Assumption - Note: the range tested in the sensitivity analysis is 10°C – 30°C
Thermal conductivity of pipe material (medium grade steel)	kW/mK	0.03	Stated in Domestic Water Services Schematic for case study HN. Thermal conductivity value from (The Engineering ToolBox, 2005)
Thermal conductivity of pipe insulation (phenolic foam)	W/mK	0.018	- Stated in Domestic Water Services Schematic for case study HN. Thermal conductivity value from ( <i>Phenolic foam insulation</i> , no date) - Note: the range tested in the sensitivity analysis is 0.005 W/mK – 7.0 W/mK. - Insulation levels given in terms of thermal conductivity, k, because pipe insulation thickness varies across distribution system. - Pipe insulation thickness ranges from 15mm to 25mm. - The range in U-value would be 0.3 W/m <sup>2</sup> K – 2 W/m <sup>2</sup> K for a pipe insulation thickness of 15mm.

The assumption in the distribution system model that the supply and return temperatures are maintained at their design set points is required because the demand data used in the model also corresponds to design day conditions, which is likely to lead to the supply and return temperatures reaching their design values. Furthermore, temperature control of the case study HN involved maintaining the supply temperature at the set point only (R. Hanson-Graville, personal communication, September 2019), as opposed to predictively adjusting temperatures (i.e., for night time set back) where temperature changes can be up to 10°C (Guelpa, 20201), and thus the assumption of a constant supply temperature in this HN is a safe assumption as it is likely that the supply temperature fluctuated around the set point. The temperature can also

fluctuate naturally during the night-time due to the smaller demand and, thus, lower the mass flow rate to the extent that the thermal losses have a much larger impact. This effect is not considered in the distribution system model, as it would require modelling the distribution system as a thermo-fluid dynamic model where mass, momentum, and energy conservation equations are solved and where the interconnection of pipes is represented in a graph system of nodes and branches, which, on balance with other components of work in the thesis, would have been prohibitively time-consuming.

### 3.7.1 Pipe Sizing Methodology

Each pipe in the distribution system model was sized to meet the peak aggregate demand acting in that segment of the system. For example, a pipe serving 10 dwellings downstream of it would be sized to meet the peak aggregate demand of 10 dwellings. A set of flow rates, and therefore a set of flow velocities, are then derived based on the operating temperatures of the HN and the peak aggregate demand for a range of pipe diameters. The smallest practicable pipe diameter for which the flow velocity falls within the recommended ranges is then selected for that part of the distribution system. To reflect the real case study, medium grade steel pipes were selected in the models. In keeping with accepted guidance (discussed in Sections 2.5.2 and 2.6), the minimum flow velocities for pipes in the model are defined as being equal to 0.5 m/s, with the velocity upper bounds being 1.5 m/s for pipes smaller than DN50 and 3 m/s for pipes larger than DN50. Table 3.5 gives the flow velocity constraints that apply for each diameter of pipe required in the model (HardHat Engineer, 2023; Stevenson Plumbing, no date).

Table 3.5: Flow velocity constraints for the range of pipe diameters used in the sizing methods

Pipe Diameters (mm)	Flow Velocity Bounds (m/s)
6, 8, 10, 12, 15, 20, 25, 32, 40, 50	0.5 – 1.5
65	0.5 – 3.0

For an example, take a lateral transport pipe serving 30 dwellings. In order to determine the pipe sizing for such a pipe, the aggregate peak demand for 30 dwellings is required. Take the peak demand to be 73 kW (this is the real demand at this level of aggregation found in the case study HN). This demand value ( $Q$ ), along with the operating temperatures of the HN ( $\Delta T$ ) are used to obtain a mass flow rate ( $\dot{m}$ ) for that segment of pipe as described by the equation below.

$$Q = \dot{m}c\Delta T$$

(3-6)

This mass flow rate is then used to determine a set of flow velocities that correspond to set of pipe diameters using the equations that follow where  $\dot{V}$  is the volume flow rate (kg/s),  $\rho$  is the density of water,  $D$  is the diameter of the pipe,  $A$  is the area of a circle and  $v$  is the flow velocity (m/s).

$$\dot{V} = \frac{\dot{m}}{\rho}$$

(3-7)

$$A = \frac{\pi D^2}{4}$$

(3-8)

$$v = \frac{\dot{V}}{A}$$

(3-9)

Table 3.6 below gives the flow velocities obtained according to the above calculations for a set of pipe diameters. As shown in Table 3.6 below, the smallest pipe for which the velocity falls within the recommended velocity bounds is selected for the segment of the distribution system. In this example, a pipe of diameter 20 mm is chosen for the lateral transport pipe that needs to serve 30 dwellings. A full list of standard pipe sizes is given in Appendix D, Section 14.1 and a full list of the pipe sizing results for all scenarios can be found in Appendix D, Section 14.2.

Table 3.6: Selecting the smallest practicable pipe for an example pipe section

Pipe Diameter (mm)	Resulting Flow Velocity (m/s)	Velocity Bounds for Pipe Diameter	Within Bounds?
6	19.5	0.5 – 1.5	No
8	11.0	0.5 – 1.5	No
10	7.0	0.5 – 1.5	No
12	4.8	0.5 – 1.5	No
15	3.1	0.5 – 1.5	No
20	1.8	0.5 – 1.5	Yes

The pipe thicknesses of each diameter of pipe are given in Appendix D, Section 14.1. Pipe thickness has been selected based on pipe diameter according to the Schedule 10. Insulation levels are dependent on pipe diameter and follows the criteria described in Table 3.7. The insulation levels in the model reflect the real insulations levels specified in the real HN design.

Table 3.7: Pipe insulation thickness is dependent on the pipe diameters

Pipe diameter (mm)	Insulation thickness (mm)
< 15	25
15 - 22	30
22- 42	35
> 42	40

Note that the pipe sizing is determined only for DHW demands rather than DHW and SH demands together. This is of course not how most real HNs are sized, nor should they be. This means that the results obtained, for example the reduced pipe sizing post storage installation which practitioners may view as something to aim for, are not intended to be taken as explicit recommendations or benchmarks without careful discernment. The driving force of this work is to understand the interplay between storage, diversity and demand and the extent to which that can impact design. In that same vein, the results are intended to be viewed as a guide that demonstrates what is possible. Having said this, there are certain conditions under which certain results could reasonably be taken as practical

recommendation, and these will be outlined and justified as they come up through the thesis. The full implications of the omission of SH demands are discussed in the Discussion Chapter in Section 8.3.2.

### 3.7.2 Network Topology

Figure 3.11 illustrates the layout of a floor, showing the relative locations of 1 and 2 bed dwellings, the staircase, and the riser cupboard. According to accepted guidance on HIU placement, the HIUs are located within the dwellings such that total pipe length is minimised. Figure 3.12 shows a close up of one segment of the floor plan in which HIU and pipe placement is shown. Figure 3.13 gives a plan view of the building and each of the six floors. The right-hand side of the network in the plan view corresponds to the segment of the floor plan shown to be vertical in Figure 3.11. Similarly, the left-hand side of the network shown in the plan view corresponds to the segment of the floor plan shown to be horizontal in Figure 3.11. Note that only part of this case study HN will be modelled and used in the analyses. This is due to demand data of sufficient quality being available for 96 dwellings. Therefore, the part that will be modelled is a part containing 96 dwellings out of the ~150 dwellings on the HN.

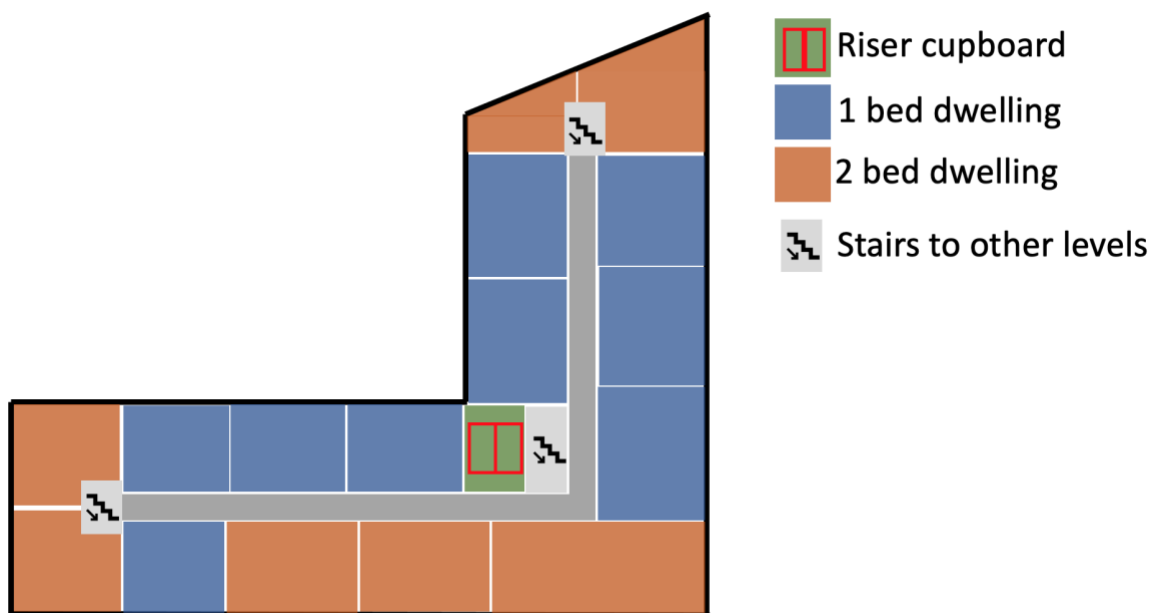


Figure 3.11: Floor plan showing dwellings, riser cupboard and stairs on one floor. This plan applies to all floors.

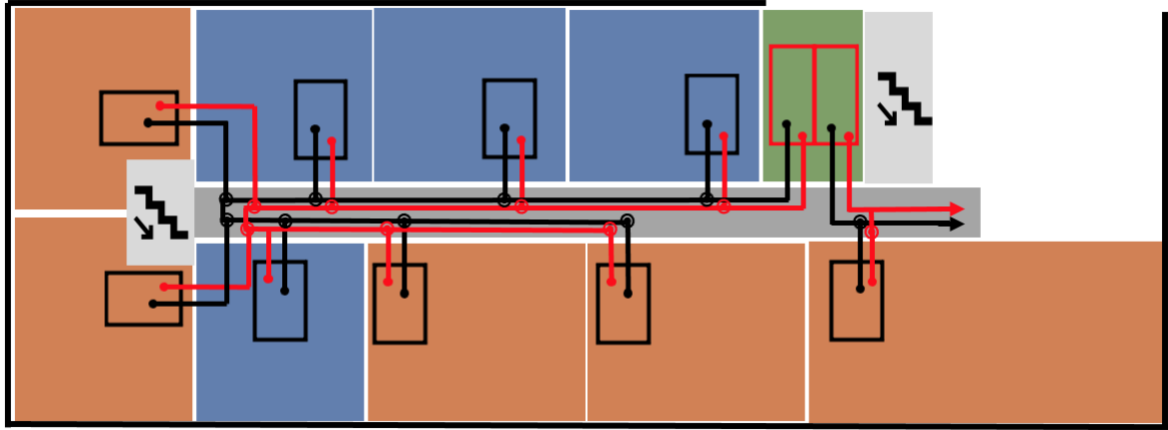


Figure 3.12: Network connection between dwellings within a floor and across floor. Black and red circles indicate where pipe cross floors

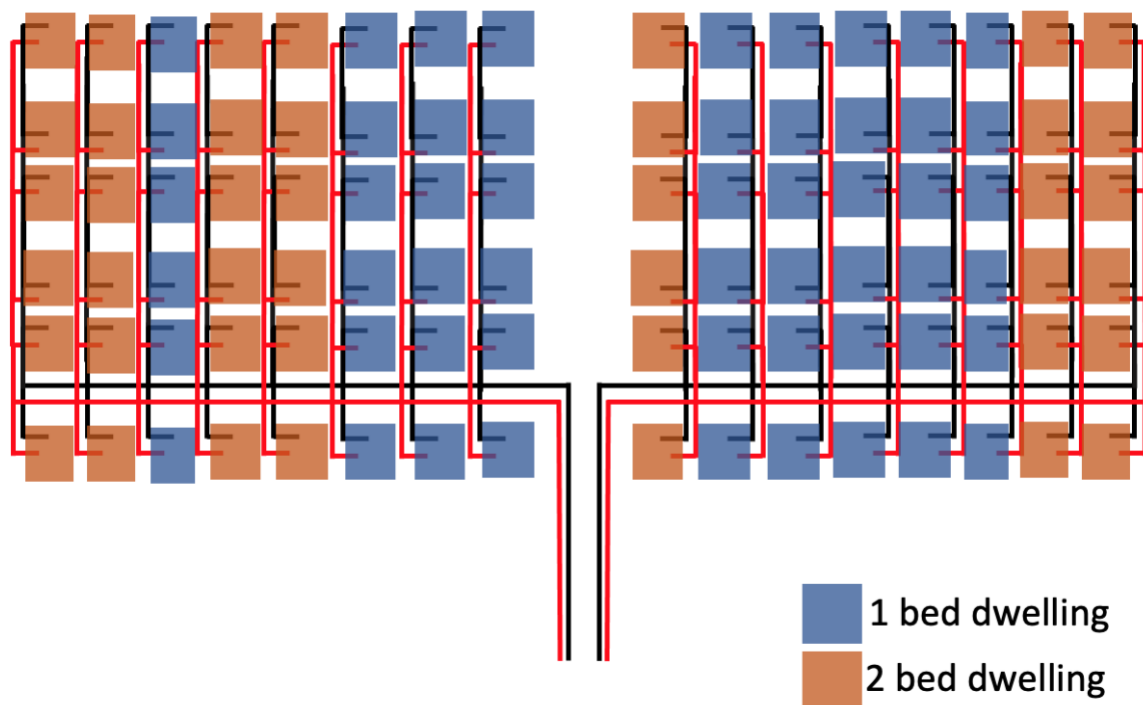


Figure 3.13: Real distribution system and dwelling plan of the case study CHN, showing all 6 floors and the type of dwellings within each floor

### 3.7.3 Distribution System Thermal Mass

Studies have considered the incorporation of the thermal mass of a distribution system as storage in HNs (Guelpa and Verda, 2019; Hoshino et al, 2023; van Easteren, 2022). In large HNs the thermal mass of the distribution system is significant, and the possibility of using this mass to the benefit of the operation of the HN could be considered, as pointed out by Werner (2013). The case study network in this work is small and contained within a single building. Pipes in the case study HN are smaller than 54 mm in diameter across the network, compared to district scale networks where pipes can be larger than 0.2 m in diameter (Zhang

et al, 2021). This is a reasonable size given the small scale of the network; one can compare it to the networks investigated by Zhang et al. (2021), where a HN serving 165 dwellings had a total volume of water of 2.2 m<sup>3</sup> in its network. Based on the network layout and the design diameters of the real HN, the total volume of fluid within the modelled part of the case study network amounts to 0.66 m<sup>3</sup>. For diameters in the storage scenarios, the total volume will be less than 0.66 m<sup>3</sup> as diameters will be smaller than design diameters. The total volume of DHW stores is 33.12 m<sup>3</sup>. Since the capacity of the network and the stores are based on similar temperature differences, the capacity of the network is relatively small compared to the capacity of the TES in the network.

### 3.7.4 Distribution System Heat Loss

Heat losses in the distribution pipes of a HN are influenced by insulation, the conditions of the surrounding environment, the pipe system dimensioning and layout, and the temperature of the fluid in the pipes (Keçebaş, 2011; Li et al., 2016). In the calculation of thermal losses from the distribution system, a constant temperature is assumed for the surrounding environment. The supply and return temperatures are also assumed to be constant. It is assumed that heated water is pumped through the distribution system at a constant velocity under steady-state steady-flow control volume conditions. The model does not include the impact of pressure drops resulting from flow friction or the heat gain due to friction.

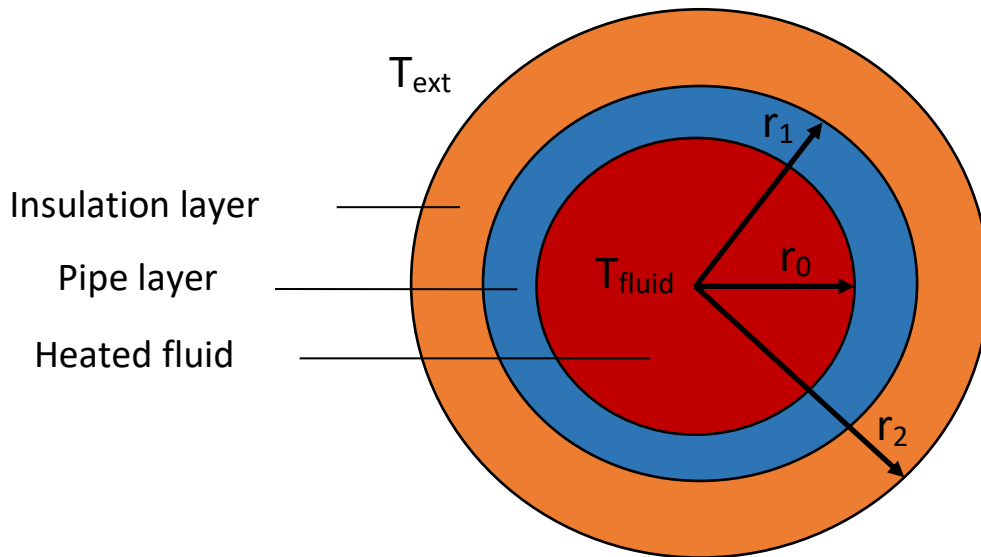


Figure 3.14: Schematic of pipe layers

The heat loss through a meter of pipe,  $Q_{loss}$ , can be expressed in terms of the fluid temperature,  $T_{fluid}$ , the temperature of the external environment,  $T_{ext}$ , and the overall heat transfer coefficient of the pipe and insulation layers,  $U$ , as described in Equation (3-).

$$Q_{loss} = \pi D_2 U (T_{fluid} - T_{ext}) = \pi D_2 U \Delta T \quad (3-7)$$

The diameters,  $D_i$ , of each layer of the insulated pipe is simply the double of the radius of each cylindrical layer as expressed in Equation (3-8), where  $i = 0, 1$ , and 2. The radii,  $r_0$ ,  $r_1$ ,

and  $r_2$  represent the radii from the centre of the pipe to the three surrounding cylindrical layers as shown in Figure 3.14.

$$D_i = 2r_i \quad (3-8)$$

The overall heat transfer coefficient,  $U$ , is the inverse of the internal resistance of the insulated pipe,  $R_{p,ins}$ , as shown in Equation (3-7) below.

$$U = \frac{1}{R_{p,ins}} \quad (3-9)$$

The total internal resistance of an insulated pipe, a summation of the conductive and convective heat transfer, and surface resistance of the layers of the pipe, is described by Equation (3-) below.

$$R_{p,ins} = \frac{D_2}{D_0 h_i} + \frac{D_2 \ln\left(\frac{D_1}{D_0}\right)}{2k_p} + \frac{D_2 \ln\left(\frac{D_2}{D_1}\right)}{2k_{ins}} + \frac{1}{h_{air}} \quad (3-10)$$

Where  $k_p$  and  $k_{ins}$  are the thermal conductivity of the pipe layer and the layer of insulation material respectively. The two middle terms of Equation (3-) represent the conductive heat flow through the pipe and insulation layers respectively. The convective heat transfer coefficients of the inside and outside surfaces,  $h_i$  and  $h_{air}$ , are calculated as described in Equation (3-) where  $Re$  is the Reynold's number and  $Pr$  is the Prandtl number, and Equations (3-) - (3-19) respectively (Holman, 1992).

$$\frac{h_i D}{k_i} = 0.023 Re^{0.8} Pr^{0.4} \quad (3-11)$$

The term above is typically negligible compared with the other terms in the total resistance of the insulated pipe equation, Equation (3-10), and thus will be ignored. The final term of the total resistance equation represents the convective and radiative heat loss from the surface of the insulation layer. Its calculation is described in Equations (3-12) -(3-19) where  $Nu$  is the Nusselt number.

$$h_{air} = h_{radiation} + h_{convection} \quad (3-12)$$

$$h_{radiation} = \frac{\sigma \varepsilon (T_{surface}^4 - T_{ext}^4)}{T_{surface} - T_{ext}} \quad (3-13)$$

$$h_{convection} = \frac{Nu_{combined} k_{air}}{r_2} \quad (3-14)$$

$$Nu_{combined} = (h_{forced}^4 + h_{free}^4)^{0.25} \quad (3-15)$$

The radiative heat transfer coefficient,  $h_{radiation}$ , is determined using the difference between the temperature of the external environment and the surface temperature of the insulation layer,  $T_{surface}$ , the Stefan-Boltzmann constant,  $\sigma$ , and the surface emissivity,  $\varepsilon$ , of the top surface of the insulation. The convective heat transfer coefficient,  $h_{convection}$ , is made up of two components,  $h_{forced}$  and  $h_{free}$ , which represent forced and free convection respectively. They can be determined using the correlation by Churchill and Bernstein, and Churchill and Chu correlations respectively, as shown in Equations (3-) - (3-) given below (Bergman et al, 2002).

$$Nu_{forced} = 0.3 + \frac{0.62Re^{\frac{1}{2}}Pr^{\frac{1}{3}}}{\left[1 + \left(\frac{0.4}{Pr}\right)^{\frac{2}{3}}\right]^{\frac{1}{4}}} \left(1 + \left(\frac{Re}{282,000}\right)^{\frac{5}{8}}\right)^{\frac{4}{5}}$$

(3-16)

$$h_{forced} = \frac{Nu_{forced}k_{air}}{r_2}$$

(3-17)

$$Nu_{free} = \left\{ 0.6 + \frac{0.387Ra^{\frac{1}{6}}}{\left[1 + \left(\frac{0.559}{Pr}\right)^{\frac{9}{16}}\right]^{\frac{8}{27}}} \right\}^2$$

(3-18)

$$h_{free} = \frac{Nu_{free}k_{air}}{r_2}$$

(3-19)

The  $h_{air}$  component was calculated by assuming a pipe with properties equal to the mean of all pipes in the distribution system. This value was then applied for all pipes in the distribution system.

The heat loss through a meter of pipe,  $Q_{loss}$ , can then be summarised by the following expression.

$$Q_{loss} = \frac{\pi D_2 \Delta T}{R_{p,ins}} = \frac{\pi D_2 \Delta T}{\frac{D_2 \ln\left(\frac{D_1}{D_0}\right)}{2k_p} + \frac{D_2 \ln\left(\frac{D_2}{D_1}\right)}{2k_{ins}} + \frac{1}{h_{air}}}$$

(3-20)

### 3.8 Applicability of Results and Limitations

As of 2018 there were about 17,000 HNs across the UK, 11,500 of which were communal HNs (ADE, 2018; BEIS, 2017; BEIS 2020a). This amounts to 500,000 connected consumers, of which a large majority are domestic consumers. Of the domestic consumers, the majority are connections to small flats and maisonettes (ADE, 2018). Given that the case study HN from which data was collected is a residential building made up of flats, it is likely that the case study site represents the majority of HNs in the UK. Government surveys also found that consumers on networks were more likely to be renting from a local authority or housing association (BEIS, 2017). The consumers at the case study site represent the majority of HN consumers in this regard also given that their properties are rented; however, they may differ in terms of specific type of tenure. Equally, reports suggest that dwellings on networks are likely to have 0-1 bedrooms, whereas the studied dwellings have between 2 and 3 bedrooms and therefore may be larger than typical dwellings served by HNs (BEIS, 2017). Reports also found that consumers on networks lived in newer homes (BEIS, 2017). Building age information is unavailable for the dataset, and thus a comparison cannot be made. In the years since the report, HNs are likely to have seen some growth, and resultantly the characteristics of HNs today may have changed significantly from previously.

In order to understand the extent to which findings can inform the technical standards for future HNs, the extent to which the studied case represents future networks must be assessed. Future HNs do not yet exist, and thus their characteristics are unknown. A comparison to existing networks can be made instead on the basis that future networks are likely to share characteristics with existing ones, e.g., existing networks were found to be likely located in large urban areas such as London, and will likely evolve in predictable ways, e.g., operating temperatures reducing, space demands decreasing as dwellings become more thermally efficient, more integration with smart grids, and more storage integration to support the connection of renewable heat sources (BEIS, 2017; BEIS, 2020a). The preceding paragraph outlines similarities between existing networks and the case study site and shows a fair amount of representation; the case study is not atypical compared to other existing HNs. Taking this together with the study being designed such that a number of the aforementioned future outcomes are represented, it is likely that the findings from the study will have reasonable applicability to future HNs. Having said this, the findings will be more applicable to networks that are similar to the studied case, serving dwellings with similar design and occupancy characteristics.

The graphs relating to diversity and aggregate demands produced in this study use the individual heat demands of the case study HN and is therefore best used in designing networks that will serve dwellings with similar design and similar occupancy characteristics, i.e., communal HNs serving residential buildings with similar enclosed dwellings to those in the study. For example, the diversity curve may be used in determining the aggregate load at various points across the distribution system and therefore be used for sizing pipes, given that connected dwellings are similar to those in the study. Results will be less applicable to district HNs, which are likely to contain different kinds of heat demands (e.g., an anchor heat load like a hospital or a school) and may therefore have a characteristically different aggregate demand. In terms of informing standards, since this diversity curve will likely be one of the very first based on empirical data from UK dwellings, there may be a case to consider its use in the design process where the Danish curve, also based on data from a residential building but with the drawback of not being UK data, would usually be used.

When it comes to findings regarding storage, the results illustrate only the impact on this particular case and may be indicative of the impact that storage would have on any network, but this cannot be confirmed without further studies. Results will be more applicable where the storage has similar design, controls, and strategies to those modelled. For example, where other kinds of storage materials, storage control, or strategies are used, the resulting residual profiles will be different, as will the aggregate demand. Having said this, the storage scenarios were designed to represent likely future scenarios, and thus it is likely that the findings will be applicable to networks developed in the near future. Similarly, findings regarding the impact of storage on network design and performance illustrate only what is possible for one case. For example, using a different topology would affect the impact that storage has on design and performance. However, even though findings may not be directly applicable to systems with different topologies, dwelling designs, storage etc., they may provide a qualitative indication of the direction and magnitude of the effects of some design decisions.

Data collection started during the COVID pandemic, which will have an impact on the findings of the study. For example, heat demand patterns will be different because of differences in occupancy patterns that result from the working from home guidelines from the UK government. This will have implications for the generalisability of findings in the study to periods when working from home guidelines are no longer in action.

## 4 Data Collection

The Heatweb server is a server which was set up by Heatweb Ltd. to collect data from 100s of Heat Interface Units (HIU) across multiple HNs. Sensors installed in individual HIUs transmit data to a central server in an Internet-of-Things set-up, which can be connected to from a remote server in order to download the transmitted data. Although only certain variables are monitored by the sensors directly, some of which are shown in Table 4.1, measurements taken whilst commissioning the HIUs enable the practitioners at Heatweb Ltd. to estimate other variables as a function of the commissioning measurements and the monitored variables together. The estimated variable data is also transmitted across the server. This novel system enables the collection of a rich dataset, made up of dozens of variables collected at high frequency, that can describe in detail the operation of and the energy flows across the HIUs. Data collection started February 2021.

Heatweb Ltd. set up and calibrated the data collection hardware and software. The author connected to the data server via their laptop, observed the data as it was being collected and helped maintain data quality by observing discrepancies or faults and reporting the details back to Heatweb Ltd. The monitoring and storage strategy and parts of the software used for directing the data from the server evolved as a result of discussions between the author and Heatweb Ltd. depending on the needs of the research and what was feasible within the system (e.g., due to memory constraints). The author cleaned the data independently once the data was collected.

*Table 4.1: Variables measured directly from sensors and heat meters in the HIU*

<b>Measured Variables</b>
Flow rate to hot water (l/m)
Network return from hot water (°C)
Primary hot supply temperature (°C)
SH valve positions (steps)
DHW valve positions (steps)
Heat meter flow rate (l/m)
Heat meter power (kW)
Heat meter volume (m <sup>3</sup> )
Heat meter return temperature (°C)
Heat meter flow temperature (°C)

Altogether, the data collection system set up by Heatweb Ltd. is a combination of meters, sensors and other hardware from which data collection is supported by linked software programs. There are two sets of sensors in the HIU; the sensors that make up the heat meter and the remainder of sensors that are located outside of the heat meter. Each set is collected via two separate data collection systems. The data system was built to aid effective monitoring and control of the HN and has now been made available for academic research. At the time of writing, only the author had access to the data stream for the purposes of research.

The section below describes the key parts of the hardware and connections. The section following that describes how data is collected through the hardware system and linked software.

The section is structured such that the process of data collection is laid out from start to finish, using the hardware as a reference to key points in the journey of the data in order to provide an intuitive understanding of the system and processes involved. However, a key piece of software must be explained first in order that the data system is understood. This is the Node-Red Software.

## 4.1 Node-Red Software

Node-red is a flow-based visual programming tool for connecting hardware devices supporting internet-of-things set-ups. Heatweb Ltd. use it as a logic controller to control the data flow through some parts of the data collection system.

Note: when the terms upstream and downstream are used they refer to positions in the chain of data transmission. ‘Upstream’ refers to processes or hardware furthest away from the point of measurement (i.e., the sensors). Conversely, ‘downstream’ refers to points close to the point of measurement.

## 4.2 Data Hardware

### 4.2.1 Located in the HIUs

#### 4.2.1.1 *Heat Meter*

As mentioned above, the data is transmitted from the sensors in the HIU via two separate networks. The heat meters record data at intervals of one second and continuously store these values in their own on-board persistent (meaning that no data is lost upon being turned off and on) memory. At every second it is also deriving variables such as power, total power consumed, etc.

#### 4.2.1.2 *HIU Sensors*

Sensors installed in the HIU (not those of the heat meter), which will be referred to as the *HIU sensors*, are connected to the electronic controller in the HIU using wires. The HIU sensors also monitor on a secondly basis. Derived variables are calculated further upstream, not at the HIU.

The electronic controller and the heat meter in each HIU are wired up, through an Ethernet and mains cable, respectively, to a Node-HIU Switch, which connects to 8 HIUs.

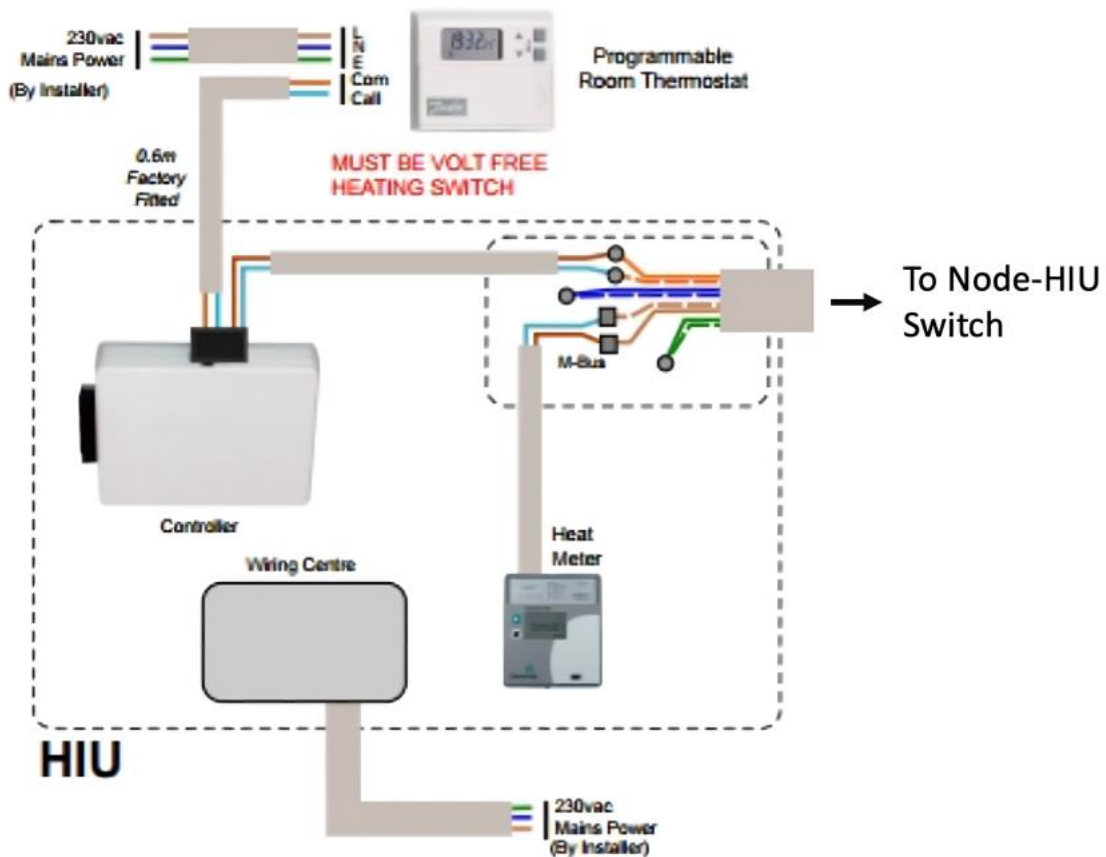


Figure 4.1: Shows connected key hardware and interconnections within the HIU (Heatweb Ltd., no date b)

## 4.2.2 Located Externally to the HIUs

### 4.2.2.1 Node-HIU Switch

The Node-HIU Switch is a Raspberry Pi and other infrastructure connecting the Ethernet and mains cables from 8 HIUs to respective devices in the plant room. There are, therefore, a group of Node-HIU Switches installed throughout the site. The endpoints of the ethernet cables and mains cables will be described in the Plant Room Hardware section.

Although both wires are housed in the same container, the Ethernet cables transferring HIU sensor data and the mains cables transferring heat meter data are on two separate wiring systems. The heat meter data is on an M-bus system, and the HIU sensor data is on what will be called a Node-HIU system. The separate systems and their impact on the data collection will be explained in detail in proceeding sections.

The heat meters are connected via a series of terminal blocks (an insulated block that secures wires together) into a common-wire network, meaning every device shares the same two wires (Figure 4.2). The circuit topology is a mix of series and parallel. The network of wires connects all the heat meters to the M-Bus Master in the plant room.

The Ethernet cables are connected via the Raspberry Pi in the Node-HIU Switch to the Power over Ethernet (PoE) Ethernet Switch. The Raspberry Pi runs Node-Red software enabling remote control of the data collection at the switches. The Switch is controlled to filter the large volumes of data it receives before sending it upstream. The Switch filters the data such that data is allowed through only if it is an update to the previous value. This is called



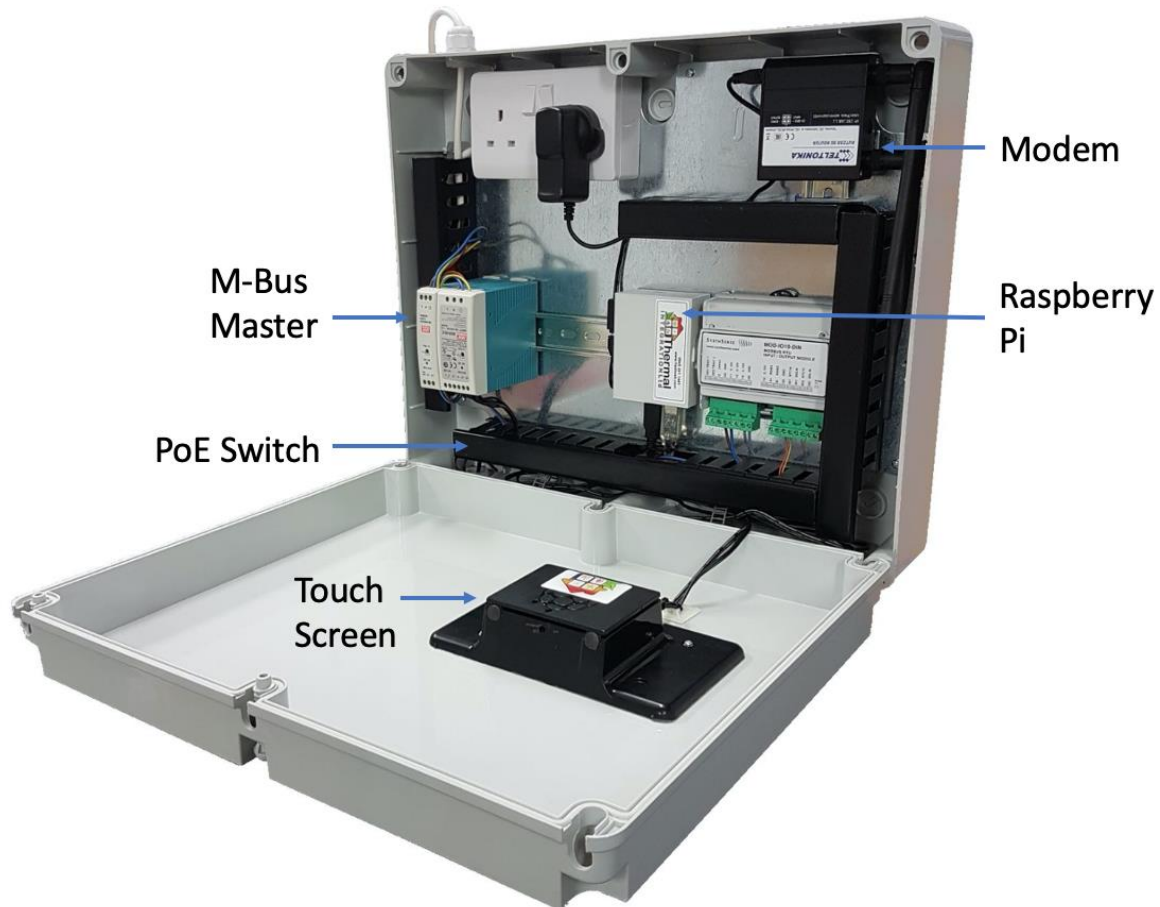


Figure 4.3: The home of Plant Pi and other pieces of hardware- this kit is housed in the plant room (Heatweb Ltd., no date b)

There data streams through several servers before reaching their end point. The purpose of each server is described in the following section.

#### 4.2.3 Software and Servers

The MQTT server is a network protocol that enables message transports between devices. The hw1 server is the main server that subscribes to the data being published to the MQTT server to anonymise it. After anonymisation at the hw1 server, the data is sent to hw12, server ready for download by the author. Simple routing functions such as the function to put data in Dropbox is carried out at this server.

#### 4.2.4 Summary of the Data Collection System

Figure 4.4 below illustrates the data collection hardware and how they connect to one another. The data collection will be summarised in the following points. Please refer to the diagram to supplement the information below.

- All heat meters on site are connected in one circuit with the M-Bus Master located in the plant room. This means there are only two wires going into the Master on the heat meter side.

- The HIU sensors in all the HIUs are connected via the electronic controller in each HIU to a Node-HIU Switch.
  - The Node-HIU Switch holds wiring for 8 HIUs, both sensor data wiring and heat meter wiring.
  - The Node-HIU Switch also contains a Raspberry Pi running Node-Red software which allows HIU sensor data filtering.
- Through the Node-HIU Switches, the heat meters and the HIU sensors connect to the M-Bus Master and the PoE Ethernet Switch respectively.
- The PoE Ethernet Switch located in the plant room panel provides power and internet to the connected devices.
- The Modem connected to the PoE Ethernet Switch provides it with an internet connection.
- The M-Bus Master allows the heat meter data to be collected in the form of a report.
- The Ethernet PoE Switch connects the Node-HIU Switches and the M-Bus Master to Plant Pi.
- Plant Pi refers to the Raspberry Pi in the plant room panel running Node-red and connected to the MQTT Server.
- Heat meter and HIU sensor data is sent though Plant Pi to the MQTT Server.

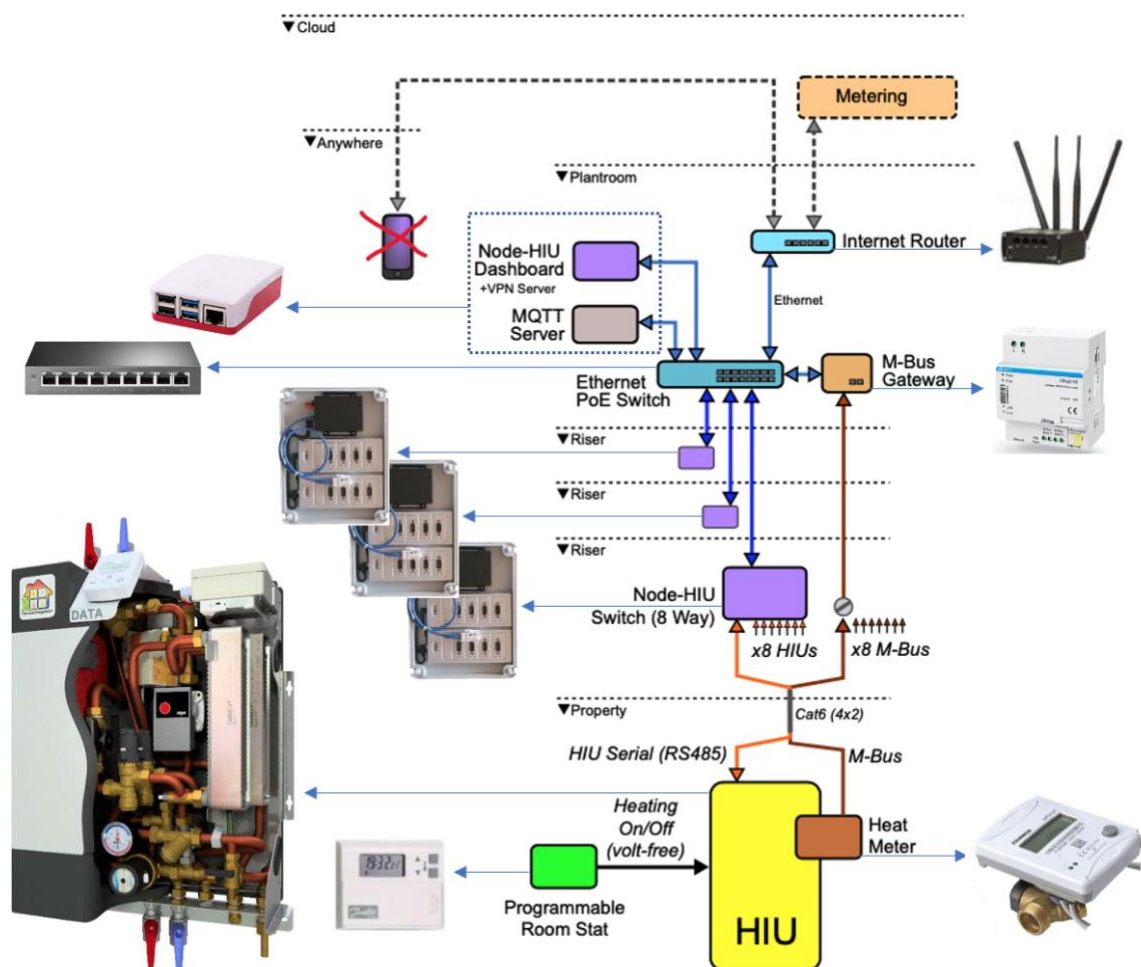


Figure 4.4: Depicts the flow of data from the sensors and the heat meters in an HIU to the data receivers

### 4.3 Node-HIU System

The Node-HIU Switches are connected by Ethernet cables to the Ethernet PoE Switch. Through this connection the filtered data is sent to the Plant Pi which runs MQTT Server and Node-red software. Thus, the filtered data, same as the meter data coming through the M-Bus system, is admitted to the MQTT server, ready for download.

### 4.4 M-Bus System

Via the Node-HIU Switches, all the heat meters are connected to the M-Bus Master in the plant room. The M-Bus Master communicates with the M-Bus slaves, in this instance, the heat meters, to receive meter data. The slave/master set-up of the M-Bus system means that the M-bus Master can only interface with one heat meter at a time. The M-Bus Master interfaces with one heat meter to receive a set of data, then moves on to the next to do the same.

After one round of interfacing, the M-Bus Master posts the entire batch of meter data in the form of a report to the Plant Pi, in which the Node-Red and MQTT are running, via the Ethernet PoE Switch. The M-Bus Master can be controlled remotely using the M-Bus manufacturer's (Elvaco) online control programs. The M-Bus master is set to send a batch of data every 5 minutes.

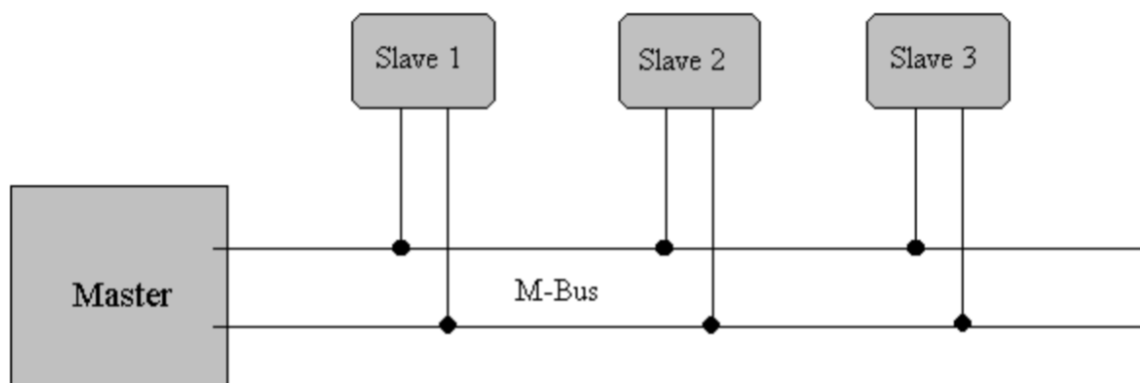


Figure 4.5: The M-bus physical layer (M-bus, no date)

### 4.5 The M-Bus Master

The M-Bus Master, CMe3100, produced by manufacturer Elvaco, is configured to readout meter readings from the connected heat meters at a defined interval, compiling the readings into the required format, ready to send to a receiver. In this case, the Master is connected through the Ethernet to the Plant Pi. Through the Plant Pi, readings are sent to the MQTT server, and then from there sent to the hw1 server for anonymisation. These readings are then collected in csv format in Dropbox.



Figure 4.6: M-Bus Master (Meter Market, no date)

The Master's readout schedule and reporting schedule can be defined through manufacturer's web interface, which will be referred to as the Elvaco interface. The readout schedule refers to the schedule at which the Master takes readings from the heat meters, through the slave/master system. To remind readers, slave/master system allows only one heat meter to be read at one time. The reporting schedule refers to the schedule of publishing for reports of the compiled readings to the designated reader, in this case, to the MQTT server. The web interface also enables the content of the reports to be defined. This will be explored in the proceeding section.

No variables are derived at the M-bus Master. It acts as a middleman who receives data and then passes it on in a defined format and according to a defined schedule.

## 4.6 The Elvaco Interface

The Elvaco web program that can be used to control the M-Bus Master and the reports that it sends is pictured below in Figure 4.7 and Figure 4.8.

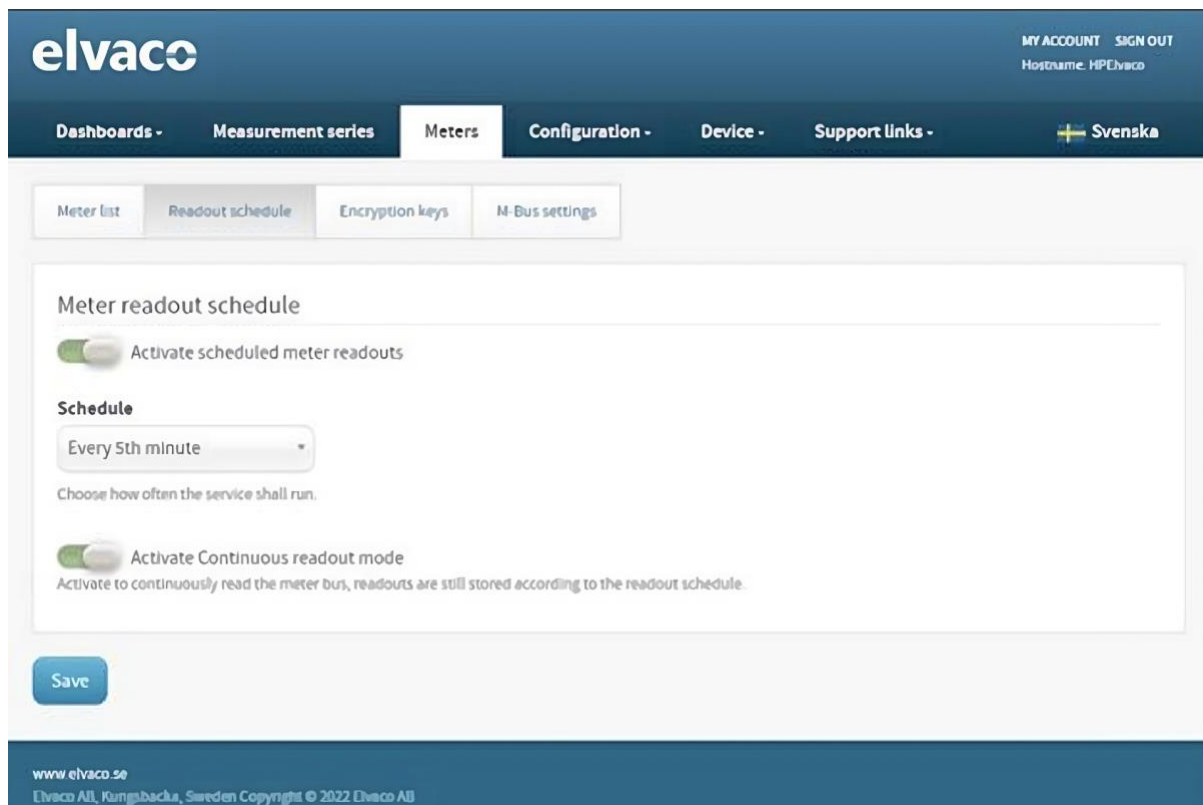


Figure 4.7: Elvaco interface showing the readout schedule

## Push Reports - Report 3

**Report type**  
HTTP

**Report template**  
3101 HTTP value report ...

**Report schedule**  
Every 5th minute  
Choose how often the service shall run.

**Meter readout schedule**  
Every 5th minute  
Current setting in Meters > Readout schedule.

### Report content

**Value period**  
5 Minute(s)  
Choose which values to include in the report based on how long ago they were stored compared to when the report is sent. For example, using settings "1 Day(s)" include all values stored within 1 day from when each report is sent.

**Value interval**  
5 minutes  
Choose "All values" to include all available values (defined by readout schedule) or choose a higher setting to create a sparse value report with a longer time between reported values.

### Report receiver

☐ Send report to default HTTP server  
Uncheck to override settings for default HTTP server settings.

**URI**  
http://192.168.1.99:1880/mbus

Figure 4.8: Elvaco interface showing push report settings

The key settings, those that underpin the understanding of the uncertainty of time created by the M-Bus system, are the ‘Value Period,’ the ‘Value Interval,’ ‘Readout Schedule’ and the ‘Report Schedule’. Readout Schedule gives the frequency at which meter values are stored in the M-Bus Master. The Report Schedule defines the interval at which the M-Bus sends reports to the MQTT server. The Value Period and the Value Interval define the content of the report. The Value Period defines the length for period back in time (before the time at which the report is sent), for which values should be included. It is given as a multiplier. Here it is set to 5 minutes, meaning values stored in the last 5 minutes will be sent. The Value Interval defines the interval between consecutive readings. The Value Interval determines the time between each reading in the reports. In this case, the Value Interval is set to 5 minutes.

The time intervals for the setting variables Value Interval, Value Period, Readout Schedule, and Report Schedule were all set to 5 minutes enables a report to be sent every 5 minutes containing the batch of data collected in the last 5 minutes. The values being stored in the Master are 5-minutely as dictated by the Readout Schedule.

## 4.7 Master Data Collection Impact on Timestamping of Meter Data

This section is a discussion of the time uncertainty in the data that is introduced by the various processes that are involved in the data collection done by the Master. To remind the readers, the data collection process is as follows. The Master connects to one heat meter at a time to collect data for all variables measured and derived by the heat meter. Once a batch (i.e., one round of data collection from the whole group of heat meters) is collected, it is stored in the Master. The Master then compiles a report using the stored data and sends it to the MQTT server. The data is then sent to the hw12 (through the hw1 server, which anonymises the data). The hw12 server routes the data into Dropbox.

The time taken for the Master to collect a batch of data will be termed  $t_{lap}$ .  $t_{lap}$  is dependent on the speed at which data travels through the wiring system and the error response mechanisms defined for the M-Bus system. The time between the start of a lap and when the Master contacts a given heat meter will be termed,  $t_{collect,n}$ , where n references the specific HIU. The order in which the Master visits the heat meters does not change. Thus  $t_{collect,1}$  will always be shorter than  $t_{collect,2}$ , for example, but the values of  $t_{collect,1}$  and  $t_{collect,2}$  itself may vary depending on the errors encountered.

$t_{publish}$  is the time between when the first datum of a batch is published (sent from the Master) and when the last datum of a batch arrives at a server to be timestamped. A subset of  $t_{publish}$  is the time taken for timestamps to be assigned to the entire batch. Timestamping occurs at the hw1 server. Timestamps are given to each reading value in the data as it comes through, resulting in a variance of around 2 seconds across the timestamps of one batch.

$t_{publish}$  is dependent purely on internet speeds that apply between the moment of publishing and moment of reception at the server.  $t_{publish}$  will be taken to be negligible because the impact of internet speeds is likely only to be significant when dealing with datasets that are considerably larger than the batches collected by the Master.

There are ~150 HIUs on site that are connected to the Master. The ‘missing’ heat meters may be because of faulty wiring leading to a subgroup of the heat meters being disconnected from the Master. Or it could be that  $t_{lap}$  is longer than the 5-minutely readout schedule, leading to the Master restarting the lap before all heat meters have been connected to. This will depend on the algorithms defined of the Master. A large number of HIUs for which the data collected was deemed of sufficient in volume and quality was selected (discussed in detail in Section 5.2).

## 4.8 Data Collection Locations

Data for this study was downloaded in two ways. Any remote server can connect to the hw12 server to collect data locally. The author’s secure laptop was set up to do so using the Node-Red software. Data collection on the laptop was ongoing, collecting readings as and when they came through on the laptop. As a back-up, Heatweb Ltd. set up the hw12 server to save data to a secure Dropbox account as well. The hw12 server sends a batch of readings at midnight every day to a secure Dropbox account. The data analysis was carried out using the data collected on the Dropbox account as it was subject to fewer disruptions than the laptop; however, there was a major period of disruption which will be discussed in a proceeding section.

## 4.9 Timestamping

### 4.9.1 Heat Meter Data

The heat meter data is time-stamped when it arrives at the hw1 server. The data is posted in 5-minutely reports by the Master. All the data in a batch is assigned a timestamp within a space of 2 seconds, as detailed in the previous section. The variance in the timestamps in a batch are because of the time it takes for the datum to be timestamped one value at a time.

### 4.9.2 HIU Sensor Data

The HIU sensor data is not limited by the M-Bus slave master set up and is transferred through the hardware on site and to the hw12 server as and when a reading is taken. Thus, timestamps are assigned individually to each reading when it arrives at hw1.

## 4.10 Data Quality Maintenance

The data collection system was unprecedented because of its high frequency nature and because it collected data from all the HIUs in the HN. Existing BMS systems monitor data but, as far as the author is aware after visiting several DHS systems (Redhill, UCL, King's Cross) and through what is documented in research literature and government literature, none monitor at the level that Heatweb Ltd. do. Moreover, the use of the collected data for demand research, or any research, is rare in the UK.

The data sets being collected by Heatweb Ltd. are not monitored by them (the HN operators were monitoring the data for operational purposes; however, the author had no communication with them), and therefore they seldom caught faults or errors. Thus, the responsibility of maintaining data quality fell on the hands of the author, with the power of controlling the data collection system being accessible only through Heatweb Ltd. In practice, this meant that the continual process of maintaining data quality, i.e., identifying issues with data, reporting it to Heatweb Ltd., Heatweb Ltd. diagnosing the issue, and fixing it, was a slow one. The author collected data by connecting to the online server but had no access to or control of the system itself. When issues were spotted in the data, these were communicated to Heatweb Ltd. who made themselves available for support in such circumstances. Because the system was new and being used for the first time, there were several issues that affected data collection that will be discussed below. Improving data quality and maintaining it to a standard was difficult due to the complexity of the system, the involvement of various other third parties that had access to certain parts of the system who were unaware of the ongoing data collection and the author not having the power to solve issues immediately as they arose.

Third parties having access to the data collection system meant that the data would need to be constantly monitored. The author decided the best way to approach this is to spend time visually inspecting data from the key variables each day for the previous day of data. The paragraphs below give examples of the kinds of data quality issues that were experienced. At the height of problems, for a period of about 4 months at the start of data collection, issues of varying nature and significance were faced weekly, and sometimes more frequently. Table 4.2 below summarises the key events, including some of the major issues encountered along the way. Some of the major data issues include a major disruptive event when an important

piece of hardware, the modem in the plant room, was stolen and had to be replaced. The metering and billing company has access to the hardware, and on at least one occasion, changed settings on the main metering hardware which led to the sampling rate of the metered variables increasing. During the Christmas holidays in 2021, the memory of the SD cards on the modem ran out. This led to a period of almost a month of zero data collection. In another instance, meter data inexplicably had periodically larger sampling times; the reading that followed the reading that came through at approximately 42 minutes past each hour came through at closer to ten minutes later. This is significantly larger than the usual sampling time which is approximately 5 minutes. The presence of this peculiarity could have been down to a number of reasons, including the relationship between the settings of the M-Bus Master controller program, Elvaco. Experimentally changing the settings to test the impact on sampling time would have potentially led to a day's worth of data with odd and inappropriate sampling times. Heatweb Ltd. are not able to diagnose errors that arise at the Master in the same way that they are able to diagnose their own Node-HIU system. Diagnosing errors that arise at the Master would require contacting the Master manufacturers, Elvaco who would charge a fee for any advice or input. Heatweb Ltd. were understandably reluctant to proceed with diagnosing Master errors beyond a certain point. Hence the periodically larger sampling time issue was left unresolved. After extensive discussions with Heatweb Ltd. about the source of the missing data, a conclusion was reached that the source cannot be known and was therefore not investigated further.

In the 1<sup>st</sup> quarter of 2021, the data collection system at Heatweb Ltd. was introduced through an online demo provided by them. The demo proved that the data being provided could be useful for the research. The author used Node-Red to connect the cloud server to the sites to enable data collected from the sites to be stored. Initial sets of variables were selected for which data was to be collected for (through Node-Red) and an increasing number of dwellings slowly came online, as they were being connected up on site by Heatweb Ltd. By the end of the 1<sup>st</sup> quarter data was being collected for up to 300 dwellings; however, a continuous stream of snags on the collection system needed to be continuously resolved. In the second quarter, with the volume of data transferred being high, the local server ran out of space, and a second laptop was connected. Data collection was also set up in Dropbox by Heatweb Ltd. as a back-up location. Data quality checks for the Dropbox data were conducted to ensure that the data quality was the same as for the local server data. In the 3<sup>rd</sup> quarter of 2021, data cleaning started, and data continued to collect. In the 4<sup>th</sup> quarter, two major data loss issues were encountered: one resulting from the modem on site being stolen, resulting in data loss that affected 1.5 months, and the second data loss relating to an accidental overwriting of data on the local server that included data from most of Q3 and some of Q4. In the 1<sup>st</sup> quarter of 2022, M-Bus settings were set to send data for meter variables every 5 minutes ready for data collection in the coldest week of the data collection period. Table 4.2 summarises the data collection process from start to finish, including notes on the major data issues encountered.

Table 4.2: Table showing the key events and processes relating to the data collection

Quarter-Year	Month	Data Process	Notes
Q1 - 2021	February	<ul style="list-style-type: none"> <li>- Scoping Heatweb Ltd. data collection system using their online demo.</li> <li>- Setting up connection to Heatweb Ltd. data system through Node-Red on local device (laptop) to begin data collection (initially for 2 dwellings only).</li> <li>- Refining architecture of data collection (i.e., which variables and dwellings).</li> </ul>	<ul style="list-style-type: none"> <li>- Data collection issue: on site SIM bandwidth which was initially restricting the volume of data being transferred was increased.</li> <li>- Data for an initial set of channels (or variables) were explored.</li> </ul>
	March	<ul style="list-style-type: none"> <li>- 300 dwellings now connected (including from a second site).</li> </ul>	<ul style="list-style-type: none"> <li>- Data collection issue: 16 dwellings communication was found to be dead due to a cable issue and resolved before the end of the month.</li> <li>- Data consistency issue: A group of dwelling were providing only 4 data points a day.</li> </ul>
Q2 - 2021	May	<ul style="list-style-type: none"> <li>- Local device ran out of space, a second laptop is set up to collect data.</li> </ul>	<ul style="list-style-type: none"> <li>- Setting up collection on Dropbox discussed.</li> </ul>
	June	<ul style="list-style-type: none"> <li>- Dropbox data collection set up.</li> </ul>	<ul style="list-style-type: none"> <li>- Dropbox data quality tested.</li> <li>- Data collection issue: Time zone issue of incorrect noted in Dropbox data and resolved in one month.</li> </ul>
Q3 - 2021	July	<ul style="list-style-type: none"> <li>- Occupancy and floor area data received in .csv files separately to the data collection system.</li> </ul>	
	September	<ul style="list-style-type: none"> <li>- Data collection continues, and quality checks are done periodically.</li> </ul>	<ul style="list-style-type: none"> <li>- Data collection issue: Site visit revealed 40 dwellings had lost connection due to a power surge and resolved by connecting back up in weeks after issue was noted.</li> </ul>
Q4 - 2021	October	<ul style="list-style-type: none"> <li>- Data cleaning begins.</li> </ul>	
	November	<ul style="list-style-type: none"> <li>- Data cleaning continues.</li> <li>- Demand estimation methods testing begins.</li> </ul>	<ul style="list-style-type: none"> <li>- Data loss issue: significant loss of data, including meter variables, (starting mid-October) due to Modem being stolen. New modem installed at the end of this month. Data loss affected 1.5 months.</li> <li>- Data loss issue: significant data loss on local device due</li> </ul>

			to accidental overwriting. Data loss affected all data from June-September.
	December	<ul style="list-style-type: none"> <li>- Stolen modem restored.</li> <li>- Demand estimation methods testing continues.</li> </ul>	- Data loss issue: data loss due to memory card in hardware on site running out resulting in data loss affecting just under a month.
Q1 - 2022	January	- MBus setting adjusted to send meter variable readings at 5-minutely intervals (initially set to one hour).	- Data from this period makes up the main set of data used in the study.
	February	- Data collection ceases.	

#### 4.11 File Format of Collected Readings

The readings are compiled into csv format files, one for each variable. The variables include measured variables (measured by the sensors installed in the HIU and the sensors of the heat meter) as well as derived variables. Data collection took place for all available variables although only a handful were required to estimate demand. This was done to make any additional analysis using the remaining variables possible if it were required at some point in the future, in the author's own work but also for other researchers that would find the data valuable. The files divided the data into three columns: a date time column, an "id" column and a value column. The date time column gave the timestamp corresponding to the reading. The anonymous "id" column gave the id of the HIU. Finally, the value column contained the value for the variable in question. For both HIU sensor data and meter data, the file formats were identical and gave readings on an event basis.

#### 4.12 Measured Variables and Measurement Errors

Decisions on which variables were measured were made by Heatweb Ltd. prior to any contact with the author and therefore was not influenced by what was required for the work in this thesis. As mentioned in the previous section, although both, the measured and derived, variables were extensive and could be valuable for other research, for the work in this thesis it was decided that the most appropriate variables to use would be a subset of the measured variables. Table 4.3 below gives the variables that were considered in the methods (described in full in Sections 5.2.2 and 5.2.4 which outline how the DHW demand and the total demand was determined), along with their sampling times and the tags they were given in the data collection system. Table 4.4 gives the measurements errors for some of the considered variables. Note that in some of the sections that follow in the thesis, the variables are referred to using their tags for clarity.

*Table 4.3: Key measured variables, their identifier tags and sampling times*

Measured Variable	Sampling Time	Unit	Tag
Instantaneous metered demand	Approx. 5-minutely	kW	meter_kw
Cumulative metered demand	Approx. 5-minutely	kWh	meter_kwh
Cold water inlet temperature	1 second	°C	dat_tCo
DHW flow rate	1 second	l/m	dat_fC

Thermostat call (used in results for illustrative purposes only)	1 second	On/off	dat_stat
Primary hot water temperature	1 second	°C	dat_tH
Primary return (from DHW heat exchanger) flow rate	1 second	l/m	dat_fHDDHW
Primary return (from DHW heat exchanger) temperature	1 second	°C	dat_tHoDHW
Primary return (from SH heat exchanger) flow rate	1 second	l/m	dat_fHCH
Primary return (from SH heat exchanger) temperature	1 second	°C	dat_tHoCH
Metered flow rate	Approx. 5-minutely		meter_fR

Table 4.4: Measurement errors of the key measured variables

Variable	Measurement Device	Measurement Error
dat_fC / cold mains flow rate	Sika VTY10 (SIKA Systemtechnik, 2023)	<b>Accuracy:</b> +/-1% of range <b>Range:</b> 1-30 l/min <b>Signal output:</b> from 0.7 l/min
dat_tCo / DHW flow temperature	Tasseron NTC sensor – short thermistor- type SNTC 10K3 A34 (Tasseron, no date)	<b>Range:</b> -20 - +105°C <b>Tolerance:</b> 3% at 60°C
dat_tC / cold mains temperature	Assumption	
dat_tHoDHW/ DHW return temperature	Tasseron NTC sensor – short thermistor- type SNTC 10K3 A34 (Tasseron, no date)	<b>Range:</b> -20 - +105°C <b>Tolerance:</b> 3% at 60°C
dat_xDHW/ DHW stepper motor position	Valve: MUT VDE-ML (Mut Thermal Systems Solutions, 2023) Actuator: Sonceboz stepper motor 7217 -4.0 (Sonceboz, no date)	No measurement error
dat_fHDDHW/ DHW return flow rate	Internal estimate	Unquantified
dat_tH/ primary hot water temperature	Tasseron NTC sensor – short thermistor- type SNTC 10K3 A34 (Tasseron, no date)	<b>Range:</b> -20 - +105°C <b>Tolerance:</b> 3% at 60°C
dat_xCH/ SH stepper motor position	Valve: MUT VDE-ML (Mut Thermal Systems Solutions, 2023) Actuator: Sonceboz stepper motor 7217 -4.0 (Sonceboz, no date)	No measurement error
dat_fHCH/ SH flow rate	Internal estimate	Unquantified
dat_tHoCH/ SH return temperature	Tasseron NTC sensor – short thermistor- type SNTC 10K3 A34 (Tasseron, no date)	<b>Range:</b> -20 - +105°C <b>Tolerance:</b> 3% at 60°C

### 4.13 Uncertainty in Meter Variables

There are several sources that introduce complexity to the uncertainty in the metered variables, the key variable being the meter\_kw variable. The uncertainties that apply to the meter\_kw variable is described in the following points.

- The meter\_kw variable is derived from the flow and return temperatures, and the flow rate measured in the heat meters. These variables have a measurement error introduced by the physical limits of the flow and temperature sensors. However, the following was stated by the primary practitioner at Heatweb Ltd. about the uncertainty in the heat meters used at the case study site: "Heat meters have matched sensors and therefore have a different level of accuracy compared to sensors elsewhere; heat meter sensors are substantially more accurate. They also fall under a different category of standards because they are finance and billing related" (Hanson-Graville, personal communication, September 2019). This suggests that the meter sensor measurement uncertainty is much smaller than for the other sensors in the system.
- There is a time lag between when a meter\_kw data point is collected from a heat meter by the Master and when that data point arrives in the server where timestamping occurs. This leads to a time lag between what shall be called the *real* timestamp and the *given* timestamp of a data point.

The uncertainty referred to in the first point can be derived by treating the measurement errors as random errors and applying the appropriate error propagation rules. The background for understanding the uncertainty in time, referred to in the second point above, is given in Section 4.4 and Section 4.7, where the processes of meter data collection are described. To restate the relevant part, the time lag between when a datum is collected and when it is timestamped is dependent on how far into  $t_{lap}$ , the time taken for the Master to complete one round of data collection from the HIUs, the datum was collected and  $t_{publish}$ , the time taken for that batch to be received at the 'hw12' server after being published by the Master. For example, the time lag may be larger if many errors were encountered in the data collection which would increase  $t_{lap}$  altogether. Thus, for a given HIU, if there were many errors encountered after its datum was collected, the lag time for that particular datum increases. Although  $t_{lap}$  and  $t_{publish}$  are not directly quantifiable, they can be qualified in the following way.

The primary practitioner at Heatweb Ltd. assured the author that  $t_{lap}$  is shorter than the readout schedule, the time interval between two batches of data being collected, which is equal to 5 minutes.<sup>4</sup> Although there is a possibility that  $t_{lap}$  exceeds 5 minutes, such an event would be extremely rare (perhaps resulting from an inordinate amount of errors being encountered in the data collection), and thus, on the authority of Heatweb Ltd. it is assumed that  $t_{lap}$  is shorter than 5 minutes.<sup>5</sup> Considering that  $t_{publish}$  can be assumed to be negligible

---

<sup>4</sup> The report schedule, the time interval at which a batch of data is published, also comes into play, but can be considered as having no real effect when it is set to equal the readout schedule, which it was.

<sup>5</sup> One way in which quantifying  $t_{publish}$  and  $t_{lap}$  could be attempted is by systematically changing the settings on Elvaco to change the report schedule and the report content. If  $t_{lap}$  is longer than the readout schedule it would mean that the Master is forced to publish the batch of data before completing data collection from all HIUs resulting in an incomplete batch of data being published. Thus, as a test, the readout schedule could be systematically changed to investigate the impact it has on the number of heat meters from which data is

due to it being dependent on internet speeds, it can be concluded that the real timestamps of the readings are in the 5 minutes prior to the time stamps being assigned. Thus, for a given reading, it can be said that the maximum lag between the real timestamp and the given timestamp is a maximum of 5 minutes. Given this, an upper bound of ~ 5 minutes can be defined for this uncertainty. Note that the order in which the M-Bus Master interfaces with the heat meters is the same every time it collects a batch of data, thus it is likely that the last HIU in the line-up will have the smallest uncertainty and vice versa, albeit all below 5 minutes.

---

*collected. If increasing the readout schedule to 1 hour leads to data being collected for 170+ meters, it can be concluded that  $t_{lap}$  must lie somewhere between 5 minutes and 1 hour. However, doing so would mean that the resulting data would have a much larger sampling time of around 1 hour. Thus, although testing could inform the time uncertainties at play, it risks limiting the data and producing messy variance, which would in turn impact the analysis. For this reason, no such testing took place, and the data that resulted from the reporting schedule and content set by Heatweb Ltd. was deemed appropriate for the analysis that is required in this work.*

## 5 Results 1 – Generating Demand Profiles

### 5.1 Introduction and Relevant Objectives

The key results of this chapter are the estimated demand profiles, which are presented along with an examination of the methods by which they were obtained. This chapter pertains to the research question and objective in bold below:

- *What is the real diversity effect in UK HNs?*
  - **Estimate the individual demand profiles of dwellings on a real HN using measured data.**
  - Analyse the impact that aggregation, over number of dwellings and over time, has on the demand.

This chapter begins by describing the earliest cleaning stages that the data were put through which involved assessing over 50 variables for their data volume and identifying the variables for which the data volume was sufficiently high. The chapter then goes on to assess the methods by which the identified variables could be used to determine the DHW demand and the total demand. The latter sections of the chapters present the demand estimations obtained using the selected methods. The chapter closes with a summary and discussion of the key results.

### 5.2 Methods

With the intention of making full use of the richness of the available multi-variate data, several variable option sets were investigated in order to determine demand. Considerable effort was focussed on generating comprehensive, reliable, and accurate demand profiles by considering each of the viable variable sets. The processes that this required can be broken down into the following stages: cleaning of the data set, selecting variables that are eligible for use in determining demand, defining the different routes through which the variables could be used to determine demand, and finally testing the routes.

The following section describes the variable option sets, deriving the uncertainty associated with the use of each, and selection of the most appropriate given these findings.

#### 5.2.1 Data Quality and Cleaning

This section gives an overview of the dataset and describes the earliest stages of cleaning by illustrating the range of variables (51 in total) and the variability between dwellings (337 in total) with regards to how much data was available for each variable. The period from which data was used was the month of October in 2021. The intended analysis focussed on the heating season and October was the most recent coldest month for which data was available at the time at which data cleaning began and was therefore used to indicate the quality of data for the rest of the heating season. As the data quality was being assessed, the data collection system was being adjusted to provide data in the format that was most appropriate for the research and being corrected for faults as they were being discovered (described in full in Section 4.10). For example, multiple days' worth of data was missing for meter measurements due to the data collection system failing to connect to the server. As a result of these adjustments and fault corrections, the data quality of the data being collected after

October is significantly higher than it was in October. This improvement is expressed fully in Section 5.3.

The diagrams below give a map of the reading count across all measured and derived variables and across dwellings for the two HNs for which there was data. Derived variables refer to those calculated internally in the data collection system. White spaces indicate that no readings of the given variable are present for the given dwelling. As can be seen, there are some variables for which many dwellings provide similar amounts of readings. To select a set of variables for which there was enough readings for each individual dwelling to be used in the key analyses, the variable set was put through a process of iterative cleaning, starting by removing the variables with 0 readings across all dwellings.

Figure 5.1 gives the reading counts for all dwellings across both HN sites; the largely grey and largely pink blocks indicate the dwellings from each HN. The labels on the right-hand side (predominantly pink blocks) are dwellings from Site I, and the remaining labels are for Site W. This chart shows that there is more data available for a larger number of dwellings for Site W compared to Site I. Thus, for determining demand, data from Site W will be used.

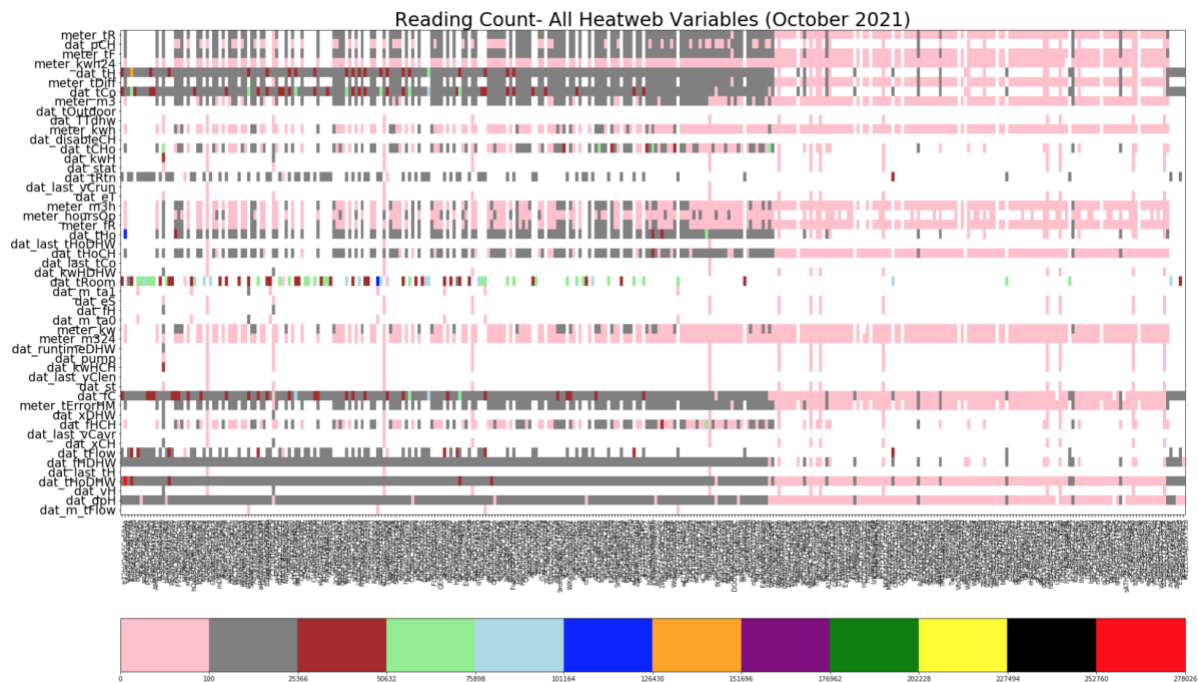


Figure 5.1: Reading count map for all variables and dwellings across both HNs. Note that x-axis markers are dwelling IDs and are provided only as an indication of the number of dwellings and are not meant to be legible. The y-axis gives the variables in their original tags.

Figure 5.2 gives the reading counts for the subset of HIUs from Site W alone. Figure 5.2 also shows that there are some variables for which the majority of dwellings do not have any readings. To study diversity in demand, the size of the group of dwellings studied must be of a substantial enough size to capture the full effect. Therefore, the data was cleaned based on the criteria that a given variable must have data for more than 30 dwellings as a minimum. Further cleaning is done to remove variables that give duplicate information. For example, ‘meter\_kwh24’ gives the daily sum of ‘meter\_kwh’ readings; the former can be calculated using the latter, and therefore, in essence, both of these variables give the same information. Variables such as these are removed.

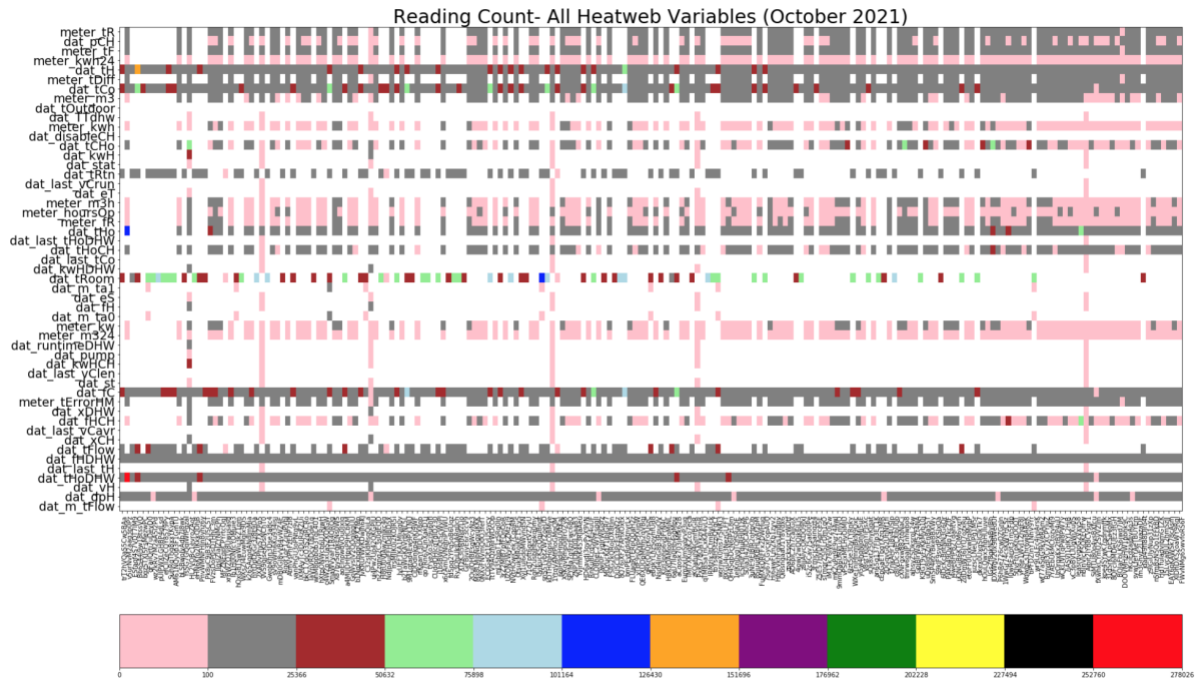


Figure 5.2: Reading count map for all variables and the subset of dwellings from Site W. Note that x-axis markers are dwelling IDs and are provided only as an indication of the number of dwellings and are not meant to be legible.

Figure 5.3 gives the reading counts for dwellings across both networks after variables with data for less than 30 dwellings were removed, as well as the variables giving duplicate information. Figure 5.4 gives the reading count for the subset of dwellings in Site W after the same cleaning processes. The remaining variables, 21 in total, show much fewer white spaces, although not completely zero.

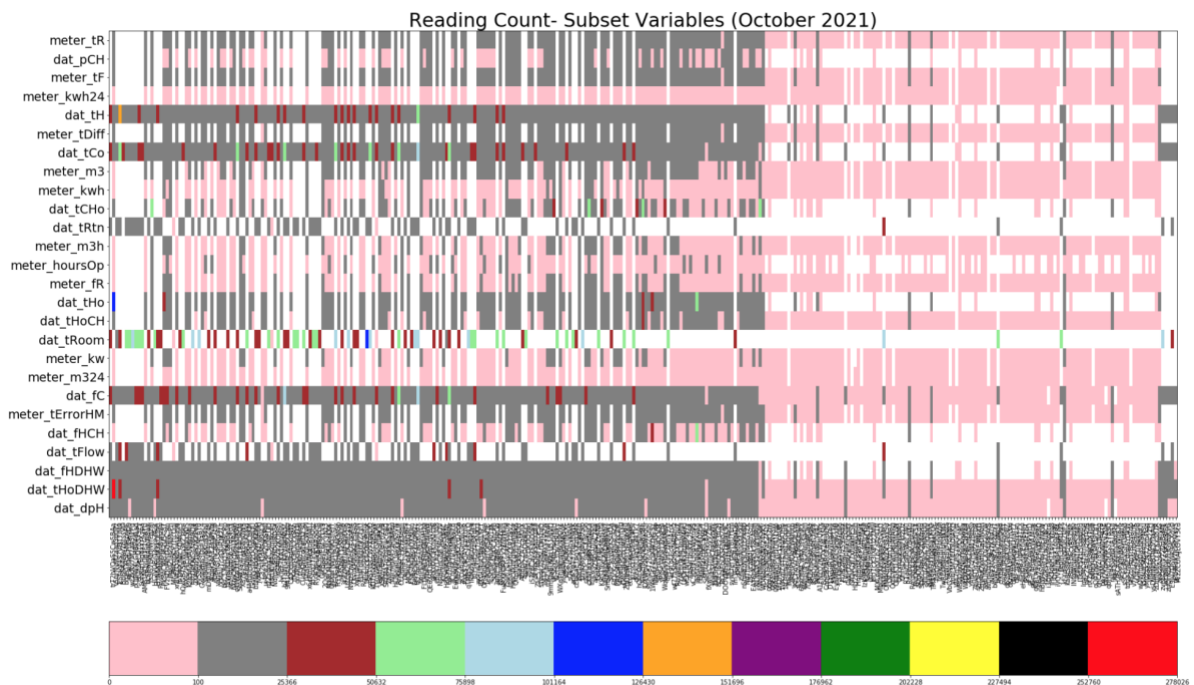


Figure 5.3: Reading count map of cleaned variables and dwellings across both HNs. Note that x-axis markers are dwelling IDs and are provided only as an indication of the number of dwellings and are not meant to be legible.

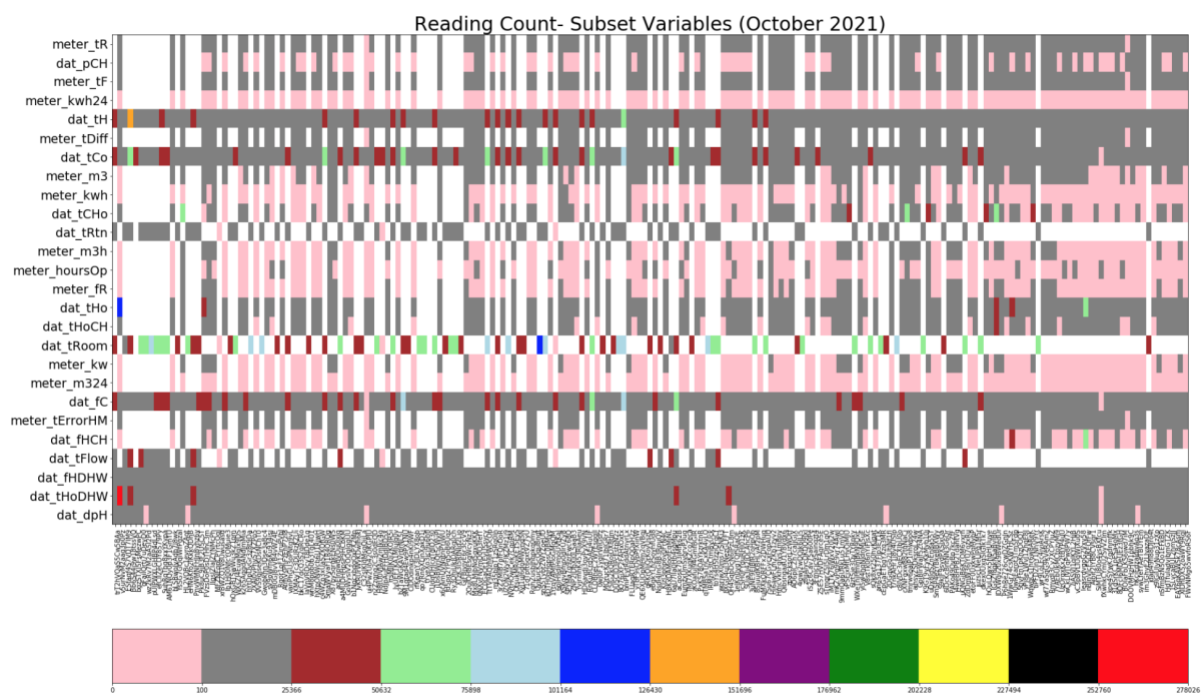


Figure 5.4: Reading count map of cleaned variables and the subset of dwellings in Site W. Note that x-axis markers are dwelling IDs and are provided only as an indication of the number of dwellings and are not meant to be legible.

The cleaned subset of variables was investigated in order to determine which of these variables could be used to produce robust estimates of demand, for example, by taking into consideration the uncertainty in resulting demand. This process is described in full in Section 5.2.2.

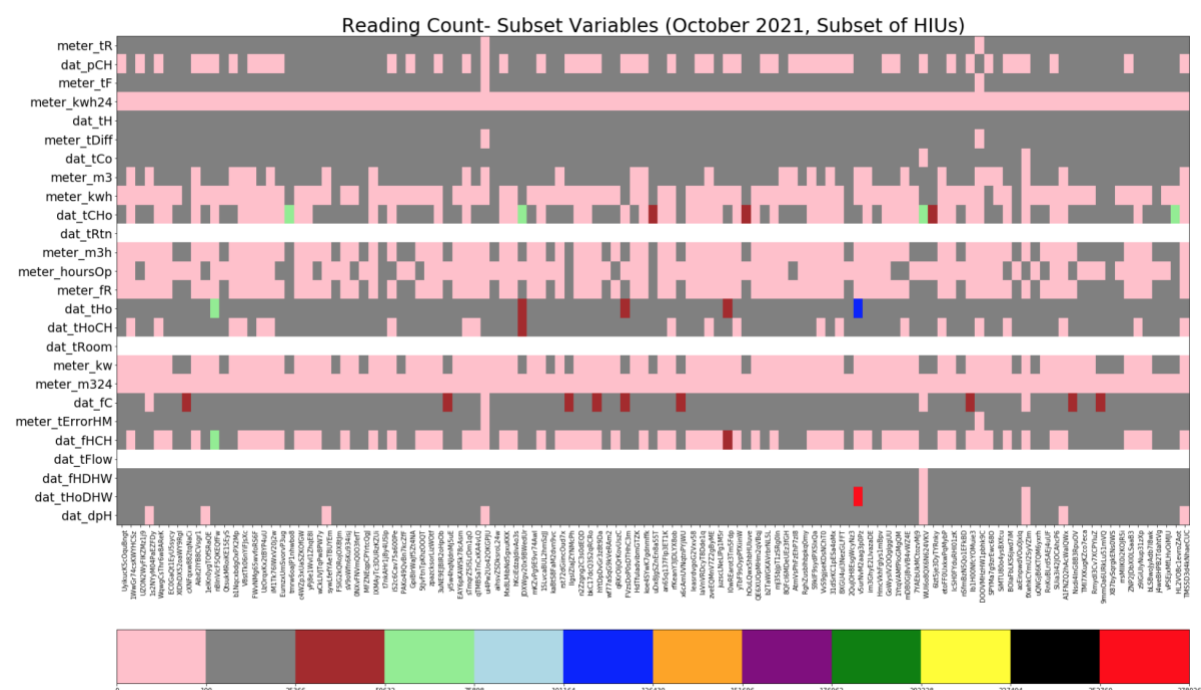


Figure 5.5: Reading count map of subset variables and subset of dwellings. Note that x-axis markers are dwelling IDs and are provided only as an indication of the number of dwellings and are not meant to be legible.

The dwellings in Site W, of which there were ~200, were put through cleaning processes to identify a subset of dwellings of 115. Dwellings where there was an absence of occupants for one or multiple days were removed by identifying the dwellings where the DHW flow rate remained at 0 l/m for a whole day. This resulted in 190 remaining dwellings. From these 190, the dwellings were further selected for data presence across all desired variables at the required frequency and for the necessary period of time. This resulted in a subset of 115 dwellings.

Out of the total selected set of 115 dwellings, for which demand was determined, 96 were selected into a further subset. For the analysis of the impact of storage on demand and HN design, a section of the case study HN, consisting of 96 dwellings chosen at random, was modelled. 96 dwellings were chosen because the part of the case study HN for which the distribution system was modelled consisted of 96 dwellings. This part of the case study HN was chosen because it constituted a self-contained network topology that had the largest number of dwellings that did not exceed the sample size for which high-quality clean data was available. The data quality for the dwellings in this subset is shown below in Figure 5.5, and Figure 5.6 and Figure 5.7 give the design occupancy and the floor area respectively for the 96 selected dwellings. For the variable of return temperature on the primary side of the DHW heat exchanger, there is one dwelling that has provided a significantly large number of readings (red block). Although unusual, this is a possibility in a system that reads by exception (i.e., event-based reading). Regardless, this variable was not used in generating demand and so further investigation was not required.

The design occupancy of 55 of the dwellings is 2 occupants (1 bed), 31 of the dwellings have a design occupancy of 4 occupants (2 bed), 6 dwellings have an occupancy of 6 people (3 bed), and finally, 4 have an occupancy of 3 occupants (2 bed), as summarised in Figure 5.6. The floor area of the dwellings has a range from 47 m<sup>2</sup> to 124 m<sup>2</sup>, with the most dwellings having a floor area of 40-49m<sup>2</sup>.

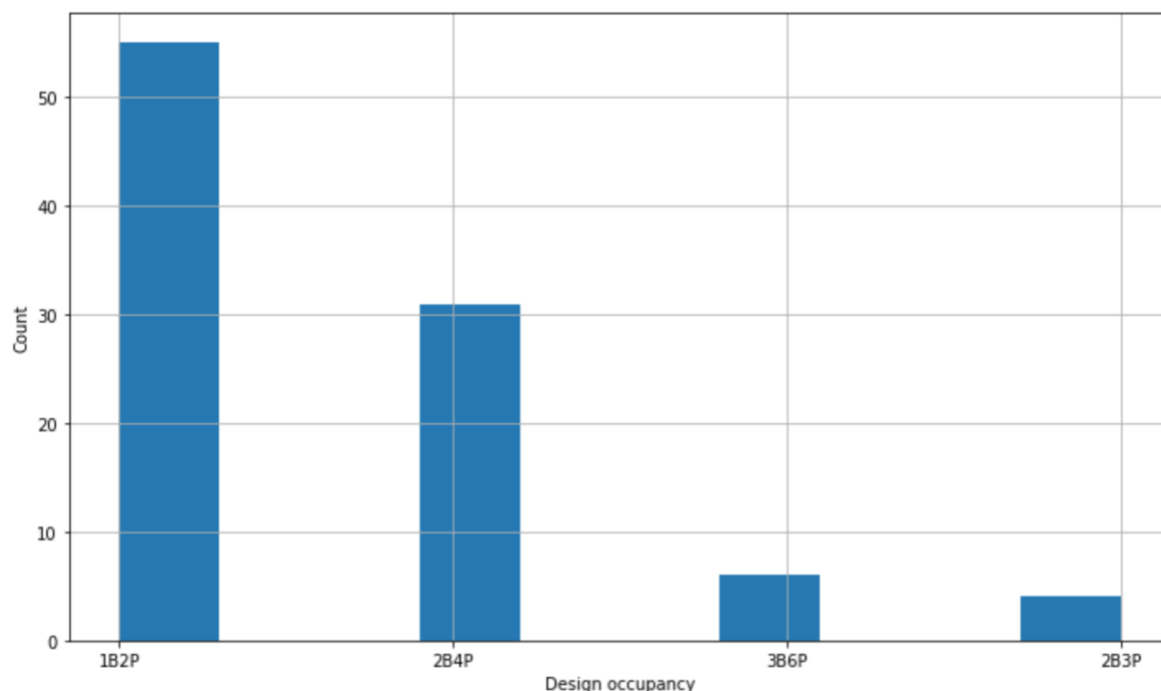


Figure 5.6: The design occupancy (P) and number of bedrooms (B) for the sample of HIUs

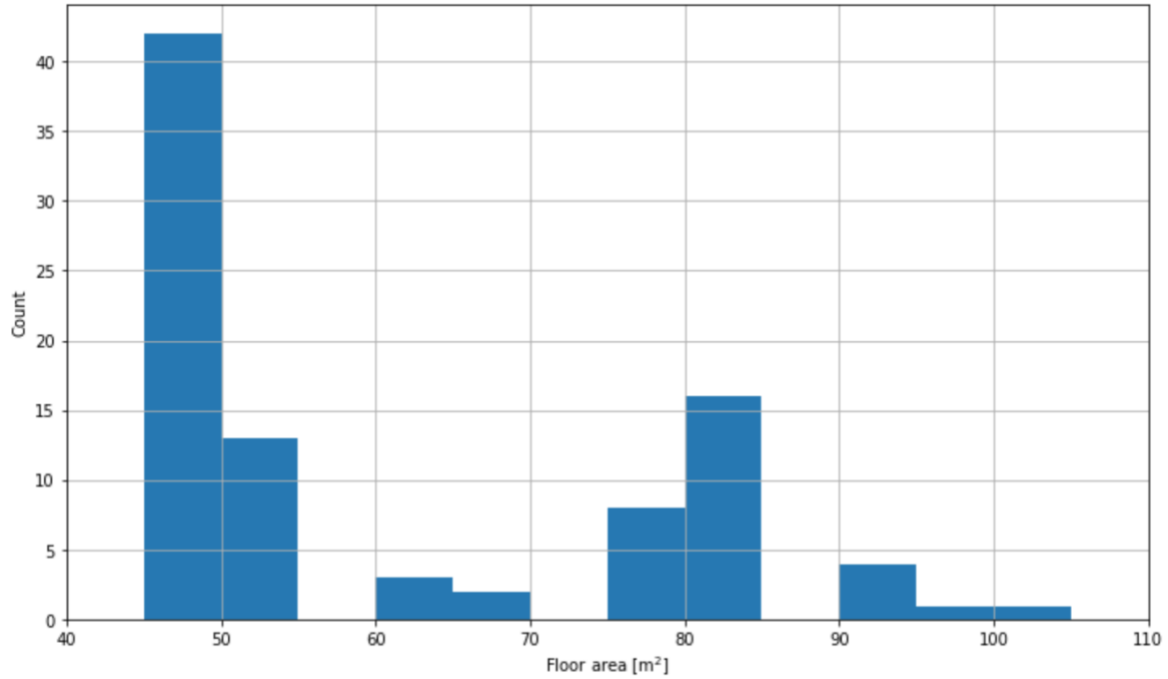


Figure 5.7: The floor area of dwellings in the case study HN

## 5.2.2 Determining DHW Demand

### 5.2.2.1 Selecting Measured Variables

The following section describes the variable option sets viable for use in determining demand and the uncertainty associated with using each. From the subset of variables that resulted after the cleaning stages, described in the previous section, the author identified the sets of variables with which demand profiles could be generated. In order to select the most viable set, the uncertainties in each set and the resulting uncertainty on demand were considered at length. The schematic shown in Figure 5.8 below gives the key sensor locations and denotes the variable measured at that location; shorthand tags are used to denote the measured variable.

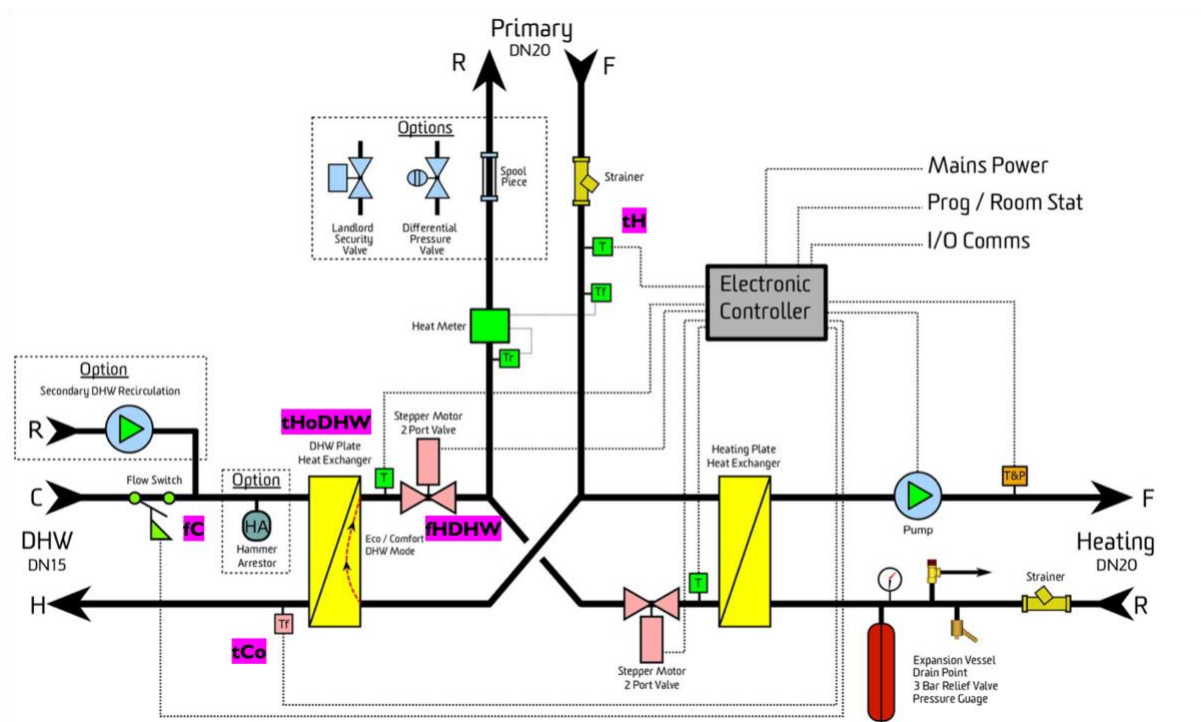


Figure 5.8: Schematic of the HIU where the key measured variables considered in determining DHW demand and the rough positions of the corresponding sensors are denoted (Heatweb Ltd., no date c)

In estimating the DHW demand, there are three sets of variables that can potentially be used;

1. Primary flow temperature (denoted by the tag 'tH'), primary return temperature ('tHoDHW'), and estimated DHW circuit primary flow rate ('fHDHW'),
2. Secondary outlet temperature ('tCo') and secondary cold mains flow rate ('fC') with assumed mains cold temperature,
3. Metered flow rate (monitored at heat meter- green box in Figure 5.8) and primary flow temperature ('tH'), and primary return temperature ('tHoDHW').

The primary flow rate of the DHW circuit ('fHDHW') is an internal estimate (further details in Appendix A, Section 11.1) that is based on the estimated differential pressure, the measured valve position ('xDHW'), and the pressure loss curve for the valve. The logic used to estimate the differential pressure is dependent on several measured variables, as well as on an assumed cold mains inlet temperature. Its error is therefore a function of the error in the assumed cold inlet temperature and the error in the other determining parameters. The differential pressure estimate can be updated only during stable tap operation, resulting in an uncertainty that is higher still when assuming differential pressure for non-stable periods of operation, which is taken to be the value of differential pressure during the last stable period of operation. The flow rate estimation ('fHDHW'), which carries forward the uncertainty in the differential pressure, therefore results in a complex uncertainty that is difficult to quantify.

Metered flow rates, on the other hand, have a much lower uncertainty than the estimated flow rate because they are measured directly. Having said this, the 5-minute sampling period of the metered flow rates is lower than that of the estimated flow rate ('fHDHW'). At a

sampling time of 5 minutes, the likelihood of capturing DHW events in full is significantly reduced as they occur over much shorter time periods. Due to this reason, metered flow rates will not be considered further. Since the sampling period of the meter flow rates render them inappropriate for use in capturing transient DHW events, variable set no. 3 will not be used in determining DHW demands. This leaves set 1 and set 2.

Sets 1 and 2 both assume a cold-water inlet temperature, and thus, both have an error associated with this. However, in the use of set 2, this error is applied directly to the demand, whereas in the use of set 1, this error is applied indirectly and alongside numerous other errors through the complex logic used to determine the differential pressure and therefore also the flow rates. Based on the considerations, the second set of variables ('tCo', 'fC', and assumed cold water inlet temperature), whose uncertainty comes only from the cold mains temperature assumption and the error in the temperature and flow rate sensors, and which are monitored at a frequency high enough to capture transient DHW events, are used to estimate DHW demand. This results in a demand profile that captures all DHW activity and with a low uncertainty. The cold mains temperature is evidenced to be a stable figure that corresponds to the annual mean outside air temperature which, in the UK, is around 10°C (Energy Savings Trust, 2008). The assumed cold inlet temperature is therefore taken to be 10°C. Figure 5.13 which shows the minimum hot water temperatures being ~10°C supports that this may be the case in the case study HN.

#### 5.2.2.2 DHW Demand Calculation and the Associated Error

The determinants of DHW demand in an individual dwelling for a given time,  $i$ , can be described by the equation below.

$$Q_{dhw,i} = \dot{m}_{dhw,i} c (T_{dhw,H,i} - T_{dhw,C,i}) \quad (5-1)$$

The errors in the mass flow rate,  $\dot{m}_i$ , and the temperature of hot water,  $T_{dhw,h,i}$  are random measurement errors.  $T_{dhw,c,i}$  is an assumed value with an assumed error. In the context of determining the DHW demand for a single dwelling, the error on  $T_{dhw,c,i}$  can be treated as a random error.

Thus, the resulting error on  $Q_{dhw,i}$  can be derived by applying error propagation rules for random errors.

$$\delta(T_{dhw,H,i} - T_{dhw,C,i}) = \sqrt{(\delta T_{dhw,H,i})^2 + (\delta T_{dhw,C,i})^2} \quad (5-2)$$

$$\delta Q_{dhw,i} = Q_{dhw,i} \sqrt{\left( \frac{\delta(T_{dhw,H,i} - T_{dhw,C,i})}{T_{dhw,H,i} - T_{dhw,C,i}} \right)^2 + \left( \frac{\delta \dot{m}_{dhw,i}}{\dot{m}_{dhw,i}} \right)^2} \quad (5-3)$$

#### 5.2.2.3 Data Cleaning and Filling

Due to the sheer number of dwellings, and therefore the large volume of data (>100 of dwellings, >3 variables, secondly frequency) for which demand had to be estimated, the cleaning and filling processes for the raw data required a bespoke approach that balanced the need to produce robust demand estimates for each individual dwelling and the need to keep the time spent on doing so to a reasonable minimum such that the research project could be completed in a timely manner. With this in mind, the approach taken was to visually inspect the timeseries of the raw data for each measured variable in order to build an understanding of the physical context of the raw data and therefore how that data needed to be cleaned for an individual dwelling, one at a time. Once this process was completed for one dwelling, the process began for the next dwelling. The time taken to complete the process sped up with each dwelling because the heating systems were similar and therefore tended to present similar issues.

The cleaning and filling issues that were present in the data are described below.

- Missing readings at the stopping point of DHW events in the flow rate reading timeseries.

The author identified one kind of missing data that was present in the flow rate measurements; the final measurement that should denote a flow rate of 0 l/m at the end of a DHW event. If left unaddressed, these missing readings would lead to the DHW demand appearing to have a low level 'leak' as a DHW event ended. An algorithm was built to identify and remove these phantom leaks. The missing readings were present across the majority of dwellings; it is expected that the data issue identified in one dwelling is likely to occur in another dwelling because the HIUs are identical and because they all share one data collection system. The algorithm was therefore applied to all dwellings. Finally, the timeseries for each dwelling was inspected visually to ensure that the missing values were addressed and that the 'leaks' were all successfully removed.

- Anomalous readings where the exact causes are unknown were produced at random.

This occurred rarely enough that the dwelling for which there were spurious readings could be removed entirely.

#### *Cold Water Inlet Flow Rate Data*

The timeseries of the raw data for the flow rate was forward filled and is justified as an appropriate filling method based on the data being 'event-based'; readings are filtered at the Node-HIU Switch such that readings come through only if they are different to the previous reading that was allowed through. This results in an 'event-based' series that can be forward filled to reproduce the data points that were filtered out. Figure 5.9 and Figure 5.10 below give example profiles for a single dwelling showing both the raw and the filled flow rate data.

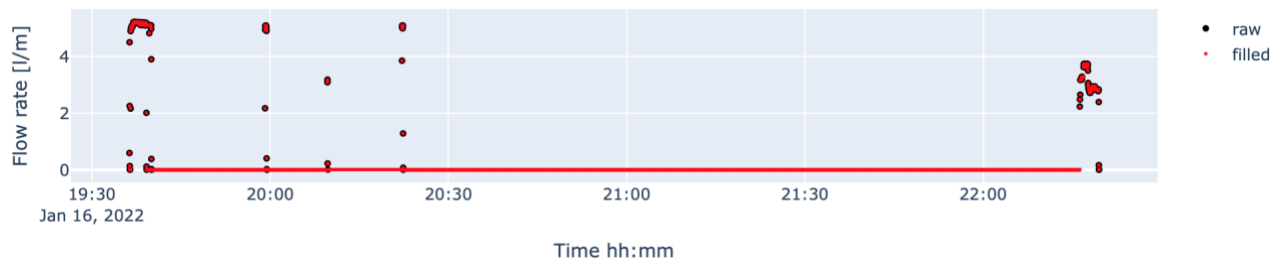


Figure 5.9: A timeseries for an individual dwelling showing the raw data for the flow rate of cold inlet water in the DHW circuit and how it is forward filled to produce a fuller timeseries



Figure 5.10: Close-up of cold flow rate for one DHW event occurring after 19:30

### Flow Temperature Data

Forward filling was applied to the flow temperature data as the raw data was event-based, like the cold-water flow rate data. Moreover, no significant kinds of missing readings were observable in the raw flow temperature data. Figure 5.11 and Figure 5.12 below give example profiles for a single dwelling showing both the raw and the filled flow temperature data corresponding to the same dwelling and event shown in Figure 5.9 and Figure 5.10.

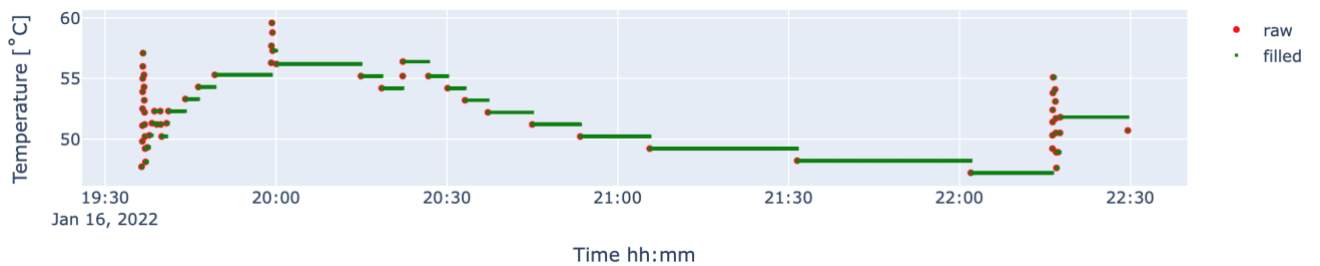


Figure 5.11: A timeseries of an individual dwelling showing the raw data for the flow temperature of the DHW and how it is forward filled to produce a fuller timeseries

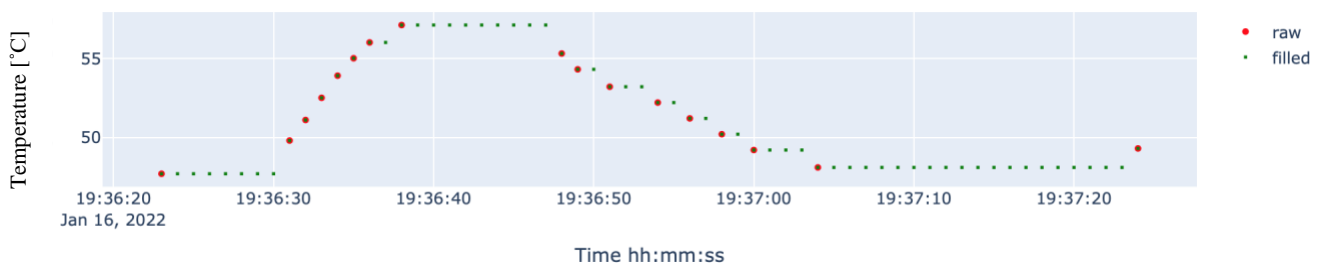


Figure 5.12: Close-up of DHW flow temperature for event occurring soon after 19:30 in Figure 5.11

Figure 5.13 shows a histogram plot for the hot water delivery temperatures across all dwellings. The mean temperature is 47.4 °C, with a maximum temperature of 60°C. The histogram shows that there is a large range of hot water delivery temperatures with two distinct peaks, the larger of which is around 50°C. An Energy Savings Trust report looking at the DHW consumption of UK dwellings found hot water temperatures between 52-54°C to be the most common temperatures (Energy Savings Trust, 2008).

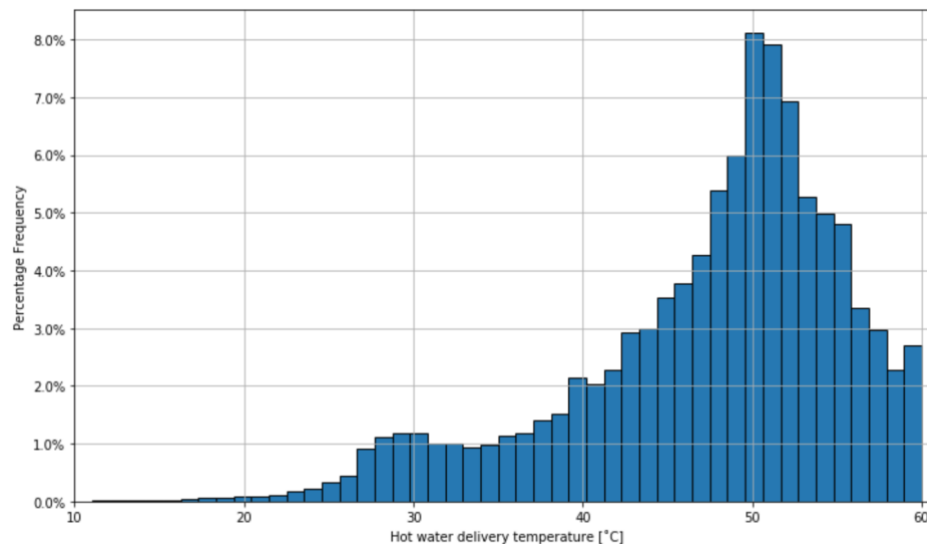


Figure 5.13: Hot water delivery temperatures for the sample of dwellings

Figure 5.14 below gives the mean daily volumetric DHW demand for each dwelling as a function of its floor area. The mean volumetric demand is 2.92 litres/m<sup>2</sup>, with a minimum and maximum of 0.43 and 9.1 litres/m<sup>2</sup> respectively. The peak in the distribution between 2 and 3 litres/m<sup>2</sup> indicate that the majority of dwellings have a daily volumetric demand around that level. Ivanko et al. (2020) did a similar analysis and found daily volumetric demand in the month of January to be ~2.25 litres/m<sup>2</sup>, which aligns with the findings in this work.

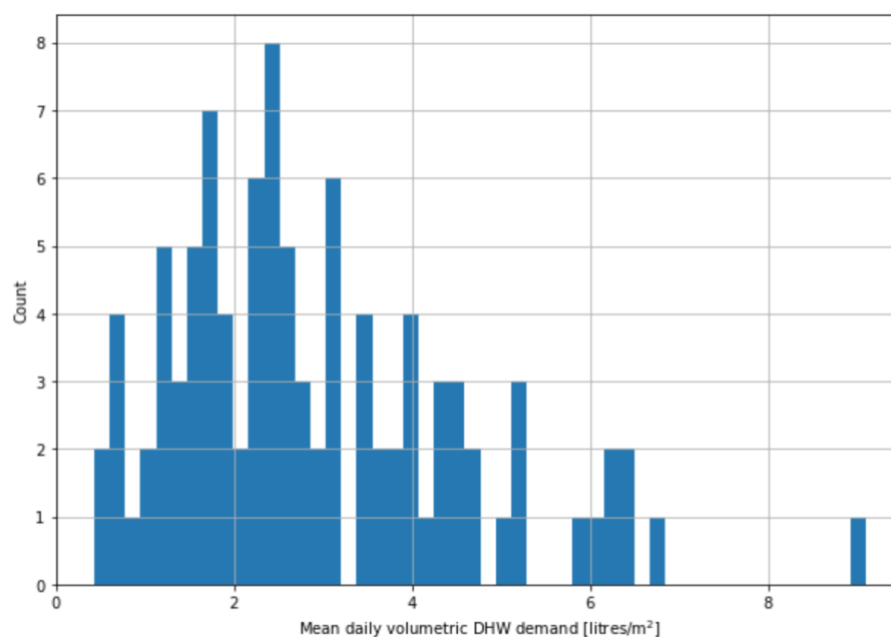


Figure 5.14: Mean daily volumetric DHW demand for the sample of dwellings

### 5.2.3 DHW Demand

Figure 5.15 and Figure 5.16 below give examples of DHW demand profiles for selected dwellings determined using the assumed cold water inlet temperature, the inlet flow rate and the flow temperature. Figure 5.15 gives the demand profile between 17:00 and 21:00 on a selected day for three example dwellings. A range of DHW events can be seen; substantial DHW draws likely to result from more demanding DHW events such as showers, for example, the event that occurs at 17:30 in the top-most profile, and smaller draws likely resulting from small tap draws, such as in the cluster occurring around 19:00 in the bottom-most profile.

Figure 5.16 gives the full daily profile of the selected day for the same dwellings; the peak times of demand in the morning and evenings are clearly seen in the profiles, with some demands in between and almost no demands in the night-time, in which occupants would be sleeping.

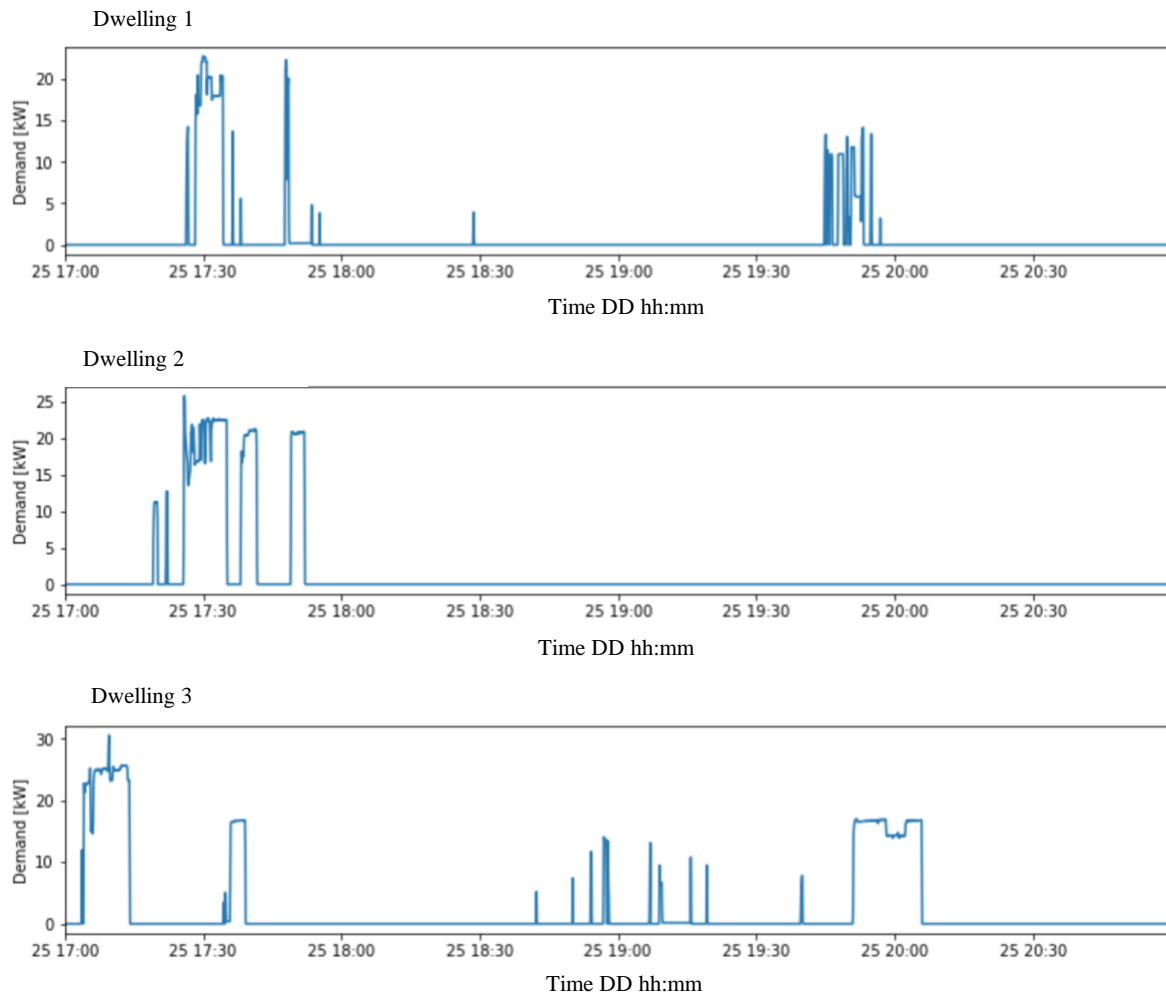


Figure 5.15: Set of three examples of DHW demand profiles on a selected day between 17:00 and 21:00

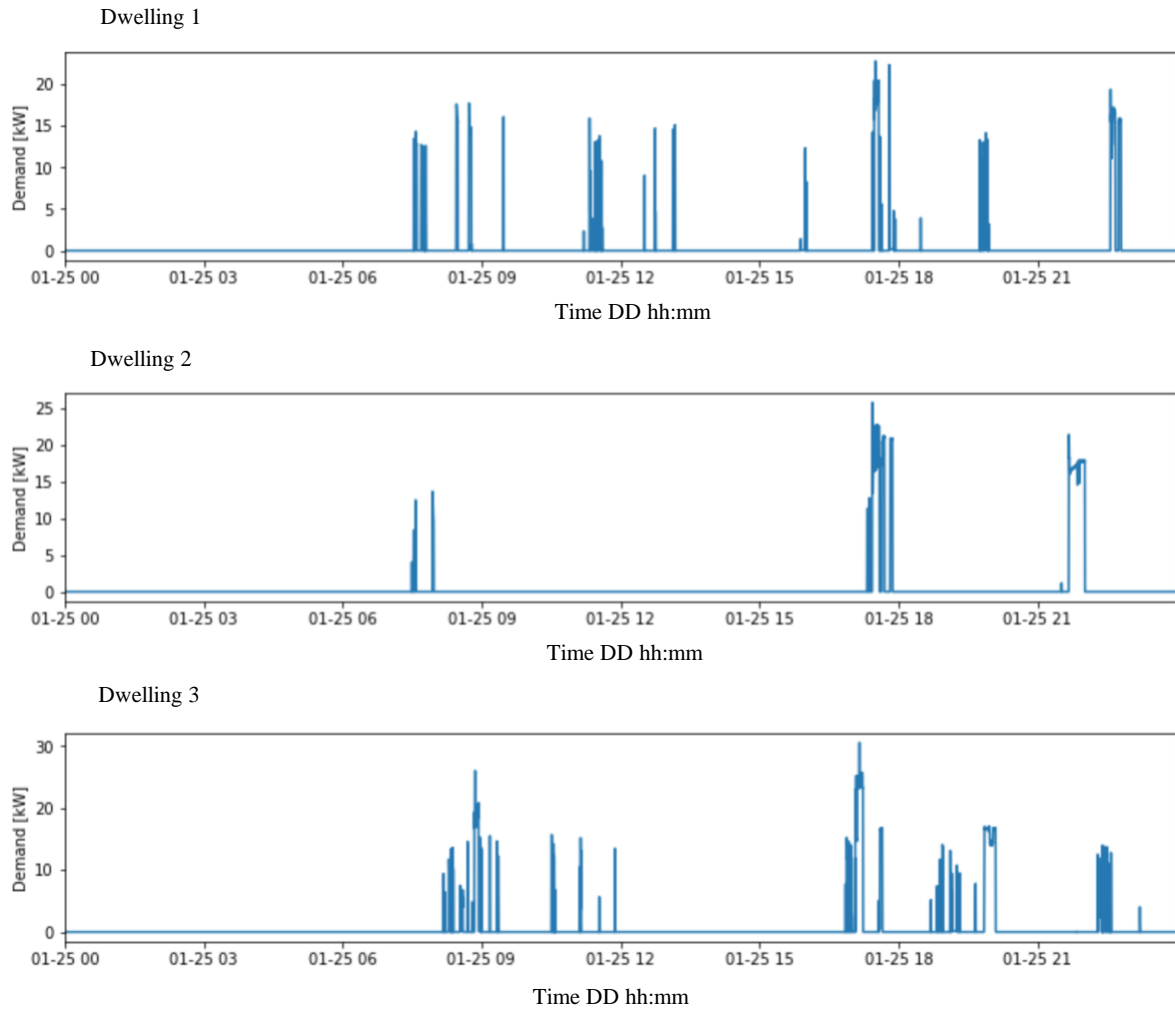


Figure 5.16: Set of three examples of DHW demand profiles over the course of a selected day

#### 5.2.4 Determining Total Demand

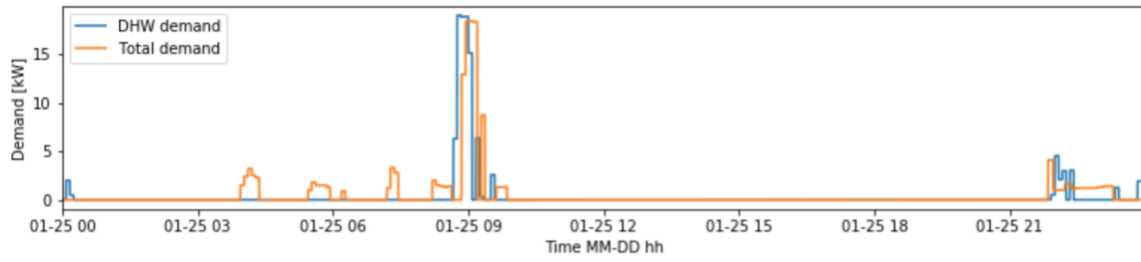
A process like that described in Section 5.2.2.1 where different sets of variables were assessed to select the most viable to use in estimating DHW demand, was carried out for SH. The result of this process, however, was that none of the options were deemed sufficient to produce robust estimates of SH demand. Thus, instead of SH demands, the total demands were estimated and used in the analyses. If some of the analysis and how the results are to be interpreted are adapted this would still allow the aims of the research to be achieved.

The measurements at the heat meter taken at a sampling time of 5 minutes, denoted by the green box labelled 'heat meter' in Figure 5.8, is used to determine the instantaneous total demand. Readers are reminded that the collection of meter data is distinct from the HIU sensor data collection system which is used for determining DHW demand. The M-Bus system consists of the meters in each dwelling connected to the 'base' of the M-Bus system. They are connected in such a way that readings from each meter can be collected only one at a time and the M-Bus settings in the case study dictate that a batch of data, meaning one reading for each measured variable and each dwelling, is to be collected every 5 minutes (refer to Section 4.4 for more detail on the M Bus system function). The time uncertainty in the metered variables is laid out in Section 4.13.

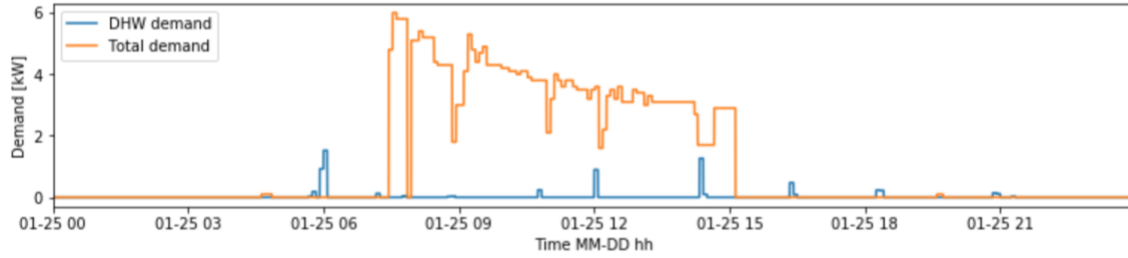
### 5.2.5 Total Demand

The meter data was backfilled to produce a timeseries profile of the total demand for each individual dwelling. Each timeseries was visually inspected to identify missing or spurious readings. The M-Bus system for data collecting, used by metering and billing companies, is highly reliable; minimal data issues were found. The demand profiles given in Figure 5.17 below show the total demand for three example dwellings on a selected day along with their estimated DHW demands which have been resampled (averaged over larger time intervals) to match the sampling time of the total demand. Due to the smaller timescales on which DHW demands occur, they are not always captured in the instantaneous demand data and are therefore not always present in the total demand profiles. A few instances of ‘missed’ events can be seen in Figure 5.17, for example, the last DHW event occurring a short time after 9:00 p.m. in the bottom most profile. Additionally, the offset in time resulting from the restrictions in the M-Bus data collection system can be seen when comparing the DHW profile to the total demand profile where DHW events in the DHW profile tend to occur a few minutes prior to those in the total demand profile. This occurs for all DHW events and is clearly visible whenever there is one in the profiles shown below. The offsets in time between the DHW demand profiles and the total demand profiles do not impact the results of the analysis because the analysis considers them separately and does not require them to be combined. The middle profile also clearly exemplifies the DHW priority function acting during the course of a SH demand event taking place between ~7:30 a.m. and ~3:00 p.m. Moreover, comparing the DHW events in the DHW demand profile to those in the total demand profile show that the events vary in magnitude. This variation is expected as the DHW demand estimates are determined using a constant assumed cold water inlet temperature. However, in reality, this temperature is likely to vary depending on the temperature conditions of the environment, thus leading to both overestimations, such as in the event occurring around 9:00 a.m. in the top-most profile, or underestimations, such as that in the event occurring around midday in the middle profile.

Dwelling 1



Dwelling 2



Dwelling 3

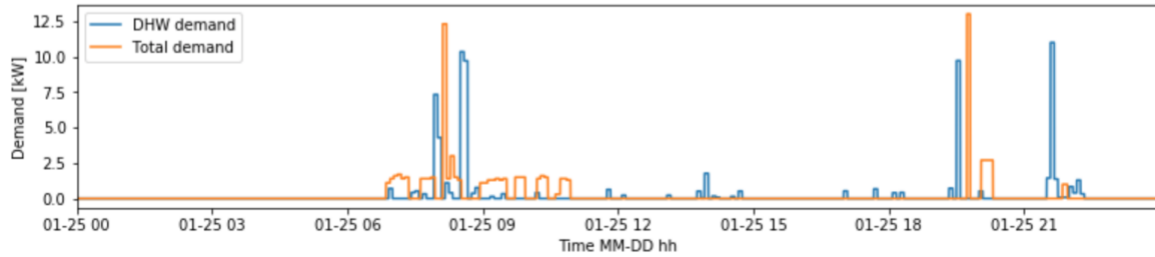


Figure 5.17: Demand profiles of three example dwellings starting at midnight and extending past 21:00 on a chosen day, showing the total demand and the DHW demands

As stated, the profiles above indicate that some DHW demands fail to be captured in the total demand profiles built using the instantaneous heat meter data. Figure 5.18 below shows the raw data points for instantaneous and cumulative demand over a period of 6 days for an example dwelling. Cumulative demand rises steadily with time as the total sum of energy used up to that point rises, whilst instantaneous demand rises and falls according to the power requirement at that instant. The difference between consecutive cumulative demand readings gives accurate information regarding the total energy use between the times of the readings. Cumulative demand readings therefore capture the real demand completely. Comparing the instantaneous demand data to the cumulative demand data can help quantify the extent to which the instantaneous demand profiles underestimate the real demand.

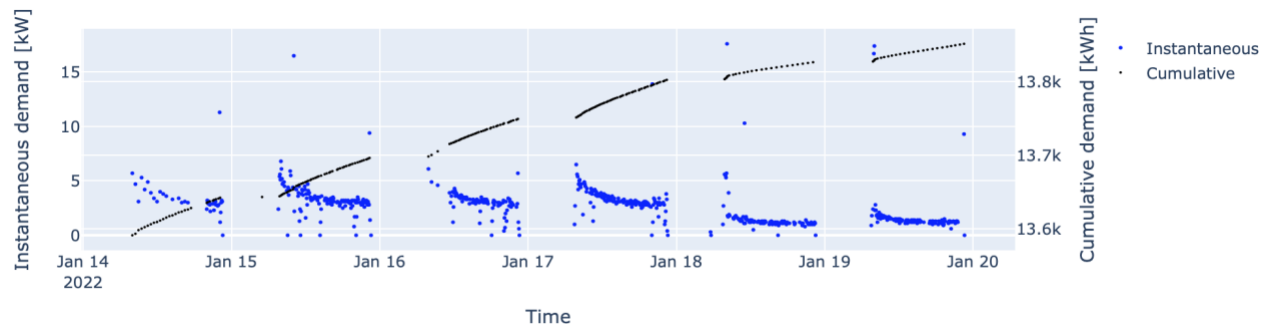


Figure 5.18: Multiple-day profile of cumulative demand (kWh) and instantaneous demand (kW) for an example dwelling

The total sum of energy used on a selected day (25<sup>th</sup> January 2022) was calculated for each dwelling using both the instantaneous demand measurements and the cumulative demand measurements. The integral of the instantaneous demand profile gives the sum of demand. The difference between the first and last cumulative demand reading of the day give the sum of energy use for that day. A regression analysis was done using the results to show the relationship between the daily sum of energy use calculated using the two different methods. Results are shown in Figure 5.19. Comparing the regression line to the 'x=y' line shows a close match indicating that the instantaneous demand measurements estimate the real demand, described using the cumulative demand, sufficiently well. Minor errors that exist at the level of the individual dwellings will cancel out as the demands are aggregated to produce the demand of the group of dwellings together, thus the impact of these errors on the final results, which are based on aggregate demands alone, will be small enough to neglect for most practical purposes.

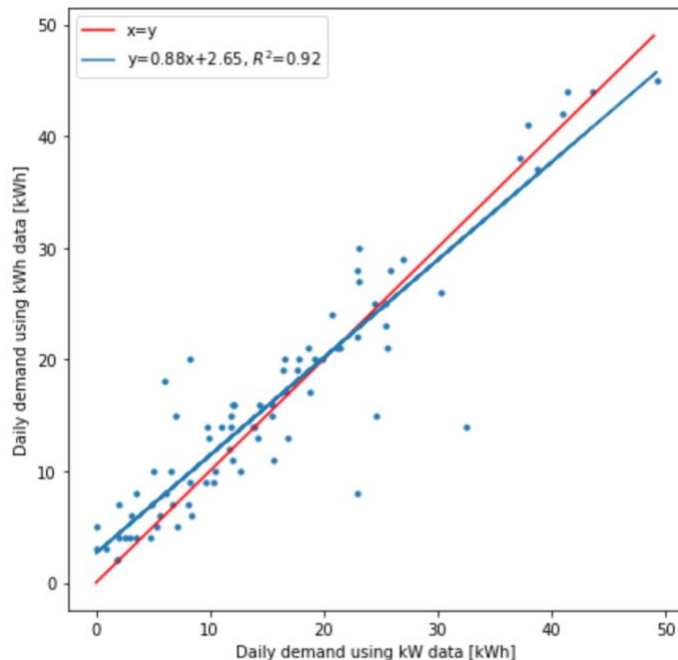


Figure 5.19: Relationship between daily demand using instantaneous data and daily demand using cumulative data; one day, all dwellings

### 5.3 Data Quality for the Selected Set of Variables

Figure 5.20 below gives the reading count (i.e., total amount of data points) for each dwelling and variable combination available for use in determining the demand for the month of October 2021, which was the time at which the early stages of cleaning took place. As mentioned in Section 5.2.1, the data quality was expected to significantly improve after the early cleaning stages in October because of the data collection system adjustments that occurred in conjunction with the cleaning process. This included the M-Bus settings being adjusted on the 22<sup>nd</sup> of January 2022 to increase the frequency of data collection, resulting in a higher volume of data for the metered variables. Figure 5.21 gives the reading count for the coldest day. It shows that the data volume for this single day alone was far greater than the data volume for the whole month of October 2021, showing the positive impact of the system adjustments. For example, for most of the dwellings, both meter variables produced less than 100 readings in total in the month of October, however on the coldest day, there were over 100 readings for each of the dwellings. No meter data was received after the 6<sup>th</sup> of February 2022.

Since the key object of this study, the distribution system sizing, is based on the demands that occur in design day conditions where external temperatures are at their lowest, demand was determined for the week containing the coldest day in the monitored period. From the period where the volume and quality of data were deemed sufficient, 22/01/2022 to 06/02/2022, demand was determined for a selected roughly one-week period spanning 24/01/2022 to the 01/02/2022. This decision was further underpinned by the need to keep computational times manageable. The following sections describe and characterise the DHW demand and the total demand estimates.

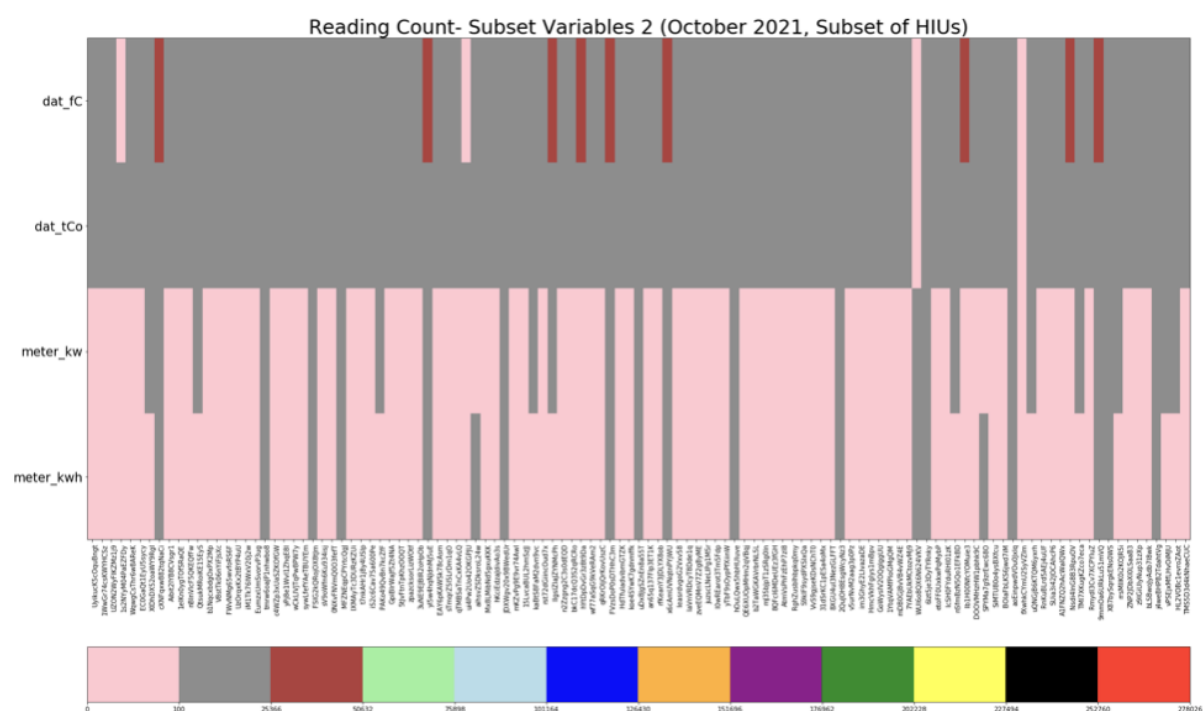


Figure 5.20: Reading count map of each variable used in determining DHW and total demands for the month of October 2021. Note that x-axis markers are dwelling IDs and are provided only as an indication of the number of dwellings and are not meant to be legible.

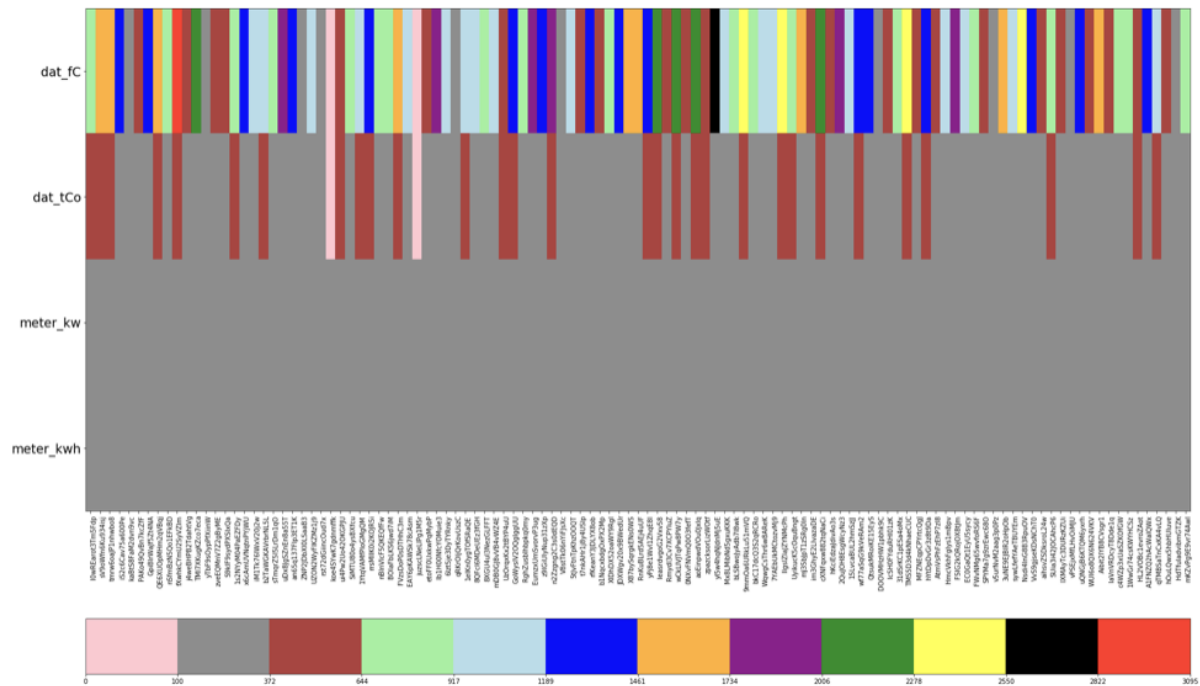


Figure 5.21: Reading count map of each variables used in determining DHW and total demand for the day of 25<sup>th</sup> of January 2022 which was the coldest day in the monitored period, chosen to represent design day conditions. Note that x-axis markers are dwelling IDs and are provided only as an indication of the number of dwellings and are not meant to be legible.

The key research objectives relate to the demand of a HN on design day conditions and to the design of HN. Accordingly, for objectives relating to HN design, data from the selected one-week cold period in January containing the coldest day in the monitored period is sufficient as it captures the peak annual demands. Figure 5.22 below shows the daily mean external temperatures for the chosen period. The plot shows that on the coldest day in the cold period, the 25<sup>th</sup> of January, the mean daily temperature was as low as 2.5 °C. The highest daily temperature, occurring on the 29<sup>th</sup> of January, was 10.2 °C. Temperatures of around 1 °C were reached on some nights of the cold period. The location of the case study HN experienced colder temperatures than the mean for the UK that month, which was 4.7 °C (Met Office, 2022). The monthly mean temperature across England for January 2022 was 0.2 °C above the monthly mean for January between the years 1991-2020 (Met Office, 2022). This indicates that the temperatures in the selected cold period are representative of the temperatures that England is likely to experience year on year. Thus, it is expected that the peak demands captured by the data closely represent the annual peak demands that the HN has experienced in previous years and will likely continue to experience year on year.

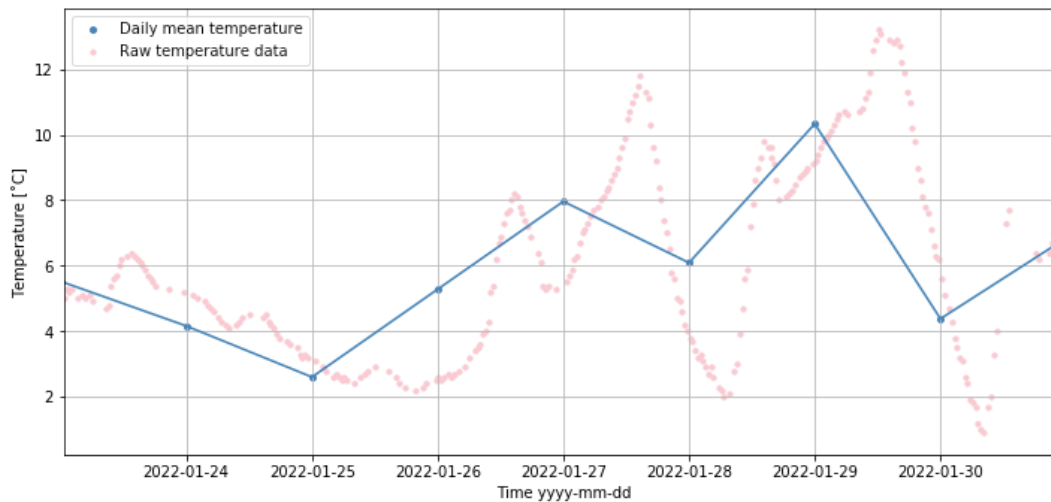


Figure 5.22: Mean daily external temperatures over the course of the selected cold period

## 5.4 DHW Demand and Total Demand

Figure 5.23 below shows the aggregate demand for DHW and the aggregate total demand (DHW and SH demand combined) of the dwelling sample (96 dwellings) over the selected cold period. The total demand profile has a sampling time of 5 minutes and the DHW demand profile has a sampling time of 5 seconds. Figure 5.24 shows the same profile as Figure 5.23; however, the DHW demand profile in Figure 5.24 has been resampled to 5-minutes, matching the sampling time of the total demand profile. Comparing Figure 5.23 and Figure 5.24, it can be seen that the DHW demand is ‘peakier’, i.e., more variable in magnitude, at the smaller sampling time. This indicates that DHW demand fluctuates at time scales smaller than 5 minutes. Figure 5.24 shows that the minimum DHW demand reaches 0 kW on some days, whereas for the total demand, the minimum demand remains above ~ 20 kW on all days. The ‘troughs’ in both profiles occur around the very start of a day at 12 a.m. where occupants are likely to be inactive and therefore unlikely to be calling for demand. The minimum total demand staying above 25 kW even during these times suggests that there may still be a demand for SH through inactive hours in some or all of the dwellings. The total demand during the inactive hours of the coldest day (25/01/2022) being significantly higher than on the warmest day (29/01/2022) suggests a relationship between the demand during these hours and the external temperature, further supporting the claim that demand during inactive hours is demand for SH. Moreover, it is unlikely that during the inactive hours, occupants will be calling for DHW, thus it can be concluded that the demand during the night-time is likely to correspond largely to SH demand. However, it is important to note that the demand during inactive hours may also include a contribution by the demand requirement of the ‘keep-hot’ function which keeps the DHW circuit in the HIUs warm, the demand from which would be captured by the metered data on the primary side of the HIU but not the sensor data on the secondary side of the HIU. Figure 5.25 shows the DHW demand and total demand at a sampling time of half an hour which gives an indication of what the demand may look like at the plant if it were serving this sample of dwellings.

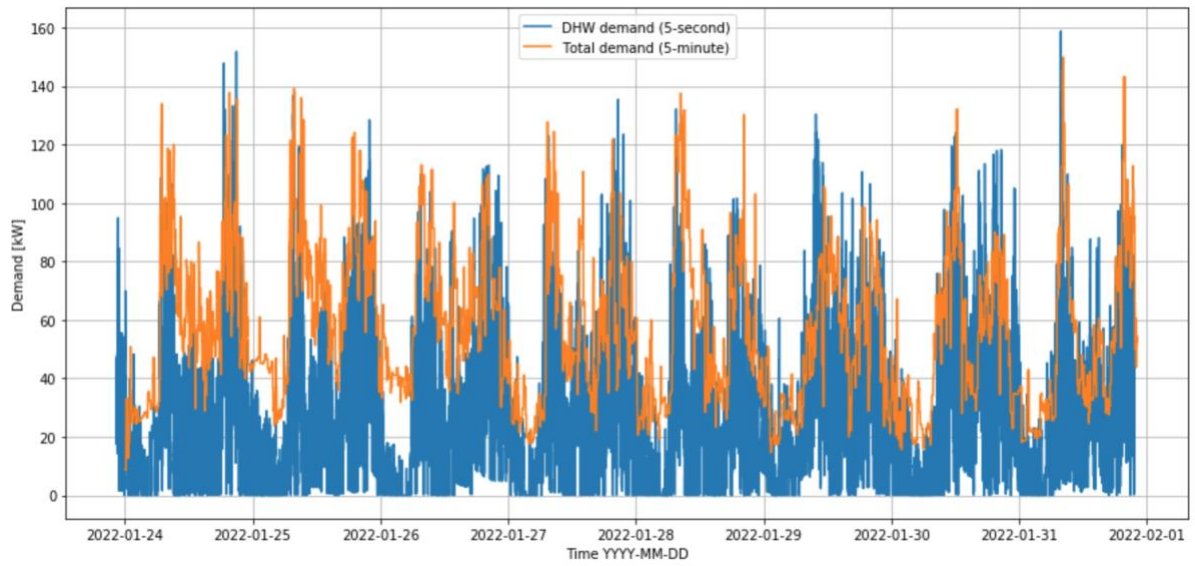


Figure 5.23: Aggregate DHW demand and total demand for the cold period at a sampling time of 5 seconds and 5 minutes respectively

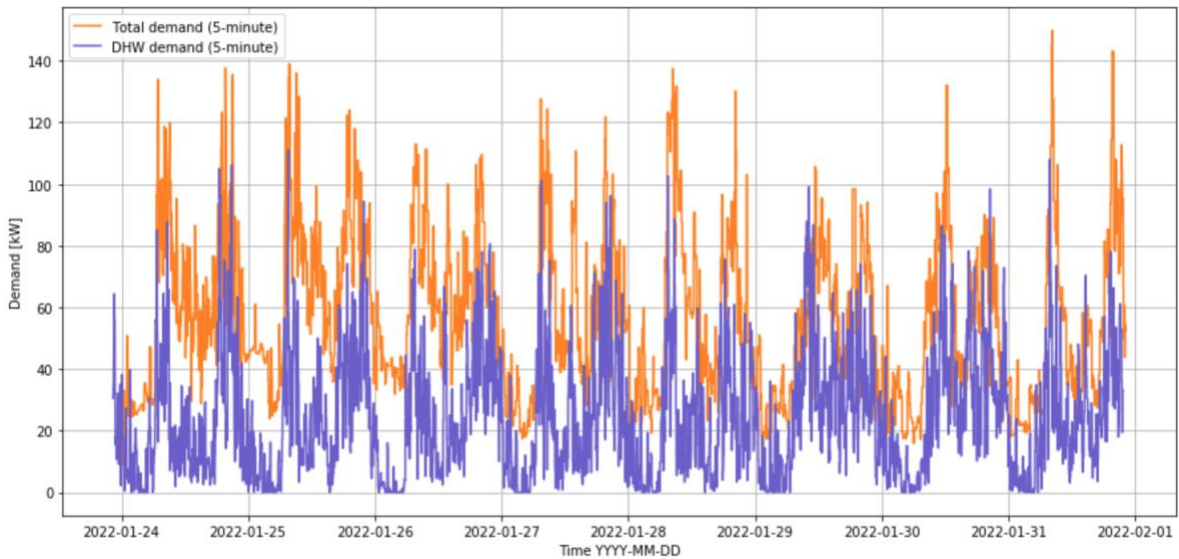


Figure 5.24: Aggregate DHW and total demand for the cold period, both at a sampling time of 5 minutes

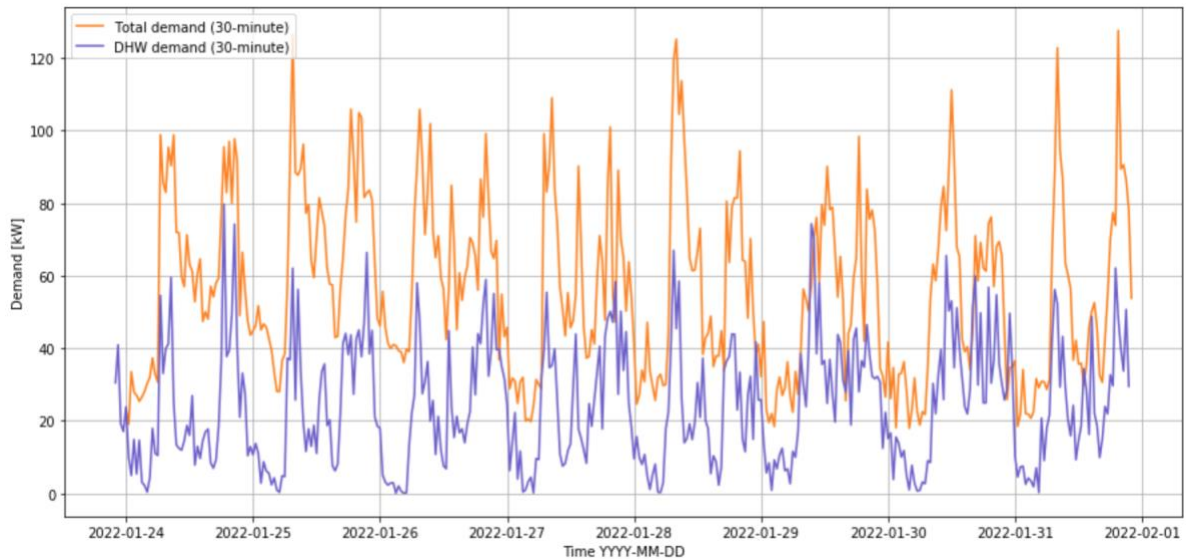


Figure 5.25: Aggregate DHW and total demand for the cold period, both at a sampling time of 30 minutes

To illustrate the range in demand across the cold period, Figure 5.26 and Figure 5.27 below show the aggregate DHW demand and aggregate total demand for the coldest and warmest days in the cold period respectively. The mean DHW demand of the cold day and warm day are 24.1 kW and 27.9 kW (15.8% higher than the cold day) respectively. The mean total demand on the cold day and warm day are 67.0 kW and 50.6 kW (24.5% lower than on the cold day) respectively. The maximum total demand on the cold day was 139.0 kW whereas on the warm day it was 105.7 kW. This suggests that DHW demand may be somewhat higher, and SH demand higher still, on days where the external temperature is lower. As is expected, this is because the SH demands are affected by external temperatures more than DHW demand because SH demands are coupled to the environmental conditions to a greater extent than DHW demands are (as described in the literature review chapter in Section 2.3).

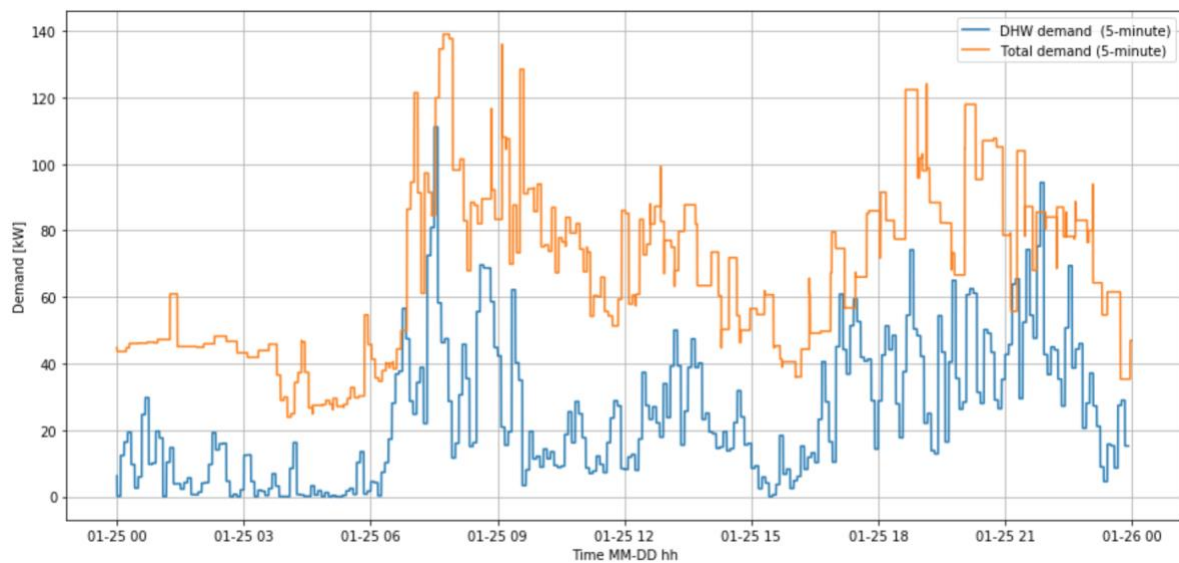


Figure 5.26: Aggregate DHW and total demand for the coldest day in the cold period

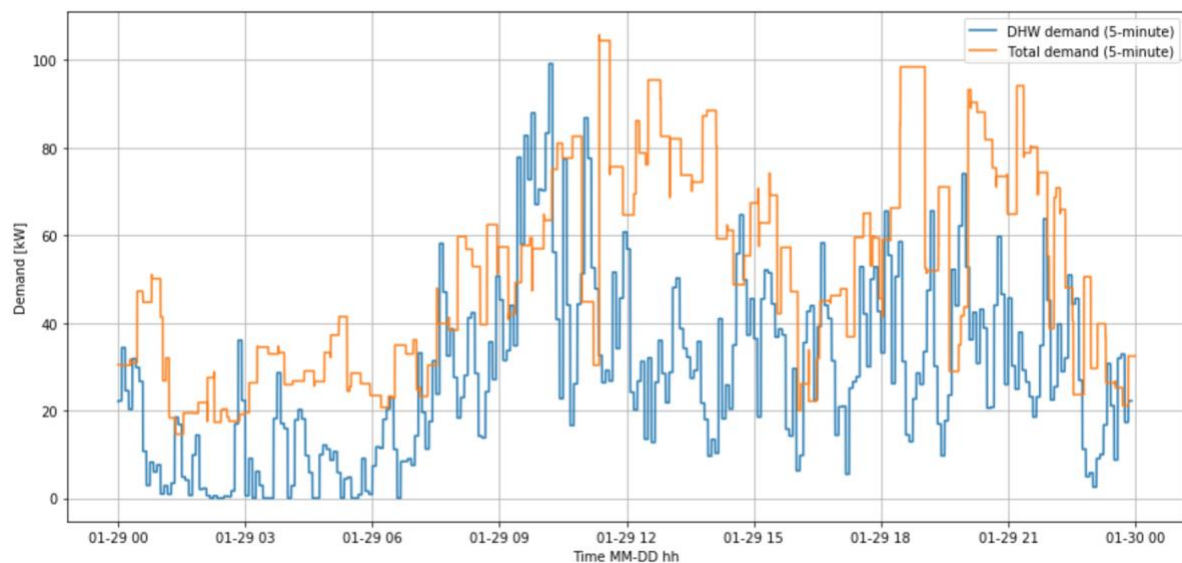


Figure 5.27: Aggregate DHW and total demand for the warmest day of the cold period

Figure 5.28 shows the mean hourly 24-hour profile for the sample of dwellings for the DHW demand and the total demand for the selected cold period. This is determined by taking a mean of the set of 96 demand values for a given time step. Which is the same as taking the aggregate demand and dividing by the number of dwellings in the group (96). Both profiles show the expected typical demand peaks occurring in the morning and evening (Gianniou et al, 2018; Summerfield et al., 2015). The highest peak for the total demand occurs in the morning, whereas for DHW demand the highest peak occurs in the evening. The profiles show that the mean total demand is at least double the mean DHW demand. Other studies have noted DHW demand to be as low as 16%, between 20-25% and between 40-50% (in energy-efficient homes) of the annual total demand (Bøhm, 2013; Erhorn-Kluttig and Erhorn, 2014; Marini et al., 2015; Marszal-Pomianowska et al., 2019; Yao and Steemers, 2005). They also point out that this proportion will rise with the trend of increasing levels of insulation. The findings here show that in the heating season, the proportion of DHW in the total demand is ~50%. This can be used to deduce that on the annual scale, which includes the off-heating season where there is no demand for SH, the proportion of DHW demand in total demand would be higher than 50%. The residential building that the dwellings in the sample are in is a new build which is likely to have higher levels of insulation compared to the wider population of dwellings which are primarily older and would therefore likely have lower levels of insulation. The dwelling sample, which sit together in one residential building, would likely have a reduced need for SH demand compared to their stand-alone dwelling counterparts as a result of having fewer external walls, with little effect on the demand for DHW (Burzynski et al, 2012; Wang et al, 2021). The combined impact of these factors may explain the high proportion of DHW demand in the total demand. The morning hourly peak for the total demand is ~0.9 kW and the hourly evening peak for the total demand is ~0.85 kW. For the DHW demand, the hourly morning peak is just above 0.4 kW, and the evening peak is higher at just under 0.5 kW, unlike for the total demand where the morning peak is higher.

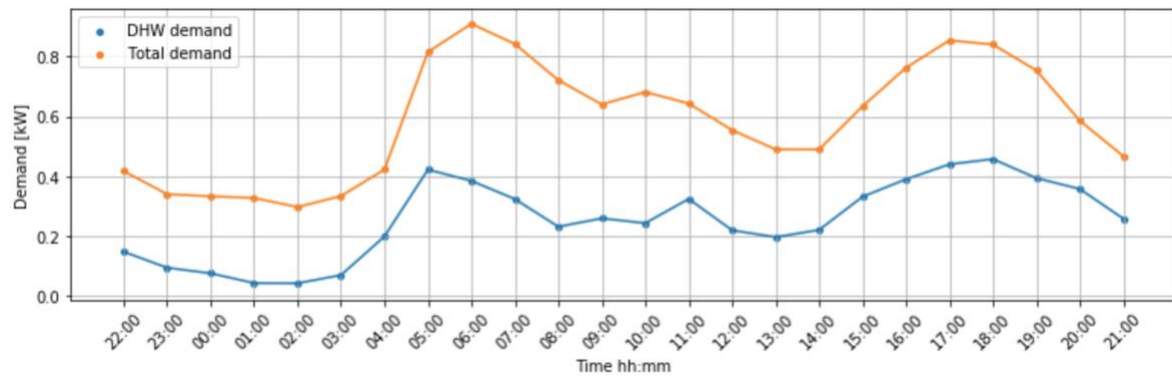


Figure 5.28: Mean hourly 24-hour profile for the sample of dwellings for DHW demand and total demand for the cold period

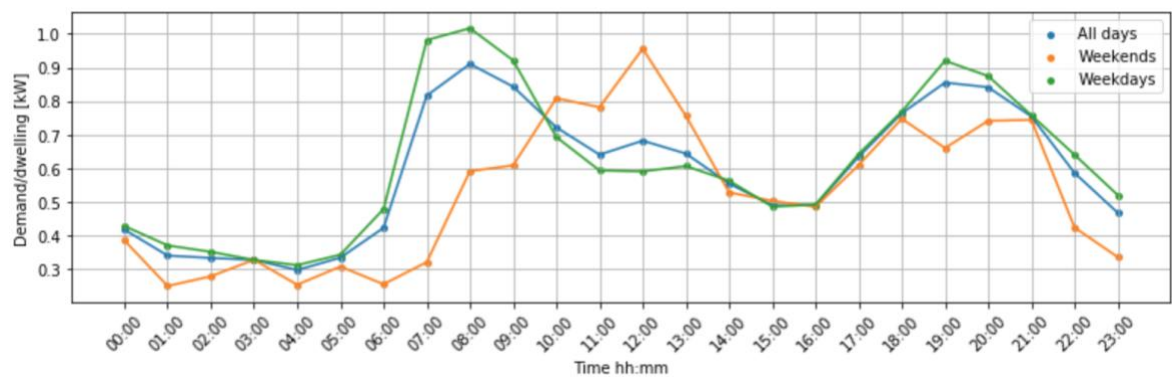


Figure 5.29: Mean hourly 24-hour profile of the total demand for the sample of dwellings for the weekend days and weekday days of the cold period

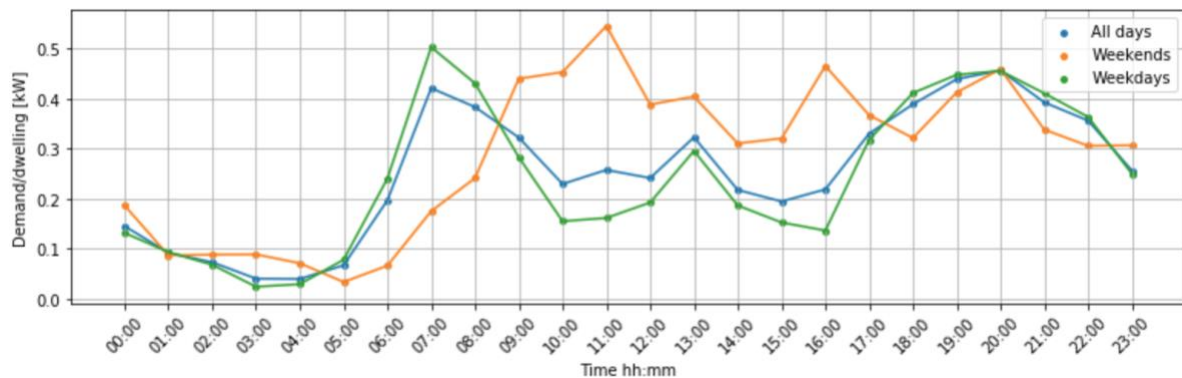


Figure 5.30: Mean hourly 24-hour profile of the DHW demand for the sample of dwellings for the weekend days and weekday days of the cold period

Figure 5.29 and Figure 5.30 above show the mean hourly 24-hour profile for the sample of dwellings for the total demand and the DHW demand respectively, both separated for the weekdays and the weekend days of the cold period. The total demand profile shows a morning peak that starts later in the day for weekends as compared with weekdays. The evening peak occurs at similar times for both the weekend and the weekdays; however, the magnitude of the peak is smaller on the weekend. The magnitude of the morning peak is smaller for the weekend as well. The delay in the morning peak on the weekend is likely explained by occupants having a slower start to the day in the absence of work commitments. The profile for the DHW demand shows that on the weekend, there is no sharply defined morning and evening peak. Instead, the demand fluctuates throughout the day after the initial rise in demand in the morning, which occurs later than it does in the weekdays, once again

reflecting the occupants' slower start to the day. Conversely, on the weekdays, there is a defined morning and evening peak, which reflect the impact that working patterns may have on occupancy and therefore also on demand.

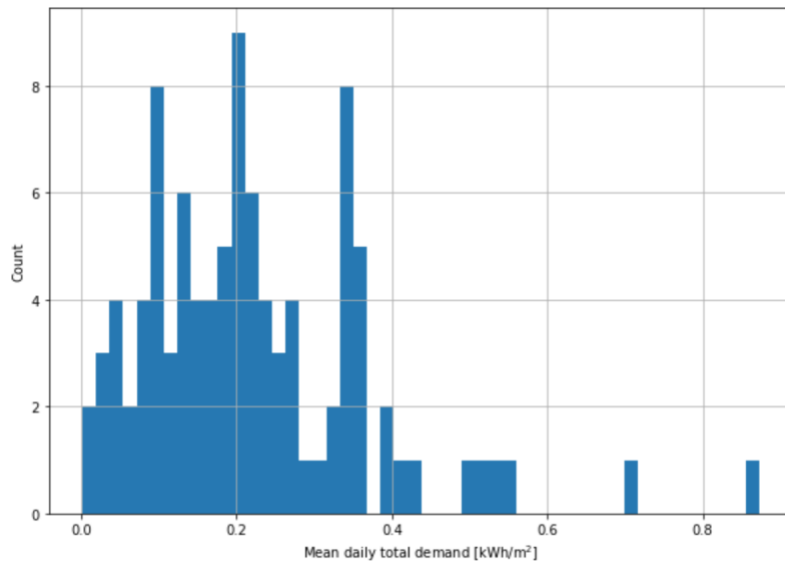


Figure 5.31: Mean daily total demand per m<sup>2</sup> of floor area

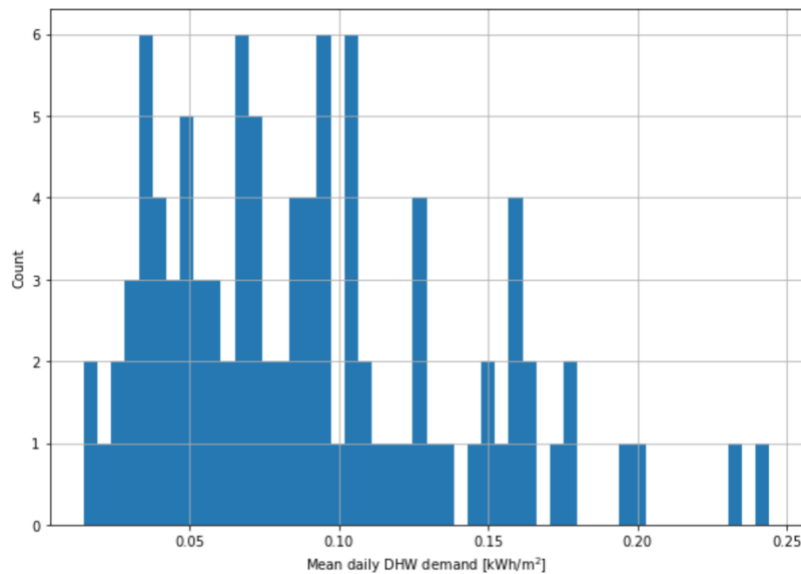


Figure 5.32: Mean daily DHW demand per m<sup>2</sup> of floor area

Figure 5.31 and Figure 5.32 show histograms of the mean daily demand per m<sup>2</sup> of floor area of the dwelling sample for the total demand and DHW demand respectively. The total daily demand for the dwelling sample varies between ~ 0 kWh/m<sup>2</sup> and 0.87 kWh/m<sup>2</sup>, with a mean of 0.22 kWh/m<sup>2</sup>. Ignoring two of the dwellings which have significantly higher demand than the rest of the dwellings, the maximum would be ~0.55 kWh/m<sup>2</sup>. A study looking at annual demand data from 450 flats in the SE of England found that the annual demand for SH can vary between 0.6 -153.5 kWh/m<sup>2</sup>a<sup>1</sup> for mid-floor flats, and between 5.8-101.6 kWh/m<sup>2</sup>a<sup>1</sup> for top or ground floor level flats (Burzynski et al, 2012). Other studies, such as Aragon et al (2022), studied 462 social housing flats in the SE of England and found the median annual

energy demand, as calculated for cluster groups, to be 20-80 kWh/m<sup>2</sup>. The characteristics of the sample in Aragon et al (2022) and in Burzynski et al (2012) are similar to the sample used in this work; both contain only flats in the SE of England. However, only data from a very cold period of the heating season is used in this work, whereas in the Aragon et al (2022) and the Burzynski et al (2012) studies, annual data is used. Ignoring the differences between the off-heating and heating seasons, the findings in Burzynski et al (2012) would translate to a daily demand of between 0.002 – 0.42 kWh/m<sup>2</sup> and 0.02 -0.28 kWh/m<sup>2</sup> for mid-floor flats and top/ground flats respectively. The mean daily total demand found in this work falls within both of those ranges. Including the demand from days in the rest of the heating season, where temperatures would have been higher, may have resulted in the mean daily demand being lower and therefore more closely aligning with the results achieved by Burzynski et al (2012). The same study found DHW consumption to vary between 2-71 kWh/m<sup>2</sup>a<sup>1</sup>. This translates to a daily demand range of 0.005-0.19 kWh/m<sup>2</sup> which closely aligns with the DHW demand in this work which is shown to vary between close to 0 kWh/m<sup>2</sup> and 0.24 kWh/m<sup>2</sup>, with a mean of 0.09 kWh/m<sup>2</sup>.

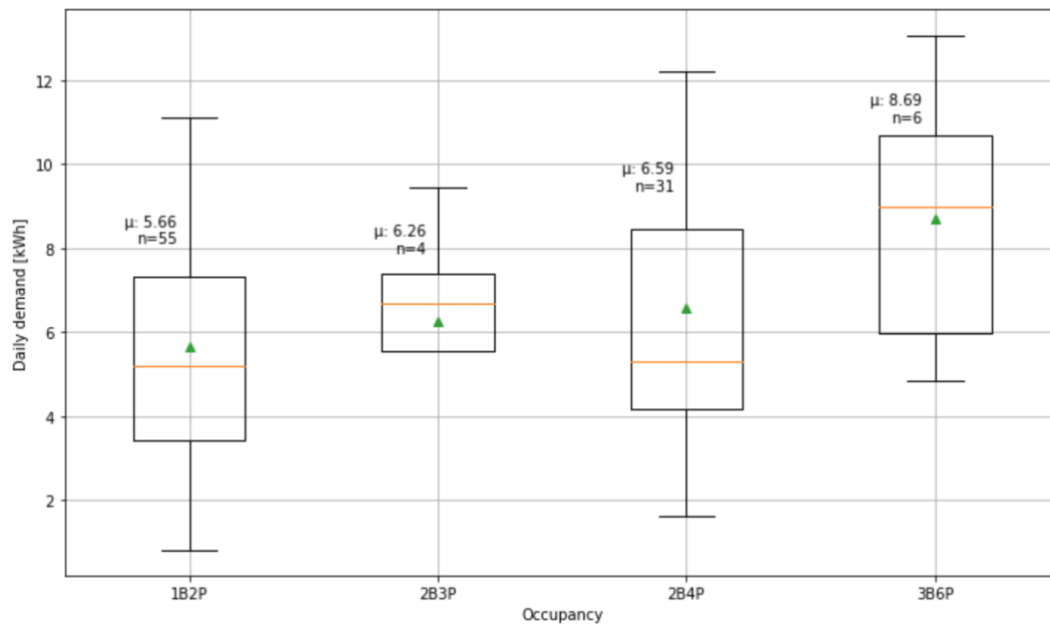


Figure 5.33: Box and whisker plot of the daily DHW demand for different dwelling occupancies where green triangles mark the mean.

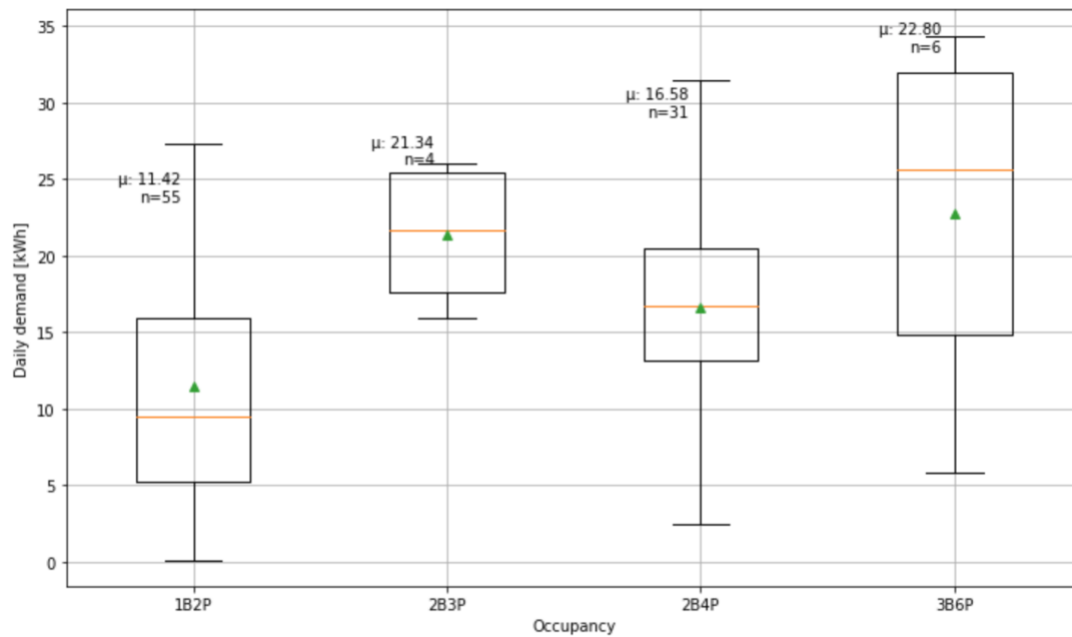


Figure 5.34: Box and whisker plot of the daily total demand for different dwelling occupancies where green triangles mark the mean.

Figure 5.33 shows the range of daily DHW demand for dwellings of different design occupancies. The mean daily DHW demand ranges from 5.66 kWh for the smallest design occupancy, 1 bed-2 people, to 8.69 kWh for the largest design occupancy, 3 bed-6 people. Figure 5.34 gives the daily total demand for dwellings of different design occupancies. The range for the mean total demand is 11.42 kWh to 22.80 kWh. The results show that the total daily demand is at least twice as much as the demand for DHW generally across all occupancy types. The sample mean for daily DHW demand was found to be 6.17 kWh, and for the total demand, the sample mean was 14.21 kWh. A report on hot water consumption by the Energy Savings Trust found a mean daily DHW demand of 16.8 MJ/day (4.6kWh/day) for their sample consisting of 112 dwellings with up to 8 occupants (Energy Savings Trust, 2008). In comparison, the mean DHW demand in this sample is higher, although not substantially. The DHW demand in the heating season has been noted as being greater than it is in the off-heating season due to holidays and slightly higher cold water inlet temperatures (as described in Section 2.3.1). The energy demand in this sample represents the energy demand of the selected cold period only. The DHW demand being higher in this sample compared to the sample in the Energy Savings Trust Report may be explained by the lack of data from the off-heating season. The lack of off-heating season data makes it challenging to compare demand results to other works which tend to use data on the annual scale (Burzynski et al, 2012). Another limitation that must be noted here is that the design occupancy may not reflect the real occupancy accurately and there may be dwellings where there are more or fewer occupants than the design intent. Furthermore, note the small sample sizes which may affect results, especially for the occupancy groups ‘2B3P’ and ‘3B6P’, which have a sample size of  $n < 10$ .

#### 5.4.1 Power Temperature Gradient

The Power Temperature Gradient (PTG) has been evaluated in previous studies, including for UK dwellings, using annual data from the Energy Demand Research Project (EDRP) smart meter field trials (Belussi and Danza, 2012; Leiria et al., 2021; Summerfield et al., 2014; Vámos and Horváth, 2023; Wang et al., 2020; Westermann et al., 2020). The PTG is a first-

order empirical metric that describes the rate of heat loss, from ventilation losses, through the building fabric and losses associated with heating system inefficiency as a function of changing external temperature conditions. It is equal to the gradient of the linear regression analysis of the daily mean demand and external temperature. The PTG is typically used as an indication of technical performance which includes a socio-technical aspect as occupant heating practices and behaviours may change with changing external conditions.

The PTG is assessed for the case study HN using data collected over the cold period between the 22<sup>nd</sup> of January 2022 and the 6<sup>th</sup> of February 2022 in the heating season (further details in Section 5.3). The data cleaning process for this analysis included removing HIUs that did not produce any meter readings at all, which amounted to 9 dwellings in total, out of a total sample of ~150 dwellings, thus leaving 138 dwellings in the sample. The number of dwellings where occupants were absent for extended periods of time (e.g., for holidays lasting one or more weeks) was limited and therefore not removed. The daily mean external temperature was obtained using temperature sensor data located outside the residential building. Ideally, the heat losses from the distribution system would be included as it is an important source of heat into the building however this data was not available.

The aggregate demand of the case study HN was calculated by summing the demands of the dwelling sample at half-hourly time steps. This demand was then split off into individual days to determine the mean demand for each day which was then divided by the total number of dwellings to give the daily mean demand per dwelling. The PTG for the case study HN, equal to the gradient of the best fit line in the plot shown in Figure 5.35 below, was found to be 40W/K.

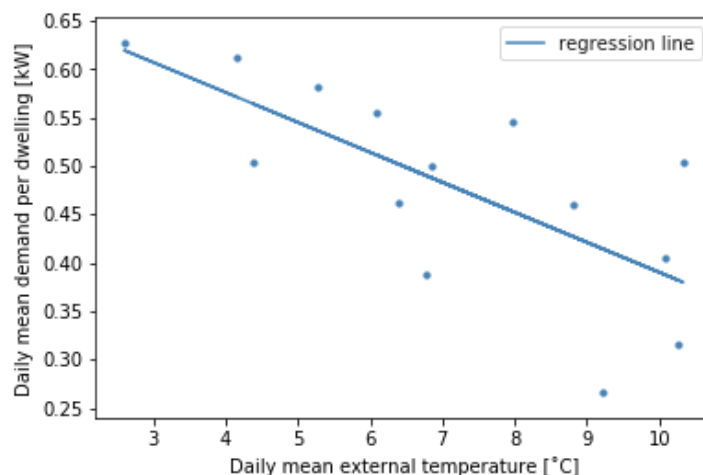


Figure 5.35: Regression of the daily demand of dwellings and external temperature in the case study HN where  $R^2 = 0.51$  and PTG = 40W/K

In Summerfield et al. (2014), a PTG study based on a UK dwelling sample, the dwellings tended to have a PTG of between 200 and 330 W/K with a full range of between 0 and 1200 W/K and in Wang et al. (2020), another similar study, the PTG was found to be 320 W/K. Both studies used gas data from dwellings collected over the period of at least 80 days by the energy provider EDF in one of the field trials in the EDRP. The data was collected for 591 dwellings in total, 304 of which were used in Wang's study, and 567 of which was used in Summerfield's study. The datasets used in these studies had an underrepresentation of flats/maisonettes, making up only 3% of the dwellings in the dataset, thus these results largely represent dwellings that are standalone dwellings, i.e., not part of a residential building, such as detached or terraced houses. In Summerfield's study, the mean PTG of the

flats/maisonettes was calculated separately and found to equal 260 W/K (Summerfield et al., 2014). The PTG found for the dwellings in the case study HN, at 40 W/K, still low even when comparing like for like, against flats/maisonettes, may be explained by the fact that heating system efficiency is not taken into account in Summerfield et al. (2014) or Wang et al. (2020). The low heat loss is potentially also explained by the case study HN being a new-build which is likely to have a lower building fabric U-value than the dwelling sample in the other studies which consist of dwellings built from before 1919 to 1980 (Wang et al., 2020). Moreover, the thermal losses from the distribution system acting as heat gains to the building, the demand of which is not considered in the PTG value, would act to further reduce the PTG of the case study HN.

## 6 Results 2 – Demand and Diversity

### 6.1 Introduction and Relevant Objectives

The research questions and objectives that pertain to this chapter are those that are stated in bold.

- *What is the real diversity effect in UK HNs?*
  - Estimate the individual demand profiles of dwellings on a real HN using measured data.
  - **Analyse the impact that aggregation, over number of dwellings and over time, has on the demand.**

In this chapter, a selection of DHW demand distributions is used to determine the minimum sampling time recommended when measuring individual dwelling demand to support the design of a HN such that it meets a given quality of service.

### 6.2 Demand Distribution

The demand distribution for DHW and total demand at varying levels of aggregation over number of dwellings and over time, as described in Section 3.5, are presented in this section. The period selected for analysis is the week (Mon-Sun) which contained the coldest day in the monitored period as is required for analysis regarding system design, as the coldest days represent the design day conditions in which demand will be at its highest. The number of dwellings whose demands were aggregated is denoted by the letter  $k$ , in reference to the equations presented in Section 3.5.

The aims of this section are as follows.

- Establish a minimum recommended sampling time appropriate for use in sizing a real HN similar to the case study to meet a defined quality of service criteria.
- Characterise (i.e., SH or DHW, real occupant demand or transient demand) the demand events that make up the notable features in the demand distributions.
- Define the extent to which findings on individual demand distribution hold for aggregate demand distributions.

The first subsection lays out the individual demand distribution plots and corresponding summary tables for different levels of aggregation over time and over dwellings in full and the final subsection gives a higher-level view of the same by summarising these distributions into two key plots.

#### 6.2.1 Individual Demand Distributions

Figure 6.1 shows the results of the demand distribution analysis for the total demand for individual demands ( $k = 1$ ) at sampling times of 5, 10, 30, and 60 minutes. Table 6.1 gives a summary of the percentile values of the distribution at each sampling time. The maximum demand (the 100<sup>th</sup> percentile) for a sampling time of 5 minutes and 10 minutes are exactly equal at 29.6 kW. At sampling times higher than 10 minutes, the maximum demand decreases; at 30 minutes it is 26.47 kW, and at an hour it is 21.44 kW. A similar pattern was

shown in a report by Cosic (2017) looking at the impact of sampling time on demand distribution; the maximum demand at sampling times equal to or lower than 10 minutes all had the same value at an individual demand level, as shown in Table 2.3 (Cosic, 2017).

Figure 6.2, Figure 6.3, and Figure 6.4 give the distribution of DHW demand of individual dwellings for the sampling times of 1, 5, 30, and 60 seconds, and 5, 10, 30, and 60 minutes. Table 6.2 gives the summary of the percentile values of the distributions at these sampling times. At a sampling time of 5 minutes, the distribution starts to resemble the distribution of total demand presented in Figure 6.1, as is expected; maximum demands are almost identical at 28.95 kW for DHW and 29.6 kW for total demand. However, the DHW demand distribution does not include the peak at ~2 kW, which is present in the total demand distribution, which suggests that the peak is largely made up of SH demands.

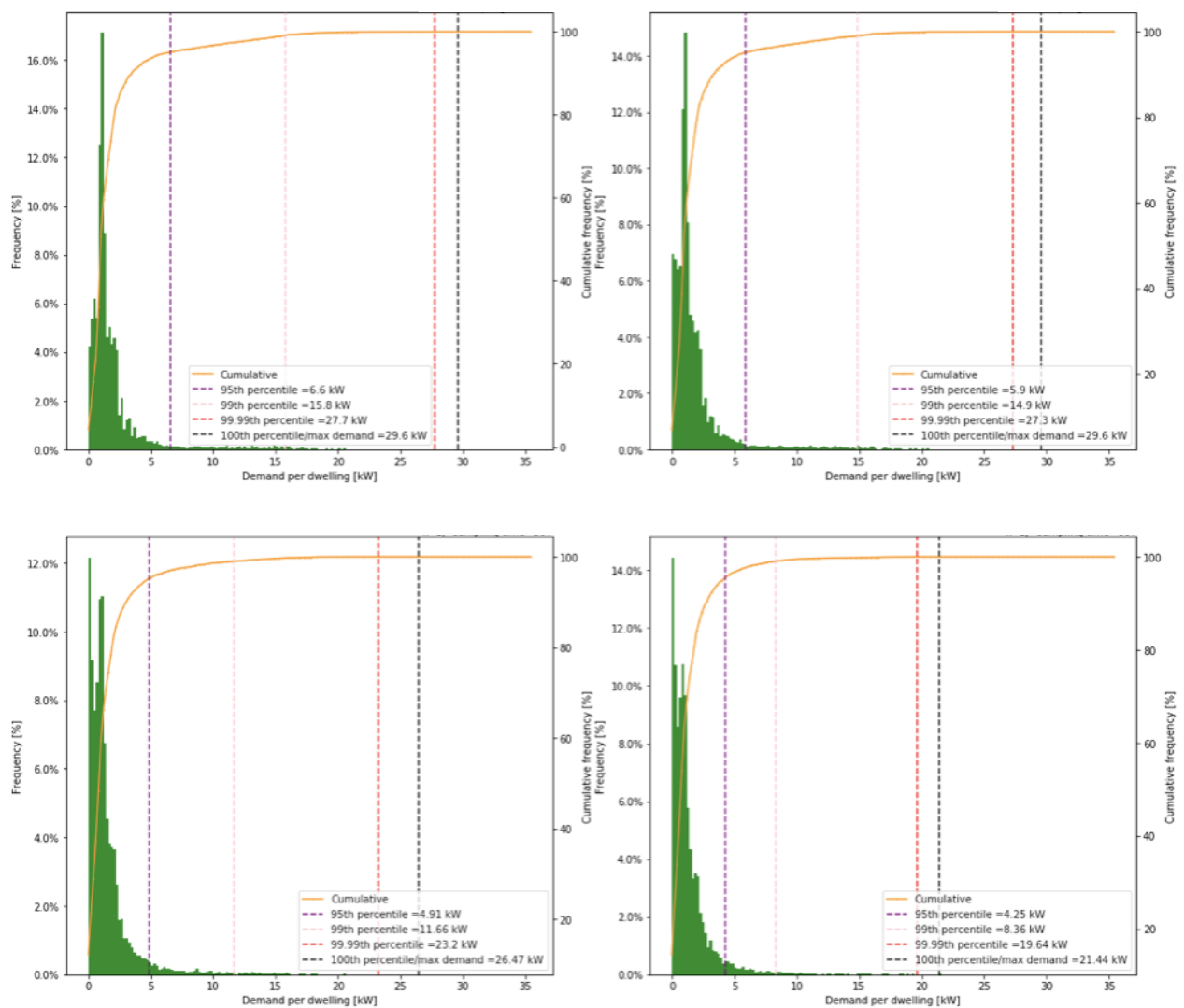


Figure 6.1: Demand distribution for the total demand at an individual demand ( $k=1$ ) level showing the impact of increasing sampling times. Top-left: 5-minute; top-right: 10-minute; bottom-left: 30-minute; bottom-right: 1-hour.

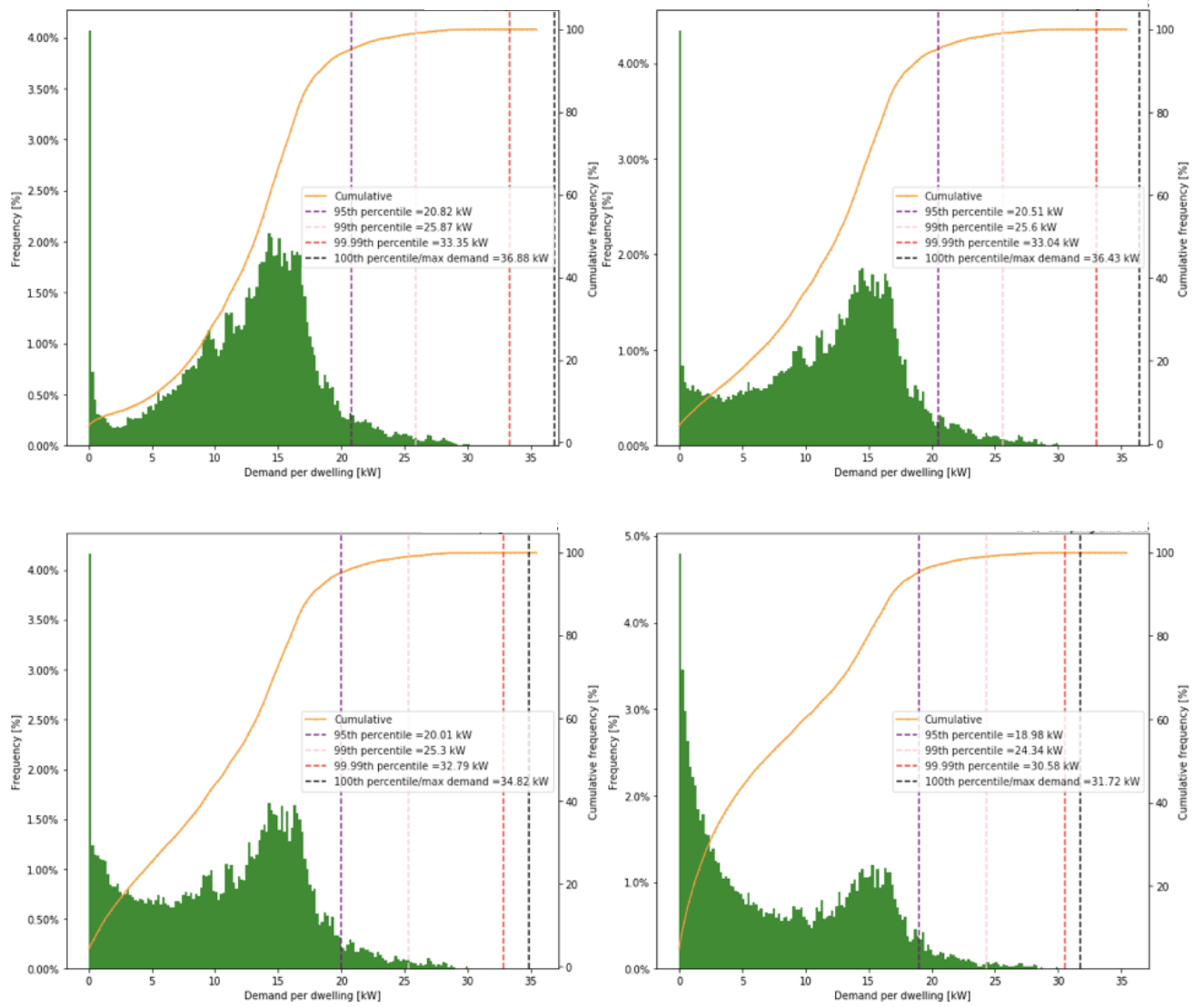


Figure 6.2: Demand distribution for the DHW demand at an individual demand ( $k=1$ ) level showing the impact of increasing sampling times. Top-left: 1-second; top-right: 5-second; bottom-left: 10-second; bottom-right: 30-second.

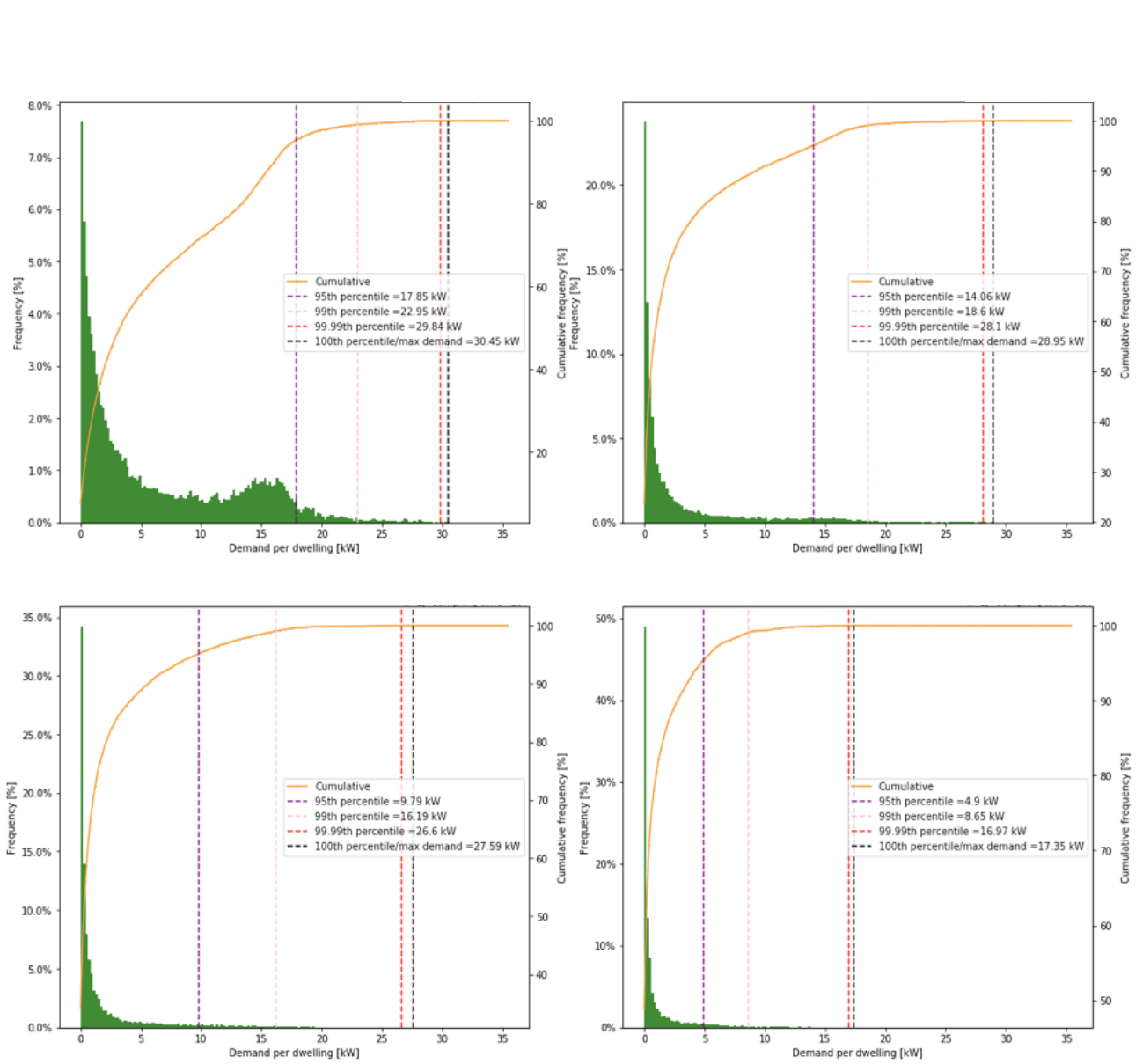


Figure 6.3: Demand distribution for the DHW demand at an individual demand ( $k=1$ ) level showing the impact of increasing sampling times. Top-left: 60-second; top-right: 5-minute; bottom-left: 10-minute; bottom-right: 30-minute.

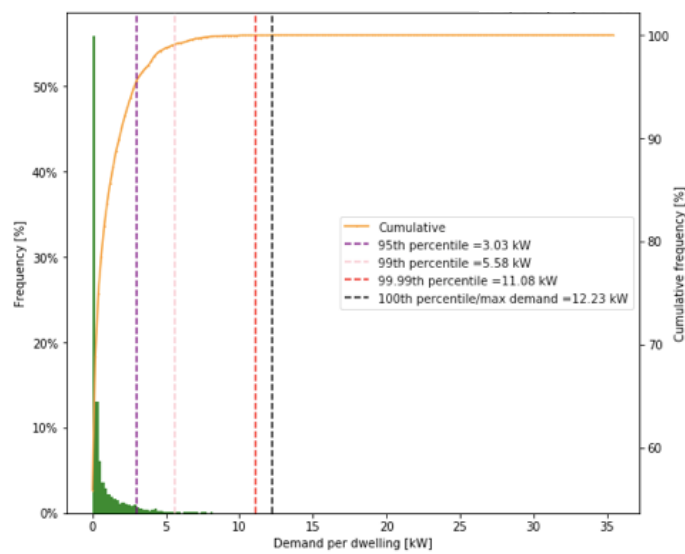


Figure 6.4: Demand distribution for the DHW demand at an individual demand ( $k=1$ ) level at a sampling time of 1 hour

Table 6.1: Summary of total demand distribution percentiles for k=1 expressed as demand per dwelling (kW)

Sampling time	95 <sup>th</sup>	99 <sup>th</sup>	99.99 <sup>th</sup>	100 <sup>th</sup>
5 minutes	6.8	15.8	27.7	29.6
10 minutes	6.05	14.9	27.3	29.6
30 minutes	4.94	11.78	23.09	26.47
1 hour	4.29	8.5	19.61	21.44

Table 6.2: Summary of DHW demand distribution percentiles for k=1 expressed as demand per dwelling (kW)

Sampling time	95 <sup>th</sup>	99 <sup>th</sup>	99.99 <sup>th</sup>	100 <sup>th</sup>
1 second	20.82	25.87	33.35	36.88
5 seconds	20.51	25.6	33.04	36.43
10 seconds	20.01	25.3	32.79	34.82
30 seconds	18.98	24.34	30.58	31.72
60 seconds	17.85	22.95	29.84	30.45
5 minutes	14.06	18.6	28.1	28.95
10 minutes	9.79	16.19	26.6	27.59
30 minutes	4.9	8.65	16.97	17.35
1 hour	3.03	5.58	11.08	12.23

Table 6.3 - Table 6.10 below summarise the percentile values for the total demand and DHW demand distributions at levels of aggregation, k, of 5, 10, 35, and 60. At a high enough level of aggregation, the SH demand may start to dominate the peak demands. At a level of aggregation of k=35, the peak total demand at a sampling time of 5 minutes exceeds, although not substantially, the peak DHW demand, which may suggest that at this level the DHW demands stop dominating the peak. This is assuming that DHW demands have been estimated accurately and match the DHW demands inherent in the total demand. Table 6.1 shows that for the total demand distribution, sampling up from 5 minutes to 10 minutes has no impact on the 100<sup>th</sup> percentile, both of which equal 29.6 kW. This suggests that at sampling times lower than 5 minutes, the maximum demand may remain at 29.6 kW. Thus, following the trend, we can say that at a sampling time of one second it may reasonably be expected that the 100<sup>th</sup> percentile of the total demand distribution is equal to 29.6 kW. Comparing this to the 100<sup>th</sup> percentile of the DHW demand distribution at a sampling time of one second, 36.88 kW, suggests that DHW demand may be generally overestimated. If this is true, then the cross-over point of k = 35 dwellings may be different. If the DHW demands are in fact lower than estimated, then the cross over point will likely also be lower than 35 dwellings.

Table 6.3: Summary of total demand distribution percentiles for k=5 expressed as demand per dwelling (kW)

Sampling time	95 <sup>th</sup>	99 <sup>th</sup>	99.99 <sup>th</sup>	100 <sup>th</sup>
5 minutes	2.7	4.06	7.48	10.58
10 minutes	2.54	3.92	7.16	9.81
30 minutes	2.12	3.49	6.27	7.05
1 hour	1.84	2.96	5.69	5.97

Table 6.4: Summary of DHW demand distribution percentiles for k=5 expressed as demand per dwelling (kW)

Sampling time	95 <sup>th</sup>	99 <sup>th</sup>	99.99 <sup>th</sup>	100 <sup>th</sup>
1 second	4.75	6.4	11.25	14.03

<b>5 seconds</b>	4.61	6.29	11.16	13.88
<b>10 seconds</b>	4.5	6.18	10.99	13.67
<b>30 seconds</b>	4.17	5.78	10.02	12.87
<b>60 seconds</b>	3.87	5.41	9.52	12.67
<b>5 minutes</b>	3.13	4.27	8.21	9.95
<b>10 minutes</b>	2.45	3.67	7.18	8.86
<b>30 minutes</b>	1.46	2.45	4.89	5.31
<b>1 hour</b>	1.1	1.76	3.43	3.53

Table 6.5: Summary of total demand distribution percentiles for k=10 expressed as demand per dwelling (kW)

<b>Sampling time</b>	<b>95<sup>th</sup></b>	<b>99<sup>th</sup></b>	<b>99.99<sup>th</sup></b>	<b>100<sup>th</sup></b>
<b>5 minutes</b>	1.87	2.78	5.2	7.0
<b>10 minutes</b>	1.81	2.68	4.86	6.46
<b>30 minutes</b>	1.63	2.35	4.06	4.31
<b>1 hour</b>	1.47	2.11	3.72	3.9

Table 6.6: Summary of DHW demand distribution percentiles for k=10 expressed as demand per dwelling (kW)

<b>Sampling time</b>	<b>95<sup>th</sup></b>	<b>99<sup>th</sup></b>	<b>99.99<sup>th</sup></b>	<b>100<sup>th</sup></b>
<b>1 second</b>	2.8	3.71	6.23	9.25
<b>5 seconds</b>	2.73	3.65	6.16	9.15
<b>10 seconds</b>	2.65	3.58	6.1	8.94
<b>30 seconds</b>	2.42	3.4	5.77	8.43
<b>60 seconds</b>	2.19	3.21	5.65	8.39
<b>5 minutes</b>	1.74	2.58	4.87	5.86
<b>10 minutes</b>	1.49	2.2	4.31	5.37
<b>30 minutes</b>	1.01	1.59	2.78	3.46
<b>1 hour</b>	0.82	1.22	1.99	2.0

Table 6.7: Summary of total demand distribution percentiles for k=35 expressed as demand per dwelling (kW)

<b>Sampling time</b>	<b>95<sup>th</sup></b>	<b>99<sup>th</sup></b>	<b>99.99<sup>th</sup></b>	<b>100<sup>th</sup></b>
<b>5 minutes</b>	1.29	1.7	2.76	3.7
<b>10 minutes</b>	1.26	1.66	2.61	3.39
<b>30 minutes</b>	1.2	1.52	2.17	2.49
<b>1 hour</b>	1.14	1.4	1.95	2.01

Table 6.8: Summary of DHW demand distribution percentiles for k=35 expressed as demand per dwelling (kW)

<b>Sampling time</b>	<b>95<sup>th</sup></b>	<b>99<sup>th</sup></b>	<b>99.99<sup>th</sup></b>	<b>100<sup>th</sup></b>
<b>1 second</b>	1.21	1.65	2.64	3.58
<b>5 seconds</b>	1.19	1.62	2.61	3.48
<b>10 seconds</b>	1.16	1.6	2.58	3.4
<b>30 seconds</b>	1.1	1.53	2.51	3.36
<b>60 seconds</b>	1.04	1.47	2.41	3.16
<b>5 minutes</b>	0.89	1.28	2.12	2.57
<b>10 minutes</b>	0.81	1.17	1.91	2.2

<b>30 minutes</b>	0.68	0.92	1.38	1.65
<b>1 hour</b>	0.6	0.78	1.19	1.42

Table 6.9: Summary of total demand distribution percentiles for k=60 expressed as demand per dwelling (kW)

<b>Sampling time</b>	<b>95<sup>th</sup></b>	<b>99<sup>th</sup></b>	<b>99.99<sup>th</sup></b>	<b>100<sup>th</sup></b>
<b>5 minutes</b>	1.16	1.46	2.3	2.55
<b>10 minutes</b>	1.15	1.43	2.15	2.29
<b>30 minutes</b>	1.11	1.32	1.72	1.77
<b>1 hour</b>	1.06	1.25	1.51	1.52

Table 6.10: Summary of DHW demand distribution percentiles for k=60 expressed as demand per dwelling (kW)

<b>Sampling time</b>	<b>95<sup>th</sup></b>	<b>99<sup>th</sup></b>	<b>99.99<sup>th</sup></b>	<b>100<sup>th</sup></b>
<b>1 second</b>	0.93	1.24	1.91	2.56
<b>5 seconds</b>	0.91	1.23	1.89	2.54
<b>10 seconds</b>	0.9	1.21	1.87	2.44
<b>30 seconds</b>	0.86	1.17	1.81	2.3
<b>60 seconds</b>	0.83	1.13	1.76	2.03
<b>5 minutes</b>	0.74	1.02	1.57	1.81
<b>10 minutes</b>	0.7	0.95	1.47	1.59
<b>30 minutes</b>	0.6	0.78	1.05	1.11
<b>1 hour</b>	0.55	0.67	0.91	0.97

Please find the demand distributions plots for higher levels of aggregation in Appendix B.

## 6.2.2 Recommended Sampling Time

At an individual demand level, DHW demand peaks dominate SH demand peaks, apart from at the hourly time scale and above. This domination is because the DHW draws need to get up to the set point temperature (if it is direct and no storage is involved) faster than is required for SH and therefore DHW requires more power. This can be enabled by the design of the HIUs which have bigger plate heat exchangers in the DHW circuit compared with the heat exchangers in the SH circuit. There is also a boost function (which involves a boost in flow rate) in the DHW circuit that enables the higher DHW power. Thus, at an individual level, the DHW dominates the peak. This can be seen in the demand profiles presented in the first results chapter, Chapter 5. Table 6.2 summarises the impact that sampling time has on the individual DHW demand distribution and shows a range of percentiles of the demand at a range of sampling times. For the following argument, assume that a sampling time of one second can be taken as being able to fully capture the **real** individual peak demand. This is a reasonable assumption to make as it is unlikely that the demand varies substantially at lower sampling times because significant demand events do not occur at time scales that small. Table 6.2 also shows that the 95<sup>th</sup> percentile of the individual demand distribution at a sampling time of one second is equal to 20.82 kW. This means that for 95% of the time the **real** demand is lower than 20.82 kW. Thus, for a quality-of-service criterion requiring the demand in a HN to be met 95% of the time, using a peak demand of 20.82 kW to size the pipes that connect directly to the HIUs would be appropriate. Equally, using any sampling time where the maximum demand (the 100<sup>th</sup> percentile) is either above or close to 20.82 kW would also be appropriate to use to size pipes directly connected to HIUs in order to achieve

a quality-of-service-criterion of 95%. For example, take a sampling time of 10 minutes where the maximum peak demand is 27.59 kW. The 95<sup>th</sup> percentile of the demand at a sampling time of one second, 20.82 kW, is less than the 100<sup>th</sup> percentile, or the maximum demand, of the demand at a sampling time of 10 minutes, 27.59 kW. Thus, a sampling time of 10 minutes or smaller is likely suitable for sizing the pipes directly connected to the HIUs in order that 95% of demands are met. At a sampling time of 30 minutes, however, the 100<sup>th</sup> percentile is 17.35 kW, which is substantially lower than 20.82 kW, which means that sizing the HN using data measured at a 30-minute sampling time won't result in the quality-of-service criterion of 95% being met.

The plot in Figure 6.5 below shows the impact that increasing sampling time has on the 95<sup>th</sup> percentile of demand (the chosen quality-of-service criterion) at varying levels of aggregation over dwellings. The plot confirms that the peak demand is highest at a sampling time of one second at the individual demand level and that as sampling time increases, and as aggregation level over dwellings increases, the peak demand decreases. If the peak demand decreases with increasing levels of aggregation over dwellings, one can expect that a sampling time that can fully capture the peak at the individual level, when it is at its highest, will also capture the peak at higher levels of aggregation over dwellings, where the peak demand is smaller. Thus, the assertion that a 10-minute sampling time will deliver a 95% quality of service criterion holds for all levels of aggregation. Thus, in practice, this sampling time is appropriate for use in sizing all pipes across the entire distribution system, not just the pipes directly attached to HIUs.

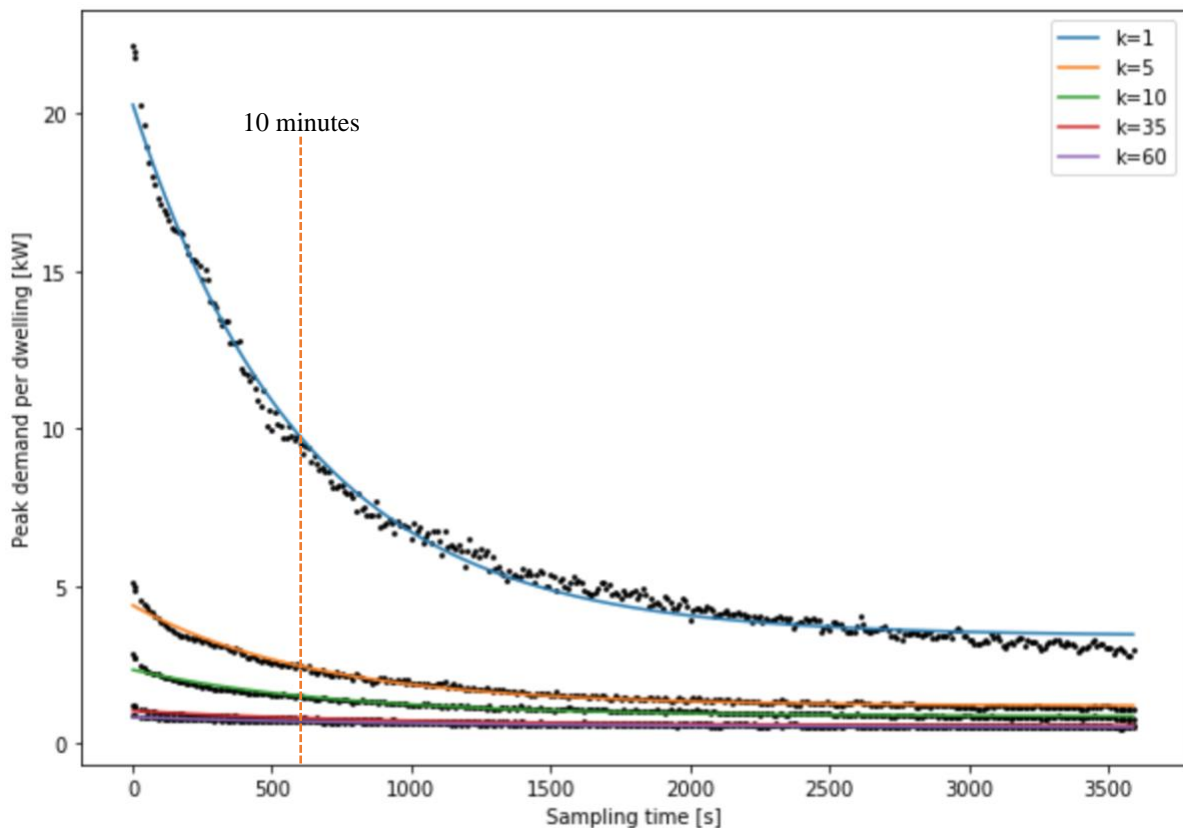


Figure 6.5: The effect that sampling time has on the 95th percentile DHW demand for varying levels of aggregation over dwellings,  $k$

The above argument stands well for the service pipes where only individual demands are relevant but what about the rest of the distribution system where aggregate demands come into play? Since DHW demands dominate up until  $k = 35$  dwellings, the above argument stands until that point. This is because if the 10-minute sampling time suffices to meet 95% of the individual DHW demand then it will also suffice to meet 95% of the demand for aggregation levels of up to 35 dwellings because of the effect of decreasing peak with increasing aggregation over dwelling described in the preceding paragraph. What about above  $k = 35$  dwellings where the DHW demand ceases to dominate the peak? At this point, where the SH demand may begin to dominate the peak demand, using the 10-minutely sampling time may result in undersized pipes that may continue to meet DHW demands but fail to deliver SH demands on top. This limitation is discussed further Section 8.3.2.

### 6.3 Total Demand Distribution Characteristics

Figure 6.6 shows several example profiles of total demand from a range of dwellings, showing both SH and DHW demand events, depicting the characteristic differences between the two. For example, as expected, DHW demand events require much higher power than SH demand events, and SH demands last substantially longer than DHW demand events, again, as expected. In the topmost profile, the first SH demand event reaches 4 kW and lasts over 2 hours. The second event in that same profile has a lower peak and lasts for the majority of the evening, likely because the thermal mass of the dwelling is charged up from the first heating event and/or heat gains from external sources such as solar gains. The SH events in the remaining profiles have a demand of around ~2 kW and last up to the duration of the whole day.

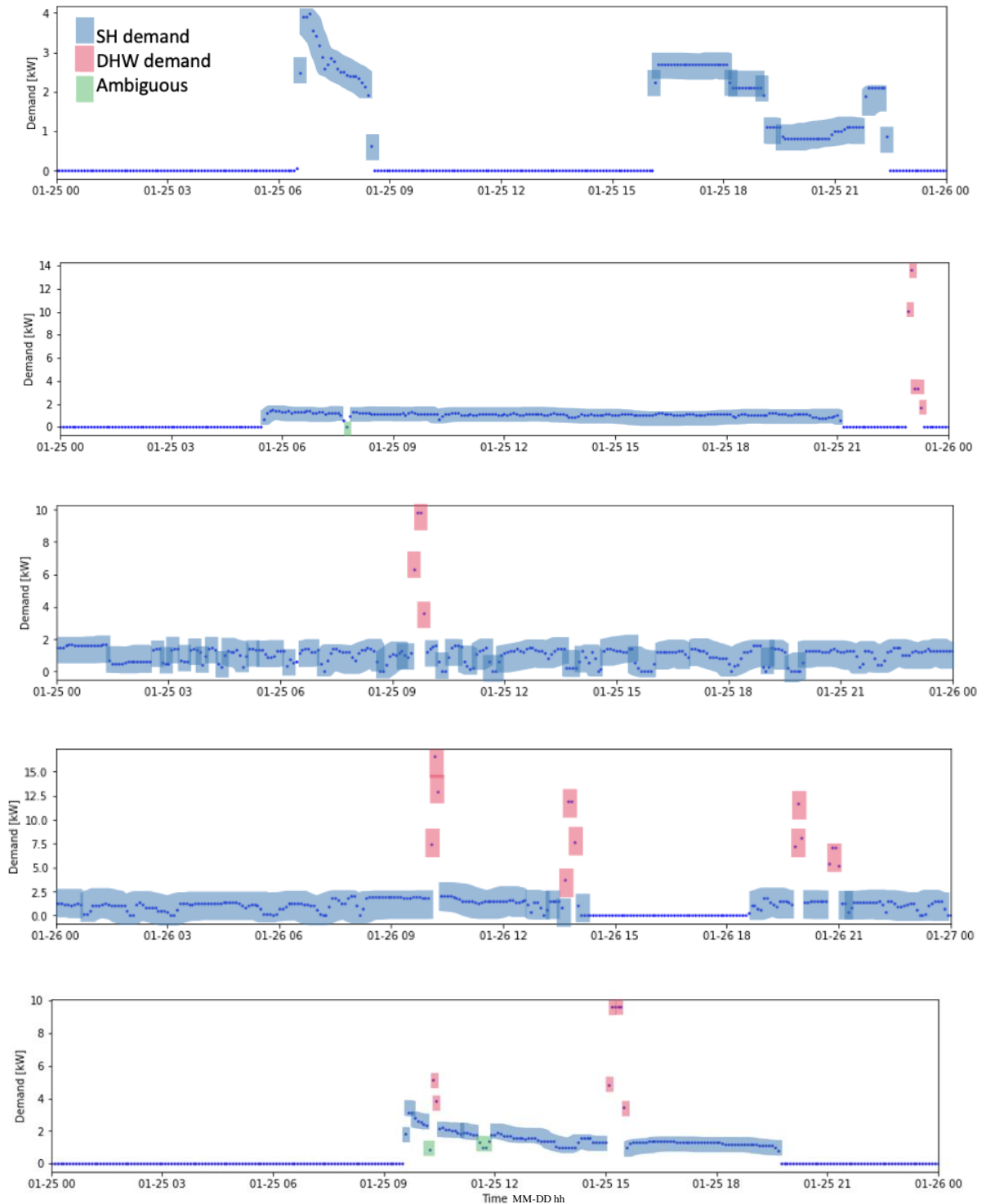


Figure 6.6: Example day-long profiles showing what could be SH, DHW and ambiguous demands which could be DHW or SH demands

The sample of profiles given in Figure 6.6 shows that SH events tend to have a mean demand of about 2 kW for the dwellings shown. SH demands across all dwellings are likely to be at a similar level given that the dwellings share the same kinds of heating systems, building fabric, and insulation properties, although solar gains and ventilation practices may introduce variance. This suggests that the prominent peak at ~2 kW in Figure 6.7 is primarily made up

of SH demand. As pointed out in Section 6.2.1, this is also suggested by the fact that the DHW demand distribution at this sampling time does not have a peak at ~2kW. The technical specification of the HIUs state that the maximum output for SH is 25 kW and the maximum for DHW is 65 kW (Heatweb Ltd., no date c). The measured demand distribution suggests that other constraints are in place in the system limiting demand to be below 35 kW. At higher demands in the distribution, the events making up that demand are likely to be made up mostly of DHW events due to them requiring a more intense load. These conclusions are summarised in Figure 6.7, which identify the parts of the distribution that are most likely to be made up of mostly SH events and mostly DHW events. The demand distribution, showing that the majority of higher demands are DHW demands, suggests that storing for DHW demand would greatly reduce the peak demands of the dwellings, allowing service pipes to be sized significantly smaller.

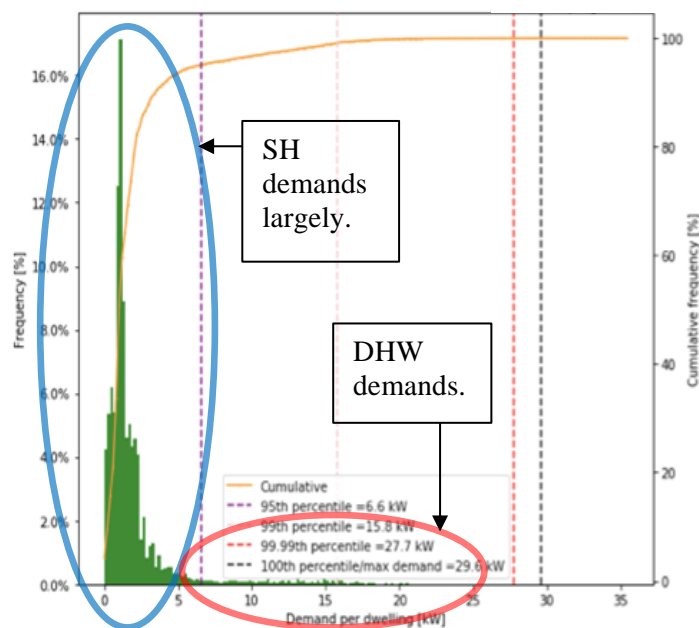


Figure 6.7: Distribution of total demand at an individual dwelling level ( $k=1$ ) and a sampling time of 5 minutes where sections of predominant SH demand and predominant DHW demands are highlighted

#### 6.4 DHW Demand Distribution Characteristic

DHW demand events typically tend to present a similar shape; as exemplified in Figure 6.8, DHW events tend to have a peak at the start before plateauing off to a steadier demand. This general shape, where DHW demand starts with a peak and then plateaus to a steady demand, is seen across all dwellings. The “peak” part of the demand event is likely to represent a “charging up” of the thermal masses that make up the DHW systems and is therefore a transient part of the demand. Additionally, the mechanics of the DHW system may also contribute to the ‘squiggle’ seen just after the peak; the thermostatic valve inside the shower mixer initially opens wide to the hot side of the valve (to compensate for the water in the pipe between the HIU and shower mixer being cold) before throttling down as the hotter water from the HIU approaches the mixer. Figure 6.9 shows a ‘zoomed out’ view of what DHW demand events look like over the timescale of several days. Figure 6.10 shows the same over a shorter span of time.

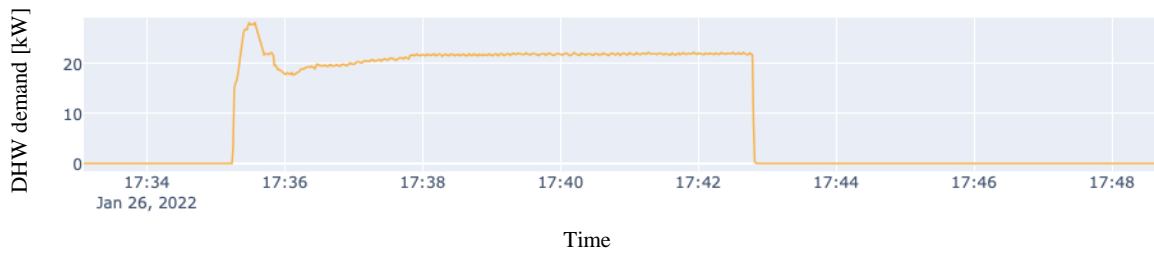


Figure 6.8: A shower DHW event, often starting with a spike and then levelling off to a constant power. More examples of this kind of event can be found in the appendix

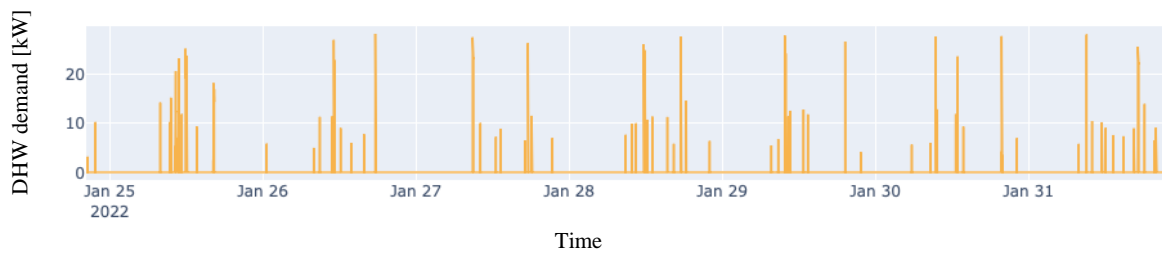


Figure 6.9: DHW demand profile spanning a number of days, showing the range of DHW events that could occur

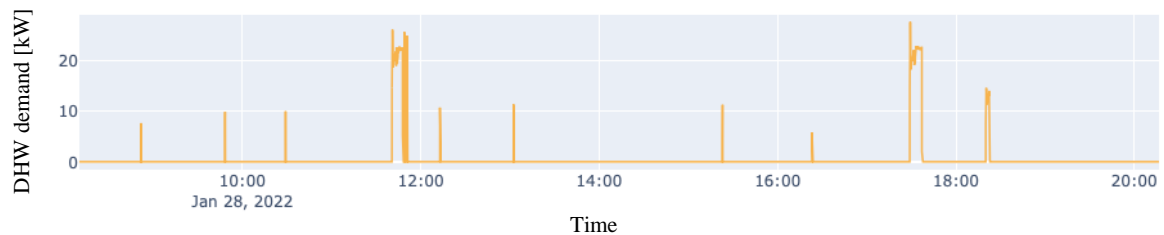


Figure 6.10: Profile showing two DHW demand events where “peak and plateau” is evident

Figure 6.11 shows instances in example profiles where there are two consecutive DHW events in which the peak of the second event is not as extreme as it is in the first event because the DHW circuit has already warmed up. The larger of these peaks are the kind of peaks which are likely to make up the right-hand side tail of the DHW demand distributions shown in Figure 6.2. The “peak and plateau” shape is also present for SH demands, as seen in the topmost profile in Figure 6.6. Like DHW transient peaks, SH transient peaks also occur at the beginning of SH demand events if the system has cooled down below a given level. However, the level of demand required to meet occupant comfort for SH can be considered a ‘moving target’ compared to the demand needed to meet comfort levels relating to DHW. This is because of the highly variable context for providing SH because SH demand is coupled to external temperature, whereas DHW is not. Additionally, DHW circuits are relatively low volume compared to SH circuits and therefore can get ‘up to temperature’ faster.



Figure 6.11: Examples of DHW events where the first in which a transient peak is present is closely followed by a second event in which the peak is less extreme

For DHW, the higher demand during the peak is also met through an increase in flow rate, as illustrated in Figure 6.12, through the boost function, which dictates that if the primary flow temperature is below a set point, the primary flow should be operating at a maximum (16 l/m) (R. Hanson-Graville, personal communication, September 2019). This is depicted in Figure 6.13. For SH thermal mass that needs to be charged up will include not only the underfloor heating system but also the thermal mass of the dwelling fabric.

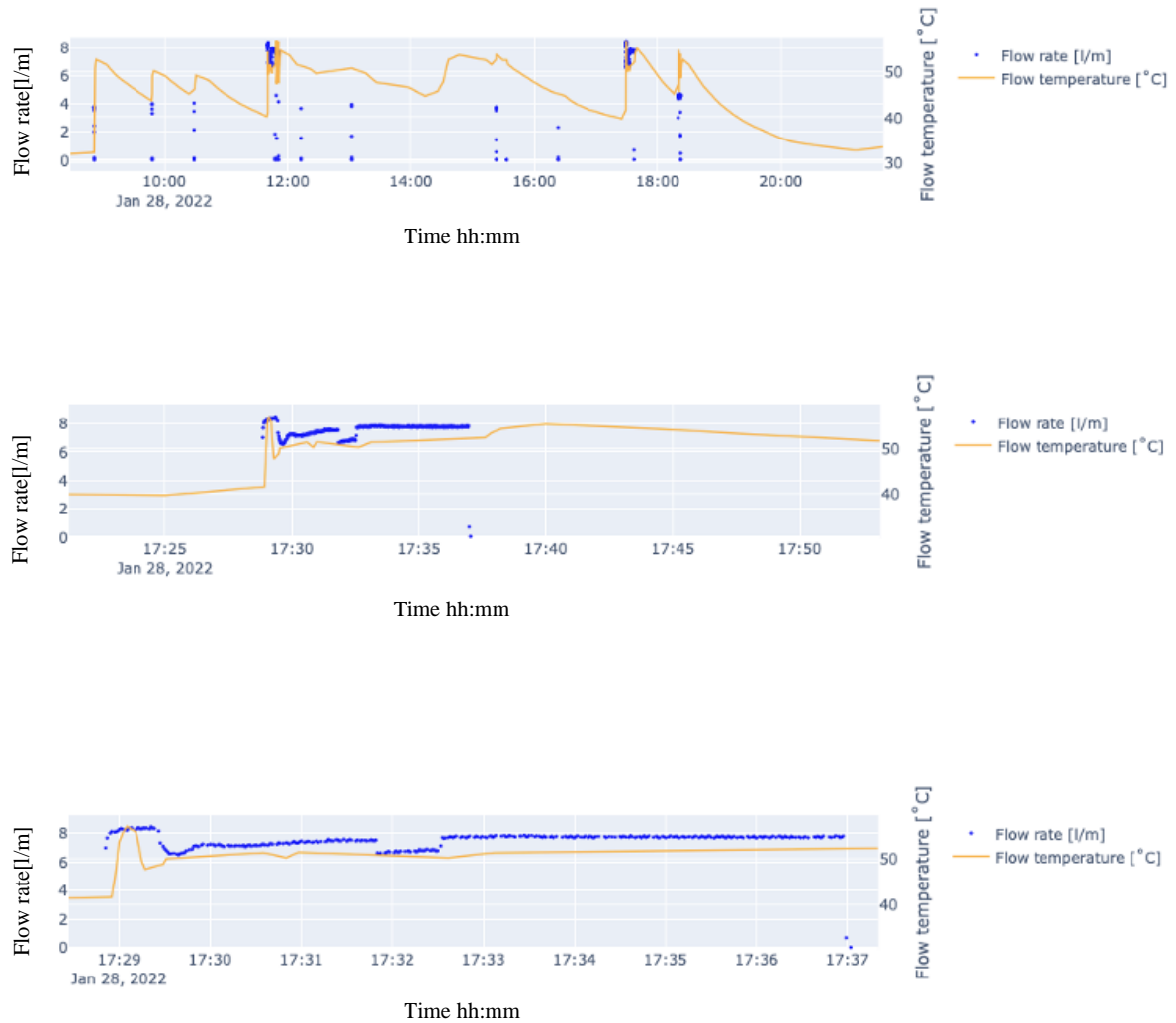


Figure 6.12: Series of plots showing the behaviour of DHW flow temperature and flow rate behaviour during a peak demand. The series increasingly zooms into the DHW peak event occurring around 17:29

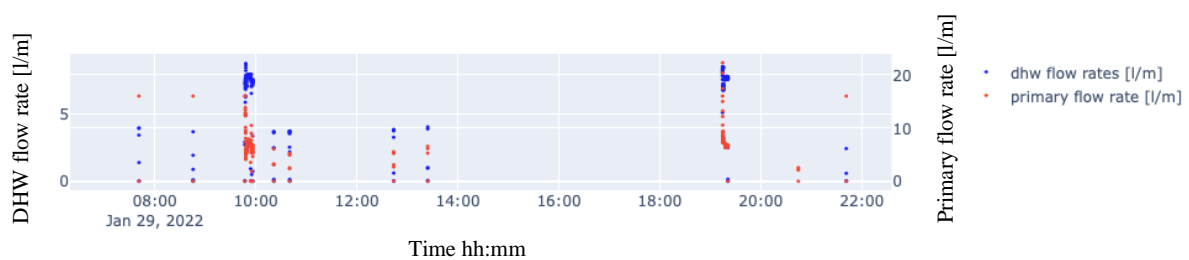


Figure 6.13: DHW flow rate and primary flow rate behaviour during peak events- showing primary flow rate reaching 16 l/s

Whilst peak demands are largely the result of the physical system (for example, by being limited by the size of the heat exchangers), the “plateau” part of the demand are steady state and are influenced largely by the requirements of the occupant and the conditions they call for during a particular event (for example, how hot do they want their shower to be). For example, the middle profile in Figure 6.11 shows that the real occupant demand would be

adequately represented by the steady demand at 15 kW. The shorter duration of the peak demands and the longer duration of the “plateau” demand are clearly visible in the demand profiles given in Figure 6.11. The large peak in the DHW demand distribution at a sampling time of one second centred at 15 kW, reproduced in Figure 6.14 below, accounts for a large proportion of the demand and is therefore likely to represent the real occupant demands that are steady and last much longer than the transient peaks. The peak of the DHW demand distribution is present for all sampling times lower than 5 minutes. The base of the peak starts at 2.5 kW and ends at 20 kW, highlighted in Figure 6.14 using a red arrow. This suggests that the “plateau”, or steady state, demands which represent real occupant demand in dwellings has a range between 2.5 kW and 20 kW and that they do not tend to last longer than 5 minutes. The transient demands that are larger than the steady demands would therefore make up the right tail of the distribution (between 20 kW and 30 kW). This suggests that the transient peaks across the group of dwellings spans 20 – 30 kW.

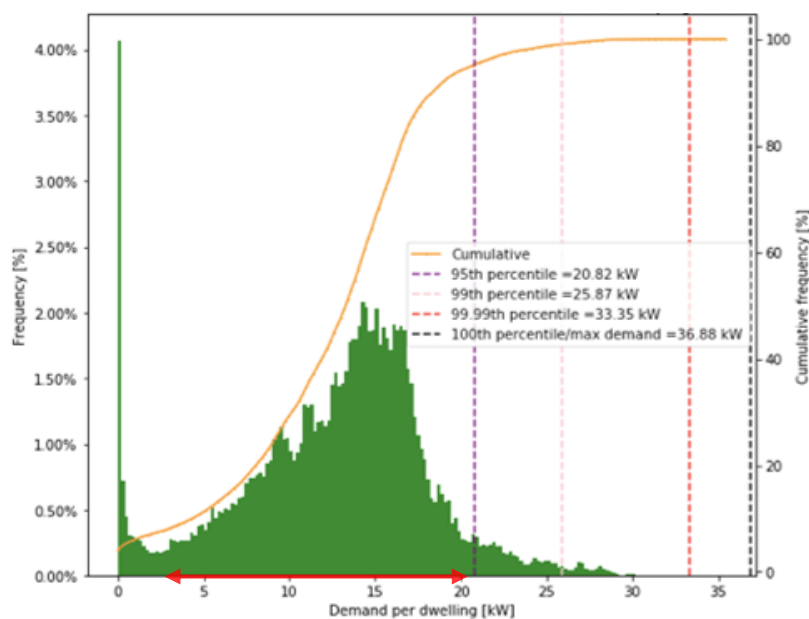


Figure 6.14: DHW demand distribution where red arrow denotes the large peak centred at 15 kW. Individual demands at a sampling time of one second.

In addition to the ‘peak and plateau’ demands, there is another kind of demand that although is present across all dwellings, is largely inconsequential to the design of the HN. These are demands that occur for a few seconds as a short, sharp spike. Two examples of such demands are shown in Figure 6.15 below. Figure 6.2, which shows the difference between the demand distribution at a sampling time of 1 and 5 seconds, where the higher range remains unchanged (remaining at around 30 kW), suggests that the demands that occur on small time frames are not peak demands. Thus, information regarding such minor demands is unlikely to have any meaningful bearing on HN design, regardless of the intended quality-of-service criterion.

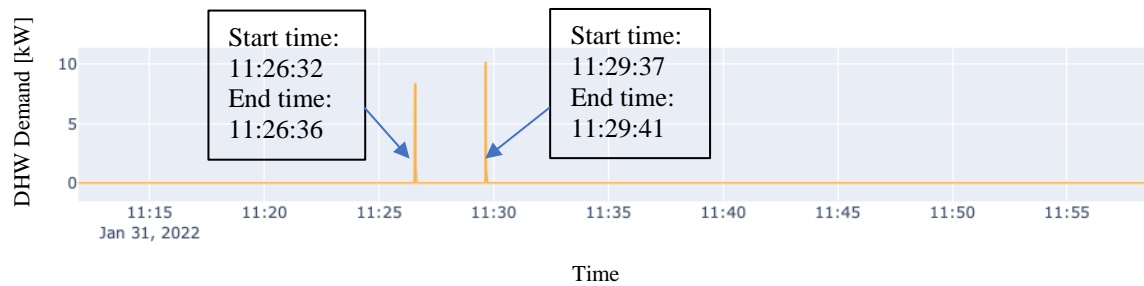


Figure 6.15: Two small demand events which often take the shape of a short, sharp spikey demand that tends to last less than 5 seconds

The key conclusions from this section are summarised in the diagram in Figure 6.16 below. Note that the higher range of demand, between 20 kW and 30 kW, could also be due to real occupant demand peak resulting from multiple outlets running at once, e.g., tap and shower being used simultaneously; however, simultaneous demands like this would be rare but may affect occupant experience (R. Hanson-Graville, personal communication, February 2022).

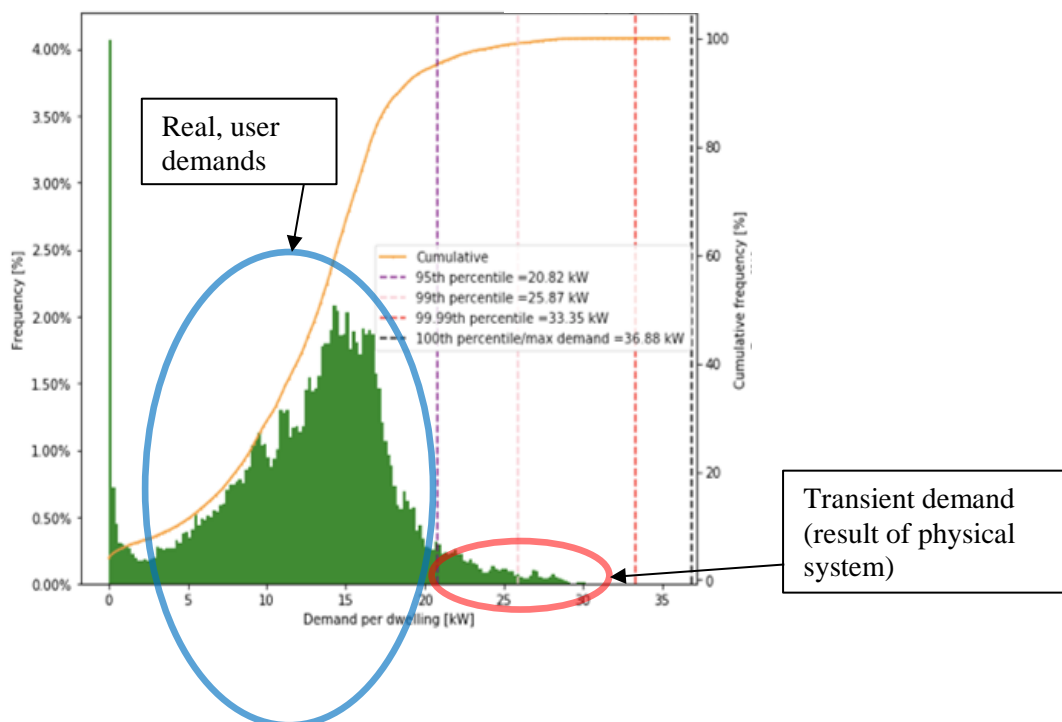


Figure 6.16: DHW demand distribution showing where the real occupant demands and transient demands are likely to be. Individual demands at a sampling time of one second.

Does the nature of the higher demands make a difference to how small the pipes serving individual dwellings could potentially be sized? The current practice for sizing the pipes that are connected directly to the HIU is to size for max HIU output (M. Cosic, Personal communication, 2022). Where the demands between 20kW and 30kW are in fact real consumer demand, pipes sized for 15 kW would not be able to meet this demand effectively; on the rare occasion that there is a shower and tap, for example, running simultaneously, the occupant's desired comfort levels would not be achieved. However, if the demand between

20 kW and 30 kW is made up of only transient heat demands (i.e., thermal mass charging up) then sizing the pipes for a peak demand of 20 kW may still preserve occupant comfort. To put another way, if the pipes were sized to 20 kW then generally, the occupants may have to wait a little longer for their water to heat up but the shower or tap draw would perform the same thereafter. Instances where two draws are happening simultaneously will, however, be affected more severely as will occupants that have real occupant demands that are above 20 kW, which are rare but do exist (topmost profile in Figure 6.11). This is an interesting point to consider because if occupants were willing to make this compromise, the benefit of the trade-off, e.g., smaller pipes and therefore lower heat losses, may be worthwhile. Note that SH demands which tend to be lower than 5 kW, shown in Figure 6.7, would also comfortably be met. In practise there is some leeway allowed when delivering heat through pipes sized to a fixed demand because higher flow rates, and therefore higher demand, can still be delivered under the right pressure conditions. The above is an argument based on a fixed pressure assumption used to illustrate the general effects of reduced pipe sizing on demand and occupant comfort. In real conditions, the likely impact of undersized pipes will be dependent on the pressure conditions available and where there is an impact, it is the dwellings at the ends of branches where such effects of will be seen first.

Additionally, this ties into the recommendation of a 10-minute sampling time for sizing the distribution system made in earlier sections. A quality-of-service criterion of 95% was the basis of this recommendation. This criterion was shown to correspond to a demand of 20.82 kW. Given that the real occupant demands (both SH and DHW) were found to be 20 kW or lower, it can be said that the selected quality-of-service criterion is sufficient in meeting all real occupant demand.

## 6.5 Real Peak Demand

Figure 6.17 shows the rate at which the dwelling per demand decreases as the number of dwellings increase for the DHW and total demand at a sampling time of 10 and 30 minutes. The curves were created by taking the maximum demand of 50 random combinations of dwellings at each level of aggregation. The half-hourly total demand curve in Figure 6.17 can be compared with a chart developed by Guru Systems, presented in Section 2.5.3 initially and reproduced here in Figure 6.18. Figure 6.18 shows the DS439 based capacity<sup>6</sup> with the measured capacity which is equal to the 99.989<sup>th</sup> percentile of half-hourly instantaneous power meter readings from a ~1000 dwelling sample across several HNs<sup>7</sup> (Personal communication, T. Noughton, May 2022). The Guru curve (SH and DHW) gives a value of 2.5 kW per dwelling at 80 dwellings, whereas the total demand half-hourly curve in this work shows a demand requirement of 1.5 kW. For 60 dwellings, the peak demand per dwelling for the dwelling sample in this work is a little above 1.5 kW, whereas for the Guru Systems sample, it is ~ 2.5 kW. For 5 dwellings, the capacity in this work's sample is ~6 kW, whereas in the Guru Systems study it was just below 10 kW. The peak demands for case study sample at all levels of aggregation are lower than they are in the Guru sample. Although it can't be confirmed, it is likely that the HNs in the Guru sample included a wide range of HNs that

<sup>6</sup> Specifically, the heat exchanger sizing method, as opposed to the pipe sizing method, described in full in Section 2.5.3 in the literature review chapter.

<sup>7</sup> For each half hour time step, a histogram containing a reading from each of the dwellings was built and normalised, following which the demand distribution for a scheme of  $n$  flats by convolving this distribution  $n$  times. Each point on the curve is determined by summing the distributions for a given  $n$ , normalising this distribution to get the distribution for an entire year, taking the 99.989<sup>th</sup> percentile and dividing by  $n$ .

included but were not limited to CHNs. Thus, there may be a good proportion of standalone dwellings in the sample whose demands are notably higher than flats/apartments which make up this work's sample in its entirety.

The capacity, as determined using the DS439, is higher than both the capacity of the Guru Systems sample and the capacity for this sample, across all levels of aggregation. Although the assumptions underpinning the calculation of the DS439 capacity is unclear, a tentative comparison can be made. Note that the DS439 curve presented in Figure 6.18 is not the method recommended in CP1.2, it is instead the heat exchanger sizing method (Personal communication, T. Noughton, May 2022). Moreover, Section 2.5.5 in the literature review makes a distinction between the real demand, which is the demand measured at a certain point in the network, and the aggregate demand which is calculated by summing the measured individual demands at each time step. The measured curves presented in Figure 6.17 and Figure 6.18 are *aggregate demands*. Guru Systems confirmed the oversizing indicated in Figure 6.18 by producing a similar graph using a large amount of bulk meter readings which are readings taken either at an energy centre or at a substations/ building entry point (Personal communication, T. Noughton, May 2022). Such a curve would be representative of the *real demand* since it comprises measurements taken directly from the distribution system. Although this does not confirm the relationship between aggregate and real demand, it does provide validation regarding oversizing claims based on aggregate demands.

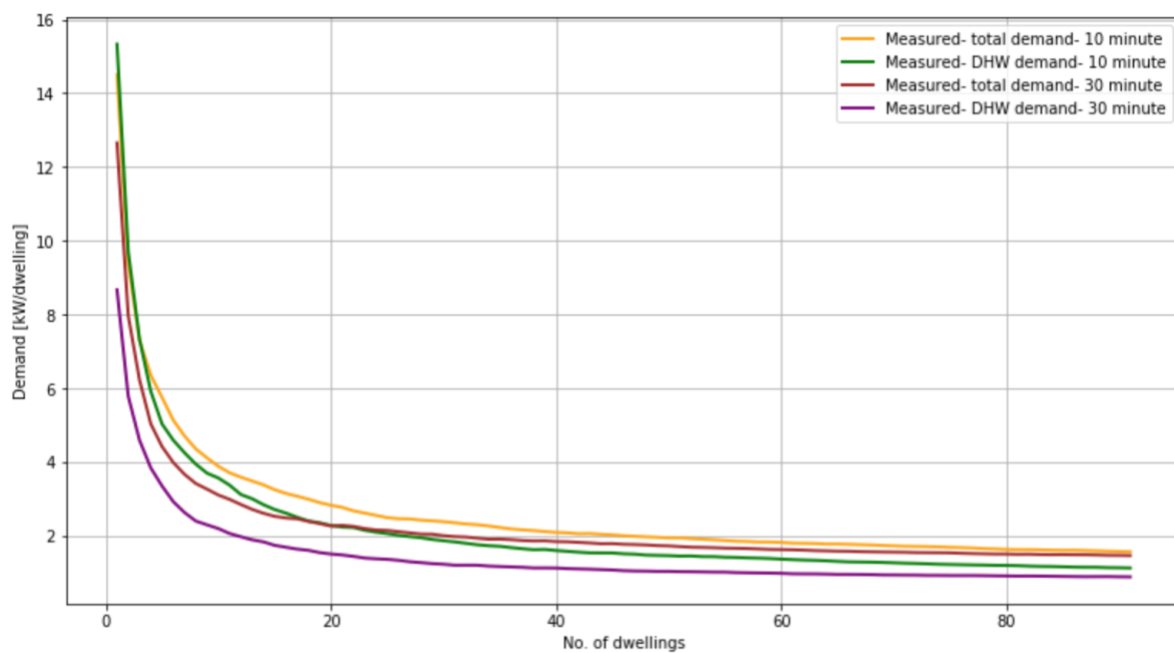


Figure 6.17: The demand per dwelling for the DHW demand and the total demand at a sampling time of 10 and 30 minutes

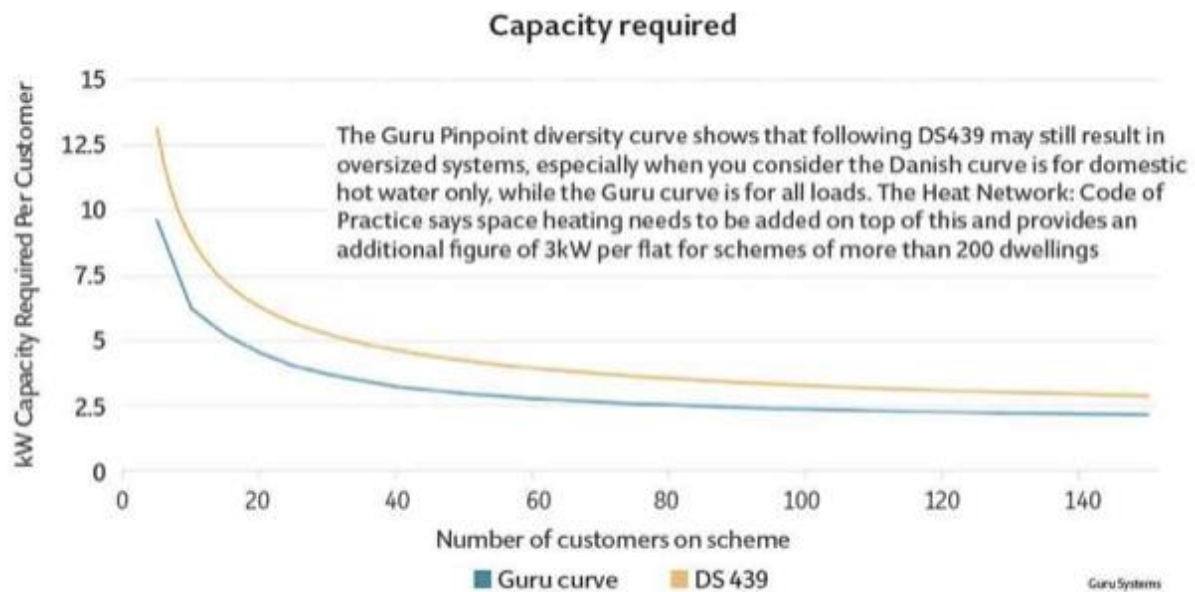


Figure 6.18: Guru diversity curve for space and DHW demand as compared with the DS439 curve (heat exchanger sizing) for DHW demand only (Smith, 2016)

Figure 6.19 shows the design capacity for the total and DHW demands, as determined using the methods recommended in CP1.2, using its Annex D as a guide, next to their measured equivalents (CIBSE, 2020). To calculate the DHW and total demand design capacities, the SH diversity factor and diversified DHW flow rate equations, presented in Sections 2.5.1 and 2.5.2, respectively were adapted and used. The design capacities are presented as ribbons showing a range of values whose calculative components are outlined in Section 13.1, Appendix C along with the adapted equations and supplementary plots. Figure 6.19 indicates that the measured peak demands are less than half of what is estimated for both DHW demand alone and for the total demand across all levels of aggregation up to and potentially beyond, 80 dwellings. Table 6.11 below specifies the design capacities, measured peak demands and the corresponding overestimation for 5, 15 and 35 dwellings showing that the overestimation remains substantial at this range. The figure also shows how closely the measured total demand and DHW demand curves follow each other. This is expected at the lower levels of aggregation where DHW peaks dominate, and thus where the peak of the total demand, which would be a DHW demand, will be equal to the peak DHW demand, but is not necessarily expected at higher levels of aggregation. The two curves slightly divert away from each other at around 5 dwellings and remain so past 80 dwellings. The difference between the two curves, at its highest at around 20 dwellings, is  $< 1$  kW. The plot also shows that the peak demands at an individual level have a mean of  $\sim 15$  kW which implies that with DHW systems, typically designed to deliver higher peaks, may often go underutilised. This may be the result of overestimated peak flow rates, as was found to be the case in other European countries (detailed in Section 2.5.4). The substantial discrepancy at the individual demand level also suggests that the smaller pipes, those serving a single dwelling, are where the most stands to be gained with respect to reducing pipe sizes and thermal loss savings. This will be further qualified in the following results chapter in the discussion around Figure 7.24 which shows high thermal loss in smaller pipes.

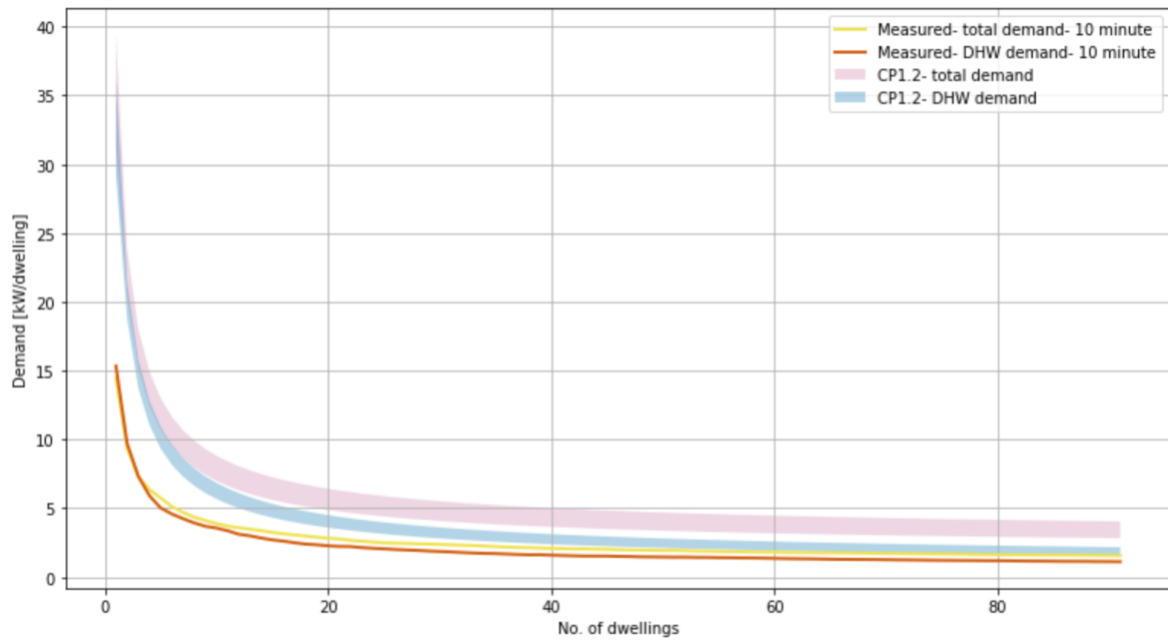


Figure 6.19: Design total demand and DHW demand capacities with the measured DHW demand and total demand peaks (10- minute sampling time)

Table 6.11: Comparison of design capacities compared with measured values for DHW and total demand

Demand type	Number of dwellings, N	Design capacity (kW)	Measured value (kW)	Overestimation (%)
<b>DHW</b>	5	9.35 - 10.91	5.01	87 – 118 %
	15	4.32 - 5.32	2.74	58 – 94 %
	35	2.57 -3.34	1.70	51 – 96 %
<b>Total</b>	5	10.74 – 13.0	5.90	82 – 120 %
	15	5.61 – 7.26	3.30	70 - 120 %
	35	3.83 – 5.23	2.23	72 – 135 %

## 7 Results 3 – DHW Storage Impact on HN Design and Demand

### 7.1 Introduction and Relevant Objectives

This chapter pertains to the research question and objectives stated below:

- *What is the impact of DHW TES on HN demand and design in the presence of diversity?*
  - Estimate the residual DHW demands that would result from DHW TES installation for the sample of dwellings.
  - Assess the impact that DHW TES has on the aggregate demand.
  - Assess the impact that DHW TES has on the distribution system pipe sizing and the resultant impact on thermal loss.

### 7.2 Thermal Store Model Results

#### 7.2.1 Mixed Thermal Store Results

The plots below show the residual demands (i.e., the modelled demand of a dwelling where storage is being utilised) obtained for an example dwelling using the mixed heat store model. The top profile in Figure 7.1 shows the residual demand and the DHW demand. The bottom profile shows the temperature of the store for the same period. The plots show that as the store starts to charge at 5 am, the temperature of the store starts to gradually increase, indicating that the store is charging up. The rate of charging slows as the temperature of the store rises, as indicated by the decreasing positive gradient of the store temperature and the decreasing negative gradient of the residual demand. When the store is full, and there is no DHW demand, like in the short period after the first charging time window ends, the store loses heat to its environment. This results in a gradual decrease in the store temperature. When there is a demand for DHW, there is a drop in temperature in the store proportional to the rate of demand. Figure 7.2 gives an example of a multi-day profile, showing the behaviour of the store model for a different dwelling. The maximum charging power in a mixed heat store model is defined such that the store can be fully charged in two hours (see Table 3.2 and Section 3.6.2). The maximum charging power varies from store to store because each store is sized according to the daily demand of a dwelling. If a dwelling has a larger daily demand, it requires a larger store to meet that demand. Hence, the maximum charging power of the store shown in Figure 7.1 is larger than the store in Figure 7.2 because the former dwelling has a larger daily demand. Although the maximum charging power is defined in this way, it does not necessarily mean a store will completely fill up in the two hour time window every time, hence the store temperatures not reaching 50 °C in certain instances such as the first charging window of the Figure 7.1. This is because the charging power is dynamic and does not remain at a fixed level as the store fills up. The maximum charging power was defined in this way as a first order approximation of the maximum charging power that would have led to a fully charged store in two-hour time window.

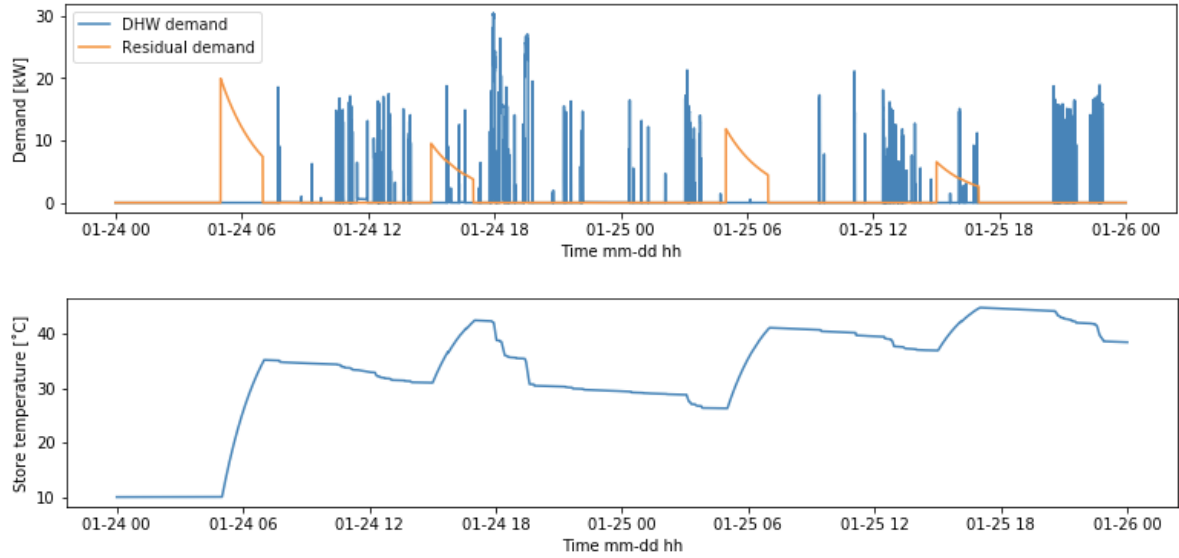


Figure 7.1: Residual demand and store temperature example profile for the mixed store model

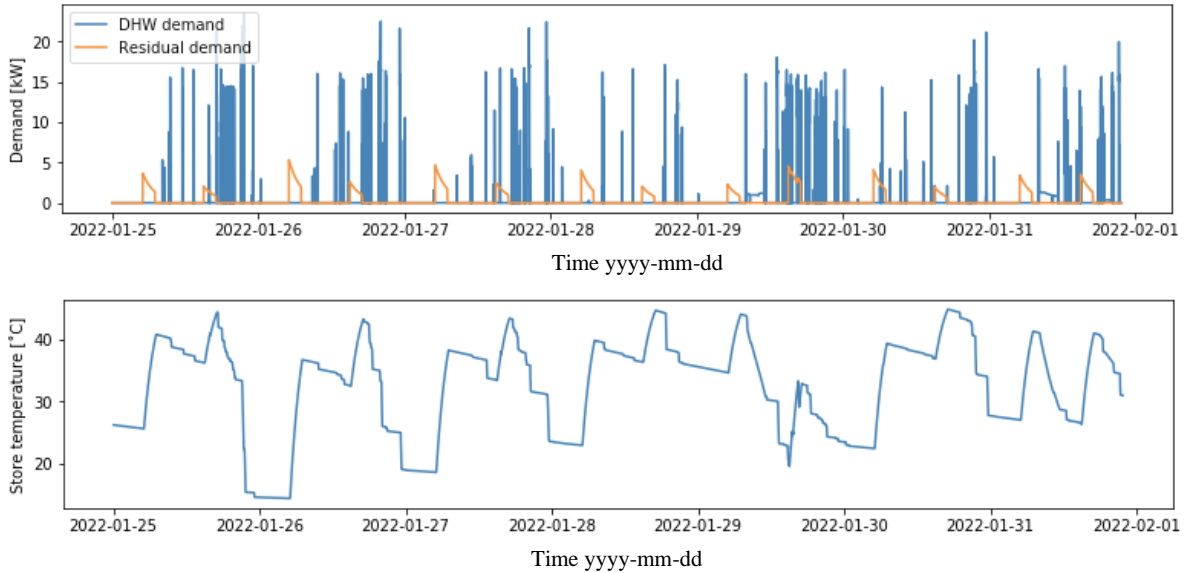


Figure 7.2: Example multiple day profile resulting from CC-mixed model

Figure 7.3 and Figure 7.4 give the fraction of the real DHW demand met by the mixed model. In both scenarios, over 90% of the demand is met for the vast majority of the dwellings. There are no dwellings for which less than 75% of the demand is met. The unmet demand is unlikely to consist only of peak demands, thus, the sizing analysis is not affected.

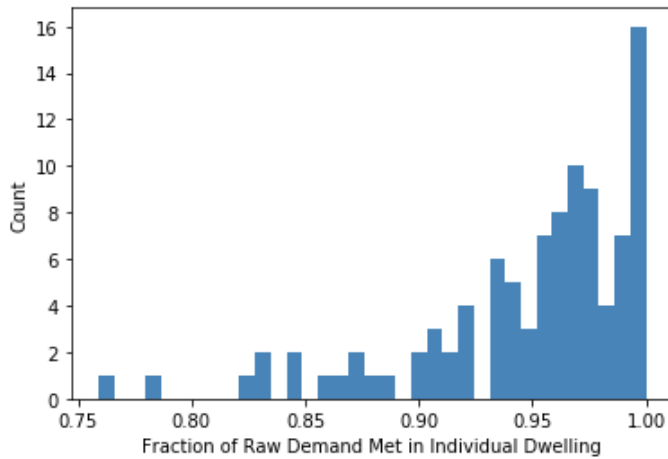


Figure 7.3: Histogram of the fraction of the real DHW demand met in individual dwellings in the CC scenario using the mixed store model

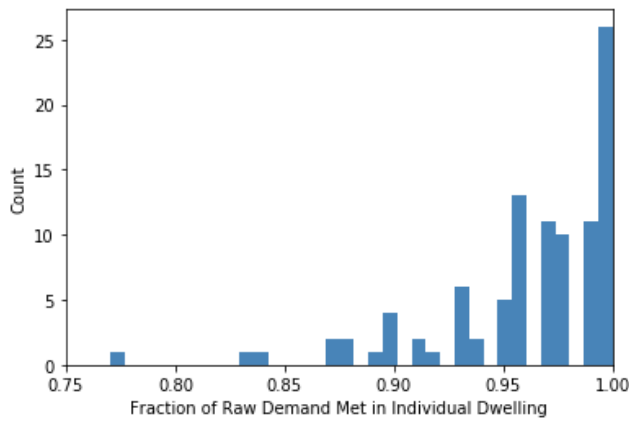


Figure 7.4: Histogram of the fraction of the real DHW demand met in individual dwellings in the SC scenario using the mixed store model

## 7.2.2 Stratified Thermal Store Results

Figure 7.5 shows the outputs of the stratified store model for an example dwelling. The residual demand (top profile) shows the store charging at a constant rate between 5 am and 7 am. The thermocline position moves from 0.45 m to 0.0 m during this time, indicating that the store has completely charged in this time. The thermocline position gradually moves back towards 0.45 m as the store loses heat to its surrounding environment. At 3 p.m. the lost heat is replaced as the store charges up again. Once the store is fully charged, the HIU keeps the store topped up as the store loses heat to surroundings gradually. This results in the cycling type residual demand pattern. The store is finished charging at 6 p.m. Figure 7.6 gives a multi-day profile of the outputs of the stratified model for another example dwelling. The numerous DHW demand events occurring between 12 p.m. and 3 p.m. deplete the store of charge, indicated by the staggered rising of the thermocline position. The heat loss profile is a mirror image of the thermocline position because the heat loss is directly proportional to the surface area of the hot zone of the store. No heat loss occurs in the cold zone, because the cold-water temperature is equal to the temperature of the environment.

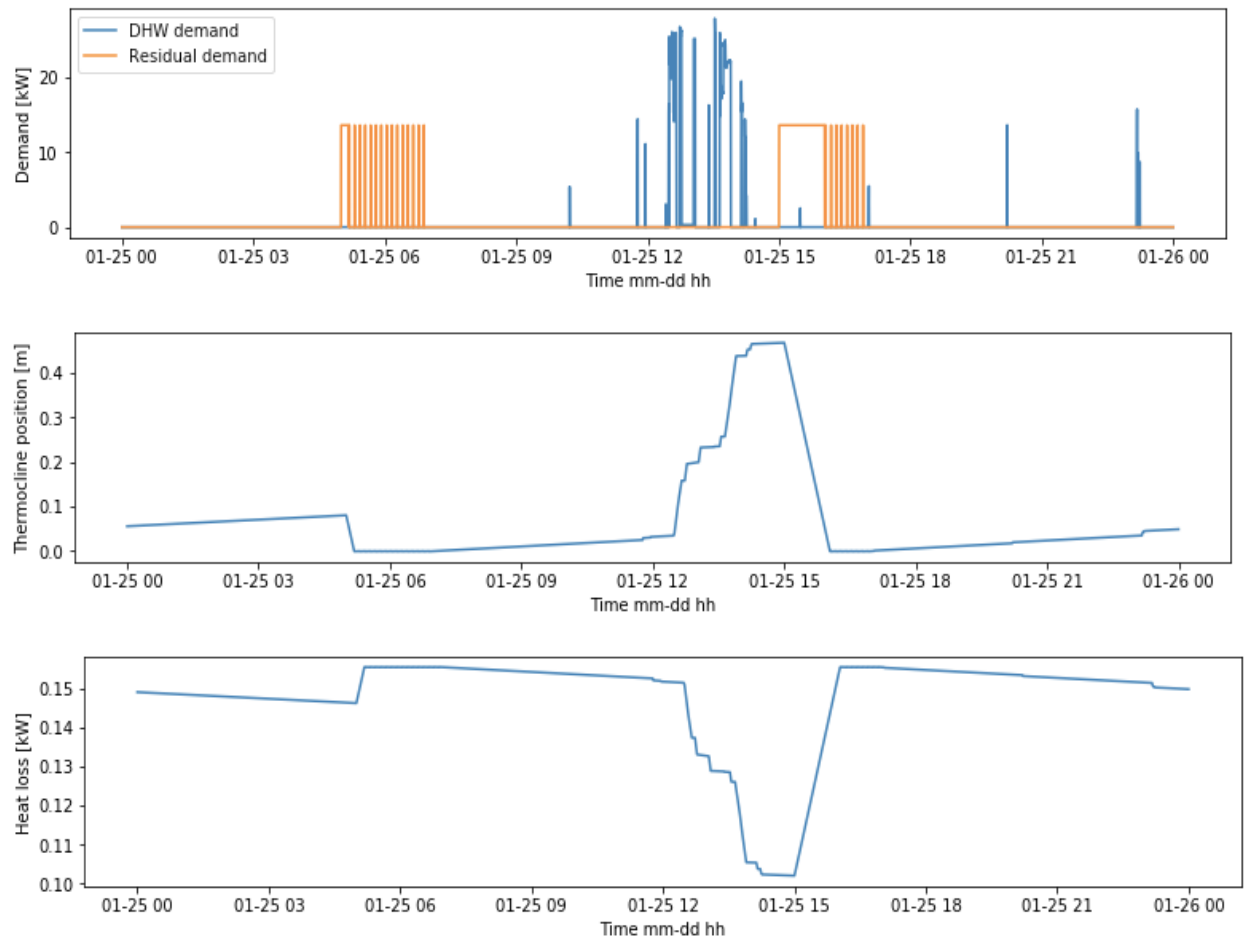


Figure 7.5: Residual and thermocline position profile of an example dwelling, obtained using the stratified store model. The height of the store is just above 0.4m. The thermocline at above 0.4 m indicates that the store is empty.

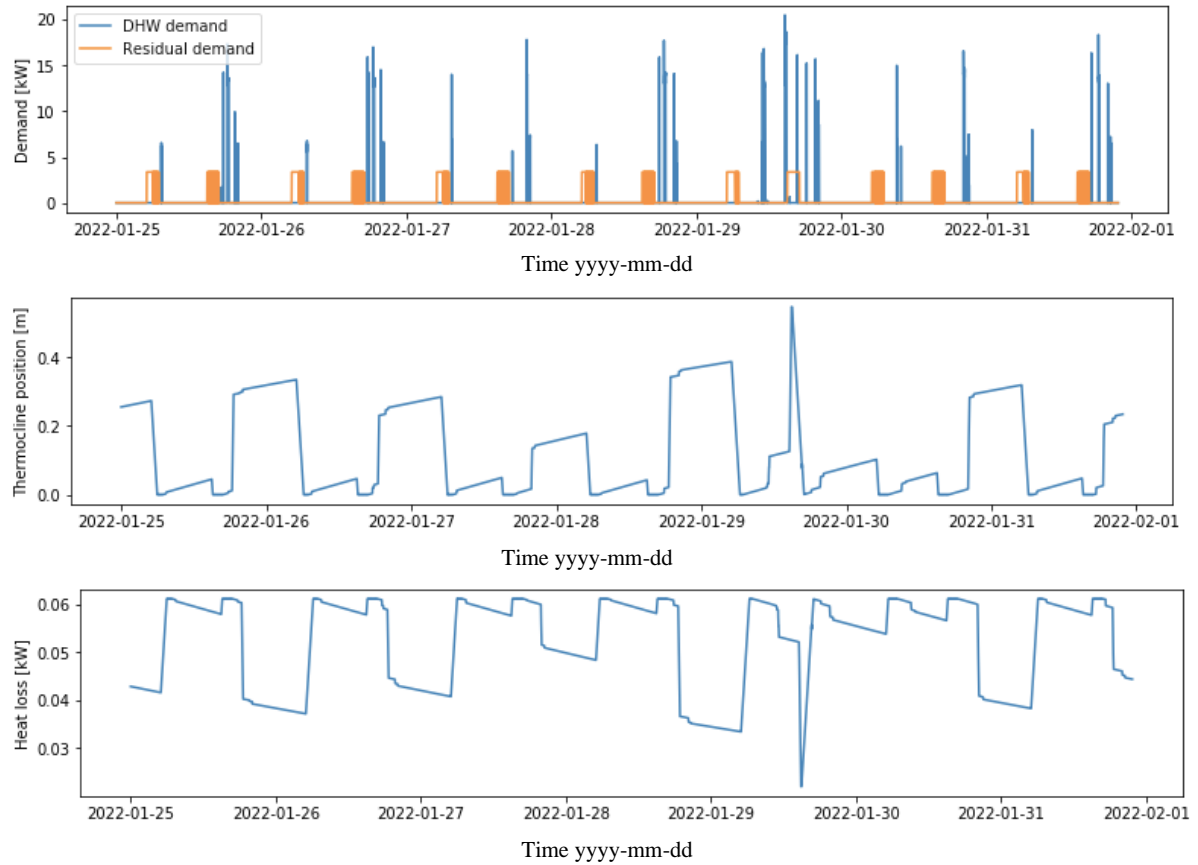


Figure 7.6: A multi-day profile for the residual demand, thermocline position and heat loss profile outputs of the stratified model. A high thermocline position indicates that the store is empty, while a thermocline position at 0.0m indicates that the store is full.

Figure 7.7 and Figure 7.8 show the fraction of real DHW demand met by the stratified store model in both storage scenarios. The histograms show that over 95% of the demand was met for a vast majority of the dwellings, and there were no dwellings with less than 80% of the real demand being met.

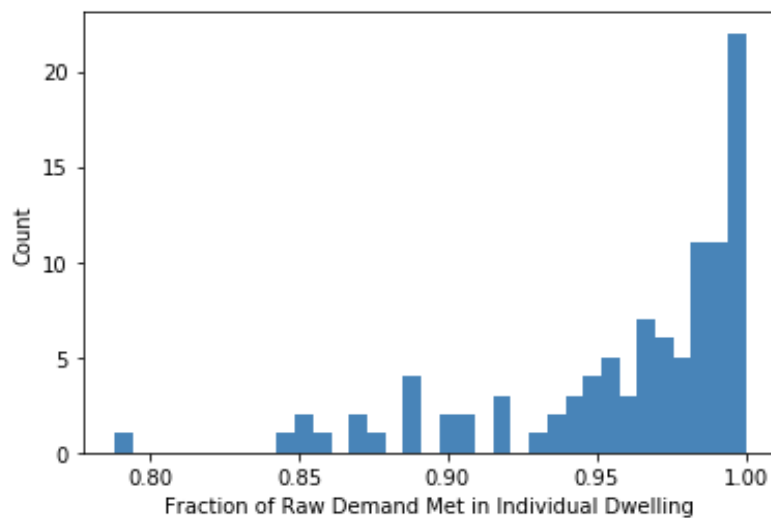


Figure 7.7: Histogram of the fraction of the real DHW demand met in individual dwellings in the CC scenario using the stratified store model

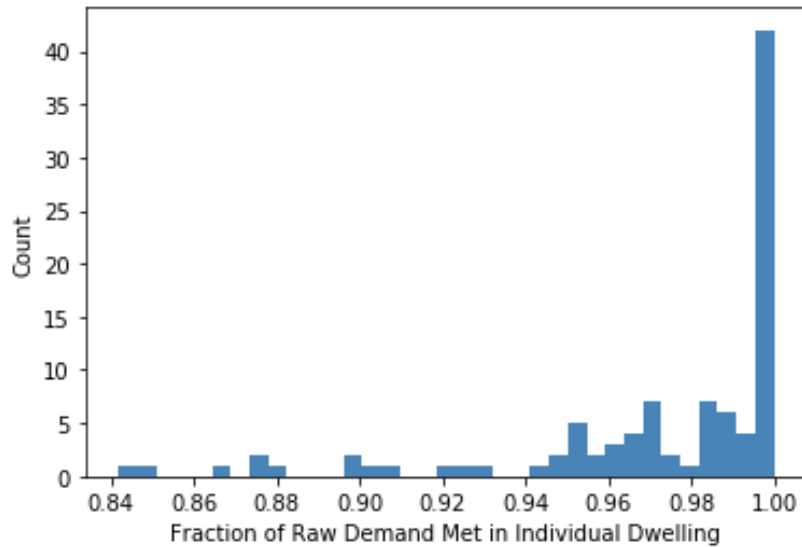


Figure 7.8: Histogram of the fraction of the real DHW demand met in individual dwellings in the SC using the stratified store model

### 7.3 Thermal Store Model Validation

Both, the stratified and the mixed models, were validated by setting the key input variables to quantities where the resulting outputs can be predicted, for example, setting the store temperature to  $0^{\circ}\text{C}$  or a substantially large temperature value to test whether model outputs were as expected. Results of the validation are given in the Appendix A Section 11.2. The results of other similar validation exercises are presented in the remainder of this section.

#### 7.3.1 Mixed Thermal Store Model Validation

To validate the heat store model, the result of adjusting selected parameters were checked against what is expected. Figure 7.9 and Figure 7.10 show the demand profile of an example store in which the heat loss factor was set to  $1 \text{ W/m}^2\text{K}$  and  $0 \text{ W/m}^2\text{K}$  respectively. The figures show that a heat loss factor  $0 \text{ W/m}^2\text{K}$  leads to 0 heat losses as expected, and the temperature of the store thus varies only due to the heat drawn from the primary network and the heat output which meets the DHW demand. Whereas, where the heat loss factor is  $1 \text{ W/m}^2\text{K}$ , in the profile shown in Figure 7.9, the heat loss from the store is larger than zero and is a function of the difference in temperature of the store fluid and the external environment.

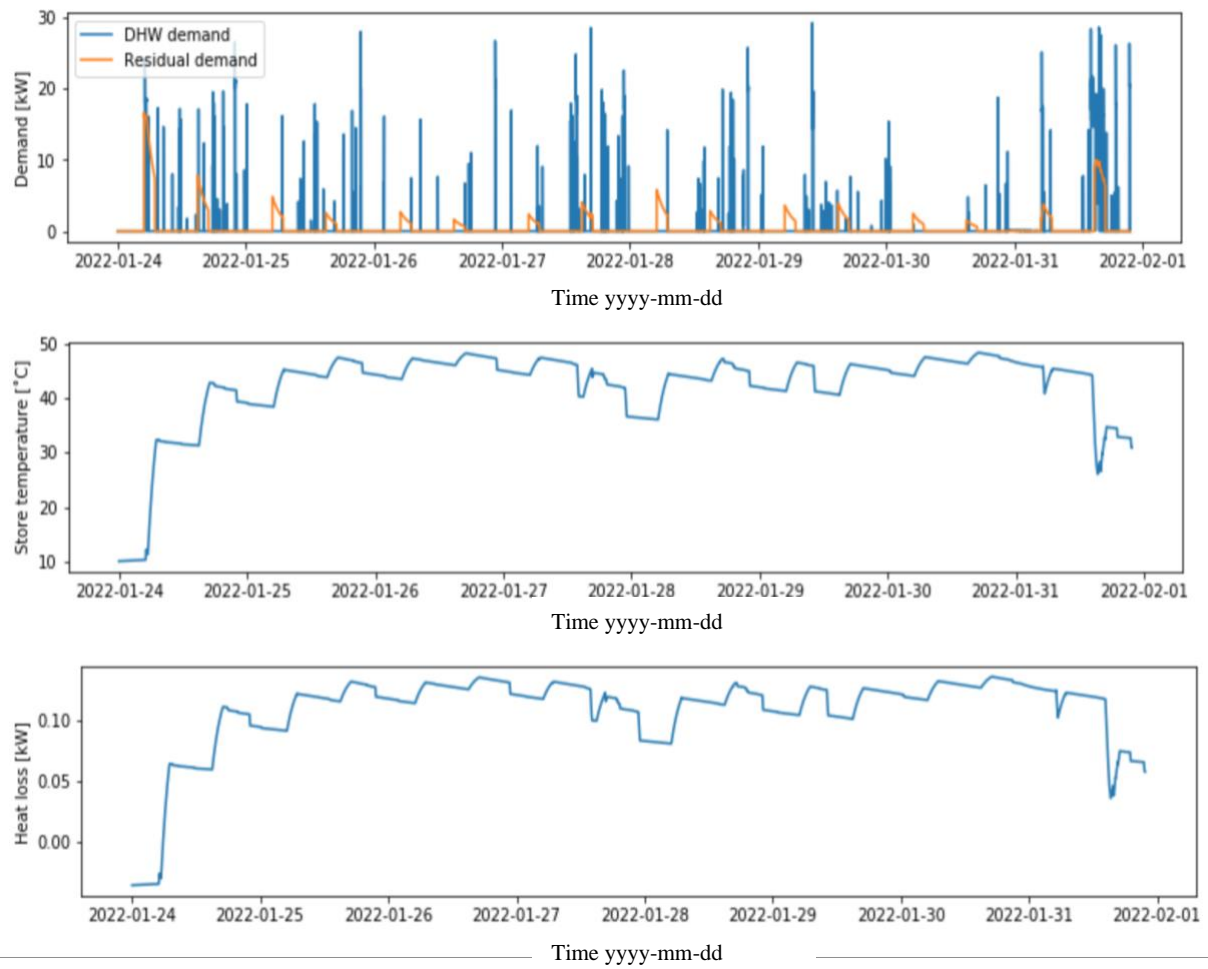


Figure 7.9: Example demand profile for a store where the heat loss factor is equal to  $1 \text{ W/m}^2\text{K}$  and ambient temperature is set to  $18^\circ\text{C}$

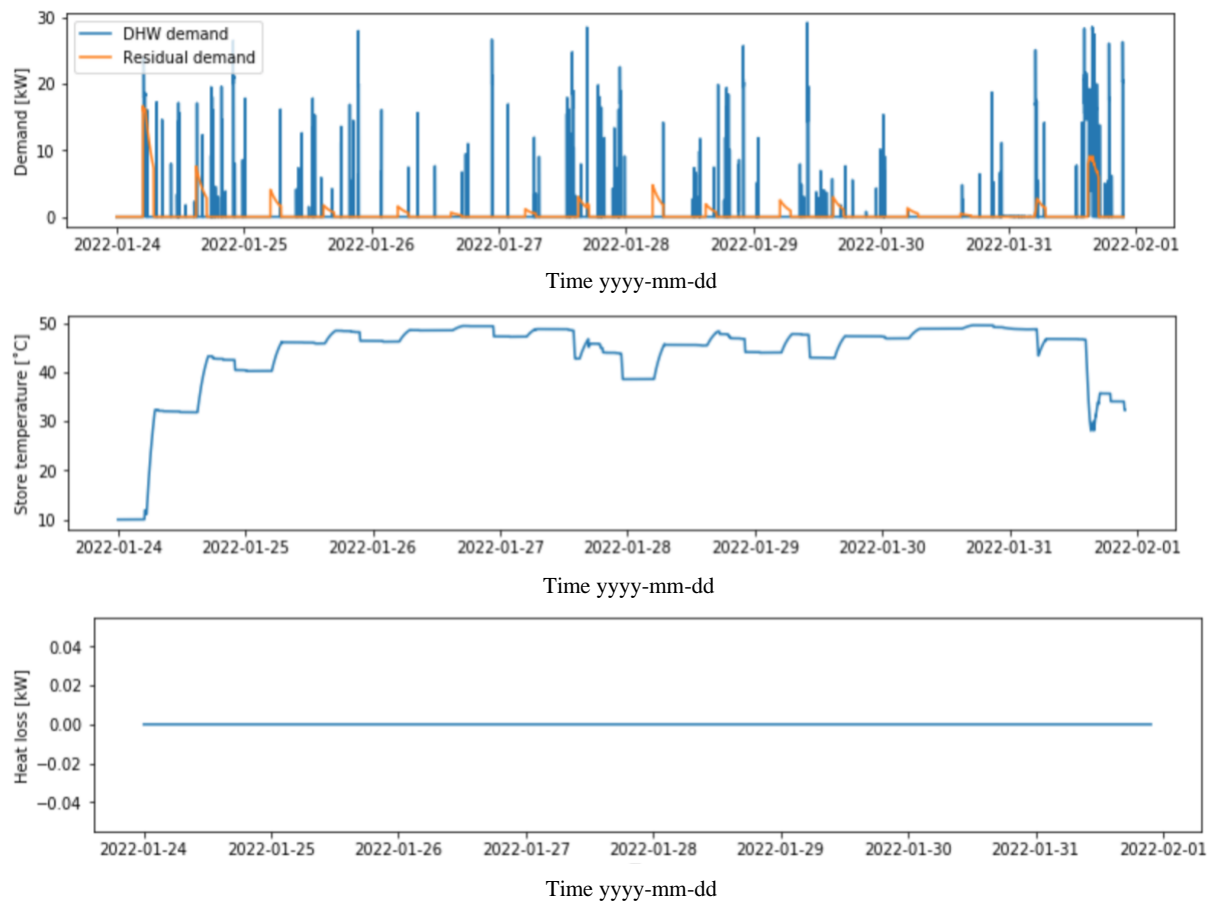


Figure 7.10: Example demand profile for a store where the heat loss factor is equal to 0 W/m<sup>2</sup>K and ambient temperature is set to 18°C

Figure 7.11 below shows the same store with the ambient temperature adjusted from 18°C, as it was in Figure 7.9, to 50°C. Figure 7.11 shows that the resulting effect is that all heat loss is in the negative, indicating that there is a heat transfer from the store environment to the store. This is expected as because an ambient temperature of 50°C will mean that the store temperature will be lower than or equal to the store environment at all times, thus creating a heat transfer that is the reverse of what typically occurs. The store temperature will then vary as a function of the net heat flow into the store which includes the heat flow from the environment to the store.

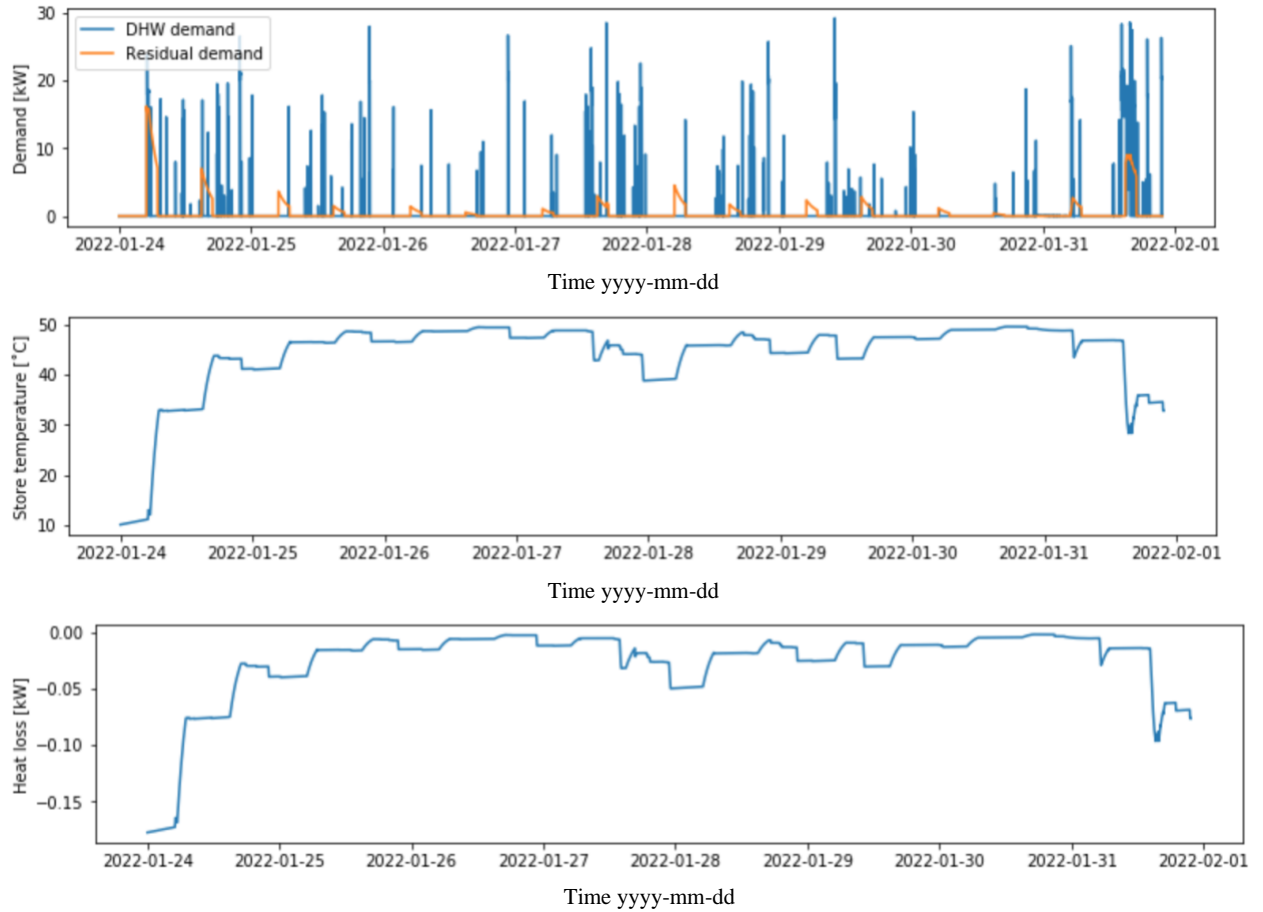


Figure 7.11: Example demand profile for a store where the heat loss factor is equal to  $1 \text{ W/m}^2\text{K}$  and the ambient temperature is set to  $50^\circ\text{C}$

### 7.3.2 Stratified Thermal Store Model Validation

Figure 7.12 shows the demand profile of an example store of which the heat loss factor is  $1 \text{ W/m}^2\text{K}$ . Figure 7.13 shows the demand profile for the same store with the heat loss factor set to  $0 \text{ W/m}^2\text{K}$ . As expected, this results in zero heat losses. The thermocline position moves as a function of the net heat flow, which comprises of only the heat drawn into the store from the primary network (defined in Section 2.2) and the heat output that meets the DHW demand. Furthermore, it can be seen that the start-stop behaviour of the store's demand (visible in Figure 7.12 but not in Figure 7.13) ceases when the heat loss is adjusted to zero because of the absence of heat loss means that when the store is up to temperature it remains full until there is a DHW demand.

Figure 7.14 shows the same store as in Figure 7.12, with the ambient temperature adjusted from  $18^\circ\text{C}$  to  $50^\circ\text{C}$ . The profile shows that heat loss falls to zero as a result of the temperature difference between the store fluid, which is held at a  $50^\circ\text{C}$ , and the store environment falling to zero. As expected, with no temperature difference across the body of the store, there is no resultant heat loss to the store environment. The thermocline position thus moves as a function of the net heat flow, comprising only the heat drawn from the primary network and the heat output that meets the DHW demand.



Figure 7.12: Example demand profile for a store where the heat loss factor is equal to  $1 \text{ W/m}^2\text{K}$  and ambient temperature is set to  $18^\circ\text{C}$

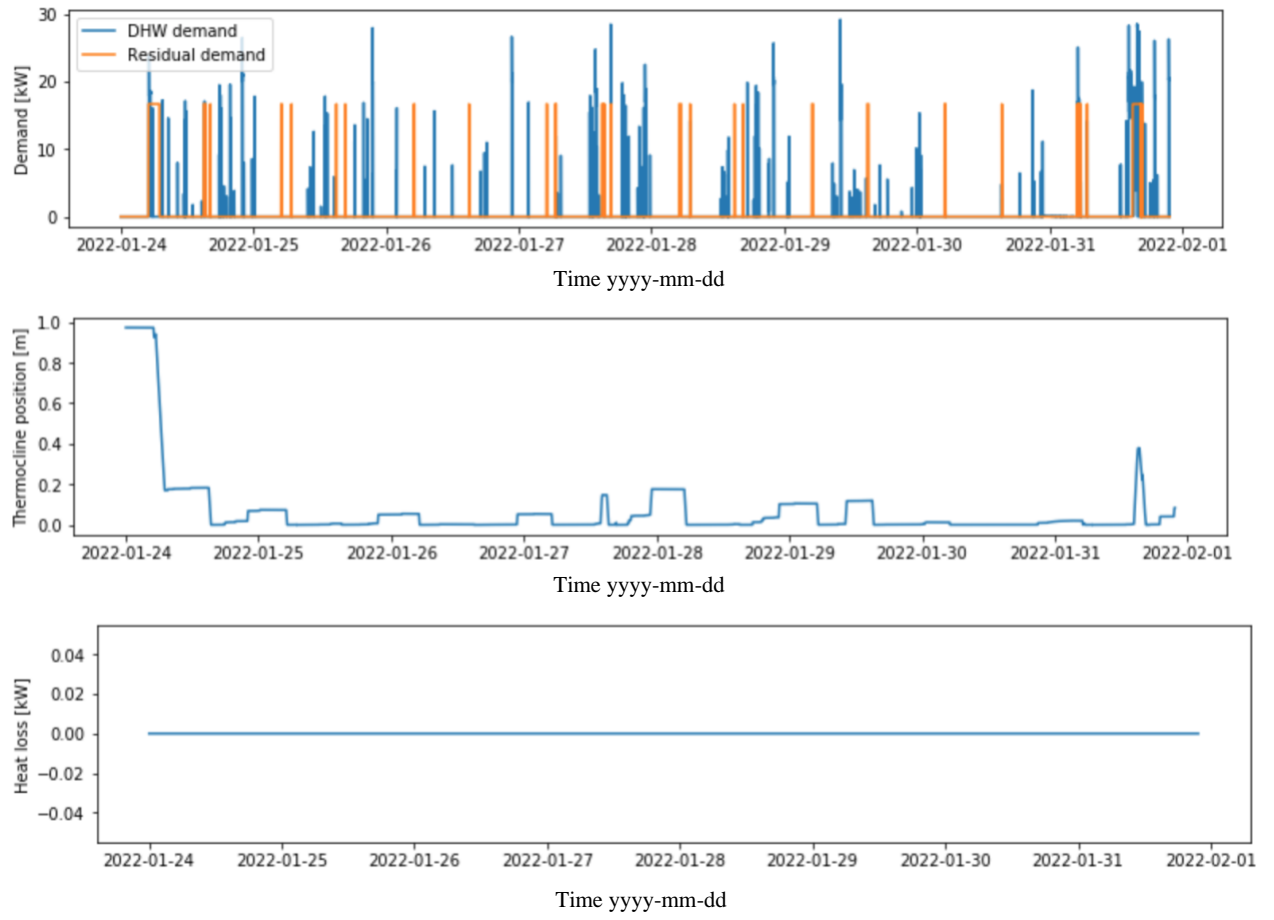


Figure 7.13: Example demand profile for a store where the heat loss factor is equal to  $0 \text{ W/m}^2\text{K}$  and ambient temperature is set to  $18^\circ\text{C}$



Figure 7.14: Example demand profile for a store where the heat loss factor is equal to  $1 \text{ W/m}^2\text{K}$  and ambient temperature is set to  $50^\circ\text{C}$

## 7.4 Aggregate Demand

Figure 7.15 below shows the demand for the SC scenario and the real DHW demand of the HN for an example day in the monitored period. The real aggregate demand shows a peak in the morning and evening, whereas the SC demand shows a peak once every two hours, reflecting the global charging strategy. The mixed store model produces an aggregate demand with minimal variation on the sub-minute scale compared to the aggregate demand produced by the results of the stratified store model. This is explained in part by the cycling behaviour present in the individual demand produced by the stratified model. The aggregate demand resulting from the stratified model has peaks that are consistently higher than the aggregate demand resulting from the mixed model. This is because the charge rates in the mixed model are a function of store temperature, whereas in the stratified model they are necessarily fixed at a maximum. This is to say that the initial charge rate in the mixed model is responsive to the state of charge of the store. If the store is completely empty, the charging will start at the maximum power. If it close to being up to temperature, the charging power will start off close to  $0\text{kW}$ . The stratified model, which does not have this capability, has a charging rate equal to the maximum charge rate whenever it is being charged, and thus starts off every charge at the maximum charge rate, resulting in higher aggregate peaks than the mixed store results in.

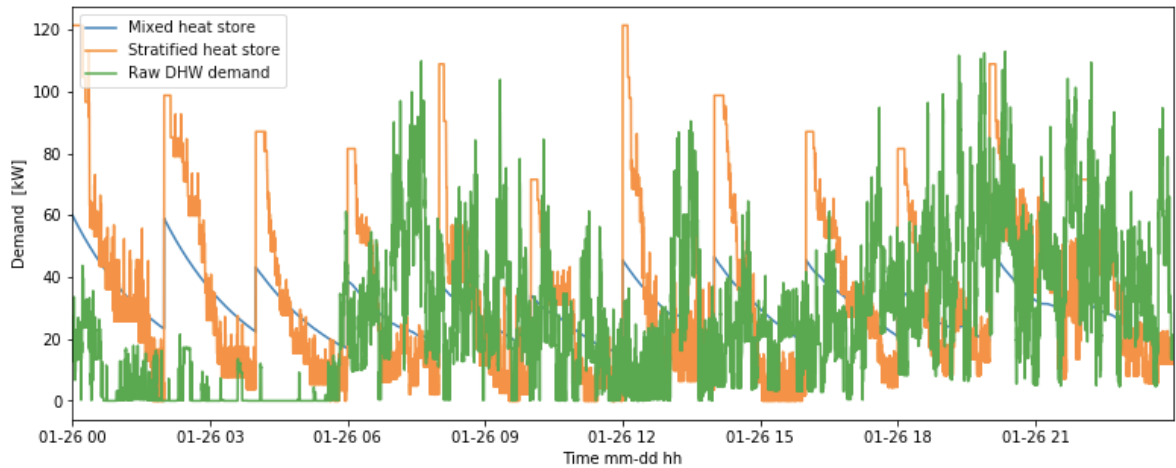


Figure 7.15: Daily demand profile of the aggregate DHW demand in the SC scenario and the real (raw) DHW demand, comprising 96 dwellings.

The daily demand profile below (Figure 7.16) shows the aggregate demand for the real DHW demand and the CC scenario. As expected, as a result of the coincident charging times of the individual domestic stores, the aggregate peak of this scenario far surpasses the aggregate peak of the real DHW demand. Therefore, if designers were to seriously consider a coincident charging regimen for their HN, it is important to consider what that would mean for the total capacity required at the plant and whether the plant, together with the distribution system, would be capable of delivering the high peak aggregate demand that would be required. As was explained in the previous section, the variation seen in the aggregate demand is a result of the start-stop behaviour that acts when a stratified store becomes full and is charged in short bursts in order to replace the standing losses.

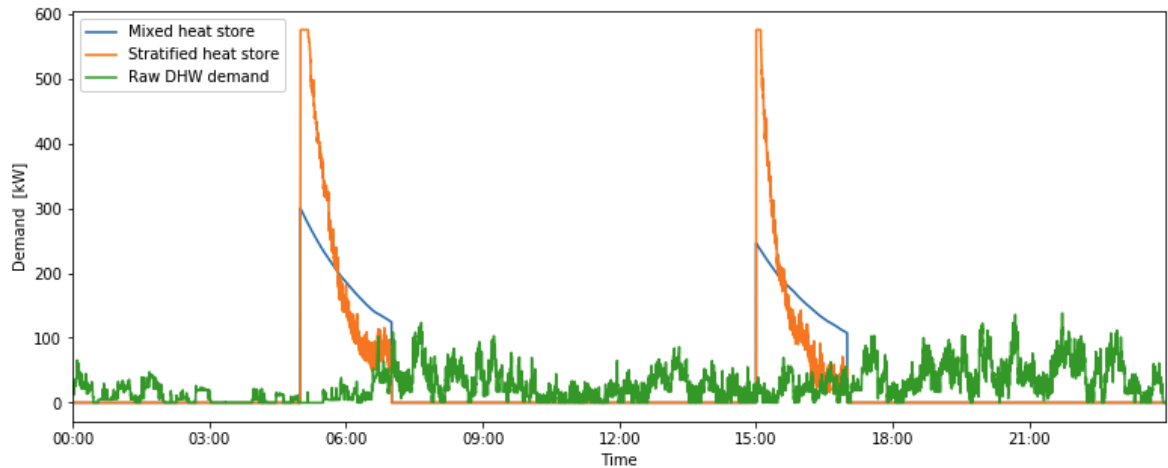


Figure 7.16: Daily demand profile of the aggregate DHW demand in the CC scenario and the real (raw) DHW demand, comprising 96 dwellings.

## 7.5 ADMD and Diversity

The ADMD curves shown in Figure 7.17 for the storage scenario are markedly flatter and remain lower than the ADMD curve for the real DHW demand scenario for all number of dwellings, as expected. This suggests that installing domestic storage in a network could result in lower distribution system losses owing to the reduction in pipe sizing required to

deliver the reduced peak demand. The ADMD curves for the storage scenarios remain relatively constant for all number of dwellings, reaching an asymptote early at around 5 dwellings (by visual inspection). The real demand scenario, on the other hand, is a strongly defined curve where an asymptote is not definitively reached within the given bounds. The ADMD curve for the CC scenario is higher than that for the SC scenario, suggesting that pipes could potentially be sized smaller across the entire network if the SC charging strategy is used. To put another way, if storage is installed, at more than 5 dwellings, the charging strategy is pivotal in whether peak loads are reduced or made larger. As expected at the individual level, and at less than 5 dwellings, storage can reduce peak regardless of the charging strategy. The impact of this on the distribution system is investigated fully in the third and final results chapter.

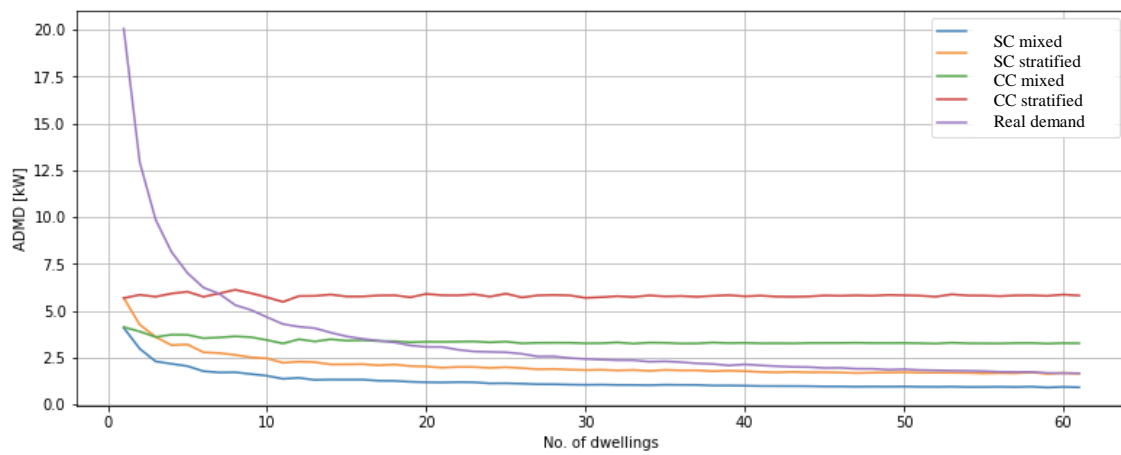


Figure 7.17: The ADMD curves for aggregate demand for both CC and SC scenarios, and for the original DHW demand

The diversity factor curve is given in the figure below. It shows that the diversity effect in the storage scenario is lower than the real demand scenario at all levels of aggregation. This is expected as there is indeed less diversity in both storage scenarios than there is in the real scenario, where DHW demand follows the highly varied occupant behaviour across the group of dwellings. At all levels of aggregation, the stratified version of the CC scenario presents a diversity factor equal to one. This is an artefact of the charging power of the stores being a constant value for each store, whereas in the mixed store, the charging power is a function of varying temperature difference. This variation also leads to the variation in individual peak demands in each scenario, which, as will be shown in the coming sections, lead to variation in the pipe sizing of the pipes serving a single dwelling.

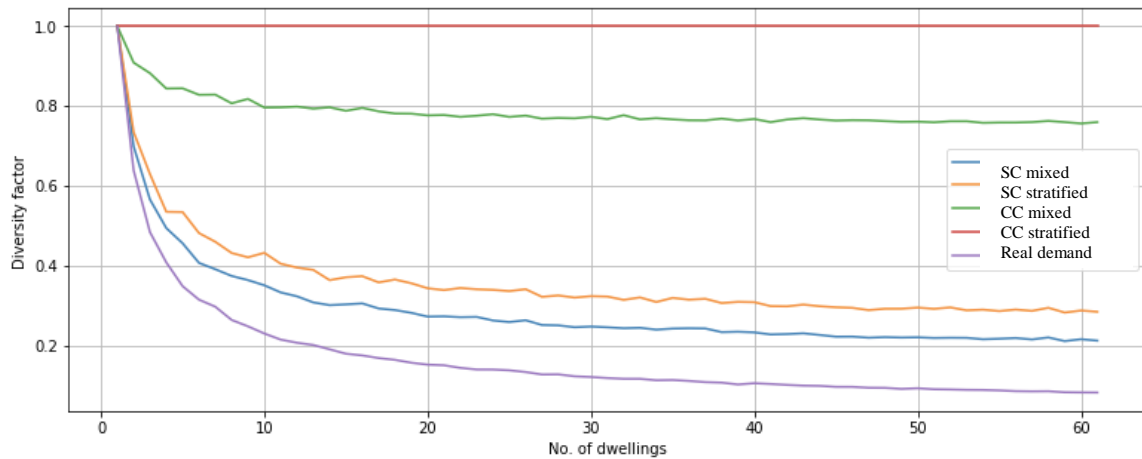


Figure 7.18: The diversity curves for the aggregate demand of both CC and SC scenarios, and for the original DHW demand

As expected, the above plots suggest that the higher the diversity, the larger the decrease in ADMD as number of dwellings increases; the ADMD in the CC scenarios, which have lower diversity than the SC scenarios, reach their asymptotes quicker than the SC scenarios. Given that lower ADMD will necessarily lead to lower distribution system sizing, it can be concluded that even when installing domestic storage, HN operators should implement a diverse charging regimen or encourage occupants to vary charging their times relative to one another. The next section looks at quantifying this benefit in terms of thermal losses in the distribution system.

## 7.6 Distribution System Sizing Results

The bar chart below summarises the topology of the modelled distribution system. For example, it shows that pipes serving a single dwelling account for 111.72 metres of pipe in the distribution system. There is 72m of pipe for pipes serving 2, 3, 4, and 5 dwellings each. Generally, the lower the number of dwellings a pipe serves, the more of that size of pipe there is in the distribution system.

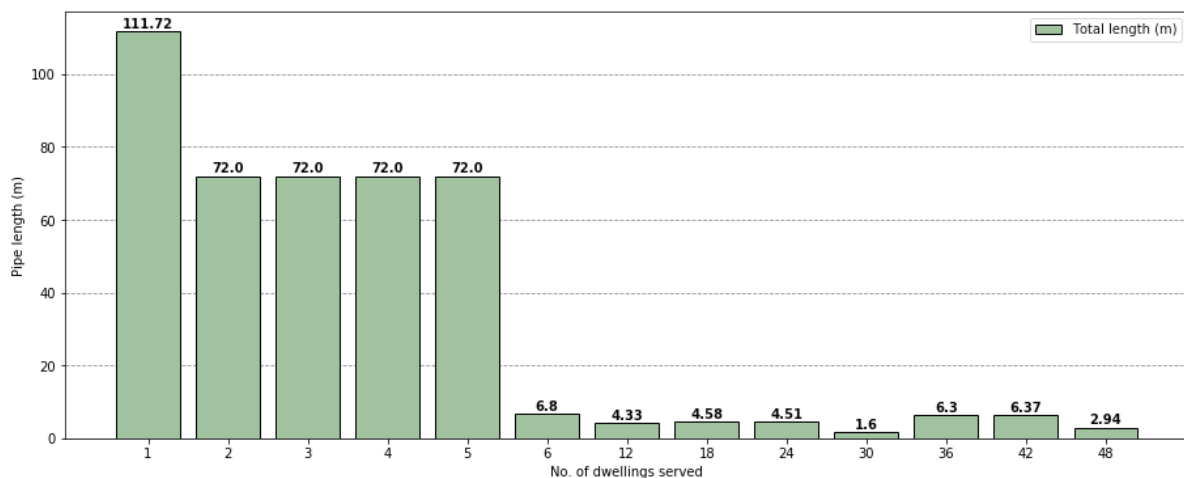


Figure 7.19: Total length of pipe in the distribution system by the number of dwellings they serve

The plot shown in Figure 7.20 gives the peak aggregate demand as a function of the number of dwellings that make up the aggregate group for each scenario. This peak value is used to size pipes for the distribution system using the method outlined in Section 3.7.1. This chart illustrates how the effect of diversity and the reduction of individual peaks introduced by introducing dwelling-level storage compete to produce the aggregate peak for different levels of aggregation. Take the aggregation at 60 dwellings; for example, the aggregate peak for the SC (stratified) scenario and the real demand scenario are similar. This is because although the real demand has much higher individual peaks, it also has a higher diversity that limits the aggregate peak at higher levels of aggregation. The CC scenarios however, where diversity is much lower, have substantially higher peaks at higher aggregate levels. The vertical blue lines indicate the number of dwellings that any single pipe in the distribution system serves. For above 5 dwellings, the CC scenario (both model types) has the highest peak demand. Below 5 dwellings, the real demand scenario has the highest peaks. This is because the individual peak demands in the real scenario are much higher than for either storage scenario. This suggests that the thermal loss from pipes serving less than 5 dwellings will be the largest in the real demand scenario, whereas for pipes serving more than 5 dwellings, the thermal loss will be highest in the CC scenario. The distribution system thermal loss overall for each scenario will depend on the thermal loss for a pipe of each size and the relative proportion of pipes of each size in the distribution system.

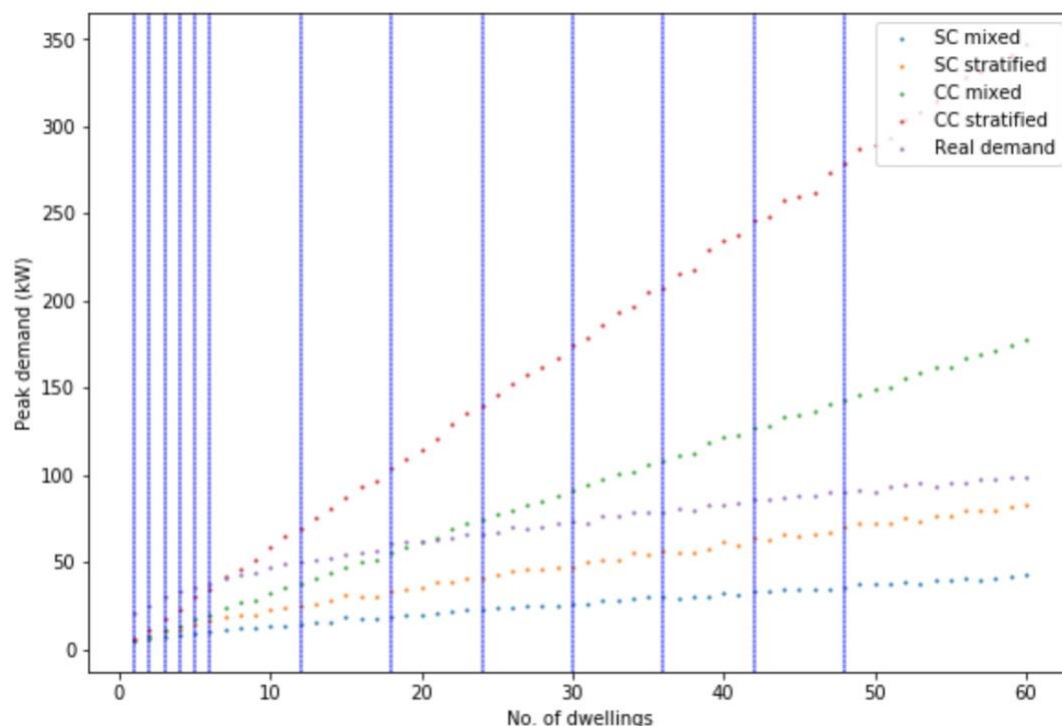


Figure 7.20: Peak demand of the aggregate demand of each scenario given as a function of number of dwellings. Blue vertical lines mark the distinct number of dwellings served by any pipe in the distribution system

Table 7.1 below gives the pipe sizes for pipes serving 4, 30 and 48 dwellings as examples. The real design of the HN (the design of the real case study as it was built) requires the largest sizes of pipe at all points across the distribution system compared with the storage scenarios. Both storage scenarios lead to smaller pipe sizes than the real sizing. Comparing the real design sizing to the sizing obtained using the real demand indicates the real oversizing of pipes; pipes serving 4 dwellings are oversized by 15 mm, pipes serving 30 and

48 dwellings are oversized by 29 mm. Find a full list of sizes of pipes in the distribution system for each scenario in Appendix D, Section 14.2.

Table 7.1: Examples of the pipe diameters required to adequately deliver where pipes are serving 4, 30 and 48 dwellings

Scenario	k= 4	k= 30	k = 48
Real (Design)	35 mm	54 mm	54 mm
SC Mixed	8 mm	15 mm	20 mm
SC Stratified	6 mm	12 mm	15 mm
CC Mixed	12 mm	25 mm	32 mm
CC Stratified	15 mm	40 mm	50 mm
Real DHW Demand	20 mm	25 mm	25 mm

The set of pie charts in Figure 7.21 show the relative proportions of pipes of each size in the distribution system for each storage scenario and for the real design scenario. The real demand and real design scenarios are compared in Section 7.8 to evaluate the real oversizing of the case study HN. The real design has the largest size of pipe, 54 mm, by far seen for any of the scenarios. Out of the remaining scenarios, the largest size of pipe is 40 mm (without counting the very small proportion of pipe of size 50 mm in the CC stratified scenario). The smallest size of pipe in the real design is 22 mm, whereas for the storage scenarios the smallest size goes down to 8.0 mm. This chart gives an overview of the size of the distribution system designed for each scenario and indicates the level of distribution system thermal loss savings that could be made with the use of DHW storage. To illustrate this point further, the plot given in Figure 7.26 gives the daily thermal losses from pipes in the distribution system for each scenario for the design day. A full list of pipe sizing results for all scenarios can be found in Appendix D, Section 14.2.

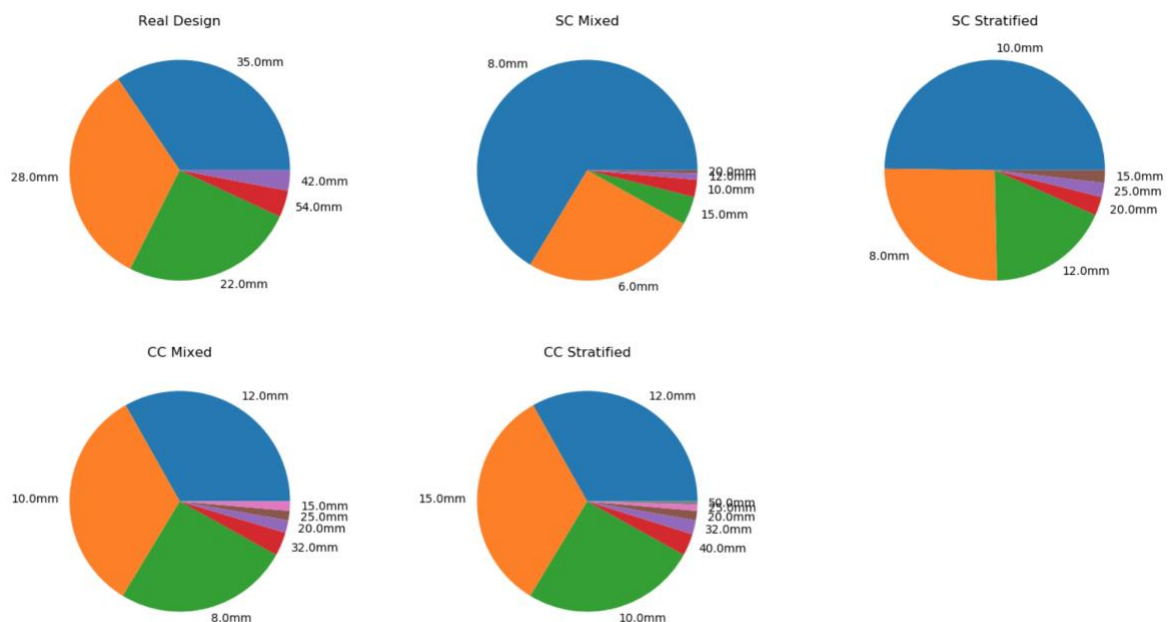


Figure 7.21: Shows the proportion of pipes of a given diameter which all together make up the whole network for each scenario

Figure 7.22 shows the direct impact of sizing of pipe on heat loss; thermal losses per meter of pipe for pipes serving more dwellings are higher because of the larger surface area of the pipe. The thermal loss for pipes serving one dwelling is below 0.09 kWh/m for all storage scenarios, whereas for the real case, the thermal loss for this size of pipe is 0.11 kWh/m. For the group of pipes serving 48 dwellings, which is the largest size of pipe in the distribution system, the same general trend is seen; the thermal loss from the storage scenarios are all below 0.160 kWh/m whereas for the real case, the thermal loss is 0.168 kWh/m. Due to the lower aggregate peaks in the SC scenario, it achieves more thermal loss savings compared to the real design and the CC scenario for pipes of every kind. It can be concluded that the charging control of the domestic stores of a HN is a crucial factor in maximising the heat loss savings in the distribution system.

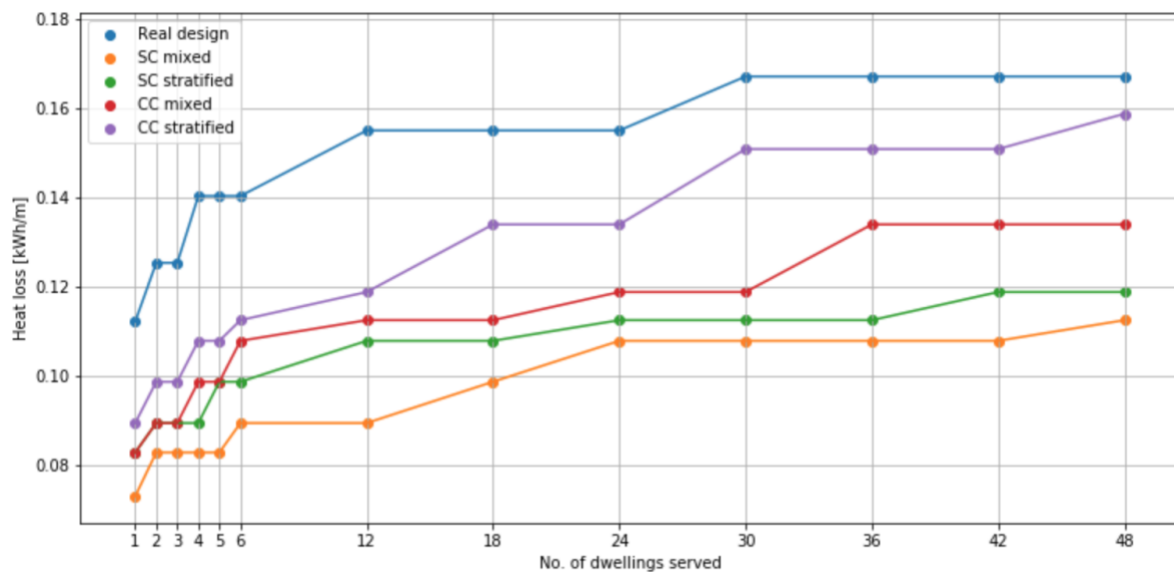


Figure 7.22: Daily heat loss per meter for each size of pipe in the distribution system

Figure 7.23 below shows the thermal loss of the storage scenarios as a percentage of the real case for different sizes of pipe in the distribution system. In the mixed SC scenario, for a pipe serving 1 dwelling, the thermal loss is reduced to 65% of that of the real design, and for a pipe serving 48 dwellings, thermal loss is reduced to 67% of that of the real design. For the CC scenarios, the percentage thermal loss savings generally increases with pipe size, although not linearly and not by much. For example, in the stratified CC scenario, for a pipe serving 1 dwelling, the thermal loss is reduced to 80% of the real design; however, for a pipe serving 48 dwellings, thermal loss is reduced to only 95%. Therefore, it can be surmised that for the SC scenario, where the diversity effect is higher, the percentage thermal loss savings per meter of pipe are comparable for smaller and larger pipes. On the other hand, for the CC scenario, where the diversity effect is lower, the larger pipes incur a smaller percentage of thermal loss savings compared to the smaller pipes. Thus, although introducing dwelling-level storage leads to a reduction in thermal loss across pipes of all sizes, the effect will be greater for larger sizes of pipe if the charging strategy is diverse. This is to say that if a HN topology were to have a larger proportion of larger pipes, the diversity effect becomes more important. This may be the case for district-wide HNs, where the plant is in a completely different locale to the dwellings served and in which the largest size of pipe is likely of substantial length.

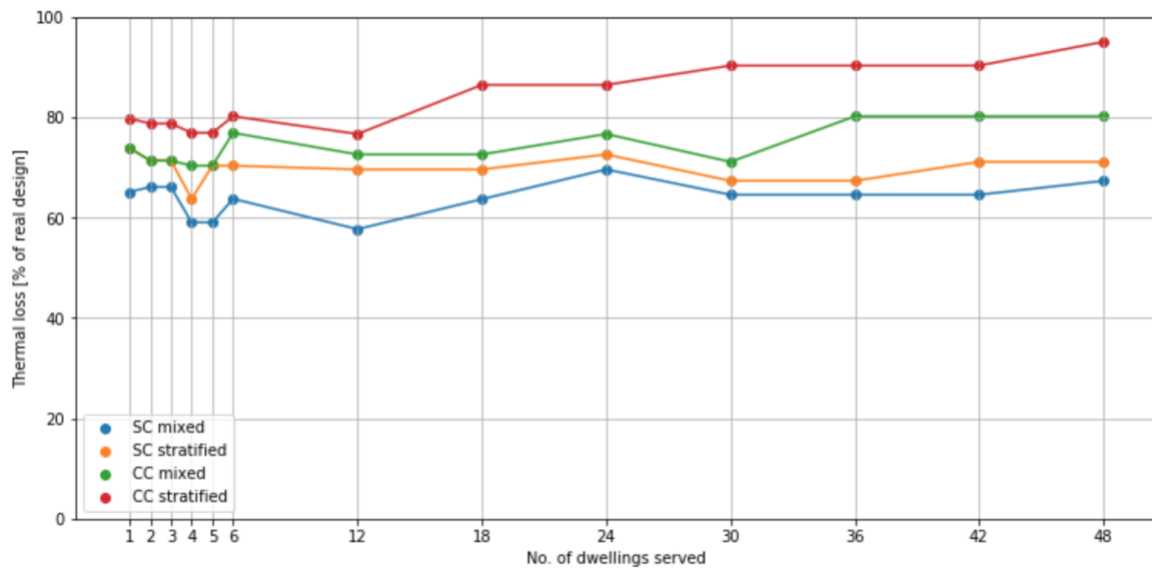


Figure 7.23: Thermal loss of pipes of a given size as a percentage of the thermal loss in the real design

Figure 7.24 shows the daily thermal losses for the total length of pipes of a given size in the distribution system. It is a direct reflection of the change in the total surface area of pipes of a given size in the distribution system that can be brought about by storage installation. The plot shows that most of the heat loss comes from pipes serving fewer dwellings, i.e., those that are closer to the dwellings. This indicates that pipework local to dwellings have large potential for thermal loss savings. Cost wise, smaller pipes don't reduce in cost with reduction in diameter as much as large pipes. In this topology, pipes that serve more than 6 dwellings have significantly less thermal loss than the pipes serving less than 6 dwellings. This suggests that the pipes closer to the dwellings should be the focus when attempting to limit thermal loss when designing HNs with similar topologies. CHNs typically have a high proportion of pipes closer to the dwelling because the distribution system of a CHN is contained in its entirety in a single building, often with the plant situated at the basement level. For district-scale HNs, which may have their plant in a different locale from the dwellings served, pipes which are closer to the plant will be longer. This would mean that heat loss from pipes closer to the plant would account for a larger proportion of the total losses from the distribution system than they do in CHNs.

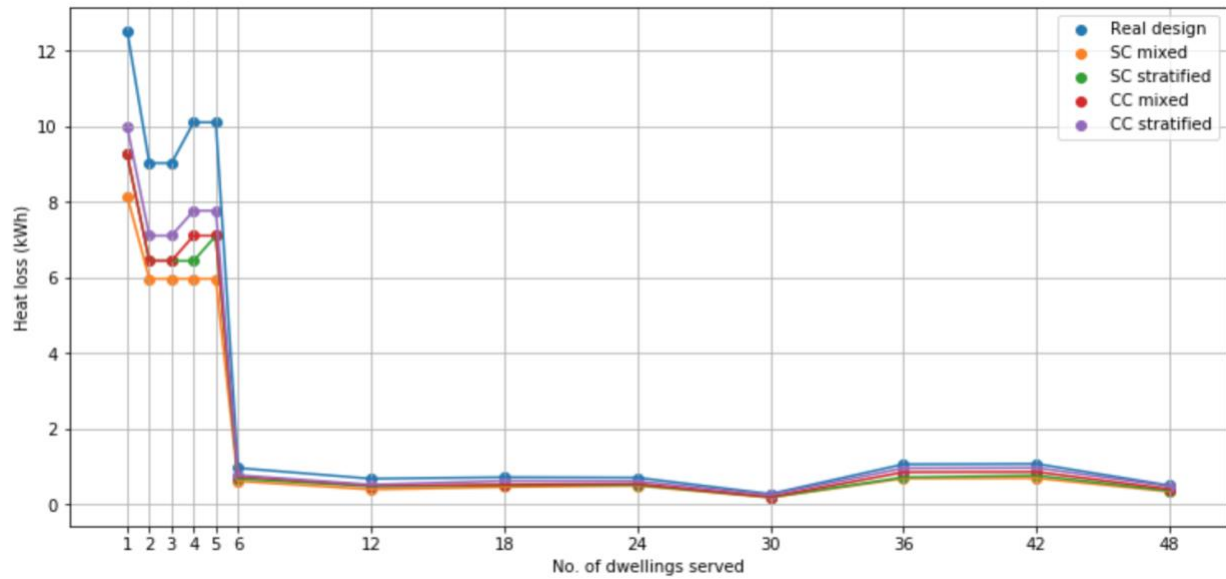


Figure 7.24: Daily thermal loss from the total length of pipes of a given size in the distribution system

## 7.7 Design Day Thermal Loss

The bar chart given below shows the storage and distribution system losses and the DHW demand across all scenarios. The distribution system losses for the real design scenario account for 8.81% of the total DHW demand, whereas for all storage scenarios the distribution system losses make up less of the DHW demand, all falling between ~ 4-6% of DHW demand. This shows that installing domestic storage will reduce distribution system losses by reducing pipe sizing although not substantially. However, taken together with the standing losses from the storage, the thermal losses in the storage scenarios are all higher than the thermal loss in the real design which comprises only distribution system losses. The storage scenarios result in a total thermal loss that make up ~17-23% of their total DHW demand. The storage losses are lower than the typical value of 1-2 kWh a day due to the optimised dimensioning and minimal surface area (CIBSE, 2020). The largest percentage of thermal loss is found in the CC scenario using the stratified model. The DHW demand is slightly different in each scenario because the DHW demand is equal to the demand of the store in the storage scenarios whereas in the real demand scenario it is the instantaneous DHW demand. Store demand can be higher than instantaneous demand depending on the interplay between the type of store, the charging strategy and the demand on the store. The extent of to which the store demand is higher than the instantaneous demand is therefore varied for each storage scenario.

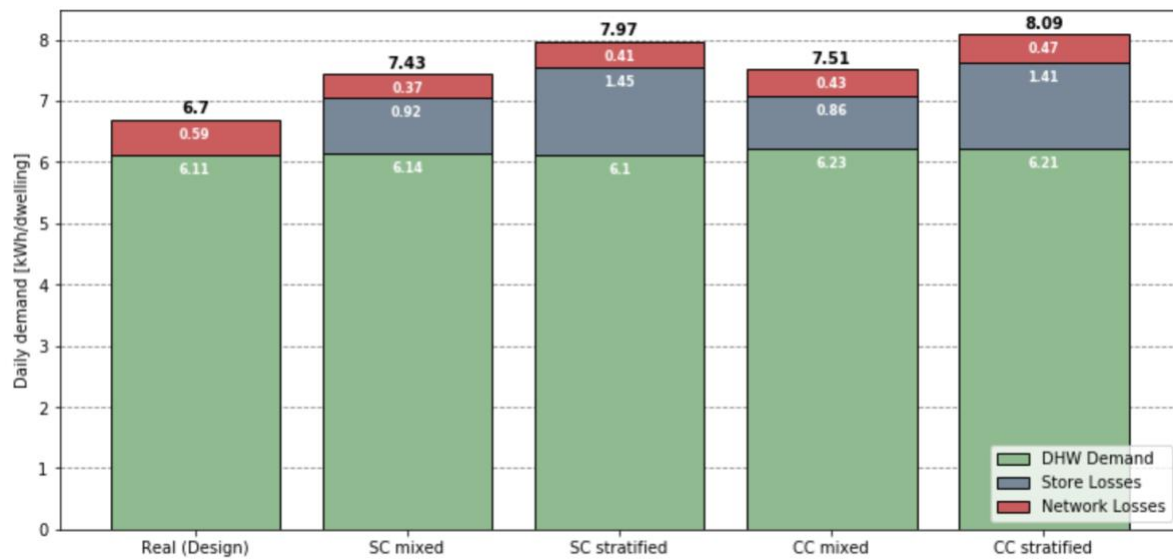


Figure 7.25: Delivered DHW demand, store losses and distribution system losses in each storage scenario

Table 7.2: Store and distribution system thermal losses given as a percentage of the DHW demand. Total losses for the coincident and spaced charging scenarios are given with the percentage difference from the real design scenario

Scenario	Store losses (%)	Distribution system losses (%)	Total losses (%)
Real design	-	8.81	8.81
SC mixed	12.38	4.98	17.36
SC stratified	18.19	5.14	23.34
CC mixed	11.45	5.73	17.17
CC stratified	17.43	5.81	23.24

The table shows that the CC scenario leads to higher distribution system losses than the SC scenarios due to the larger sizing of the pipes in the CC scenario. The storage losses in the SC scenario are slightly greater than in the CC scenario. This is because both the absolute storage losses are higher and because the demand in the SC scenario is lower than in the CC scenario, together leading to a higher fraction of store losses in the SC scenario. The absolute storage losses in the SC scenario are higher than in the CC scenario, likely because the charging times of a large number of dwellings are not aligned with the typical morning and evening peak demand times, thus leaving their stores fully charged and losing heat for the longer periods of time than in the CC scenario, where the charging times of all dwellings match up with the morning and evening peak demand times. The demand in the CC scenario being higher is likely because of the alignment of the charging times and peak demand times, which allows for more of the real DHW demand to be met. The total demand of the CC scenario is higher than the SC scenario due to the higher distribution system losses and the higher DHW demand. The storage loss of the stratified models is larger than that of the mixed models because by the nature of the stratified model the charging power is at a constant (unlike the mixed store where the charging power is a function of the temperature of the store) which leads to faster charge up times and therefore longer periods at close to full charge where thermal loss is higher. The start stop behaviour that results from the impetus of the stratified model to charge up to full when the store falls just below full means that the store is kept cycling between full and almost full, adding the above effect.

Due to the higher storage losses in the SC scenario and the higher distribution system losses in the CC scenario, the total thermal loss resulting in both scenarios is not significantly different. However, both are significantly higher than for the real design. Taking the mean between the stratified and mixed models for each scenario, the total thermal loss of both storage scenarios is  $\sim 2.7$  times greater than for the real design.

In summary, the above results show that incorporating storage into a HN design has the potential to reduce the thermal loss from the distribution system through pipe size reduction. The results also show that the extent of this reduction is dependent on the relative charging times of the dwellings; the more diverse the charging times, the greater potential for heat loss reduction. However, implementing diverse charging times is likely to lead to higher storage losses due to longer standing times. In this instance, the net effect is that the total thermal loss of the two charging scenarios ends up being almost equal. Moreover, the thermal loss of the storage scenarios compared to the real design are significantly higher due to the insufficient reduction of distribution system losses that fail to outweigh the increase in storage losses.

### 7.7.1 Sensitivity Analyses

To map the impact that the key parameters have on the storage model, the distribution system sizing and the distribution thermal loss model together, sensitivity analyses were carried out. In order to produce the plots, a testing range was defined for each of the tested variables. The distribution system loss and the store heat loss were calculated for three discrete values within this range. These results were then extrapolated to illustrate the impact on the total thermal loss for a wider range of values of the tested variable. The plots in this section show the impact that the ambient temperature of the building (the environment in which the distribution system lies), the ambient temperature in the dwellings, the thermal conductivities of the pipe insulation and the thermal conductivities of the domestic thermal stores have on the total thermal losses in design day conditions.

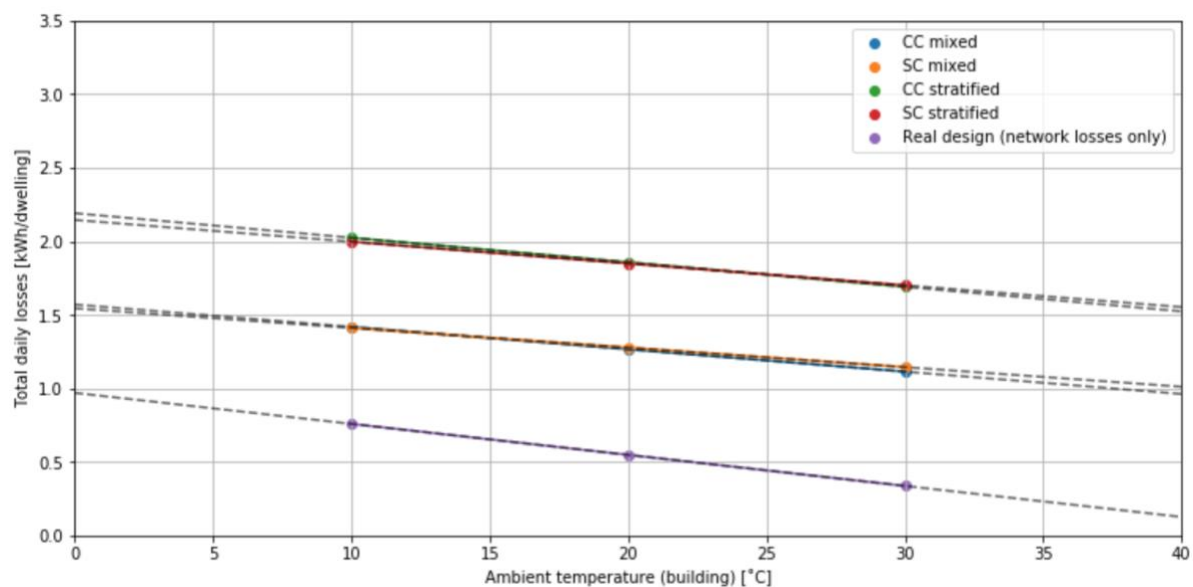


Figure 7.26: Impact of varying building temperature parameter on thermal losses

Figure 7.26 above shows the impact that increasing the temperature of the building has on the total losses in each scenario. Increasing the building temperature reduces the thermal losses

from the pipes at a higher rate for the real design than for the storage scenarios. This is because the thermal losses from the pipes are the only component in the real design total losses, whereas storage losses are included in the total losses of the storage scenarios. The upper bound of the tested temperature range is 30°C because of the high temperatures that can be reached in communal spaces due to overheating.

Figure 7.27 below shows the impact of varying the thermal conductivity of the pipe insulation<sup>8</sup>. As expected, the plot shows that decreasing the thermal conductivity of the pipe insulation leads to lower losses. This effect is more pronounced in the real design where the pipe sizes are larger. The chart also shows that the charging control becomes more important at higher thermal conductivities. This is indicated by the increasing difference between the losses in the SC and CC scenarios as the thermal conductivity of the insulation increases. This is a result of the distribution system being sized larger for the CC scenario. For extremely low thermal conductivity, where  $k < 0.01 \text{ W/mK}$ , the total loss from the CC scenario is lower than for the SC scenario because at this point the storage losses of the SC scenario start to outweigh the losses from the pipes. Note that no existing insulation material have thermal conductivities in the range  $k < 0.01 \text{ W/mK}$ . The results will be evaluated as it relates to existing kinds of insulation in the following paragraphs.

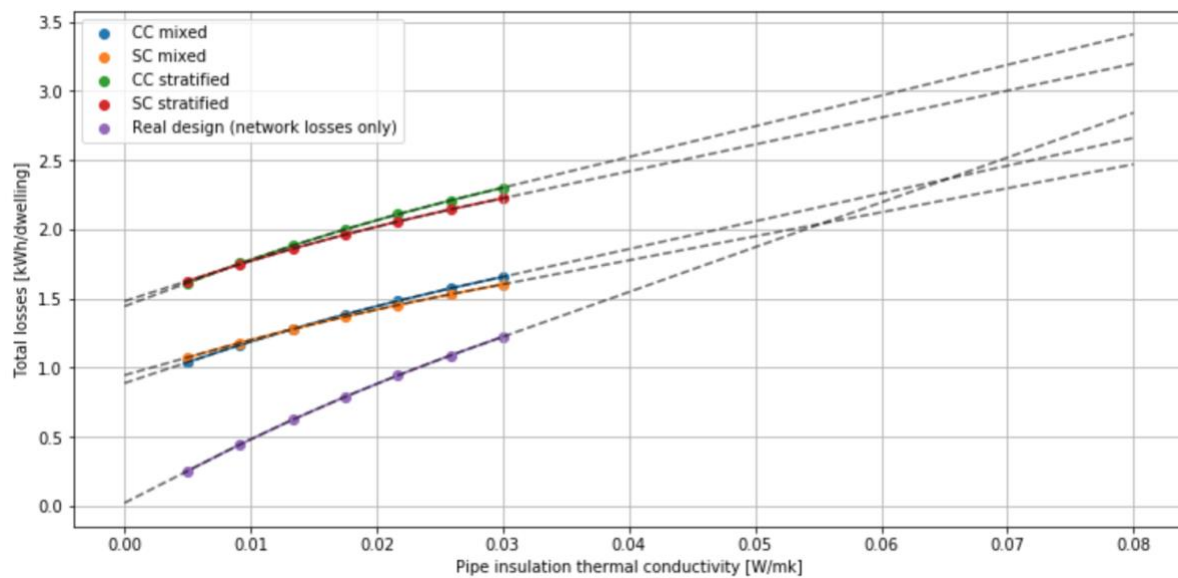


Figure 7.27: Impact of varying the thermal conductivity of the pipe insulation on thermal losses

<sup>8</sup> The heat loss of the pipes is given in terms of the fundamental property of thermal conductivity of the pipe insulation,  $k$ , rather than the heat loss factor,  $U$ . This is because the pipe thickness, which affect the  $U$  value, vary through the network.

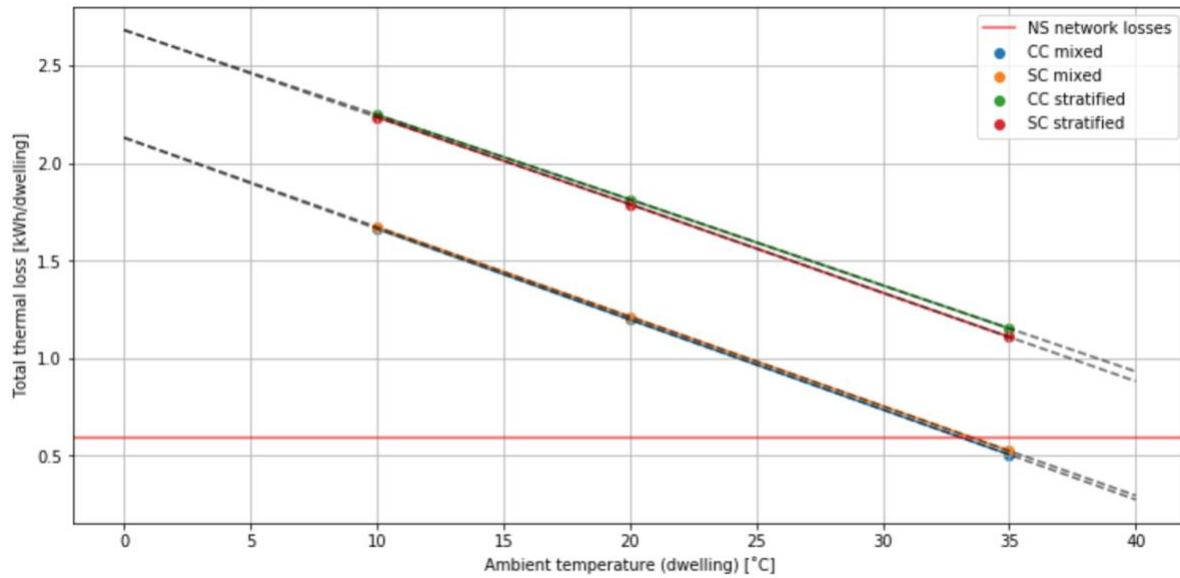


Figure 7.28: Impact of varying dwelling temperature parameter on thermal losses, where the red line demarks network losses (design day)

The dwelling temperature affects only thermal losses from the stores and thus only has an impact on the storage scenarios. The dwelling temperatures also affect heat loss from the HIU; however, these losses have not been included in the model. The plot given in Figure 7.28 shows that the thermal losses of the storage scenarios are equal to those of the real design (denoted by the red line names NS network losses) at extremely high temperatures that exceed 35°C, which are unlikely to occur in a typical dwelling. Typically, real dwelling temperatures remain within the range of 16 °C – 20 °C (Huebner et al., 2013).

The plot in Figure 7.29 shows the impact that varying the insulation levels of the domestic thermal stores have on the overall thermal losses<sup>9</sup>. As expected, reducing the heat loss factor of the store insulation reduces the overall losses of the storage scenarios. For the overall losses from the best-case storage scenarios to be similar to the losses from the real design, heat loss factors of <0.25 W/ m<sup>2</sup>K need to be achieved. A heat loss factor, or the heat loss coefficient (U-value), of 0.25 W/m<sup>2</sup>K corresponds to an insulation thermal conductivity value of around ~0.0009 W/mK assuming an insulation thickness of 2 inches and a store diameter of between 0.4 m and 1.05 m<sup>10</sup>. The range of heat loss factors tested in the sensitivity analysis, 0.5 – 1.5 W/m<sup>2</sup>K, corresponds to a thermal conductivity range of 0.0086 – 0.026 W/mK. Phenolic foam, a top-performance insulation material, has a thermal conductivity of between 0.018 W/mK and 0.023 W/mK given the same store and insulation dimension assumptions. Thus, for the overall thermal losses of the storage scenarios to be smaller than those of the real design, a material of thermal conductivity that is ~20 times (0.018/0.0009 W/mK) better performing than the best-performing Phenolic foam is needed if the insulation thickness is to be no larger than 2 inches. Alternatively, if insulation thickness was larger, the

<sup>9</sup> The heat loss from the stores is given in terms of the heat loss factor, i.e., the U-value, instead of the thermal conductivity,  $k$ , of the insulation because the thickness of insulation across all stores are the same, and thus the a given  $k$  value results in the same U value across all stores.

<sup>10</sup> The heat loss factor,  $U$ , for a given thermal conductivity,  $k$ , does not vary significantly where the diameter of the thermal store has a range of 0.4 – 1.05 meters and a fixed insulation thickness of 2 inches. All stores in the modelled HN have a diameter of between 0.4 and 1.05 meters, thus the heat loss factor does not vary significantly across the thermal stores for a given thermal conductivity.

thermal conductivity of the insulation need not be as low. As there is no commercially viable insulation material that perform better than Phenolic foam, thickness of insulation will need to be increases. This is a viable option if it is factored into the design properly.

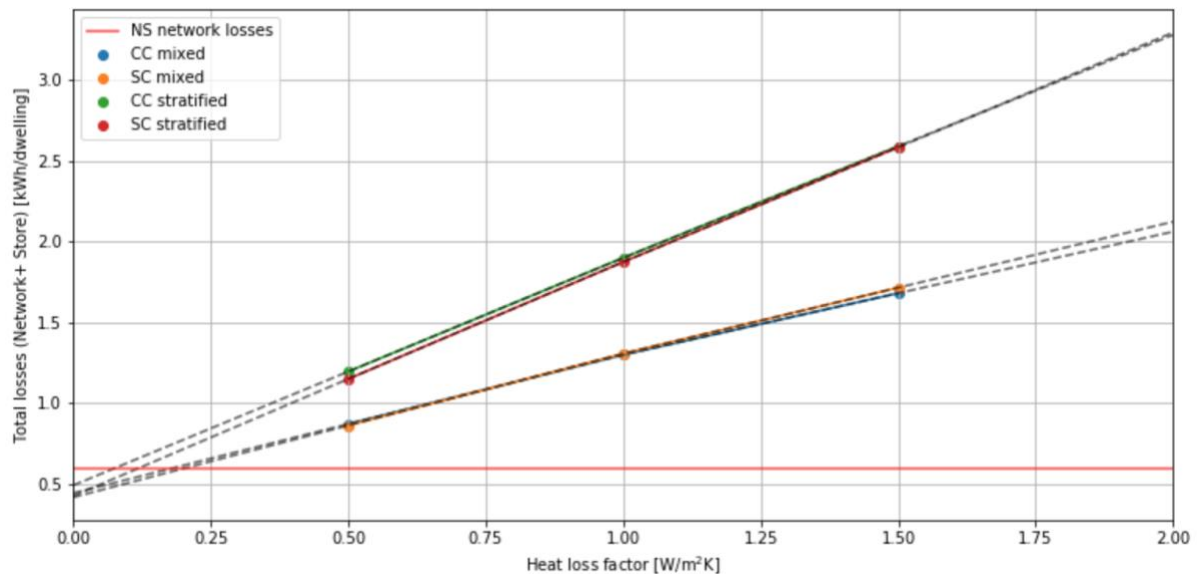


Figure 7.29: Impact of varying the heat loss factor of the thermal store on overall thermal loss, where the red line demarks network losses (design day)

Figure 7.30 below shows the impact that the thickness of Phenolic foam has on its heat loss factor. To achieve the required heat loss factor of  $0.25 \text{ W/m}^2\text{K}$ , an insulation thickness of  $\sim 0.13 \text{ m}$  (or  $\sim 5.1$  inches) is required. Thus, in order for the storage installation to result in a reduction of overall thermal loss, significantly high insulation levels may be required; phenolic foam insulation of greater than 5.1 inches thickness in this case. Thermal stores with insulation layers of greater thicknesses are available commercially but may be infeasible in domestic settings due to concerns about space.

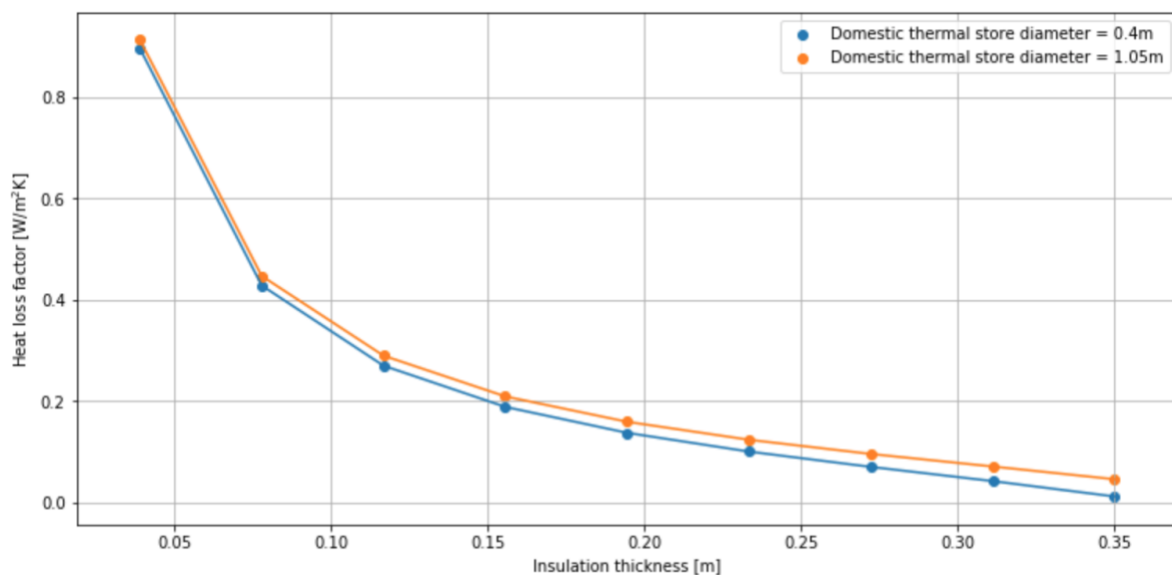


Figure 7.30: Variation in heat loss factor with increasing thickness of insulation material for a thermal conductivity of high performing Phenolic foam ( $k = 0.018 \text{ W/mK}$ )

The results of this section have shown that the conditions required for the thermal loss in either of the storage scenarios to be comparable to the real design are conditions that are

unlikely to exist. The necessary conditions are also that which are detrimental to occupant comfort, such as extremely low building ambient temperatures or extremely high dwelling ambient temperatures, are conditions that go against fundamental design guidance, such as high pipe thermal conductivity, or are likely unfeasible due to significant increased demands on space, such as 5.1-inch-thick thermal store insulation. Even with these conditions, the thermal loss of the storage and real demand scenarios would only be at similar levels. It wouldn't be the case that these conditions bring about a significant reduction in thermal loss in the storage scenarios.

The results have shown that although the aggregate peak demands can be reduced substantially with the installation of storage, the resulting reduction of thermal loss from pipes is not large enough to outweigh the losses from the domestic stores. The limited extent to which pipe thermal losses are reduced are not a result of the pipe sizing methodology. The smallest diameter of pipe (6mm) was required only in the SC scenario. This indicates that the reduction of thermal loss was not limited by the minimum available pipe size.

## 7.8 Oversizing of the Case Study HN Distribution System

In this section the real oversizing of the case study network is investigated in order to understand the impact on thermal loss. In other words, the design of the HN as it exists, using its construction drawings that give pipe dimensions, is compared to sizing determined using the method outlined in Section 3.7.1 using the real demand of the sample of dwellings. Figure 7.31 shows the daily heat loss from the pipes in the distribution system for the real design and the real demand scenarios. The pipes are presented on the x-axis in terms of the number of dwellings they serve. A pipe serving a given number of dwellings will be of a given size. The more dwellings served by a pipe, the larger the diameter of the pipes, and thus the pipe size increases with the increasing x-axis. The plot shows that all of the pipes in the distribution system could have been sized smaller and continue to meet the demand. Where the pipes are serving 2, 3, 4 and 5 dwellings are where there is a substantial potential reduction in heat loss.

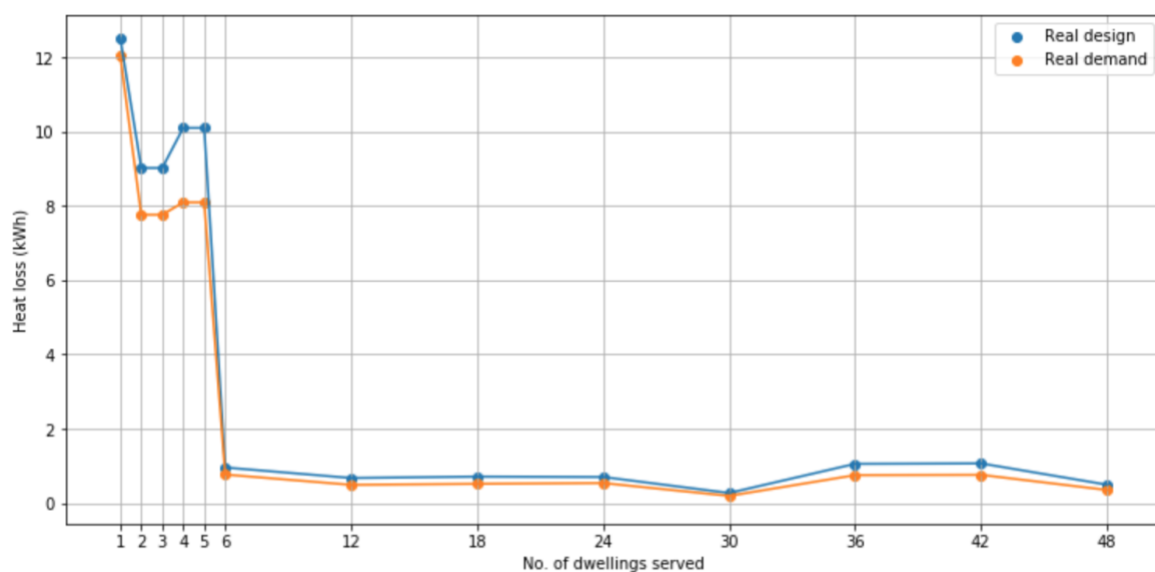


Figure 7.31: Daily heat loss from the total length of pipes of a kind (i.e., serving a given number of dwellings) in the distribution system for the real design and the real demand scenarios

Figure 7.32 below shows the proportions of pipes of a given size in the distribution system for the real design and the real demand scenarios. The real demand distribution system consists of pipes of only three different sizes, 15mm, 20mm, and 25mm. The real design consists of 5 pipe sizes, the smallest of which is 22mm, and the largest 54mm.

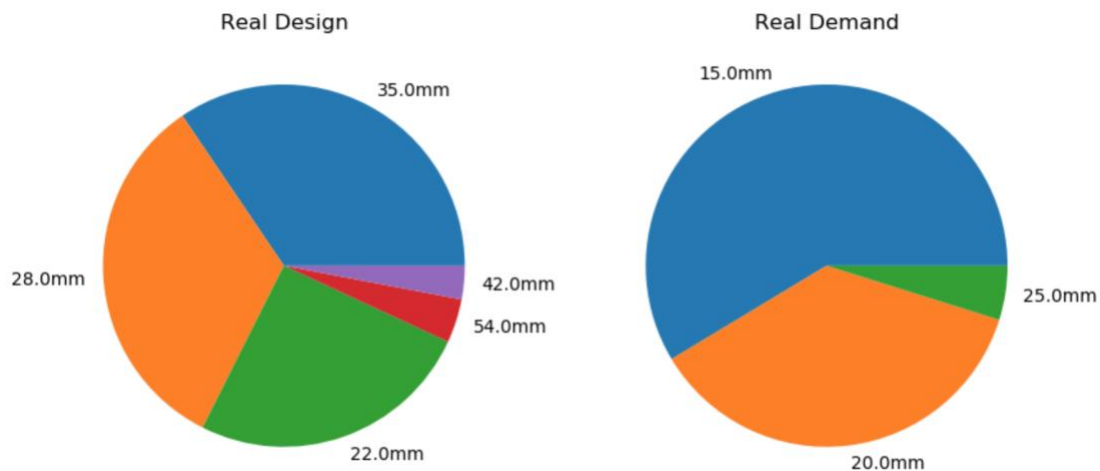


Figure 7.32: Shows the proportion of pipes of a given diameter which all together make up the whole distribution system for each scenario

In the real design the heat loss accounts for 9.7% of the daily DHW demand, whereas for the real demand scenario, the heat loss accounts for 8.2% of the DHW demand. The daily heat loss per meter of pipe for the real design scenario is 0.13 kWh/m and 0.09 kWh/m for the real demand scenario. Values reported for other case study HNs give the daily heat loss per meter of pipe as being between 0.63 kWh/m and 16.23 kWh/m (DECC, 2015). This suggests that the thermal loss in the case study HN falls on the lower end of existing HNs. This is due to the efficient design of the pipework that results in a low total pipework per dwelling. The pipework design follows the principles of CP1 and has been optimised to reduce pipe lengths (see Figure 2.14). CP1.2 states that the thermal loss from a HN must be lower than 2.4 kWh/dwelling/day (CIBSE, 2020). All tested storage scenarios, as well as the real demand and real design scenarios, had thermal losses substantially lower than this benchmark due to the efficiently designed pipework. Note that the real design may have had other reasons for the chosen sizing that are unknown to the author, and thus, the statements made here are not meant to be taken as an evaluation of the overall performance of the case study HN.

## 8 Discussion

### 8.1 Results 1 Summary and Discussion

The first results chapter, Results 1 – Generating Demand Profiles, begins by describing the dataset that was available for the task of determining the demand for a group of 115 dwellings being served by the case study HN. Although the dataset was rich, containing many variables and data from a large number of dwellings, it proved to be challenging with regards to the maintenance of data quality due to various data collection issues (explained in full in Section 4.10). The early stages of handling and cleaning this data involved identifying the variables and dwellings for which a sufficient amount of data existed such that high-frequency analysis could be conducted. After the initial stages of cleaning, where the variables for which there was a sufficient volume of data were identified, a range of methods using different combinations of variables were assessed on their merit for determining the demand. The method that produced the results with the lowest uncertainty was used to determine the DHW demand and the total demand independently for each dwelling. To determine the DHW demand, data describing the hot water delivery temperature and the flow rate, with a sampling time of one second, was used alongside an assumed cold water inlet temperature. Data of a 5-minute sampling interval describing the instantaneous metered total demand was used to estimate the total demand. Demand profiles for the DHW demand and the total demand were produced for the coldest period in the year-long data monitoring and collection period for 115 dwellings with design occupancies of 2,3,4 and 6 occupants. These were then subject to detailed analysis.

The key results from the first results chapter are summarised below.

- The daily mean external temperatures of the selected cold period spanned 2.5 - 10°C, with some hourly temperatures that dropped below 2°C.
- The daily mean aggregate DHW demand on the coldest and warmest days of the cold period were 24.1 kW and 27.9 kW respectively (15.8% higher on the cold day).
- The daily mean aggregate total demand on the coldest and warmest days of the cold period were 67 kW and 50.6 kW respectively (24.5% higher on the cold day).
- The hourly mean demand profiles for the DHW demand and the total demand present the typical morning and evening peaks (Gianniou et al., 2018). The morning and evening hourly peaks for the total demand are ~0.9 kW and ~0.85 kW respectively. For the DHW demand, the morning and evening peaks are ~0.4 kW and ~0.5 kW respectively.
- The mean daily DHW demand was found to be 0.09 kWh/m<sup>2</sup>.
- The mean daily total demand was found to be 0.22 kWh/m<sup>2</sup>.
- The mean daily total demand for dwellings with the lowest design occupancy, an occupancy of 2 people, was 11.42 kWh, and for the highest occupancy, an occupancy of 6 people, it was 22.80 kWh.
- The mean daily DHW demand for dwellings with the lowest design occupancy, an occupancy of 2 people, was 5.66 kWh and for the dwellings with the highest occupancy, an occupancy of 6 people, it was 8.69 kWh.
- The mean hot water delivery temperature was found to be 47.4°C with a range of between 11-60 °C.

The demand of the sample of dwellings in this study show similarities as well as differences when compared to samples of UK dwellings found in other demand studies. Some studies include samples with a more diverse population of dwellings, with variation in occupancy, age, heating system type and insulation levels. Whilst some other studies use samples similar to that of this work which are made up of flats in a single residential building unit located in the Southeast of England. Hot water delivery temperatures and the daily volumetric DHW consumption was found to be similar to those in studies that used a more diverse sample (Energy Savings Trust, 2008). Energy demand for DHW was lower in other studies although not by a significant amount and is likely explained by the lack of off-heating season data (Aragon et al., 2022; Burzynski et al., 2012). Taken together, the sample of dwellings in this work are found to have a similar demand compared to samples of the wider population of UK dwellings, and where differences are found, they can be explained by the difference in sample characteristics. The main limitations in the results include that the demand represents heating-season demand only and thus makes it difficult to compare like for like in other studies as other studies, where similar samples were used, evaluated the demand on an annual basis. Other limitations include that the design occupancy may not reflect the real occupancy in the dwellings.

As was set out in the objectives stated at the beginning of the first results chapter, Results 1 – Generating Demand Profiles, the demand has been estimated for a group of 115 dwellings for the coldest period of one week in the monitored period. Demand for DHW and the total demand was estimated independently and align with demands found for UK dwellings in other studies; both kinds of demand have been characterised and found to align with other dwelling demand studies when comparing heating patterns and daily demand (Aragon et al., 2022; Burzynski et al., 2012; Energy Savings Trust, 2008; Ivanko, 2020; Wang et al., 2021). The demand estimations were then used to investigate the impact that sampling time has on the ADMD of DHW demand and total demand, to estimate residual storage demand for the sample of dwellings, and to investigate the impact that storage has on the aggregate demand and HN distribution system sizing.

## 8.2 Results 2 Summary and Discussion

In the second results chapter, the demand estimated in the previous chapter was further validated by taking a whole HN perspective. The demand distributions for the total demand and the DHW demand were investigated in order to identify the key features and link it back to the socio-technical factors that they result from. In conjunction with individual demand profiles the demand distributions were used to distinguish the real occupant demand from the transient demands. By comparing the demand distribution for the total demand to that of the DHW demand, the level of influence of SH and DHW at different levels of aggregation were defined. The impact of sampling time on aggregate demand was investigated and used to assess the sampling time required to deliver demand at a defined quality-of-service criterion.

The following points summarise the key results of this chapter.

- The PTG for the case study HN was found to be 40 W/K.
- The maximum demand in the total demand distribution at sampling times of 5 and 10 minutes were exactly equal at 29.6 kW. The maximum demand in the DHW demand distribution at a sampling time of 5 minutes was 28.95 kW. This confirms that the DHW demand estimates are a reliable indication of the real demand as the total demand is derived from reliable metered data.

- The maximum demand (the 100<sup>th</sup> percentile) and the 95<sup>th</sup> percentile in the DHW demand distribution (Figure 6.2, top left) at a sampling time of one second were 36.88 kW and 20.82 kW respectively. The maximum demand in the DHW demand distribution at a sampling time of 10 minutes was 27.59 kW. Given that this is higher than the 95<sup>th</sup> percentile of the demand at a sampling time of one second, a sampling time of 10 minutes would be sufficient to use in sizing a HN similar in demographic and topology to the case study HN to meet 95% of its demand. This is useful for HN designers that intend to make their own measurements of demand when sizing the distribution system pipes, as is recommended in CP1.2.
- The total demand distribution (Figure 6.1, top left) presents a sharp peak at ~ 2 kW, and the DHW demand distribution (Figure 6.2, top left) presents a broad peak at ~15 kW; demands in these ranges are those that occur more frequently and are therefore likely to be meaningful occupant demands. The DHW demand distribution does not have a peak at ~2 kW which is present in the total demand distribution. This suggests that the peak in the total demand likely represents the occupant SH demand alone.
- The peak centred at ~15 kW in the DHW demand distribution (Figure 6.2, top left) is present at all sampling times lower than 5 minutes, which suggests that the real occupant demands tend to last no longer than 5 minutes. This peak starts at 2.5 kW and ends at 20 kW, suggesting that real occupant demand spans 2.5 – 20 kW.
- The tail of the DHW demand distribution (Figure 6.2, top left), i.e., the higher demands, which are between 20 - 30 kW, are likely transient demands that are associated with the DHW system. Since the peak demand at a sampling time of 10 minutes is 20.82 kW, sizing a system to this level would mean that all meaningful occupant demand can be met.
- At an aggregation level, k, of around 35 and above, the total demand peak exceeds the DHW demand peaks, which suggests that SH demands begin to dominate the peak demands at these levels.
- It is likely that the only information lost when using a sampling time of 5 seconds, compared to a sampling time of one second, is information relating to very minor demand that would have no meaningful bearing on HN design, regardless of the intended quality-of-service criterion.
- Comparing the measured DHW and total demand peaks to the design capacities, determined using the DS439-based methods recommended in CP1.2, showed that the measured peaks were less than half of the design estimates across all levels of aggregation, up to and potentially beyond, 80 dwellings.

The results in this chapter characterised the high frequency DHW and total demands of a sample of dwellings on a HN, which has been called for in previous studies (Fuentes et al., 2018; Ivanko et al., 2020; Marszal-Pomianowska et al., 2019; Weissmann et al., 2017). Moreover, the results in this chapter have explicitly demonstrated the validity of using a given sampling time in the design of a HN with an intended quality-of-service criterion. Industry guidance has assumed that lower sampling times are unlikely to hold information that has a meaningful bearing on sizing but has not proven it explicitly. Thus, the results in this chapter demonstrating the validity of using a 10-minute sampling time is a novel result that can be used to inform the technical guidance that supports the growing UK HNs industry. Investigation of the individual demand profiles in conjunction with the aggregate demand distributions has been used to draw conclusions about the nature of the demands at different levels of aggregation and to make claims about the implications of these findings on the use of the selected sampling time in sizing a HN. The results in this chapter have focussed

on the relationship between the sampling time, the level of aggregation, and the peak demand, showing the rate at which, as the sampling time increases and the level of aggregation increases, the peak demand values decrease. By comparing the relationship between the total demand and the DHW demand with the aggregation level, it was clear that DHW demand dominates the peak demands up until a level of aggregation of around 35 dwellings where SH begins to dominate. The individual impact of DHW demand on diversity, as separate to the impact of SH demand, has not been found to be the subject of any previous research literature, and thus the findings in this work are the first of its kind. Relevant industry guidance was used to compare to the real demand and to explicitly show where guidance was valid and where it could be further improved.

### 8.2.1 Applicability

The findings in this chapter have highlighted the importance of using real demand data from a sample of dwellings on a real HN to inform UK HN guidance in several important ways. Firstly, the demand estimates for the sample of dwellings were shown to be significantly lower than the demand for a sample of standalone dwellings in the wider population, likely owing to them being new-builds with fewer external walls (Summerfield et al., 2014; Wang et al., 2020). Hitherto, most studies related to the demand and the diversity of demand conducted with the aim of informing UK HN industry guidance have been based on demand data from standalone dwellings. In this work, the demand in the sample of dwellings, that all sit in a residential building together, was found to be lower than the demand in the wider population. CHNs make up a sizeable proportion of HN existing today and those to be developed in the future (Department for Energy Security and Net Zero, 2023). As described in Section 2.1 in the Literature Review chapter, CHNs are those that serve dwellings in a single residential building unit. Thus, the findings in this thesis are likely to be applicable to a significant proportion of future UK HNs. Larger HNs are likely to have a larger diversity effect, one reason being that in larger networks, the return flow takes longer to reach the plant. Thus, to inform the design of larger HNs, such as DHS, conducting a study similar to this with the use of a real district-wide HN is recommended. Furthermore, in larger networks, the occupant density is also likely to vary more significantly than in CHNs; Weismann et al. (2016) found that diversity is sensitive to changes in user profile when occupant density is higher. HNs could also be used to deliver heat to campus buildings such as student residences where the occupants are likely to have routines that are aligned to a greater extent than the wider population (CIBSE, 2020). Thus, the author recommends that similar studies be conducted for the different kinds of HNs expected to be developed in the UK, where key characteristics such as occupant density, size and occupancy type may vary.

### 8.2.2 Sampling Time

A sampling time of 10 minutes was deemed appropriate for use in sizing the distribution system of a HN similar in occupancy and topology to the case study HN to satisfy a quality-of-service criterion calling for demand to be met 95% of the time. Typically, quality-of-service criteria are higher than 95% in UK HNs and are defined based on annual demands which include off-heating season demands (Personal communication, T. Noughton, May 2022). In this work, heating season demands from the coldest periods were used. This results in a stricter criterion than when using annual demands because lower demands are not included. Thus, if a HN were sized using a 10-minute sampling time, over 95% of the annual demand, including for the off-heating season, will likely be met.

The DHW demand distribution produced in a study conducted by Cosic (2017) using data from 40 dwellings over a period of 112 days covering the heating season differs from the results in this work in a few key ways (Cosic, 2017). Firstly, for the demand distribution of individual demand, the impact of sampling time on peak demand is significantly less than it was found to be here. In this work, the peak demand at 5 seconds and 1 hour is 36.43 kW and 12.23 kW respectively, whereas in the Cosic report, the peak demands are 35.0 kW and 34.0 kW respectively. The peak demand has reduced by less than 3% in their work, whereas here, there is a reduction of 66.4%. This is because the methods used in Cosic (2017) use a recasting calculation that takes demand data from dwellings not on HNs and recasts them, so that it fits within the constraints imposed within a HN. One of the constraints is a limit on demand of 35 kW. For example, if a measured demand event exceeds 35 kW that demand event is transformed in such a way that demand doesn't exceed 35 kW, but the length of the event is increased such that the total energy consumed remains consistent. This forces an over representation of demand at the level of 35 kW, which may be the reason that sampling times of up to one hour still capture demands as high.

Furthermore, in Cosic (2017) results, the demand distribution tends to have multiple peaks, whereas the distributions produced in this work had singular peaks. Figure 8.1 below shows an example distribution from the Cosic (2017) where multiple peaks can be seen.

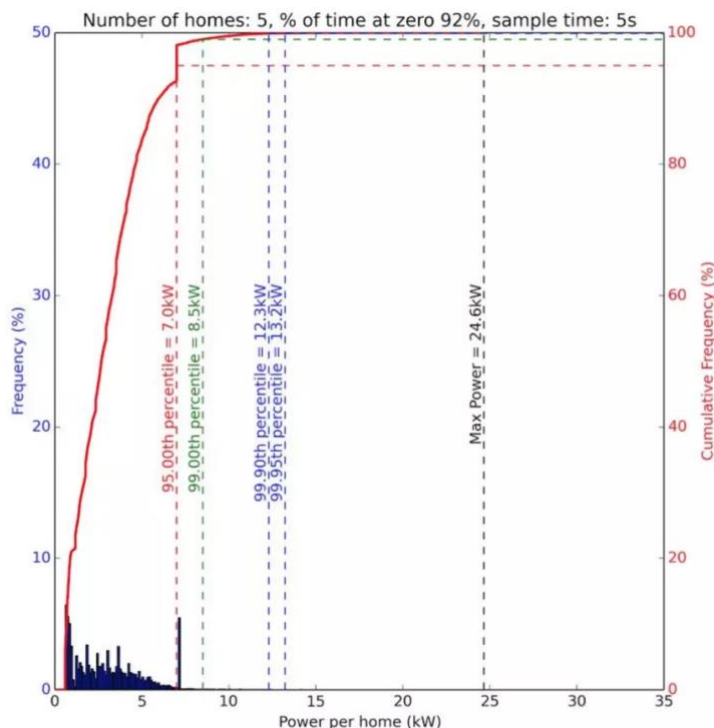


Figure 8.1: Demand distribution for the aggregate demand of 5 homes at a sampling time of 5 seconds (Cosic, 2017)

Data in this work was collected from dwellings in one HN in a single residential building, whereas Cosic (2017) used the Energy Savings Trust data set, which covered a range of dwelling types and occupancy and from various locations. The presence of multiple peaks in their results, compared to the singular peak present in this work, is likely explained by the much wider range of occupancy, heating systems, and building of the Cosic (2017) sample. Occupancy behaviour may also vary as a result of adapting to the heating system; for

example, residents of flats in some residential buildings have learned that the cold water tends to be at a temperature that is high enough not to cause discomfort, and therefore, where they would usually use the hot water tap, they instead use the cold water tap (M. Cosic, Personal communication, 2022). The minimum hot water temperatures in the case study HN reached a minimum of 11 °C (as shown in Figure 5.13) which suggests that cold water temperatures can reach the temperatures typically expected of cold inlet water of around ~ 10 °C as shown in Figure 2.2.

When a quality-of-service criterion is defined, the basis of the definition must be on annual data. Although it is reasonable to assume that the demands in the cold periods are higher, and therefore, adding in off-heating season data may not necessarily alter the peak demand, the results in this section are best confirmed using annual data before it is used to inform design guidance. The results do, however, demonstrate the behaviour of HN demands using a novel dataset and uses the demands to highlight where the design guidance may have drawbacks. The results confirm previous findings deriving from other datasets. However, this work is the first to be based on data from a real HN.

### 8.2.3 Validity of Technical Guidance

The DS439 diversity methods have been critiqued relating to its application in the design of UK HNs because of the resulting oversizing (Smith, 2016). There are two sizing methods in the DS439, one intended for heat exchanger sizing and the other for pipe sizing. The heat exchanger sizing method was shown explicitly to oversize capacities in HNs (Open Data Institute, 2017; Smith, 2016). There have been no studies demonstrating oversizing as a result of using the pipe sizing method until this work (Section 6.5). CP1.2 refers to the pipe sizing method and caveats its use by recommending that data measured at a minutely sampling time be used where it is available to develop empirical diversity curves. Results in Section 6.2.2 demonstrate that a sampling time of 10 minutes may be appropriately used for sizing to meet a quality-of-service criterion of 95%.

There is no shortage of studies showing a discrepancy between measured DHW flow rates and those recommended across a range of European design standards. In these studies, the authors suggest that the reasons for the discrepancy may be the drastic changes in the DHW systems since the design standards were developed and changes in occupant consumption behaviour (Fuentes et al., 2018; Jack et al., 2017; Kõiv and Toode, 2005; Kõiv and Toode, 2006). Additionally, the Energy Savings Trust (2008) showed that measured DHW temperatures are lower than those assumed in commonly used standards. These findings were supported by measured DHW temperatures in this work. Lower flow rates and lower temperatures than what is assumed in technical standards could lead to real peak demands at the individual level being significantly lower than estimated. Use of overestimated individual peak demands to estimate aggregate peak demands would lead to an overestimation despite the validity of the formulation of diversity. Recommendations for future work include considering how the pipe sizing method and heat exchanger method vary in their application in UK HN design (i.e., clarify the extent to which industry practitioners use each), evaluating the merits and demerits of each (including evaluating the extent to which each overestimates peak demands) and making suggestions as to how each could be treated such that resulting estimations could become more valid.

Future work should aim to bring pumping costs into account in a cost-benefit study; although reduced pipe sizing reduces heat loss, it increases the pumping costs. Furthermore, the

difference in the cost of the pipes themselves should be considered even though they are unlikely to be substantial compared to pumping costs and costs due to heat loss.

#### 8.2.4 Distribution System Sizing

At levels of aggregation higher than 35 dwellings, the peak demand was shown to be dominated by SH demand. This means that for all pipes serving 35 dwellings or less, the DHW demand is the key consideration in sizing. For pipes serving more than 35 dwellings, SH demands may be a more important consideration. The guidance found in CP1.2 does not make a distinction between using SH or DHW for sizing different parts of the distribution system, but instead suggests that SH and DHW diversity can be calculated for each pipe section independently and then combined in order to obtain a total flow rate. The findings in this chapter have shown the difference in the peak total demand compared with the peak DHW demand at aggregation levels above 35 dwellings are not substantially different. Below this level, the DHW peaks are higher than the total demand peaks. This suggests that for parts of the distribution system that are closer to the dwellings, sizing the distribution system for DHW demand alone will not restrict the delivery of SH. Thus, a sizing method based on DHW demand alone would be sufficient in sizing some parts of the distribution system to deliver both SH and DHW. A key limitation here is the distinction made in the literature review section (Section 2.5.5) between the real demand and aggregate demand. The assumption being made here is that the aggregate demand is accurately representing the real demand at a given point in the distribution system. In other words, it is being assumed that the aggregate demand for 10 dwellings, for example, is equal to the real demand measured at a section of pipe in the distribution system downstream of which there are 10 dwellings. To verify this assumption, measurement studies that collect flow data from different locations along the distribution system itself would be required. One would expect the real demand profiles to be ‘flatter’ than the aggregate demands due to mixing in the pipes resulting from non-uniform fluid velocity.

### 8.3 Results 3 Summary and Discussion

The aim of the third results chapter was to investigate the impact that DHW storage has on HN demand and on the sizing of the distribution system. To achieve this aim, domestic heat storage was modelled to take the real demand of an individual dwelling as inputs and produce a residual demand, i.e., the demand of the thermal store itself. Two kinds of heat store were modelled: a mixed heat store and a stratified heat store. The results of each act to bookend the possible behaviour of a real heat store. The residual demands were aggregated to give the HN demand. The ADMD and diversity curves for the different scenarios of storage and the resulting impact on distribution pipe sizing was analysed and compared. The thermal losses from the distribution system and the thermal stores for the different storage scenarios were calculated. For the design day, the thermal losses from the thermal stores and from the distribution system were compared to the DHW demand for each storage scenario. Sensitivity analysis allowed the mapping out of how key parameters of the thermal store and distribution system models affect the results. Additionally, the real oversizing of the case study HN was analysed, showing the potential for reduced sizing in the distribution system. The key findings in this chapter are summarised in point form below.

- Generally, the ADMD of the storage scenarios is lower than for the real scenario at lower levels of aggregation, whereas at higher levels, the ADMD of the storage scenarios tended to be higher than for the real scenario.

- Analysis of the total lengths of pipes of a given size in the case study network showed that the longest total pipe length was for pipes serving a single dwelling. Generally, the more dwellings a pipe serves downstream of it, the less total length there is of that size of pipe in the distribution system.
- Both the CC and the SC storage scenarios require smaller pipe sizing across the distribution system than the real sizing. For example, pipes serving 4 dwellings could be sized to a diameter of 6 mm with the installation of storage, whereas currently it has a diameter of 35 mm. Pipes serving 48 dwellings, could be sized to a diameter of 15 mm with storage installation, which is 39 mm smaller than its current sizing.
- Comparing the sizing for the real demand scenario against the real sizing of the distribution system shows that pipes could have been sized smaller across the distribution system. For example, pipes serving 30 dwellings could have been sized 29 mm smaller.
- Pipe sizing in the storage scenarios could be as low as 6 mm, whereas the smallest pipe in the real case was 22 mm.
- Thermal loss results, evaluated in terms of thermal loss per meter of pipe, show that thermal losses from the real design were consistently higher than thermal loss for any of the storage scenarios for all sizes of pipe. For example, for the largest pipes in the distribution system, the pipe serving 48 dwellings, the thermal loss is lower than 0.160 kWh/m for every storage scenario, whereas for the real case, the thermal loss is 0.168 kWh/m.
- Across all scenarios, pipes serving less than 6 dwellings are responsible for a large majority of the total heat loss from the distribution system. Pipes serving less than 6 dwellings have a daily heat loss of above 6 kWh. Whereas for pipes serving 6 or more dwellings, the highest daily thermal loss is ~1 kWh. This suggests that the smaller but more numerous pipes, which are those that are closer to the dwellings, ought to be the focus of any attempts to reduce thermal loss in the distribution system when designing HNs where the topology is similar to that of that case study HN.
- The distribution system losses in the real scenario make up 8.8% of the total DHW demand on the design day. For the storage scenarios, the thermal loss of the distribution system makes up ~4-6 % of the DHW demand. Thus, showing that installation of domestic storage will reduce the thermal losses of the distribution system.
- However, the total thermal loss of any storage scenarios is higher than the thermal loss of the real design scenario which comprises only distribution system thermal loss.
- The total thermal loss of the storage scenarios makes up ~17-23 % of their respective total DHW demand.
- Sensitivity analyses of the domestic thermal store model and the distribution system model showed that the conditions required for the thermal loss in any storage scenario to be comparable to that of the real design are conditions that are prohibitively detrimental to occupant comfort (i.e., extremely low ambient temperatures) or are conditions which are infeasible due to increased demands on space (i.e., 15-inch-thick thermal store insulation)

### 8.3.1 Implications for Design Guidance and Industry Practice

In the earlier chapters of this thesis, the contention with the UK HNs industry regarding the benefit of domestic storage in reducing overall thermal loss and the role that diversity plays therein was made evident. The uncertainty was evident in personal communications that the author had with industry practitioners as well as in the conflicting official guidance within the

industry. The results of the work in this thesis have brought about some clarity to the question that has remained unanswered hitherto; does DHW storage bring about an overall reduction in thermal loss? In short, no; although adding DHW storage will reduce thermal loss from the distribution system due to reduced pipe sizing, the additional losses from the stores themselves are too great to be able to bring an overall reduction in the total thermal loss. This was shown to be the result in all cases where conditions were those that could be reasonably expected, i.e., not unreasonably high ambient temperatures or overly thick insulation levels.

Although neither of the storage scenarios resulted in a total reduction of thermal loss, the work in this chapter was able to quantify the impact of the diversity effect by modelling two different storage scenarios, bringing about clarity to the understanding of the role that diversity plays in reducing pipe sizing in different parts of the distribution system. Like for smaller pipes, the reduction of the size of larger pipes is brought about by reduction in individual demand, however, unlike to smaller pipes, reduction is furthered through the effect of diversity. This is partly why the SC scenario outperforms the CC scenario even though they both have comparable reductions to individual peaks; the increased diversity effect of the SC scenario decreases the sizes of the larger pipes further. The reduction of sizing of larger pipes resulting from a reduction in individual peak demands and increase in diversity has not been explicitly demonstrated hitherto and thus makes one of the novel findings of this work. If the UK HN industry were to build HNs with domestic storage it is of paramount importance that technical guidance specific to designing with domestic storage be developed. The work in this thesis could be a starting point for such guidance. The results in this chapter have shown that the collective charging times of domestic stores are able to have a marked impact on the aggregate demand because of impact it has on the diversity effect and therefore technical guidance would have to be specific to different charging times of the domestic stores.

In terms of heat loss per meter of pipe, the pipes serving a single dwelling were responsible for the least amount of heat loss, however, taking the heat loss from the total length of pipes of a given size, they were responsible for the most amount of heat loss. To put another way, taking the distribution system as a whole, the smaller but more numerous pipes, brought about the most thermal loss savings of any size of pipe due to their having the greatest collective surface area. The smaller pipes should therefore also be the focus of any kind of thermal loss reduction efforts, such as through insulation. This is emphasized in the guidance in CP (Objective 3.9.1) (CIBSE, 2020). Moreover, although results have shown that pipes can be sized as small as 8 mm, the implications of having such small pipe sizes and the impact that these have on the distribution system need to be considered. Smaller pipes require more pumping energy and therefore higher costs for electricity. Small pipes are also mechanically weaker than larger pipes and their durability need to be taken into consideration. The difference in the thermal loss between smaller pipes and larger pipes are noted in a study by the Department and Energy and Climate Change (DECC) who published a report considered to have used the most comprehensive dataset characterising UK HNs at the time of publishing (DECC, 2015). The report looked at 14 HNs, all of network length >1,000 m and varying peak supply capacities. The relative heat loss in these HNs were found to range from 3% to 43%. The results show that there is a significant difference in heat loss in bulk schemes, where the mean relative heat loss is 6% and non-bulk schemes where the mean is 28%. Bulk schemes are where the main network operators deliver heat in bulk to the main distribution points but don't have the responsibility for final delivery to end consumer. Thus, in bulk-schemes, the heat loss from internal pipes is not included in the distribution losses. Non-bulk schemes are where the network operators are responsible to the final delivery to

end consumer. The discrepancy in relative heat losses is attributed to poor pipe insulation, of which there have been more accounts of in non-bulk schemes. The heat loss in kWh/m of pipe length shows losses of orders of magnitude higher in non-bulk schemes. The ground pipes have stricter insulation standards than internal pipes, and thus it is likely that the high losses are largely due to the internal pipes. The report adds that internal losses will occur in all CHS (a system contained in a single building) regardless of whether it is connected to a wider HN or not, and that the issue of internal losses and poorer standards for internal pipe insulation should be considered a building services design and maintenance issue. Due to the longer pipe lengths in large scale HNs the heat loss is a significant consideration at the design stage. The case study HN used in this work, in which the consumers and plant are in a single building, and where the total network length is equal to ~450 m, would be considered a small-scale HN (detailed in Section 3.4).

### 8.3.2 Limitations

The assumption that store height is equal to diameter may not be ideal in terms of practical space considerations, however such a criterion was chosen in order to reduce the surface area and therefore determine the lowest possible thermal losses in order to understand the 'best case' scenario. In the mixed model stores, the maximum charging power is defined as the fixed value of power required to fill up the store in 2 hours however, because in operation the charging power responds to the state of charge of the store, the store doesn't fill up all the way in the given time. This means that the mixed store models don't reach a 'full' level as much as the stratified stores which may result in lower thermal losses from the stores when comparing the mixed stores with the stratified stores. If the mixed stores were to fill up in the 2 hours, they would require a maximum charging power that was higher than what has been defined. This means that the peak demands in the mixed models would have been higher. This would result most notably in the service pipes being sized larger to meet this higher peak demand. This in turn results in more thermal losses from the service pipes in the scenarios that use mixed stores.

The distribution system thermal loss model is based on the assumption of constant return and flow temperatures which are equal to the operating temperatures required for delivering peak demands in the case study. In reality, the temperatures across a distribution system will not be spatially or temporally constant. For example, in the pipes serving a single dwelling the peak demands exist for shorter periods of time, and thus the operating temperatures will also only be reached for shorter periods of time, compared to the pipes closer to the plant. Having said this, some HNs have a keep hot function that prevents the final branches of a distribution system from dropping below a given temperature. This allows comfortable temperatures to be reached faster. The implication of this assumption on the results is that the difference in the thermal loss between the smaller pipes and the larger pipes may not be as pronounced as the results indicate. Moreover, the distribution system thermal loss savings in the storage scenarios is limited by the pipe sizing methodology used to size the pipes. An avenue of further study would be to incorporate an optimisation algorithm for pipe sizing. If pipe sizes are found to be reducible beyond what is allowed in existing sizing methodology, greater amounts of thermal loss savings are possible. Furthermore, storage would allow for the use of intermittent supply in the off-heating season which would lead to lower losses from the distribution system from local pipework being allowed to cool for periods of time. This was not captured in the model due to the use of constant flow and return temperatures. For simplicity, and because it was deemed unnecessary for studying thermal losses for the design day, which is a relatively short time scale, the effects of the thermal mass of the distribution

system were ignored in the distribution system model. To recapitulate: thermal mass acts like thermal storage within the distribution system itself however, the capacity of the distribution system as storage is negligible compared to the collective capacity of the DHW stores and was thus could reasonably be ignored in the distribution system model. Including the effects of the thermal mass of the distribution system would have necessitated the construction of a thermo-fluid dynamic model. Such a model would be more instructive than a steady state model on the time scale of a year, but less so when evaluating under the much stricter conditions of a design day, which is of shorter time scale and therefore where thermal conditions vary significantly less.

Thermal losses may not always be wasted energy per se. They could also be useful heat gains depending on the time of year. During the heating season, storage losses could ideally contribute entirely to SH demand. In the shoulder months, the thermal losses may provide just the right amount of heat to prevent the activation of the SH system. The same could be said for thermal losses from the distribution system that enter the communal spaces and potentially permeate through the to the dwellings through warmed walls. These losses could also be considered a useful source of heat to dwellings. On the other hand, thermal losses into communal spaces have been shown to contribute to overheating in the summer periods. The evaluation of thermal loss in this work has been for the design day alone, which is a day that would naturally occur in the heating season and therefore where the thermal losses could appropriately be defined as useful internal heat gains that contribute to SH demand. Had this work defined storage losses as a contribution to the SH demand, the SH demand would have reduced, however the total demand would have remained unchanged because the demand from the store would go to either SH or DHW. Taking all the above into consideration, a potential avenue for further study could take a more holistic view and build a thermal model comprising the dwellings and the communal spaces and where useful heat gains and how they vary throughout a typical year are considered.

The pipe in parts of the distribution system closer to the dwellings will have to be greater than a minimum set by the SH demand and the pipe in parts of the distribution system further away from the dwellings will have to be greater than a minimum determined by DHW demand depending on the design of the network. The distribution systems in the storage and real demand scenarios were sized based solely on DHW demand, rather than the total demand. For pipes closer to the dwellings, where DHW dominates the peak, using DHW demand-based sizing is appropriate. However, further upstream of the dwellings, where total demand peaks exceed DHW demand peaks (as shown in Figure 6.19) using DHW demand alone to size pipes may lead to undersized pipes. Due to limitations in SH demand data, this thesis considered DHW demand only when assessing storage and determining reduced pipe sizing. Despite this, from the available data on total demand, it can be shown that for the storage scenarios the SH demand can be met at least where service pipes are concerned. The smallest pipe diameter for a service pipe found in any scenario was 6 mm in the SC scenario with the mixed thermal store. This size of pipe was based on a demand of 4.34 kW. Figure 6.7 shows that the vast majority of individual SH demands fall below ~5 kW. This suggests that at the service pipes, a 6 mm pipe sizing would likely be able to meet the DHW demand as well as a large majority of the SH demands. A similar yet more comprehensive study involving a modelled storage system that considers both DHW and SH demands and their respective  $\Delta T$ s at the heat exchangers would be required to state the above conclusion with more confidence as well as to determine sizing for pipes throughout the distribution system beyond the service pipes. Considering the time and resource constraints as well as limitations in the data, the work in this thesis has focussed on DHW demand in its aim to investigate the

effects of storage on the network demand and sizing. As such, the storage results should not be seen as a rigid benchmark when designing HNs. The results are intended rather to demonstrate the key design considerations that relate to the interaction between storage, demand and diversity so that designers are more informed in their decision making. Having said this, results that relate to parts of the distribution system nearer the dwellings are more valid due to the DHW dominance in that region. Future work should involve similar studies using both SH and DHW demands together to investigate how the effects of both combined, with and without storage, and what that could mean for network demand and design. The consideration of both SH and DHW demands may result in more readily practicable take-aways for the design of all the entire distribution system rather than the parts closer to the dwellings.

Evaluations of the real demand showed that DHW demand dominates the peak below levels of aggregation less than around 35 dwellings. If this claim holds for the storage scenarios, then it can be said that since much of the pipes in the distribution system serve less than 35 dwellings, using the DHW demand alone would have been appropriate for a large portion of the distribution system; results relating to parts of the distribution system closer to the dwellings would be more valid than parts that are further away. Does the claim hold for the storage scenarios? This depends on how storage impacts DHW demand and SH demands independently of each other, which in turn depends on whether storage losses are treated as useful heat gains or not. If storage losses are taken to contribute to SH demand, the total demand remains unchanged. If storage losses are taken as not contributing to SH demand, the total demand increases. If the total demand increases, and the distribution system was sized using total demand, in the sections where DHW does not dominate the peak, pipes would have had to be sized larger. If the total demand remained unchanged, the pipe sizes would also remain unchanged. For the results obtained, which are based on the design day, which is in the heating season, one can reasonably assume that the storage losses contribute entirely to SH demands. Thus, total demand would have remained unchanged, as would have the pipe sizes in the distribution system where DHW does not dominate the peak. For the shoulder months and the off-heating seasons, the case would be different; the shoulder months, where storage losses would contribute to SH demand, would have meant that the total demand remains unchanged, and in the off-heating season, DHW demand peaks would have reduced, and sizing based on purely DHW demand would be appropriate since there is no SH demand.

Higher velocities are allowed with instantaneous demand because the high velocities would only act for short periods of time. The guiding principles of the velocity bounds recommended in CP1.2 are not stated and thus it is not possible to know whether they were defined to be more liberal with the above in mind or not. If they were not, for the instantaneous demand scenario, the velocity bounds allowed could have been higher than for the storage scenarios, resulting in the pipe sizing for the real demand scenario being smaller.

The temperatures in the distribution system are dynamic and respond to a number of factors including the demand on the network, state of the bypasses, as well as operational factors that may aim to reduce heat losses by letting the network go cold whilst still preventing Legionella growth. The temperatures of a distribution system will vary seasonally. In the winter months where SH demand is active, there is a more consistent demand on the network. Whereas in the summer, when only DHW demands acts, the demand on the network is less consistent. Adding domestic storage to a network not only impacts distribution system thermal losses through reduction in distribution system sizing but will impact losses through fundamental changes to the demand. For example, the CC scenario which allows DHW

demand charging at given time slots may allow the network to go cold in between the charging time slots in the summer when there is no SH demand, thus reducing the thermal losses significantly. To assess the full impact of storage, future work could extend to using annual DHW and SH demand as inputs in a dynamic thermal network model. Modelling the distribution system using node methodology would enable the determination of a temperature field across the network, which in turn could be used to give the demand profile of the key heat sources, as well as the profile of thermal losses from the distribution system. Knowing the impact on demand at the plant would be useful in achieving a full techno-economic analysis of the storage and real demand scenarios as well.

There are many sources of energy losses in a HN, including efficiency losses, such as those in the heat generators, heat exchangers or pumps. These sources of thermal loss were not considered in the models in this work because compared to the effect that storage has on pipes, the effect that storage would have on these other thermal loss sources would be insignificant, however for a more holistic understanding of thermal loss a model would involve all sources of thermal loss, and thus future work could involve these sources.

In drawing conclusions about the impact of storage on distribution system sizing it is assumed that the heating systems within the dwellings operate with DHW priority. In an instantaneous system, DHW priority is more acceptable because the demands are shorter. In a storage system however, the demands of the store last longer. This means that giving DHW priority leads to SH demands being interrupted for longer. In reality, occupants will likely control their stores so that SH service is not interrupted. However, in this study, the control of the stores is assumed to be set by the HN operator. Thus, there is a trade-off to consider between implementing a HN wide control strategy of stores and the occupants' desire for their SH to not be interrupted. The 2-hour charging window was chosen with this in mind; in order to balance giving the store enough time to charge against having a short enough interruption to the SH service that occupants would not find unacceptable.

### 8.3.3 Applicability of Results

The results in this chapter pertain to a case study CHN with a specific network topology. There are 17,000 HNs in the UK, 11,500 of which are CHNs (ADE, 2018). The majority of existing HNs, and those likely to be built in the future in the UK will be CHNs. Thus, because of similar topologies, similar pipe environments, and the similar occupant demands that CHNs tend to have, the results will likely be instructive for a large proportion of UK HNs. However, care must be taken when making claims about HNs that have any characteristic differences to the case study. For example, where distribution system pipes are in different environments, say underground as opposed to in riser cupboards, thermal losses may be higher or lower than results indicate here due to different ambient temperatures. Similarly, if topological differences mean that the collective length of larger pipes are longer than that of shorter pipes, the thermal losses from the larger pipes could outweigh those of the smaller pipes. In such a case, leveraging the diversity effect to reduce the pipe sizes of the larger pipes would be of paramount importance. On the other hand, the pipes serving a single dwelling could be longer (this may be the case for particularly large dwellings), and thus have an even greater collective length. This would lead to an even greater discrepancy between the collective thermal loss of the small pipes and the large pipes. Moreover, the findings in this work relate to a CHN where the occupant demands are similar to one another. In district scale HNs that are likely to be mixed mode, where demands from different users will be more varied, the diversity effect at play will predictably be greater. Following the

measured data principles of this thesis, it is recommended that real demand data is collected from mixed mode users and used in a diversity study similar to that in this thesis. For example, at a district scale, it is likely that there are users that have long and steady demands compared to residential users such as hospitals or swimming pools. The diversity effect that acts when demands from users such as these get aggregated will be different to that found for residential occupants in this work.

HNs of the future will become increasingly lower temperature, which means that losses from the distribution system will decrease, and therefore so will any potential thermal loss savings from pipe size reduction. With the growth of 4<sup>th</sup> and 5<sup>th</sup> generation HNs, where a core principle is reduced operating temperatures, and where there will be a need for other accompanying developments such as a requirement for a different configuration of storage and/or the installation of heat pumps for upgrading temperatures nearer the dwellings, the diversity effect at play and its impact on network sizing and thermal losses could look substantially different to the findings in this work. It is recommended that high-frequency demand data is collected from a 4<sup>th</sup> or 5<sup>th</sup> generation HN and studied using the methods used in this thesis to produce findings similar to those in this study but that relate to the characteristically different HN generations. This will enable standards to continue to be informed as the core principles driving HN design develop.

#### *8.3.3.1 Estimating Real Demand*

Heat demand at the taps or radiators in a dwelling would be met instantaneously by the HIU if there was no lag time or thermal inertia in the heating circuits. Lag time describes the time it takes for heated water to travel to a point where it can be experienced by consumers and is therefore dependent on the design and operation of the distribution system. Thermal inertia is also dependent on the design and operation of the heating system. The thermal inertia of a radiator system is a measure of how quickly it can get up to temperature and can be calculated using catalogue data, like was done by Karlsson and Fahlén (2008) in which a time constant of 23-26 minutes was used corresponding to the thermal inertia of a radiator system with a  $\Delta T$  of 55/45°C. They also use a lag time of 10 minutes estimated as a practical limit based on the length of piping of the radiator system in their study.

The above describes how thermal inertia and lag time act in a domestic system. Thermal inertia and lag time also act across the distribution system of a HN, and therefore, when using the raw dwelling demand data to estimate the real demand elsewhere in the network, such as a point upstream in the distribution system or at the central plant, the thermal inertia and the lag time that acts between the relevant points must be accounted for. For example, because of the thermal inertia and lag in the system, demand at the dwellings is not experienced immediately at the central plant. Similar to the domestic heating circuits, the thermal inertia and lag in the distribution system depends on its operation and design. Thus, thermal inertia and lag time is an important consideration when using demand aggregate demand made up of individual demand at HIUs to represent the demand at a given point in the distribution system. To be clear, this would be using the aggregate of 10 individual demand profiles, measured at 10 different HIUs, to represent the demand through a pipe in the distribution system that serves 10 dwellings. To measure such a demand directly would require a prohibitively inordinate number of resources including expensive measuring equipment and access and rights to install such equipment in a case study HN that is likely to disrupt the service to occupants. Thus, the next best alternative is to use the aggregate demand of individual demand profiles.

In addition to the above, it is important to consider the added complexity that arises from the physical limits imposed by the sensing equipment itself, for example the finite time taken for a temperature sensor to warm up. There is also the process of digitisation which acts to further degrade the signal. Besides real distortions, equipment could also record readings that don't correspond to any physical reality. However, it's unlikely that any of the above distortions or uncertainties occur at time scales over the order of a second and thus are unlikely to have affected the demand profiles or related results.

## 9 Conclusions

In this chapter, the key findings of this thesis are framed by the key questions and objectives that drove the research. This section concludes by outlining potential avenues for research that could build on the findings in this thesis.

- *What is the real diversity effect in UK HNs?*
  - Estimate the individual demand profiles of dwellings on a real HN using measured data.
  - Analyse the impact that aggregation, over number of dwellings and over time, has on the demand.

This objective above relates to estimating and understanding the individual demand profiles of a sample of dwellings in the case study CHN for which data was collected. The objectives here also relate to characterising the aggregate demands that could be built from the individual demand. In order to fulfil these objectives, high frequency, multivariate, measured data from 115 HIUs in a case study CHN in the Southeast of England was used to estimate the total and DHW demands for a mixed occupancy sample for the period of the coldest week in the heating season. The demands estimated in these objectives were used as inputs in the models built to achieve the remaining objectives, the main aim of which was to inform design guidance in the UK HN industry by removing uncertainty around the case for domestic storage, as well as informing guidance in other ways such as by setting a benchmark for the sampling times required when measuring demands.

Evaluating the effect of sampling time of the aggregate demand showed that a 10-minute sampling time could be used to meet 95% quality-of-service criterion at all levels of aggregation. This finding is relevant to HN design guidance, specifically, where it is advised to use own empirical measurements when evaluating sizing of the distribution system and plant. Conventional industry guidance has operated on the assumption that shorter sampling intervals are unlikely to provide meaningful data for sizing, although it has not definitively confirmed the extent to which this is the case. The comparison of total demand and DHW demand at varying levels of aggregation showed that at an aggregation level of around 35 or more dwellings, the total demand peak exceeds the DHW demand peak, suggesting that SH may dominate the peak at these levels. The impact of DHW demand independent from SH demand on diversity has not been the subject of any previous research literature making the findings in this work the first of its kind. Lastly, many studies looking at diversity in UK HNs have used a sample of standalone dwellings (Summerfield et al., 2014; Wang et al., 2020). Thus, the work in this thesis is the first of its kind to use real data from dwellings on a real HN. The results pertaining to these objectives constitute novel findings pertinent to the HN industry and its design guidance.

- *What is the impact of DHW TES on HN demand and design in the presence of diversity?*
  - Estimate the residual DHW demands that would result from DHW TES installation for the sample of dwellings.
  - Assess the impact that DHW TES has on the aggregate demand.
  - Assess the impact that DHW TES has on the distribution system pipe sizing and the resultant impact on thermal loss.

The second and final set of objectives were designed to answer the main question that the thesis centres on which is ‘does domestic storage bring an overall reduction in thermal loss?’ In order to answer this question, a number of storage scenarios were modelled using two types of storage model and compared to the real design of the case study HN and the scenario of the real demand of the case study HN. The scenarios were evaluated in terms of their diversity, their peak demands, the resultant required distribution system pipe sizing, and their thermal losses.

The ADMD of the storage scenarios was found to be lower than for the real scenario at lower levels of aggregation. At higher levels of aggregation, the ADMD of the storage scenarios were found to be higher. Both storage scenarios allowed for pipes to be sized smaller than in the real design of the HN; for the storage scenarios some pipes could be sized as small as 6 mm, whereas the smallest sizing of real pipe was 22 mm. Across all scenarios, pipes serving less than 6 dwellings were found to be producing the majority of the thermal loss in the distribution system. This suggests that when designing network topologies similar to the case study, efforts to minimise thermal loss in the distribution system should prioritise the smaller yet more numerous pipes located closer to the dwellings. Thermal loss evaluations showed that distribution system thermal loss for the storage scenarios was lower than for the real design. The distribution system losses in the real scenario are 8.81% of the DHW demand on the design day. For the storage scenarios, the thermal loss of the distribution system equal ~4-6 % of the DHW demand. Considering the thermal loss from the distribution system together with those of the domestic thermal stores shows that total thermal loss is not reduced with the installation of storage. Sensitivity analyses of the domestic store model and the distribution system thermal loss model showed that the conditions required for the thermal loss in any storage scenario to be comparable to the real design are conditions that are nonoptimal for occupant comfort (i.e., extremely low ambient temperatures) or are conditions which are infeasible due to increased demands on space (i.e., 15 inch thick thermal store insulation).

No studies to date have attempted to evaluate the impact that storage has on the thermal losses of HN by modelling the impact on distribution system sizing. Thus, the results above constitute novel findings that can be used to inform the UK HN industry. Firstly, by producing an empirical ADMD curve using real data from a UK HN that may be used as a supplement to the sizing guidance in CP1.2. Secondly, by showing that storage is unlikely to bring about a substantial overall reduction in thermal loss in HNs similar to the case study CHN. Both above points, as well as the requirement of a validated sampling time for use when measuring demand for HN design, have been hitherto a point of contention within industry. With these novel findings, the design guidance can be clarified and made more robust in order that future HNs will be built to high standards and be able to be effective in their role in decarbonising heat in the UK.

### 9.1.1 Future Research

The case study HN used in this work was a CHN and thus the findings apply primarily to CHNs of similar topology and occupancy. Similar studies should be conducted for HNs that vary in size, topology and consumer sample. A further avenue of study could be to use an optimisation algorithm for pipe sizing. If pipe sizes are found to be reducible beyond what is allowed in existing sizing methodology, more thermal loss savings are possible. The use of a model that incorporates the effects of thermal mass and lag would enable an assessment of the annual thermal loss rather than thermal loss solely on the design day. An estimation of

annual losses would provide insight into how the impact of storage may vary in the off-heating seasons and the shoulder months, where the definition of ‘useful heat’ may vary.

## 10 References

- Abokersh, M. H., Saikia, K., Cabeza, L. F., Boer, D., & Vallès, M. (2020). 'Flexible heat pump integration to improve sustainable transition toward 4th generation district heating', *Energy Conversion and Management*, 225(August). <https://doi.org/10.1016/j.enconman.2020.113379>
- ADE. (2018). Market Report: HNs in the UK. *The Association for Decentralised Energy*, (January), 20. Retrieved from [https://www.theade.co.uk/assets/docs/resources/HNs in the UK\\_v5 web single pages.pdf](https://www.theade.co.uk/assets/docs/resources/HNs%20in%20the%20UK_v5%20web%20single%20pages.pdf)
- Allison, J., Bell, K., Clarke, J., Cowie, A., Elsayed, A., Flett, G., Tuohy, P. (2018). 'Assessing domestic heat storage requirements for energy flexibility over varying timescales', *Applied Thermal Engineering*, 136(November 2017), 602–616. <https://doi.org/10.1016/j.applthermaleng.2018.02.104>
- Aragon, V., James, P. A. B., & Gauthier, S. (2022). 'The influence of weather on heat demand profiles in UK social housing tower blocks', *Building and Environment*, 219(September 2021), 109101. <https://doi.org/10.1016/j.buildenv.2022.109101>
- ASHRAE. (1997). ASHRAE Fundamentals Handbook.
- Ballico, M. J., & Van Der Ham, E. W. M. (2013). 'A simple method for the measurement of reflective foil emissivity', *AIP Conference Proceedings*, 1552 8(September 2013), 740–745. <https://doi.org/10.1063/1.4819634>
- BEIS. (2017). Heat Networks Consumer Survey: Results Report. *BEIS Research Papers*, (27), 71. Retrieved from <https://goo.gl/kzdp1h>
- BEIS. (2019). Leading on Clean Growth. Retrieved from [https://assets.publishing.service.gov.uk/media/5da5c1f4e5274a392aa9582b/CCS0819884374-001 Government Response to the CCC Progress Report 2019 Web Accessible.pdf](https://assets.publishing.service.gov.uk/media/5da5c1f4e5274a392aa9582b/CCS0819884374-001_Government_Response_to_the_CCC_Progress_Report_2019_Web_Accessible.pdf)
- BEIS. (2020a). Heat Networks: Building a Market Framework, (February), 1–84. Retrieved from <https://www.gov.uk/government/consultations/heat-networks-building-a-market-framework>
- BEIS. (2020b). Energy Consumption in the UK (ECUK) 1970 to 2018. *Energy Policy*, 62(July 2019), 82–93.
- Belussi, L., & Danza, L. (2012). 'Method for the prediction of malfunctions of buildings through real energy consumption analysis: Holistic and multidisciplinary approach of Energy Signature', *Energy and Buildings*, 55, 715–720. <https://doi.org/https://doi.org/10.1016/j.enbuild.2012.09.003>
- Bergman, T., Lavine, A., Incropera, F., & Dewitt, D. (2002). *Fundamentals of Heat and Mass Transfer*.

- Bøhm, B., & Larsen, H. V. (2005). *Simple models of district heating systems for load and demand side management and operational optimisation*. Technical University of Denmark.
- Bøhm, B. (2013). 'Production and distribution of domestic hot water in selected Danish apartment buildings and institutions. Analysis of consumption, energy efficiency and the significance for energy design requirements of buildings.', *Energy Conversion and Management*, 67, 152–159. <https://doi.org/10.1016/j.enconman.2012.11.002>
- Borri, E., Zsembinszki, G., & Cabeza, L. F. (2021). 'Recent developments of thermal energy storage applications in the built environment: A bibliometric analysis and systematic review', *Applied Thermal Engineering*, 189, 116666. <https://doi.org/10.1016/j.applthermaleng.2021.116666>
- BSRIA. (2011). *Energy Efficient Pumping Systems - A Design Guide (BG 12/2011)*.
- Burzynski, R., Crane, M., Yao, R., & Becerra, V. M. (2012). 'Space heating and hot water demand analysis of dwellings connected to district heating scheme in UK', *Journal of Central South University of Technology (English Edition)*, 19(6), 1629–1638. <https://doi.org/10.1007/s71-012-1186-z>
- Cai, H., Ziras, C., You, S., Li, R., Honoré, K., & Bindner, H. W. (2018). 'Demand side management in urban district heating networks', *Applied Energy*, 230(May), 506–518. <https://doi.org/10.1016/j.apenergy.2018.08.105>
- Collazos, A., Maréchal, F., & Gähler, C. (2009). 'Predictive optimal management method for the control of polygeneration systems', *Computers & Chemical Engineering*.
- Cao, B., Zhu, Y., Li, M., & Ouyang, Q. (2014). 'Individual and district heating: A comparison of residential heating modes with an analysis of adaptive thermal comfort', *Energy and Buildings*, 78, 17–24. <https://doi.org/10.1016/j.enbuild.2014.03.063>
- Carpaneto, E. and Chicco, G. (2006) 'Probability distributions of the aggregated residential load', *2006 International Conference on Probabilistic Methods Applied to Power Systems* [Preprint]. doi:10.1109/pmaps.2006.360235
- Carpaneto, E., & Chicco, G. (2008). 'Probabilistic characterisation of the aggregated residential load patterns', *Generation, Transmission & Distribution, IET*, 2, 373–382. <https://doi.org/10.1049/iet-gtd:20070280>
- CCC. (2020). The Sixth Carbon Budget: The UK's path to Net Zero. *Committee on Climate Change*, (December), 448. Retrieved from <https://www.theccc.org.uk/publication/sixth-carbon-budget/>
- Chen, Y., Athienitis, A. K., & Galal, K. E. (2014). 'A charging control strategy for active building-integrated thermal energy storage systems using frequency domain modeling', *Energy and Buildings*, 84, 651–661. <https://doi.org/10.1016/j.enbuild.2014.09.004>

- Chesser, M., Lyons, P., O'Reilly, P., & Carroll, P. (2020). 'Probability density distributions for household air source heat pump electricity demand', *Procedia Computer Science*, 175, 468–475. <https://doi.org/10.1016/j.procs.2020.07.067>
- CIBSE. (2016). Guide B1 Heating. In *Guide B1* (p. 148).
- CIBSE. (2014). Heat Networks: Code of Practice for the UK.
- CIBSE. (2020). Heat Networks: Code of Practice for the UK. Second Edition.
- CIPHE. (2002). Plumbing Engineering Services Design Guide.
- Cosic, M. (2017) *COHEAT 5G Heat Network demonstration*. <https://www.slideshare.net/MarkoCosic/coheat-5g-heat-network-demonstration-final>.
- Compton, P. (2015). A solution to overheating in common corridors of high rise buildings. Retrieved January 12, 2023, from <https://blog.coltinfo.co.uk/a-solution-to-overheating-in-common-corridors-of-high-rise-buildings>
- Cruikshank, C. A., & Harrison, S. J. (2010). 'Heat loss characteristics for a typical solar domestic hot water storage', *Energy & Buildings*, 42(10), 1703–1710. <https://doi.org/10.1016/j.enbuild.2010.04.013>
- Dansk Standard. (2009). Code of Practice for Domestic Water Supply Installations, 75.
- DECC. (2015). *Assessment of the Costs, Performance, and Characteristics of UK HNs*.
- Department for Energy Security and Net Zero. (2023). *HN Procurement Pipeline: 2023 Q1*. Retrieved from [https://assets.publishing.service.gov.uk/government/uploads/system/uploads/attachment\\_data/file/1169995/heat-networks-procurement-pipeline-jan-mar-2023-q1.pdf](https://assets.publishing.service.gov.uk/government/uploads/system/uploads/attachment_data/file/1169995/heat-networks-procurement-pipeline-jan-mar-2023-q1.pdf)
- Do Carmo, C. M. R., & Christensen, T. H. (2016). 'Cluster analysis of residential heat load profiles and the role of technical and household characteristics', *Energy and Buildings*, 125, 171–180. <https://doi.org/10.1016/j.enbuild.2016.04.079>
- Easteren, J. van. (2022). *The Potential of Thermal Energy Storage in combination with District Heating to deliver Winter Peak Load. PhD Thesis*. <http://resolver.tudelft.nl/uuid:2bd73389-f2b6-4ef8-bd80-1ee013ae1123>
- Energy Savings Trust. (2008). Measurement of domestic hot water consumption in dwellings. *Energy Savings Trust*, 1–62. Retrieved from [https://www.gov.uk/government/uploads/system/uploads/attachment\\_data/file/48188/3147-measure-domestic-hot-water-consump.pdf](https://www.gov.uk/government/uploads/system/uploads/attachment_data/file/48188/3147-measure-domestic-hot-water-consump.pdf)
- Erhorn-Kluttig, H., & Erhorn, H. (2014). *Selected examples of Nearly Zero-Energy Buildings Detailed Report*. Retrieved from [http://www.epbd-ca.eu/wp-content/uploads/2011/05/CT5\\_Report\\_Selected\\_examples\\_of\\_NZEBs-final.pdf](http://www.epbd-ca.eu/wp-content/uploads/2011/05/CT5_Report_Selected_examples_of_NZEBs-final.pdf)

- Faraj, K., Khaled, M., Faraj, J., Hachem, F., & Castelain, C. (2021). 'A review on phase change materials for thermal energy storage in buildings: Heating and hybrid applications', *Journal of Energy Storage*, 33(September), 101913. <https://doi.org/10.1016/j.est.2020.101913>
- Fischer, D., Wolf, T., Scherer, J., & Wille-Haussmann, B. (2016). 'A stochastic bottom-up model for space heating and domestic hot water load profiles for German households', *Energy and Buildings*, 124(April), 120–128. <https://doi.org/10.1016/j.enbuild.2016.04.069>
- Flyvbjerg, B. (2006). 'Five Misunderstandings About Case-Study Research', *Inquiry*, 12(2), 219–245. <https://doi.org/10.1177/1077800405284363>
- Foteinaki, K., Li, R., Péan, T., Rode, C., & Salom, J. (2020). 'Evaluation of energy flexibility of low-energy residential buildings connected to district heating', *Energy and Buildings*, 213, 109804. <https://doi.org/10.1016/j.enbuild.2020.109804>
- Fuentes, E., Arce, L., & Salom, J. (2018). 'A review of domestic hot water consumption profiles for application in systems and buildings energy performance analysis', *Renewable and Sustainable Energy Reviews*, 81(February 2017), 1530–1547. <https://doi.org/10.1016/j.rser.2017.05.229>
- Gadd, H., & Werner, S. (2013a). 'Daily heat load variations in Swedish district heating systems', *Applied Energy*, 106, 47–55. <https://doi.org/10.1016/j.apenergy.2013.01.030>
- Gadd, H., & Werner, S. (2013b). 'Heat load patterns in district heating substations', *Applied Energy*, 108, 176–183. <https://doi.org/10.1016/j.apenergy.2013.02.062>
- Gallo Cassarino, T., Sharp, E., & Barrett, M. (2018). 'The impact of social and weather drivers on the historical electricity demand in Europe', *Applied Energy*, 229(April), 176–185. <https://doi.org/10.1016/j.apenergy.2018.07.108>
- Gallo Cassarino, T. & Barrett, M. (2022). 'Meeting UK heat demands in zero emission renewable energy systems using storage and interconnectors', *Applied Energy*, 306, 118051. <https://doi.org/10.1016/j.apenergy.2021.118051>
- Gianniou, P., Liu, X., Heller, A., Nielsen, P. S., & Rode, C. (2018). 'Clustering-based analysis for residential district heating data', *Energy Conversion and Management*, 165, 840–850. <https://doi.org/https://doi.org/10.1016/j.enconman.2018.03.015>
- Good, N., Zhang, L., Navarro-Espinosa, A., & Mancarella, P. (2015). 'High resolution modelling of multi-energy domestic demand profiles', *Applied Energy*, 137, 193–210. <https://doi.org/10.1016/j.apenergy.2014.10.028>
- Grasmanis, D., Talcis, N., & Greķis, A. (2015). 'Heat Consumption Assessment of the Domestic Hot Water Systems in the Apartment Buildings', *Proceedings of REHVA Annual Conference 2015*. <https://doi.org/10.7250/rehvaconf.2015.024>
- Guadalfajara, M., Lozano, M., & Serra, L. (2014). 'Analysis of Large Thermal Energy Storage for Solar District Heating', *Eurotherm Seminar #99 Advances in Thermal*

- Energy Storage*, (August), 1–10. Retrieved from [http://publicationslist.org/data/miguel.a.lozano/ref-186/cc103\\_EUROTHERM99-01-089Paper.pdf](http://publicationslist.org/data/miguel.a.lozano/ref-186/cc103_EUROTHERM99-01-089Paper.pdf)
- Guan, J., Nord, N., & Chen, S. (2016). ‘Energy planning of university campus building complex: Energy usage and coincidental analysis of individual buildings with a case study’, *Energy and Buildings*, 124(1), 99–111. <https://doi.org/10.1016/j.enbuild.2016.04.051>
- Guelpa, E. (2021). ‘Impact of thermal masses on the peak load in district heating systems’, *Energy*, 214, 118849. <https://doi.org/10.1016/j.energy.2020.118849>
- Guelpa, E., Barbero, G., Sciacovelli, A., & Verda, V. (2017). ‘Peak-shaving in district heating systems through optimal management of the thermal request of buildings’, *Energy*, 137, 706–714. <https://doi.org/10.1016/j.energy.2017.06.107>
- Guelpa, E., & Verda, V. (2019). ‘Thermal energy storage in district heating and cooling systems: A review’, *Applied Energy*, 252(June), 113474. <https://doi.org/10.1016/j.apenergy.2019.113474>
- Hanson-Graville, R. (September 2019). Personal communication.
- Hanson-Graville, R. (September 2020). Personal communication.
- Hanson-Graville, R. (January 2021). Personal communication.
- Hanson-Graville, R. (February 2022). Personal communication.
- Happle, G., Fonseca, J. A., & Schlueter, A. (2020). ‘Impacts of diversity in commercial building occupancy profiles on district energy demand and supply’, *Applied Energy*, 277. <https://doi.org/10.1016/j.apenergy.2020.115594>
- HardHat Engineer (2023). *A Complete Guide to Pipe Sizes and Pipe Schedule – Free Pocket Chart*. Retrieved January 17, 2023, from <https://hardhatengineer.com/pipe/pipe-schedule-chart-nominal-pipe-sizes/>
- Heat Trust. (2021). Heat Trust. Retrieved May 31, 2021, from <https://heattrust.org/>
- Heatweb Ltd. (no date a). *Heatweb- Integrated Thermal Technology*. Retrieved May 31, 2021, from <http://www.heatweb.co.uk/>
- Heatweb Ltd. (no date b) *Node-HIU Switch*. [https://www.heatweb.co.uk/w/index.php?title=Node-HIU\\_Switch](https://www.heatweb.co.uk/w/index.php?title=Node-HIU_Switch)
- Heatweb Ltd. (no date c) *The DATA HIU - Heatweb Wiki*. [https://www.heatweb.co.uk/w/index.php?title=The\\_DATA\\_HIU#Documents](https://www.heatweb.co.uk/w/index.php?title=The_DATA_HIU#Documents).
- Hennessy, J., Li, H., Wallin, F., & Thorin, E. (2019). ‘Flexibility in thermal grids: A review of short-term storage in district heating distribution networks’, *Energy Procedia*, 158, 2430–2434. <https://doi.org/10.1016/j.egypro.2019.01.302>

- Hlebnikov, A., Siirde, A., & Paist, A. (2007). 'Basics of optimal design of district heating pipelines diameters and design examples of Estonian old non-optimised district heating networks', Doctoral School of Energy- and Geo-technology.
- Holman, J. P., (1992). *Handbook of Heat Transfer, seventh edition. McGraw-HillBook Co.* <https://doi.org/10.1002/9783527630868.ch4>
- Holmberg, S. (1987). *Ventilationsteknik [Ventilation Technology]. PhD Thesis.* Royal Institute of Technology Stockholm Sweden.
- Hoshino, H., Koo, T. J., Chu, Y.-C., & Susuki, Y. (2023). 'Model Predictive Control of Smart Districts Participating in Frequency Regulation Market: A Case Study of Using Heating Network Storage'. Retrieved from <http://arxiv.org/abs/2305.07198>
- Hot Water Association. (no date). *Sizing a Hot Water Cylinder*. Retrieved January 9, 2025, from <https://www.hotwater.org.uk/sizing-a-hot-water-cylinder/#:~:text=Obviously%20larger%20houses%20will%20have,45%20litres%20for%20every%20occupant.>
- HWA. (2018). *Design Guide Stored Hot Water Solutions in HNs 2018 Stored DHW in HNs - Design Guide HWA/DG1*. Retrieved from <https://www.hotwater.org.uk/uploads/5B053A7597A5F.pdf>
- Huang, T., Yang, X., & Svendsen, S. (2020). 'Multi-mode control method for the existing domestic hot water storage tanks with district heating supply', *Energy*, 191, 116517. <https://doi.org/10.1016/j.energy.2019.116517>
- Huebner, G. M., McMichael, M., Shipworth, D., Shipworth, M., Durand-Daubin, M., & Summerfield, A. (2013). 'The reality of English living rooms – A comparison of internal temperatures against common model assumptions', *Energy and Buildings*, 66, 688–696. <https://doi.org/10.1016/j.enbuild.2013.07.025>
- Ilha, M. S. de O., Oliveira, L. H. de, & Gonçalves, O. M. (2008). 'Design flow rate simulation of cold water supply in residential buildings by means of open probabilistic model', *W062 - Proceedings of the 34th International Symposium on Water Supply and Drainage for Buildings*, (1), 36–49.
- Ivanko, D., Taxt Walnum, H., Lekang Sørensen, Å., & Nord, N. (2020). 'Analysis of monthly and daily profiles of DHW use in apartment blocks in Norway', *E3S Web of Conferences*, 172, 1–7. <https://doi.org/10.1051/e3sconf/202017212002>
- Jack, L., Patidar, S., & Wickramasinghe, S. A. (2017). 'A proposed new UK framework for the sizing of domestic hot and cold water systems for medium-large scale residential buildings', *CIBW062 Symposium 2017*, 1–11.
- Jebamalai, J. M., Marlein, K., & Laverge, J. (2020). 'Influence of centralized and distributed thermal energy storage on district heating network design', *Energy*, 202, 117689. <https://doi.org/10.1016/j.energy.2020.117689>

- Jonsson, E. (1993). *Bidrag till beräkningen av vattenledningarnas maximibelastning* [Contribution to the calculation of water mains' maximum load], VVS, Nr 5.
- Karlsson, F., & Fahlén, P. (2008). 'Impact of design and thermal inertia on the energy saving potential of capacity controlled heat pump heating systems', *International Journal of Refrigeration*, 31(6), 1094–1103. <https://doi.org/10.1016/j.ijrefrig.2007.12.002>
- Kavvadias, K., Jiménez-Navarro, J. P., & Thomassen, G. (2019). *Decarbonising the EU Heating Sector. EUR 29772 EN, Publications Office of the European Union*. <https://doi.org/10.2760/943257>
- Keçebaş, A., Ali Alkan, M., & Bayhan, M. (2011). 'Thermo-economic analysis of pipe insulation for district heating piping systems', *Applied Thermal Engineering*, 31(17–18), 3929–3937. <https://doi.org/10.1016/j.applthermaleng.2011.07.042>
- Kensby, J., Trüschel, A., & Dalenbäck, J. O. (2017). 'Heat source shifting in buildings supplied by district heating and exhaust air heat pump', *Energy Procedia*, 116, 470–480. <https://doi.org/10.1016/j.egypro.2017.05.094>
- Kõiv, T., & Toode, A. (2005) 'Investigation of the domestic hot water consumption in apartment buildings', *Proceedings of the Estonian Academy of Sciences. Engineering*, 11(3), p. 207. doi:10.3176/eng.2005.3.03
- Kõiv, T., & Toode, A. (2006). 'Trends in domestic hot water consumption', *Proc. Estonian Acad. Sci. Eng.*, 72–80. Retrieved from [http://www.kirj.ee/public/va\\_te/eng-2006-1-6.pdf](http://www.kirj.ee/public/va_te/eng-2006-1-6.pdf)
- Leiria, D., Johra, H., Marszal-Pomianowska, A., Pomianowski, M. Z., & Kvols Heiselberg, P. (2021). 'Using data from smart energy meters to gain knowledge about households connected to the district heating network: A Danish case', *Smart Energy*, 3, 100035. <https://doi.org/10.1016/j.segy.2021.100035>
- Li, Y., Rezgui, Y., & Hanxing, Z. (2016). 'Dynamic Simulation of Heat Losses in a District Heating System: A Case Study in Wales', In *2016 IEEE Smart Energy Grid Engineering (SEGE)*.
- Lowe, R. (March 11, 2024). Personal communication.
- Luc, K. M., Li, R., Xu, L., Nielsen, T. R., & Hensen, J. L. M. (2020). 'Energy flexibility potential of a small district connected to a district heating system', *Energy and Buildings*, 225, 110074. <https://doi.org/10.1016/j.enbuild.2020.110074>
- Lund, H., Østergaard, P. A., Chang, M., Werner, S., Svendsen, S., Sorknæs, P., ... Möller, B. (2018). 'The status of 4th generation district heating: Research and results', *Energy*, 164, 147–159. <https://doi.org/10.1016/j.energy.2018.08.206>
- M-bus (no date). *Physical Layer – M*. Retrieved August 24, 2024, from <https://m-bus.com/documentation-wired/04-physical-layer>

- Ma, Z., Knotzer, A., Billanes, J. D., & Jørgensen, B. N. (2020). 'A literature review of energy flexibility in district heating with a survey of the stakeholders' participation', *Renewable and Sustainable Energy Reviews*, 123(February). <https://doi.org/10.1016/j.rser.2020.109750>
- Marini, D., Buswell, R. A., & Hopfe, C. J. (2019). 'Sizing domestic air-source heat pump systems with thermal storage under varying electrical load shifting strategies', *Applied Energy*, 255(February), 113811. <https://doi.org/10.1016/j.apenergy.2019.113811>
- Marszal-Pomianowska, A., Zhang, C., Pomianowski, M., Heiselberg, P., Gram-Hanssen, K., & Hansen, A. R. (2019). 'Simple methodology to estimate the mean hourly and the daily profiles of domestic hot water demand from hourly total heating readings', *Energy and Buildings*, 184, 53–64. <https://doi.org/10.1016/j.enbuild.2018.11.035>
- Martin-Du Pan, O., Woods, P., & Hanson-Graville, R. (2019). 'Optimising pipe sizing and operating temperatures for district heating networks to minimise operational energy consumption', *Building Services Engineering Research and Technology*, 40(2), 237–255. <https://doi.org/10.1177/0143624418802590>
- McBride, P. (December 16, 2022). Personal communication.
- McKenna, R., Hofmann, L., Merkel, E., Fichtner, W., & Strachan, N. (2016). 'Analysing socioeconomic diversity and scaling effects on residential electricity load profiles in the context of low carbon technology uptake', *Energy Policy*, 97, 13–26. <https://doi.org/10.1016/j.enpol.2016.06.042>
- Met Office. (2022). *Monthly Summary: January 2022*. Retrieved from [https://www.metoffice.gov.uk/binaries/content/assets/metofficegovuk/pdf/weather/learn-about/uk-past-events/summaries/uk\\_monthly\\_climate\\_summary\\_202201a.pdf](https://www.metoffice.gov.uk/binaries/content/assets/metofficegovuk/pdf/weather/learn-about/uk-past-events/summaries/uk_monthly_climate_summary_202201a.pdf)
- Meter Market (no date). *Elvaco CMe3100 M-bus Gateway*. Retrieved August 24, 2024, from <https://www.metermarket.co.uk/product/elvaco-cme3100-m-bus-gateway-up-to-256-meters-on-1-fixed-network>
- Mosbech, H. (1983). 'Optimal Operation of Heat-Storage Units in Systems with Cogeneration of Heat and Electrical Power', *Int. Symp. Appl. Control and Identification*.
- Mut Thermal Systems Solutions. (2023). Product Index. Retrieved from [https://www.mutmeccanica.com/downloads/Catalistino-ING\\_senza\\_prezzi\\_2023\\_REV00\\_singole.pdf](https://www.mutmeccanica.com/downloads/Catalistino-ING_senza_prezzi_2023_REV00_singole.pdf)
- Noughton, T. (2022). Personal Communication.
- Noussan, M., Jarre, M., & Poggio, A. (2017). 'Real operation data analysis on district heating load patterns', *Energy*, 129, 70–78. <https://doi.org/10.1016/j.energy.2017.04.079>
- Oliveira, L. H., Cheng, L. Y., Gonçalves, O. M., & Massolino, P. M. C. (2013). 'Modelling of water demand in building supply systems using fuzzy logic', *Building Services Engineering Research and Technology*, 34(2), 145–163. <https://doi.org/10.1177/0143624411429381>

- Open Data Institute. (2017). Guru Systems improving energy efficiency through open data. The ODI. Retrieved May 31, 2021, from <https://theodi.org/project/case-study-guru-systems-improving-energy-efficiency-through-open-data/>.
- Pakere, I., Purina, D., Blumberga, D., & Bolonina, A. (2016). 'Evaluation of Thermal Energy Storage Capacity by Heat Load Analyses', *Energy Procedia*, 95, 377–384. <https://doi.org/10.1016/j.egypro.2016.09.040>
- Paris Agreement*. (2015). United Nations Framework Convention on Climate Change, Paris, France, Dec. 12, 2015. Retrieved from [https://unfccc.int/sites/default/files/english\\_paris\\_agreement.pdf](https://unfccc.int/sites/default/files/english_paris_agreement.pdf)
- Phenolic foam insulation* (no date) *Phenolic foam insulation - Designing Buildings*. Available at: [https://www.designingbuildings.co.uk/wiki/Phenolic\\_foam\\_insulation](https://www.designingbuildings.co.uk/wiki/Phenolic_foam_insulation)
- Rämä, M., & Wahlroos, M. (2018). 'Introduction of new decentralised renewable heat supply in an existing district heating system', *Energy*, 154, 68–79. <https://doi.org/10.1016/j.energy.2018.03.105>
- Romanchenko, D., Kensby, J., Odenberger, M., & Johnsson, F. (2018). 'Thermal energy storage in district heating: Centralised storage vs. storage in thermal inertia of buildings', *Energy Conversion and Management*, 162(January), 26–38. <https://doi.org/10.1016/j.enconman.2018.01.068>
- Rosato, A., Ciervo, A., Ciampi, G., Scorpio, M., Guarino, F., & Sibilio, S. (2020). 'Energy, environmental and economic dynamic assessment of a solar hybrid heating network operating with a seasonal thermal energy storage serving an Italian small-scale residential district: Influence of solar and back-up technologies', *Thermal Science and Engineering Progress*, January, 100591. <https://doi.org/10.1016/j.tsep.2020.100591>
- Rydberg, J. (1945). *Beräkning av maximala tappnings- effekten for varmvattensberedningsanlaggningar [Calculation of the maximum tapping effect for hot water treatment plants]*.
- Sajjad, I., A. Chicco, G., & Napoli, R. (2014). 'A Statistical Analysis of Sampling Time and Load Variations for Residential Load Aggregations', *2014 IEEE 11th International Multi-Conference on Systems, Signals & Devices (SSD14)*. Retrieved from <https://ieeexplore.ieee.org/stamp/stamp.jsp?tp=&arnumber=6808851>
- Sajjad, M. I. A., Chicco, G., & Napoli, R. (2016). 'Definitions of Demand Flexibility for Aggregate Residential Loads', *IEEE Transactions on Smart Grid*, 7, 1. <https://doi.org/10.1109/TSG.2016.2522961>
- SAV Systems. (2013). *Design and Product Guide: Danfoss FlatStations*. Retrieved from [https://issuu.com/mikeglanfield/docs/sav\\_flatstation\\_design\\_guide\\_-\\_rev](https://issuu.com/mikeglanfield/docs/sav_flatstation_design_guide_-_rev)
- Schuchardt, G. K. (2016). 'Integration of decentralized thermal storages within district heating (DH) networks', *Environmental and Climate Technologies*, 18(1), 5–16. <https://doi.org/10.1515/rtuect-2016-0009>

- Schütz, T., Harb, H., Streblow, R., & Müller, D. (2015). 'Comparison of models for thermal energy storage units and heat pumps in mixed integer linear programming', *ECOS 2015 - 28th International Conference on Efficiency, Cost, Optimization, Simulation and Environmental Impact of Energy Systems*, (July).
- SIKA Systemtechnik. (2023). Turbine flow sensors // VTY10 Technical Datasheet. Retrieved from [https://www.sika.net/fileadmin/products/corporate/datasheet/turbine\\_flow\\_sensors/Datasheet\\_Turbine\\_Flow\\_Sensors\\_VTY10.pdf](https://www.sika.net/fileadmin/products/corporate/datasheet/turbine_flow_sensors/Datasheet_Turbine_Flow_Sensors_VTY10.pdf)
- Skea, J. (2010). 'Valuing diversity in energy supply', *Energy Policy*, 38(7), 3608–3621. <https://doi.org/10.1016/j.enpol.2010.02.038>
- Smith, A. (2016). *On a mission: using data to optimise heat networks*. CIBSE Journal. <https://www.cibsejournal.com/technical/on-a-mission-using-data-to-optimise-heat-networks/>
- Sonceboz. (no date). Liner Actuators 7217. Retrieved from <https://ivb-antriebstechnik.com/wp-content/uploads/7217-4.0.pdf>
- Stevenson Plumbing. (no date). *British Standard Pipe Thread (BSPT)*. Retrieved January 17, 2023, from <https://www.stevensonplumbing.co.uk/bspt.html>
- Stirling, A. (2009). Multicriteria diversity analysis. *Energy Policy*, 38(4), 1622–1634. <https://doi.org/10.1016/j.enpol.2009.02.023>
- Summerfield, A. J., Oreszczyn, T., Hamilton, I. G., Shipworth, D., Huebner, G. M., Lowe, R. J., & Ruyssevelt, P. (2015). 'Empirical variation in 24-h profiles of delivered power for a sample of UK dwellings: Implications for evaluating energy savings', *Energy and Buildings*, 88, 193–202. <https://doi.org/10.1016/j.enbuild.2014.11.075>
- Svensk Fjärrvärme (2007) *Kulvertkostnads katalog [District Heating Pipe Cost Catalogue]*, Rapport. [https://www.energiforetagen.se/globalassets/energiforetagen/det-erbjuder-vi/publikationer/kulvertkostnads katalog\\_2007-1.pdf](https://www.energiforetagen.se/globalassets/energiforetagen/det-erbjuder-vi/publikationer/kulvertkostnads katalog_2007-1.pdf).
- Tasseron. (no date). Temperature Sensor - TSC Series - Technical Datasheet. Accessed January 9, 2024. Retrieved from [https://static1.squarespace.com/static/575837b259827e26b5694200/t/57fcf3f1ff7c50b4250f2d31/1476195314513/Tasseron Clip-on temperature sensor TSC v3.2.pdf](https://static1.squarespace.com/static/575837b259827e26b5694200/t/57fcf3f1ff7c50b4250f2d31/1476195314513/Tasseron+Clip-on+temperature+sensor+TSC+v3.2.pdf)
- The Engineering ToolBox (2005) *Metals, metallic elements and alloys - thermal conductivities*. [https://www.engineeringtoolbox.com/thermal-conductivity-metals-d\\_858.html](https://www.engineeringtoolbox.com/thermal-conductivity-metals-d_858.html).
- The Engineering ToolBox (2018) *Air – Prandtl number*. [https://www.engineeringtoolbox.com/air-prandtl-number-viscosity-heat-capacity-thermal-conductivity-d\\_2009.html#:~:text=The%20Prandtl%20Number%20%2D%20Pr%20%2D%20is,free%20and%20forced%20convection%20calculations.](https://www.engineeringtoolbox.com/air-prandtl-number-viscosity-heat-capacity-thermal-conductivity-d_2009.html#:~:text=The%20Prandtl%20Number%20%2D%20Pr%20%2D%20is,free%20and%20forced%20convection%20calculations.)

- Tindall, J., & Pendle, J. (2018). 'A comparison of UK domestic water services sizing methods with each other and with empirical data', *JESS*, 38, 25–35.
- Torriti, J. (2014). 'A review of time use models of residential electricity demand', *Renewable and Sustainable Energy Reviews*, 37, 265–272.  
<https://doi.org/10.1016/j.rser.2014.05.034>
- Turski, M., & Sekret, R. (2018). 'Buildings and a district heating network as thermal energy storages in the district heating system', *Energy and Buildings*, 179, 49–56.  
<https://doi.org/10.1016/j.enbuild.2018.09.015>
- Vámos, V., & Horváth, M. (2022). 'Residential Domestic Hot Water Consumption Analysis for Multifamily Buildings Supplied By District Heating', *Thermal Science*, 26(2), 1267–1276. <https://doi.org/10.2298/TSCI200505190V>
- Vámos, V., & Horváth, M. (2023). 'Evaluation of district heating patterns for Hungarian residential buildings: Case study of Budapest'.  
<https://doi.org/10.1016/j.enbuild.2023.112833>
- van den Brom, P., Hansen, A. R., Gram-Hanssen, K., Meijer, A., & Visscher, H. (2019). 'Variances in residential heating consumption – Importance of building characteristics and occupants analysed by movers and stayers', *Applied Energy*, 250(December 2018), 713–728. <https://doi.org/10.1016/j.apenergy.2019.05.078>
- Vandermeulen, A., van der Heijde, B., & Helsen, L. (2018). 'Controlling district heating and cooling networks to unlock flexibility: A review', *Energy*, 151, 103–115.  
<https://doi.org/10.1016/j.energy.2018.03.034>
- Wang, R., Cong, M., Wei, C., Zhou, Z., Ni, L., Liu, J., & Jian, C. (2021). 'The effect of unheated users on residential building in heating performance', *Energy and Buildings*, 253, 111519. <https://doi.org/https://doi.org/10.1016/j.enbuild.2021.111519>
- Wang, Z., Crawley, J., Li, F. G. N., & Lowe, R. (2020). 'Sizing of district heating systems based on smart meter data: Quantifying the aggregated domestic energy demand and demand diversity in the UK', *Energy*, 193, 116780.  
<https://doi.org/10.1016/j.energy.2019.116780>
- Weissmann, C., Hong, T., & Graubner, C. A. (2017). 'Analysis of heating load diversity in German residential districts and implications for the application in district heating systems', *Energy and Buildings*, 139, 302–313.  
<https://doi.org/10.1016/j.enbuild.2016.12.096>
- Werner, S. (2013). *District heating and cooling*. Reference Module in Earth Systems and Environmental Sciences, Elsevier. <https://doi.org/10.1016/B978-0-12-409548-9.01094-0>
- Werner, S. (2017). 'International review of district heating and cooling', *Energy*, 137, 617–631. <https://doi.org/10.1016/j.energy.2017.04.045>
- Westermann, P., Deb, C., Schlueter, A., & Evins, R. (2020). 'Unsupervised learning of energy signatures to identify the heating system and building type using smart meter

data', *Applied Energy*, 264, 114715.  
<https://doi.org/https://doi.org/10.1016/j.apenergy.2020.114715>

Winter, W., Haslauer, T., & Obernberger, I. (2001). 'Untersuchungen der Gleichzeitigkeit in kleinen und mittleren Nahwärmenetzen [Investigations of simultaneity in small and medium-sized local heating networks]', *EuroHeat&Power*, 1–17.

Wollerstrand, J. (1997). *District Heating Substations Performance, Operation and Design PhD Thesis*. Lund Technical College.

Yan, D., O'Brien, W., Hong, T., Feng, X., Burak Gunay, H., Tahmasebi, F., & Mahdavi, A. (2015). 'Occupant behavior modeling for building performance simulation: Current state and future challenges', *Energy and Buildings*, 107(6), 264–278.  
<https://doi.org/10.1016/j.enbuild.2015.08.032>

Yao, R., & Steemers, K. (2005). 'A method of formulating energy load profile for domestic buildings in the UK', *Energy and Buildings*, 37(6), 663–671.  
<https://doi.org/10.1016/j.enbuild.2004.09.007>

## 11 Appendix A

### 11.1 Internal Flow Rate Estimates

The Heatweb Ltd. server produces internal estimates of the flow rates of the DHW and SH circuits on the primary side. To estimate these flow rates, the  $\Delta P$  in the circuit, which is estimated during stable tap operation, is required. A stable period occurs when the measured output temperature of a running tap is within  $1^\circ\text{C}$  of the target temperature. Values for  $\Delta P$  during a stable tap operation are then used in the proceeding period of non-stable tap operation to determine flow rates at all times.

This process of determining the internal flow rate estimates in the DHW and SH circuits are described in three main steps below.

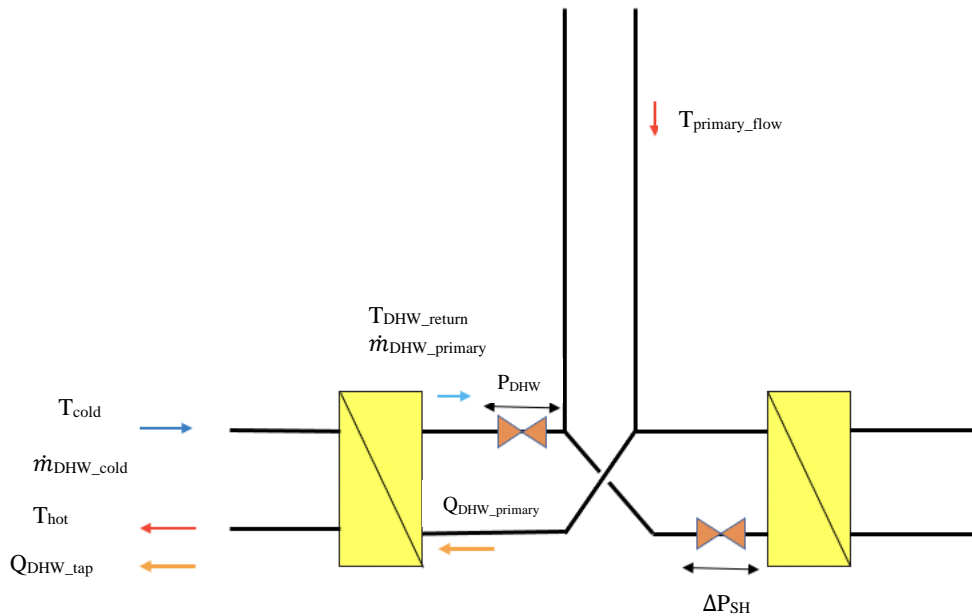


Figure 11.1: Key parameters used in determining the DHW flow rate

#### 1. Determining the primary side DHW flow rate at stable operation:

Domestic side DHW power,  $Q_{\text{DHW\_tap}}$ , is determined using an estimate of the inlet temperature,  $T_{\text{cold}}$ , (estimated by assuming that the measured primary return,  $T_{\text{DHW\_return}}$ , is around  $3\text{--}5^\circ\text{C}$  above the cold inlet temperature), the outlet temperature ( $T_{\text{hot}}$ , measured directly), and the measured domestic side flow rates,  $\dot{m}_{\text{DHW\_cold}}$ .  $T_{\text{cold}}$  can be assumed to be  $3\text{--}5^\circ\text{C}$  below  $T_{\text{DHW\_return}}$  only during stable tap operation.

$$Q_{\text{DHW\_tap}} = \dot{m}_{\text{DHW\_cold}} (T_{\text{hot}} - T_{\text{cold}})c \quad (11-1)$$

Equating the domestic side DHW power to the primary side DHW power,  $Q_{\text{DHW\_primary}}$ , the measured primary flow,  $T_{\text{primary\_flow}}$ , and primary return temperatures,  $T_{\text{DHW\_return}}$ , can be used to estimate the flow rate on the primary side of the DHW heat exchanger,  $\dot{m}_{\text{DHW\_primary}}$ .

$$Q_{DHW\_tap} = Q_{DHW\_primary} \quad (11-2)$$

$$Q_{DHW\_primary} = \dot{m}_{DHW\_primary} (T_{primary\_flow} - T_{DHW\_return})c \quad (11-3)$$

$$\dot{m}_{DHW\_primary} = \dot{m}_{DHW\_cold} \frac{T_{hot} - T_{cold}}{T_{primary\_flow} - T_{DHW\_return}} \quad (11-4)$$

The mass flow on the primary side of the DHW heat exchanger,  $\dot{m}_{DHW\_primary}$ , during stable tap operation is now obtained. This flow rate is used with the measured valve position and the valve's pressure loss curve to estimate the differential pressure across the DHW circuit,  $\Delta P_{DHW}$ , during stable tap operation.

The stable  $\Delta P_{DHW}$  is then used to determine the primary flow rates during the proceeding non-stable operation in the following way.

## 2. Determining primary side DHW flow rates during non-stable operation using $\Delta P_{DHW}$ :

The  $\Delta P_{DHW}$  from the last stable operation period is assumed to hold for the proceeding non-stable period and is used with the measured valve position (of stepper motor on DHW circuit) and the valve's pressure loss curve to determine the flow rates,  $\dot{m}_{DHW\_primary\_non-stable}$  during a non-stable operation period.

## 3. Determining the SH circuit flow $\Delta P_{DHW}$ and flow rates:

The logic that estimates SH circuit flow rates (denoted by the tag 'fHCH') takes the DP to be equal to the DP during the last stable DHW tap operation.

## 11.2 Heat Store Model Validation

The thermal heat stores were validated by adjusting the parameters to either 0 or infinite in order to check the output against an expected output. The results were the same for both stratified and mixed models and are given in the table below.

Table 11.1: Thermal store model validation results

Parameter Adjustment	Expected Results	Real Result
Ambient room temperature( $^{\circ}\text{C}$ ) set to infinite	Should result in no thermal loss from store because of the temperature of the environment being	0.0 kW of thermal loss from store
Specific heat capacity of water ( $\text{kJ/kg}^{\circ}\text{C}$ ) set to 0	Should result in no thermal storage being enabled	No thermal storage resulted in the store
Insulation thickness adjusted to infinity	No thermal loss from store	0.0 kW of thermal loss from store
Setting maximum store temperature ( $^{\circ}\text{C}$ ) to infinity (mixed model).	Temperature of the store exceed $50^{\circ}\text{C}$ (previous maximum) and continue increasing in temperature until charging window closes.	Store temperatures exceed previous maximum set temperature.

## 11.3 Convective Heat Transfer Coefficient of the Insulation Layer

The table below gives the key parameters used to determine the convective heat transfer coefficient of the insulation layer.

Table 11.2: Determining parameters for the convective heat transfer coefficient used in determining thermal loss from the network

Parameter	Value	Notes
Inner diameter, $r_0$	22mm	Mean inner diameter of available pipe sizes
Outside diameter of pipe, $r_1$	24.1mm	Assuming pipe thickness of 2.4mm, an mean pipe thickness.
Fluid temperature, $T_{fluid}$	$46^{\circ}\text{C}$	Mean temperature of flow and return temperature
Ambient temperature, $T_{ext}$	$18^{\circ}\text{C}$	Assumed constant
Wind speed	0.0m/s	Negligible wind speeds in internal space
Surface emissivity, $\epsilon$	0.03	Assumption for low emissivity foil on insulation material (Ballico et al, 2013)
Insulation thickness	20mm	Mean insulation thicknesses

Outside diameter of insulation, $r_2$	64.1mm	Adding insulation thickness to outside diameter of pipe
Surface temperature, $t_{surface}$	26.5°C	Estimated by assuming surface temperature equal to ambient temperature at first iteration and determining resultant effect of heat flow through pipe and insulation on surface temperature, until differences in iteration results become negligible.
Thermal conductivity of air, $k_{air}$	0.026W/mK	(Bergman et al, 2002)
Prandtl number, Pr	0.708	The Pr number is the ratio of momentum diffusivity to thermal diffusivity (Bergman et al, 2002). Pr is a function of air temperature and pressure, for 18°C and 1 bar of pressure (The Engineering Toolbox, 2018)
Reynold's number, Re	0.0	The Re number is the ratio of inertial forces to viscous forces occurring in a fluid and is used to determine whether flow is laminar or turbulent. Here, Re goes to 0 because of negligible wind speeds (Bergman et al, 2002).

#### 11.4 Validating the Network Thermal Loss Model

To validate the network thermal loss model, the result of adjusting a fixed parameter is checked against the expected result.

Table 11.3: Network thermal model validation results

Parameter Adjustment	Expected Results	Real Result
Pipe and insulation thermal conductivity, $k_{pipe}$ and $k_{ins}$ , respectively adjusted to 0 kW/m <sup>2</sup> K	No thermal loss from pipes.	0.0 kWh/ dwelling daily thermal losses.
Pipe and insulation thermal conductivity, $k_{pipe}$ and $k_{ins}$ , respectively adjusted to infinity kW/m <sup>2</sup> K	Maximum thermal loss from network	Infinite daily thermal loss.
Pipe thickness adjusted to infinity	No thermal loss from pipes	0.0 kWh/ dwelling daily thermal losses.
Insulation thickness adjusted to infinity	No thermal loss from pipes	0.0 kWh/ dwelling daily thermal losses.
Flow and return temperatures adjusted to equal the external temperature	No thermal loss from pipes	0.0 kWh/ dwelling daily thermal losses.

## 12 Appendix B

### 12.1 Total Demand Distributions at Aggregate Levels

The results in this section give the demand distributions for the total demand at varying levels of aggregation over dwellings greater than  $k=1$  and over time.

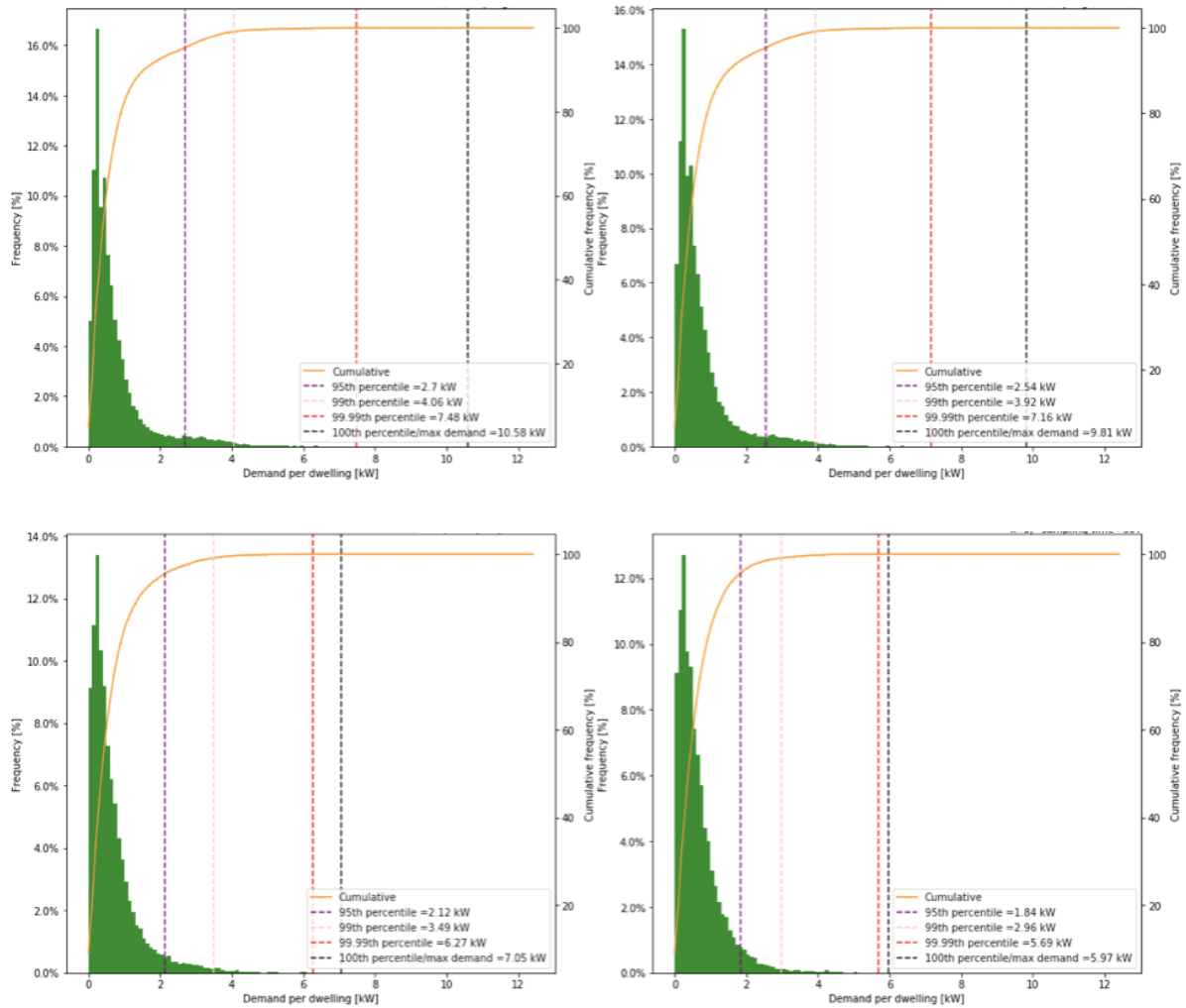


Table 12.1: Demand distribution for the total demand showing the impact that sampling times has on demand at an aggregation level of  $k=5$  dwellings. Top left: 5-minute; top-right: 10-minute; bottom-left: 30-minute; bottom-right: 1-hour.

Table 12.2: Summary of the demand distribution percentiles for the total demand at an aggregation level of  $k=5$  dwellings expressed as demand per dwelling (kW)

Sampling time	95 <sup>th</sup>	99 <sup>th</sup>	99.99 <sup>th</sup>	100 <sup>th</sup>
<b>5 minutes</b>	2.7	4.06	7.48	10.58
<b>10 minutes</b>	2.54	3.92	7.16	9.81
<b>30 minutes</b>	2.12	3.49	6.27	7.05
<b>1 hour</b>	1.84	2.96	5.69	5.97

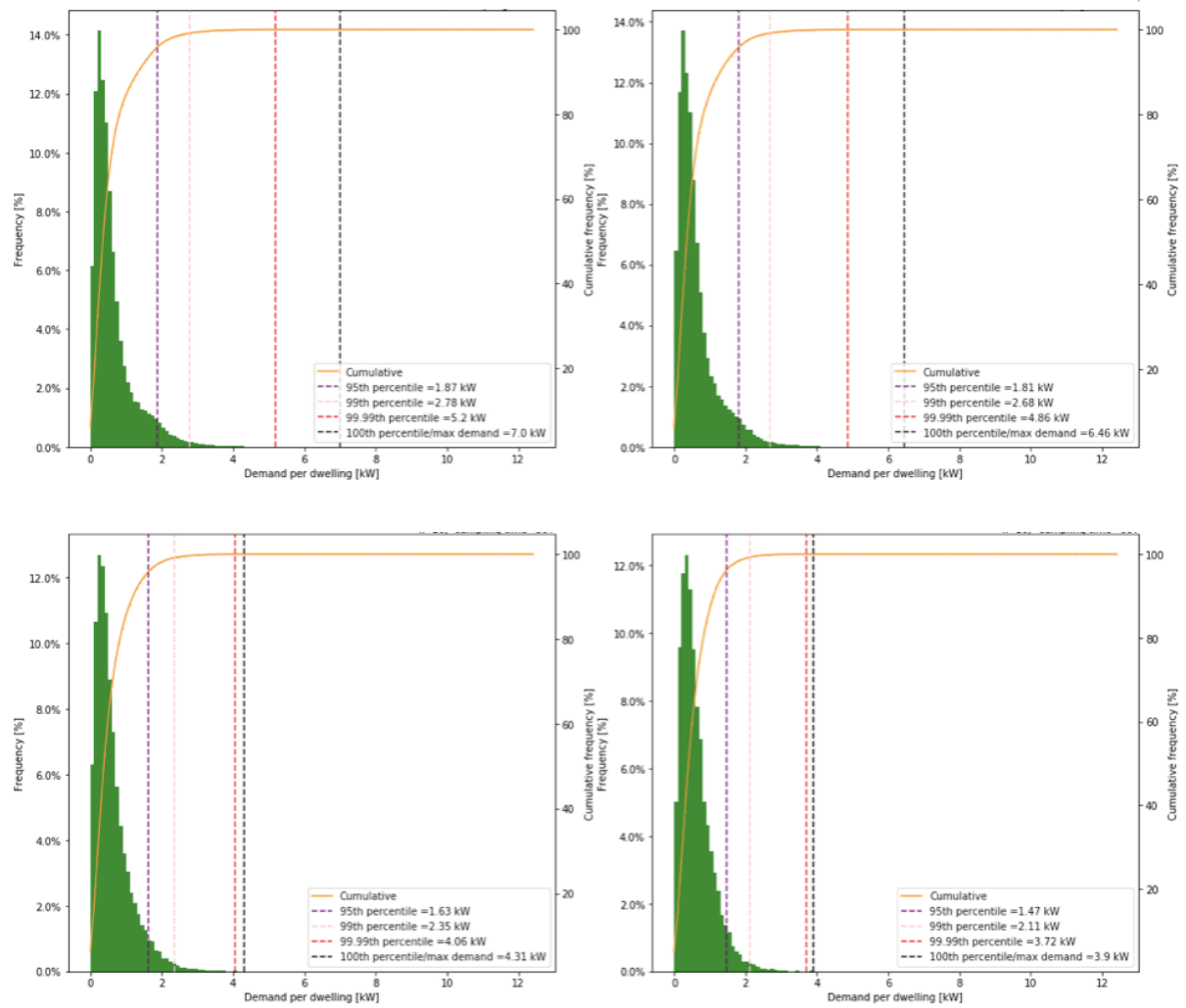


Figure 12.1: Demand distribution for the total demand showing the impact that sampling times has on demand at an aggregation level of  $k=10$  dwellings. Top left: 5-minutes; top-right: 10-minutes; bottom-left: 30 minutes; bottom-right: 1 hour.

Table 12.3: Summary of the demand distribution percentiles for the total demand at an aggregation level of  $k=10$  dwellings expressed as demand per dwelling (kW)

Sampling time	95 <sup>th</sup>	99 <sup>th</sup>	99.99 <sup>th</sup>	100 <sup>th</sup>
<b>5 minutes</b>	1.87	2.78	5.2	7.0
<b>10 minutes</b>	1.81	2.68	4.86	6.46
<b>30 minutes</b>	1.63	2.35	4.06	4.31
<b>1 hour</b>	1.47	2.11	3.72	3.9

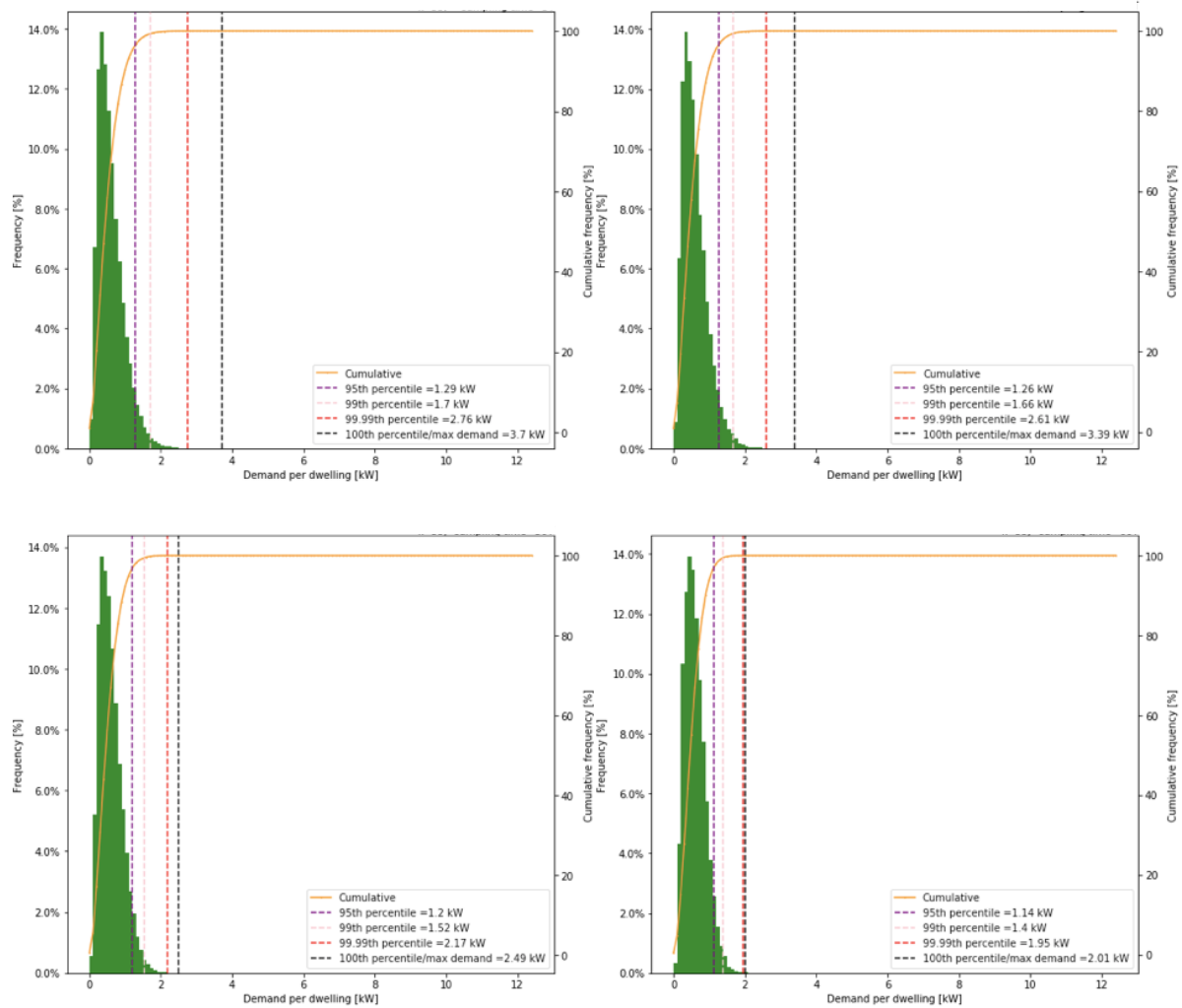


Figure 12.2: Demand distribution for the total demand showing the impact that sampling times has on demand at an aggregation level of  $k=35$  dwellings. Top left: 5-minutes; top-right: 10-minutes; bottom-left: 30 minutes; bottom-right: 1 hour.

Table 12.4: Summary of the demand distribution percentiles for the total demand at an aggregation level of  $k=35$  dwellings expressed as demand per dwelling (kW)

Sampling time	95 <sup>th</sup>	99 <sup>th</sup>	99.99 <sup>th</sup>	100 <sup>th</sup>
5 minutes	1.29	1.7	2.76	3.7
10 minutes	1.26	1.66	2.61	3.39
30 minutes	1.2	1.52	2.17	2.49
1 hour	1.14	1.4	1.95	2.01

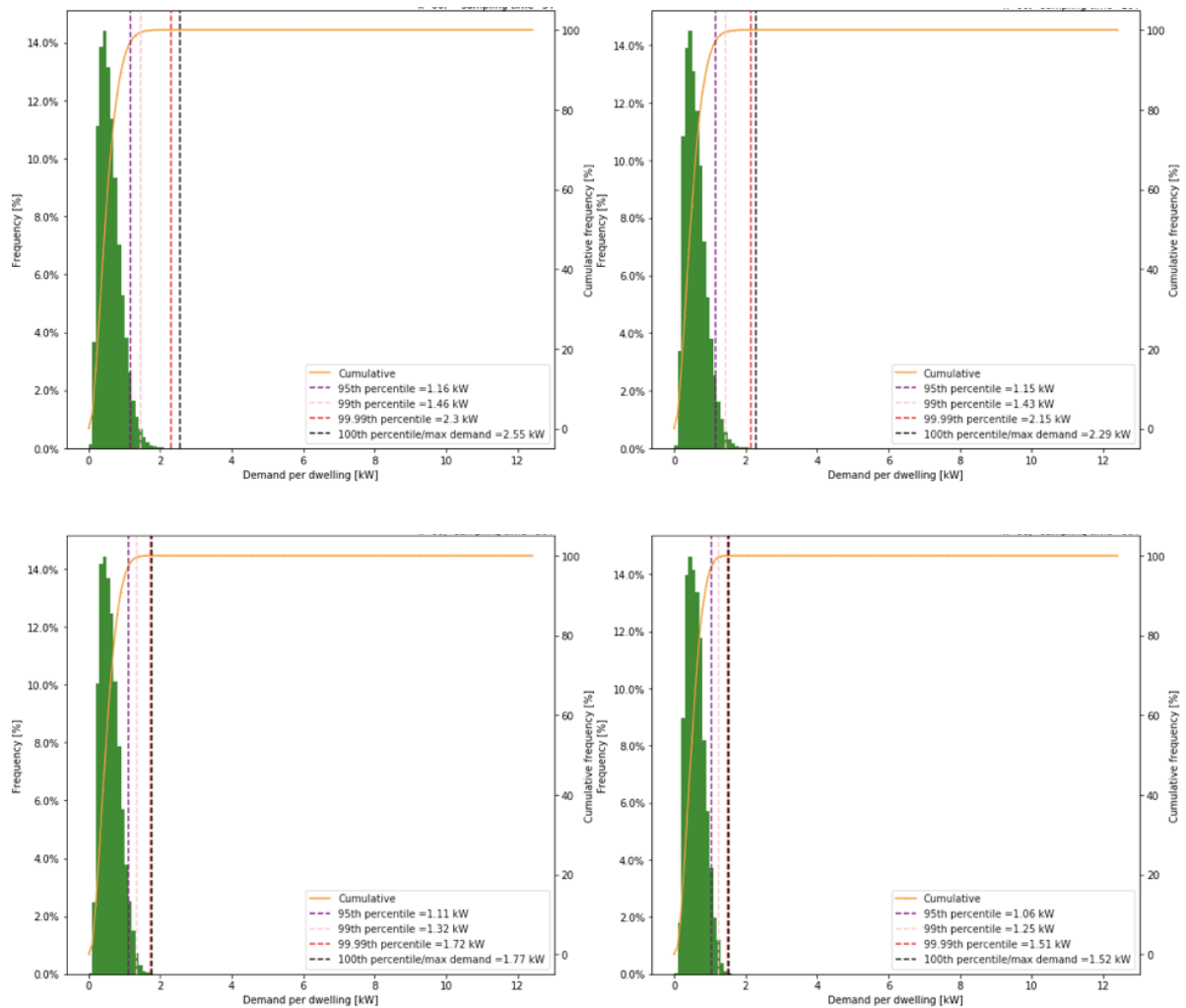


Figure 12.3: Demand distribution for the total demand showing the impact that sampling times has on demand at an aggregation level of  $k=60$  dwellings. Top left: 5-minutes; top-right: 10-minutes; bottom-left: 30 minutes; bottom-right: 1 hour.

Table 12.5: Summary of the demand distribution percentiles for the total demand at an aggregation level of  $k=60$  dwellings expressed as demand per dwelling (kW)

Sampling time	95 <sup>th</sup>	99 <sup>th</sup>	99.99 <sup>th</sup>	100 <sup>th</sup>
<b>5 minutes</b>	1.16	1.46	2.3	2.55
<b>10 minutes</b>	1.15	1.43	2.15	2.29
<b>30 minutes</b>	1.11	1.32	1.72	1.77
<b>1 hour</b>	1.06	1.25	1.51	1.52

## 12.2 DHW Demand Distributions at Aggregate Levels

This section gives the demand distributions for DHW demand across varying levels of aggregation over dwellings greater than  $k=1$  and over time.

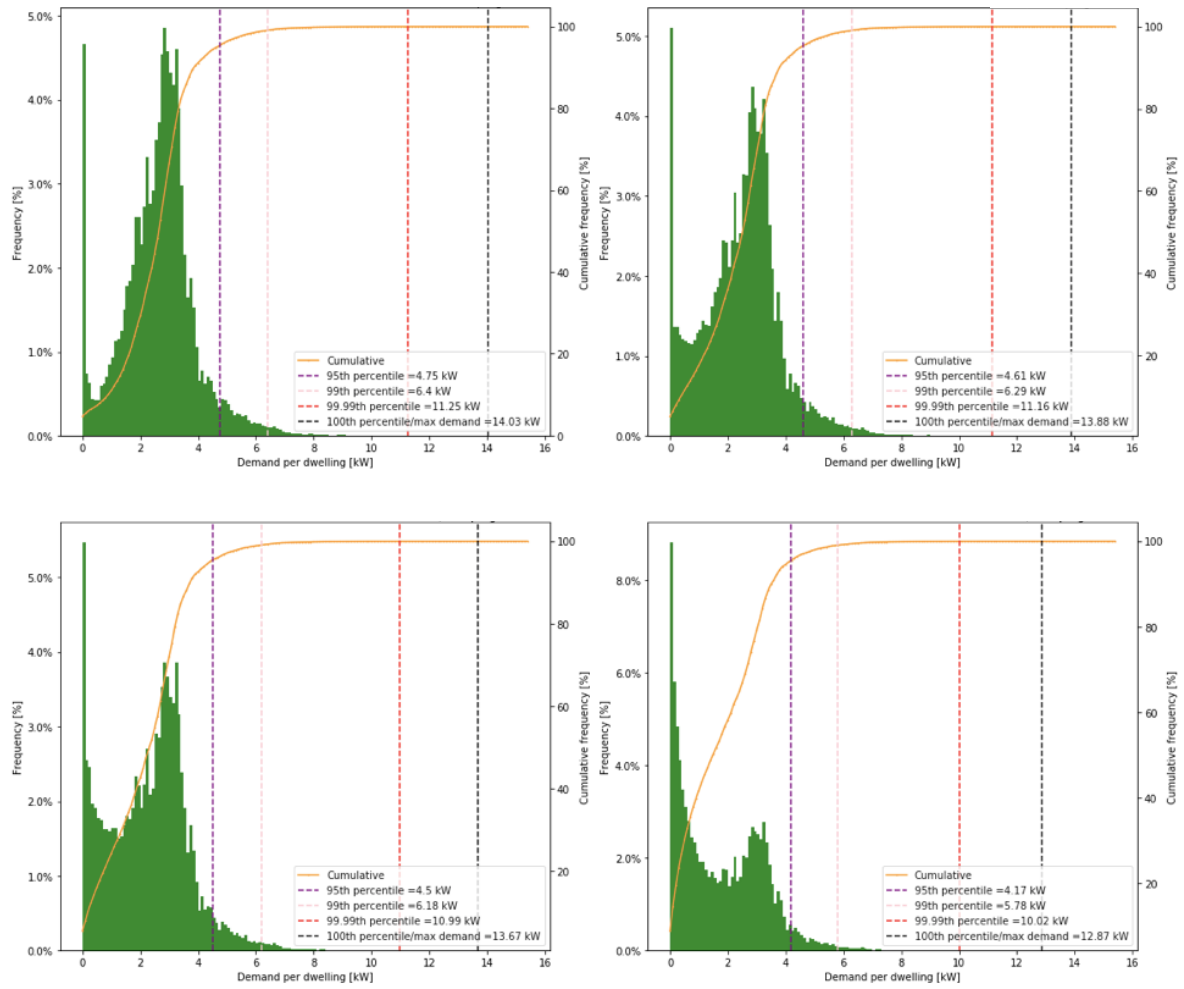


Figure 12.4: Demand distribution for the DHW demand showing the impact of increasing sampling times at an aggregation level of  $k = 5$  dwellings. Top-left: 1-second; top-right: 5-second; bottom-left: 10-second; bottom-right: 30-second.

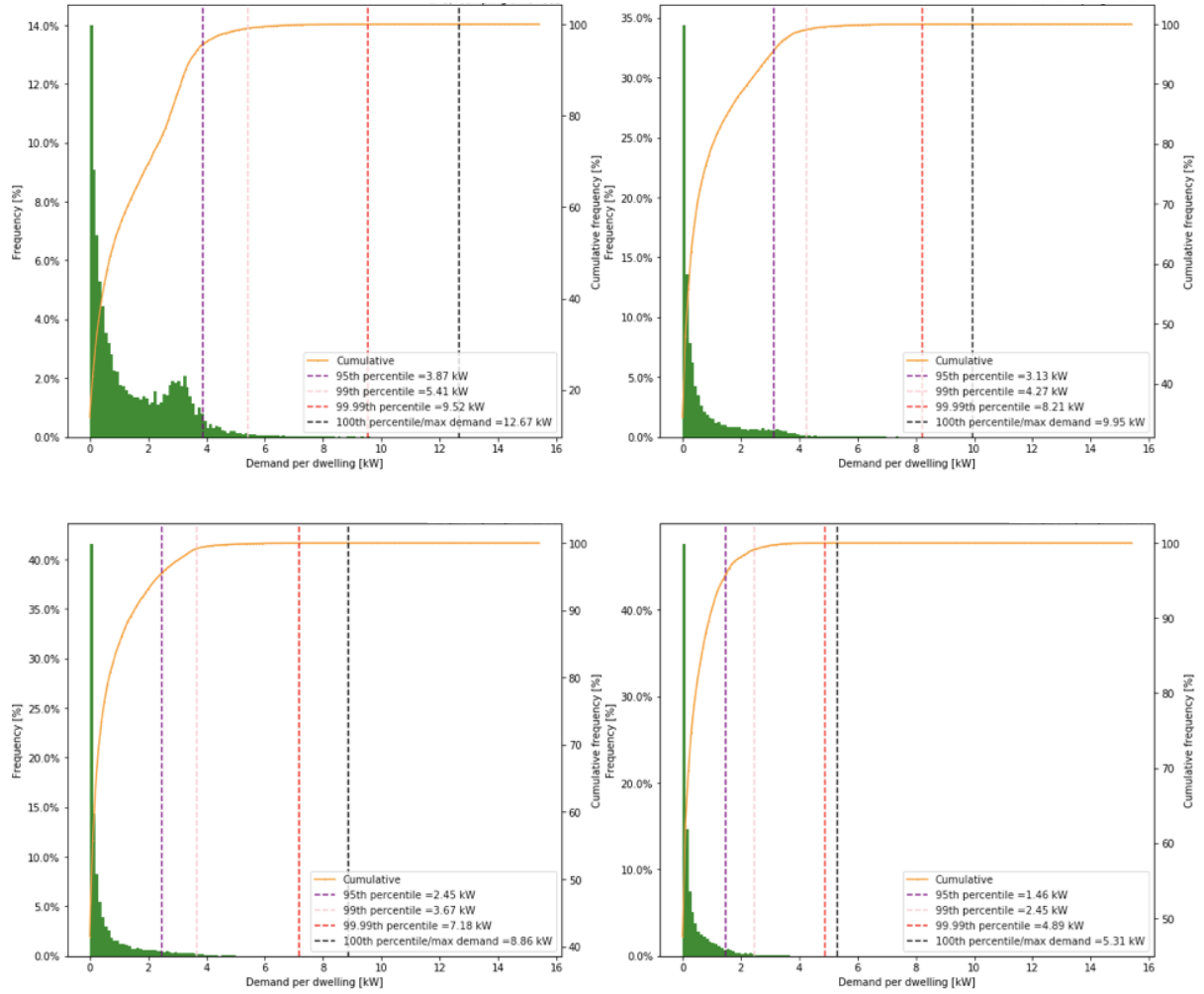


Figure 12.5: Demand distribution for the DHW demand showing the impact of increasing sampling times at an aggregation level of  $k = 5$  dwellings. Top-left: 60-second; top-right: 5-minute; bottom-left: 10-minute; bottom-right: 30-minute.

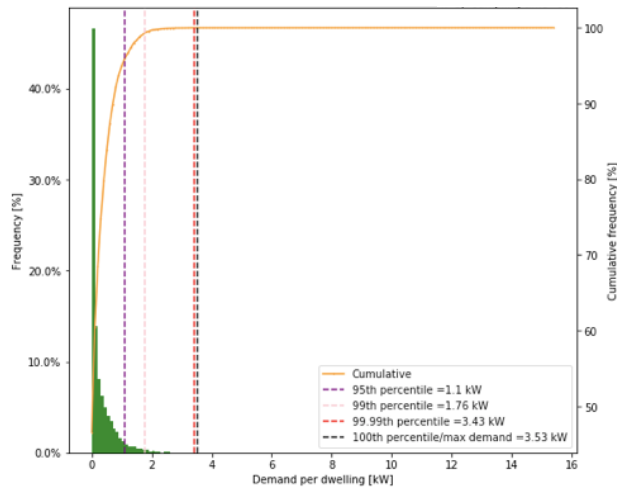


Figure 12.6: Demand distribution for the DHW demand at an aggregation level of  $k = 5$  dwellings and a sampling time of 1 hour.

Table 12.6: Summary of the demand distribution percentiles for DHW demand at an aggregation level of  $k=5$  dwellings expressed as demand per dwelling (kW)

Sampling time	95th	99th	99.99th	100 <sup>th</sup>
<b>1 second</b>	4.75	6.4	11.25	14.03
<b>5 seconds</b>	4.61	6.29	11.16	13.88
<b>10 seconds</b>	4.5	6.18	10.99	13.67
<b>30 seconds</b>	4.17	5.78	10.02	12.87
<b>60 seconds</b>	3.87	5.41	9.52	12.67
<b>5 minutes</b>	3.13	4.27	8.21	9.95
<b>10 minutes</b>	2.45	3.67	7.18	8.86
<b>30 minutes</b>	1.46	2.45	4.89	5.31
<b>1 hour</b>	1.1	1.76	3.43	3.53

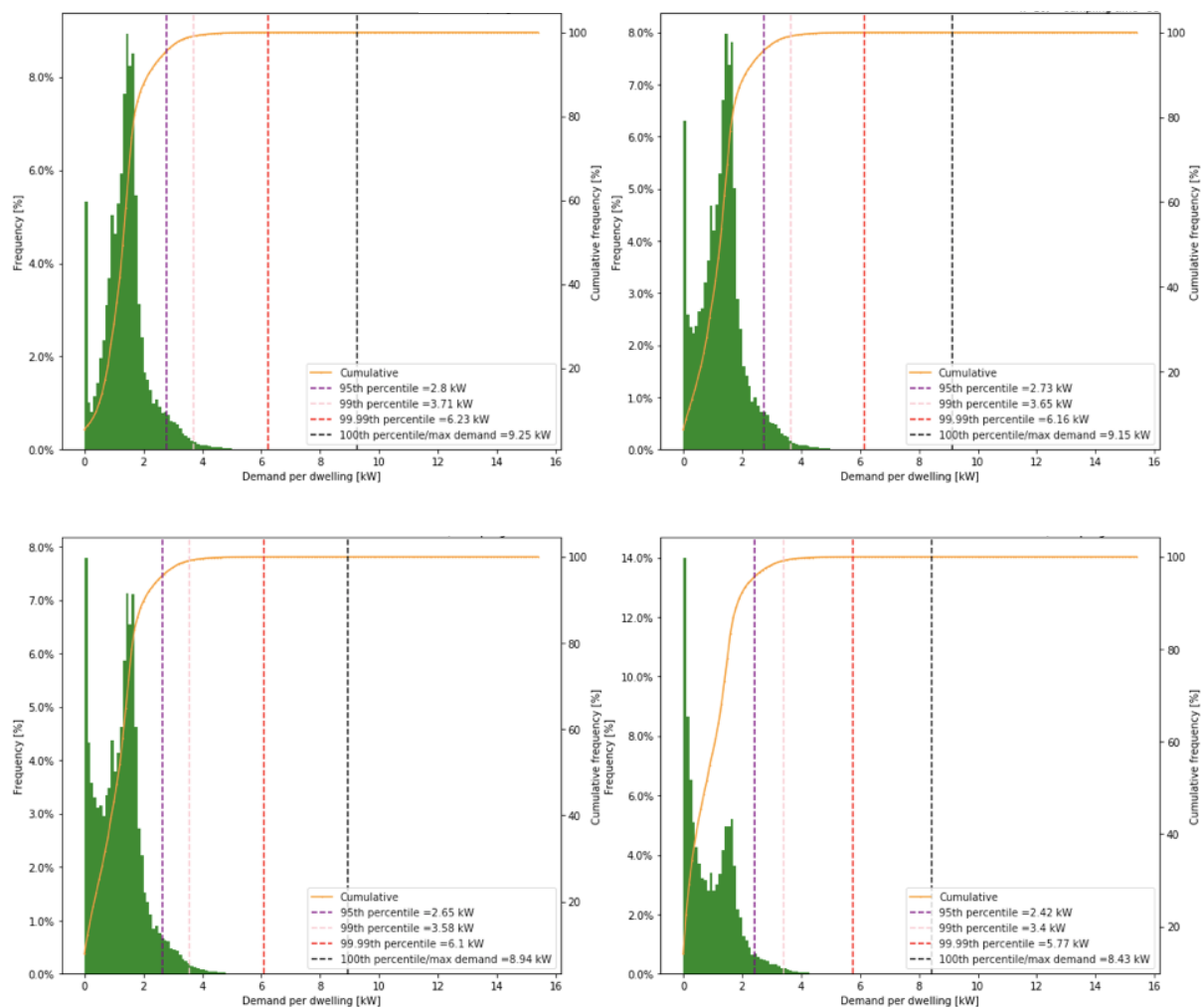


Figure 12.7: Demand distribution for the DHW demand showing the impact of increasing sampling times at an aggregation level of  $k = 10$  dwellings. Top-left: 1-second; top-right: 5-second; bottom-left: 10-second; bottom-right: 30-second.

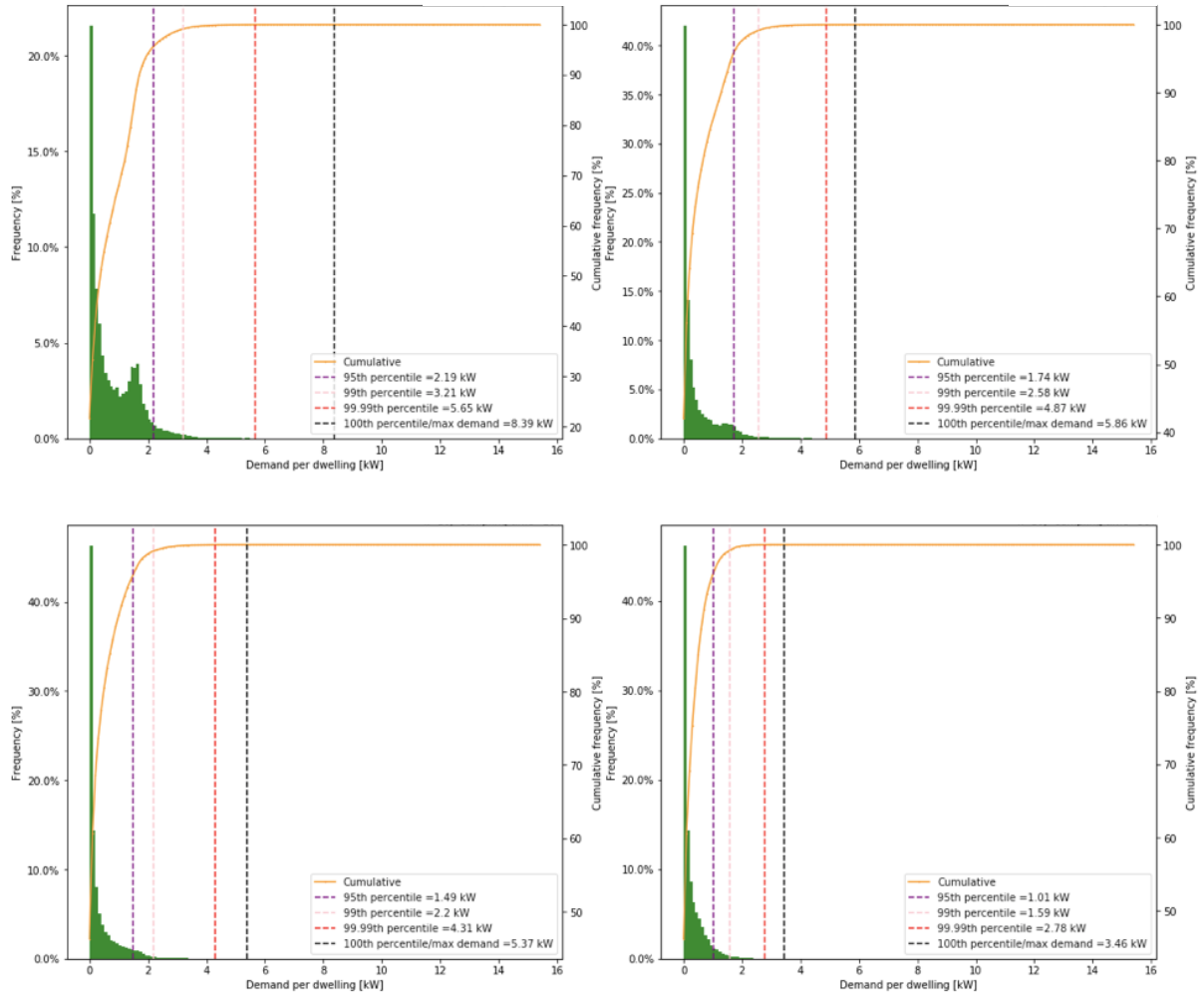


Figure 12.8: Demand distribution for the DHW demand showing the impact of increasing sampling times at an aggregation level of  $k = 10$  dwellings. Top-left: 60-second; top-right: 5-minute; bottom-left: 10-minute; bottom-right: 30-minute.

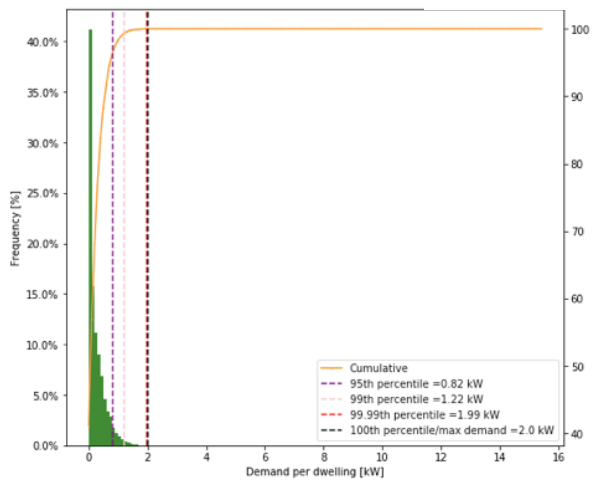


Figure 12.9: Demand distribution for the DHW demand at an aggregation level of  $k = 10$  dwellings and a sampling time of 1 hour.

Table 12.7: Summary of the demand distribution percentiles for DHW demand at an aggregation level of  $k=10$  dwellings expressed as demand per dwelling (kW)

Sampling time	95th	99th	99.99th	100 <sup>th</sup>
1 second	2.8	3.71	6.23	9.25
5 seconds	2.73	3.65	6.16	9.15
10 seconds	2.65	3.58	6.1	8.94
30 seconds	2.42	3.4	5.77	8.43
60 seconds	2.19	3.21	5.65	8.39
5 minutes	1.74	2.58	4.87	5.86
10 minutes	1.49	2.2	4.31	5.37
30 minutes	1.01	1.59	2.78	3.46
1 hour	0.82	1.22	1.99	2.0

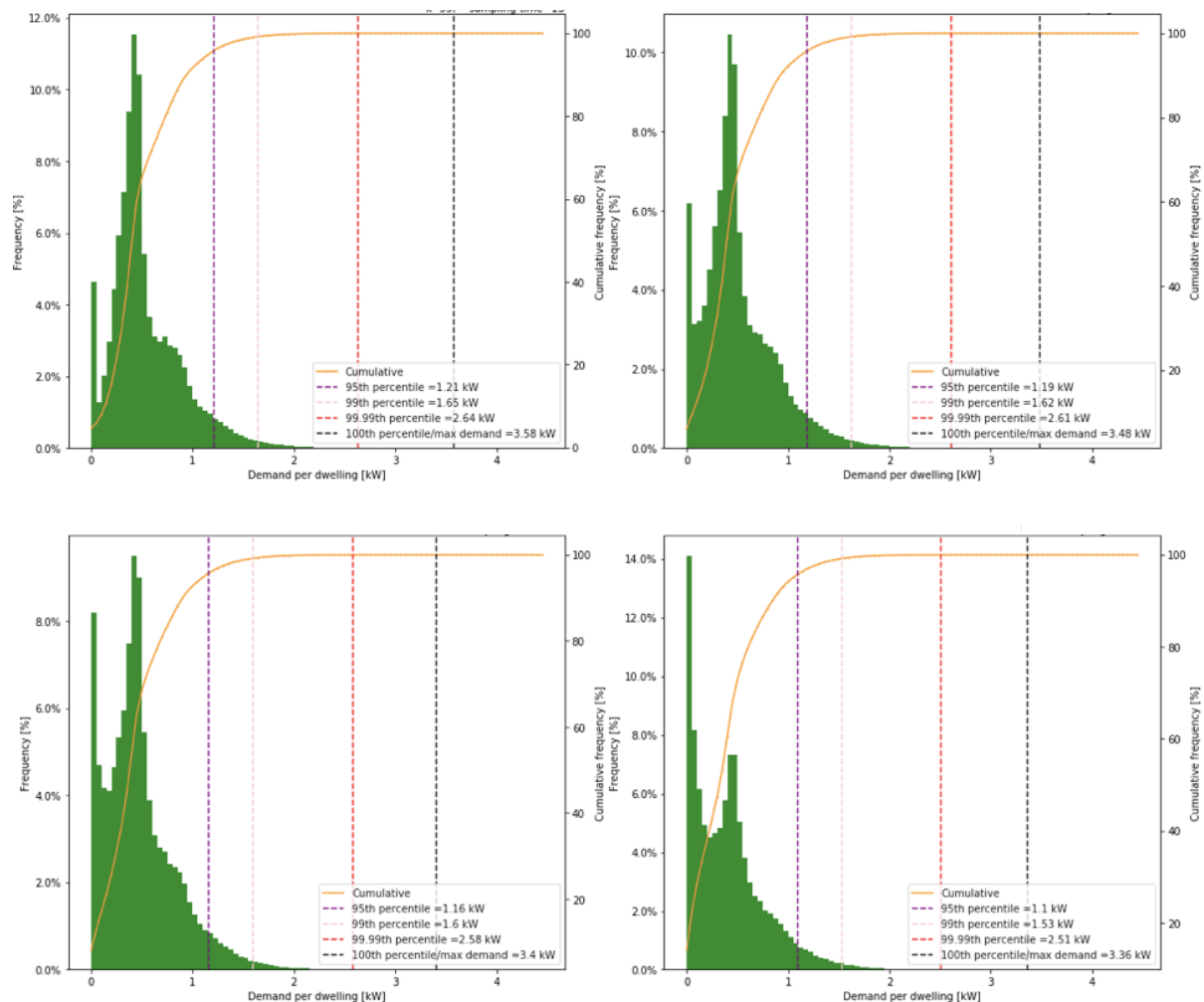


Figure 12.10: Demand distribution for the DHW demand showing the impact of increasing sampling times at an aggregation level of  $k=35$  dwellings. Top-left: 1-second; top-right: 5-second; bottom-left: 10-second; bottom-right: 30-second.

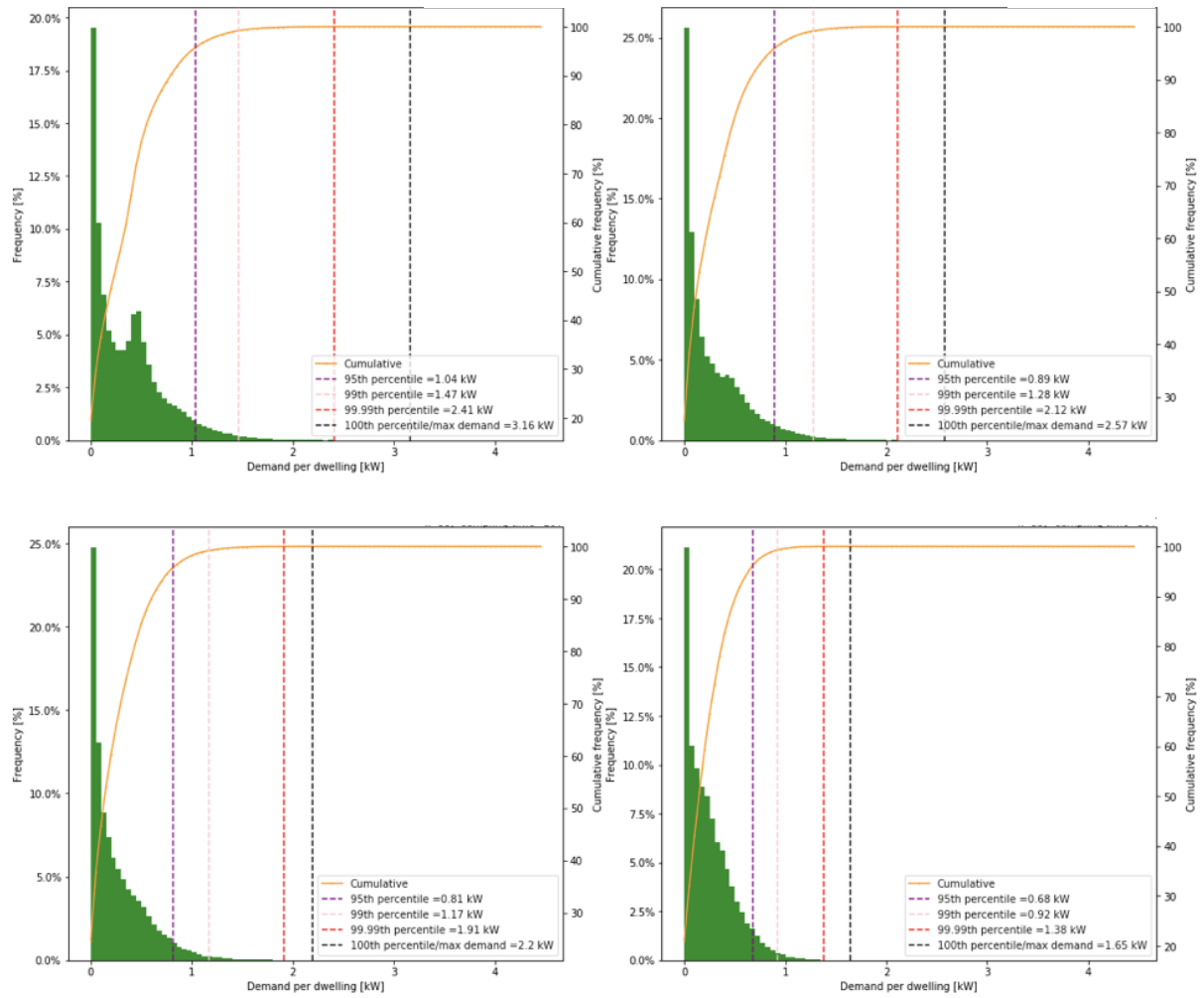


Figure 12.11: Demand distribution for the DHW demand showing the impact of increasing sampling times at an aggregation level of  $k = 35$  dwellings. Top-left: 60-second; top-right: 5-minute; bottom-left: 10-minute; bottom-right: 30-minute.

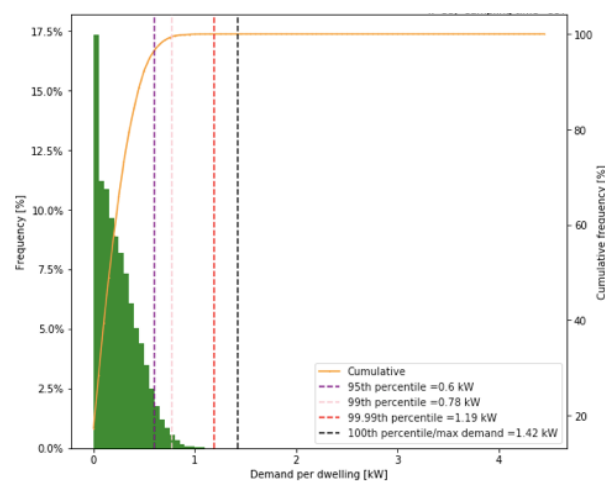


Figure 12.12: Demand distribution for the DHW demand at an aggregation level of  $k = 35$  dwellings and a sampling time of 1 hour.

Table 12.8: Summary of the demand distribution percentiles for DHW demand at an aggregation level of  $k=35$  dwellings expressed as demand per dwelling (kW)

Sampling time	95th	99th	99.99th	100 <sup>th</sup>
1 second	1.21	1.65	2.64	3.58
5 seconds	1.19	1.62	2.61	3.48
10 seconds	1.16	1.6	2.58	3.4
30 seconds	1.1	1.53	2.51	3.36
60 seconds	1.04	1.47	2.41	3.16
5 minutes	0.89	1.28	2.12	2.57
10 minutes	0.81	1.17	1.91	2.2
30 minutes	0.68	0.92	1.38	1.65
1 hour	0.6	0.78	1.19	1.42

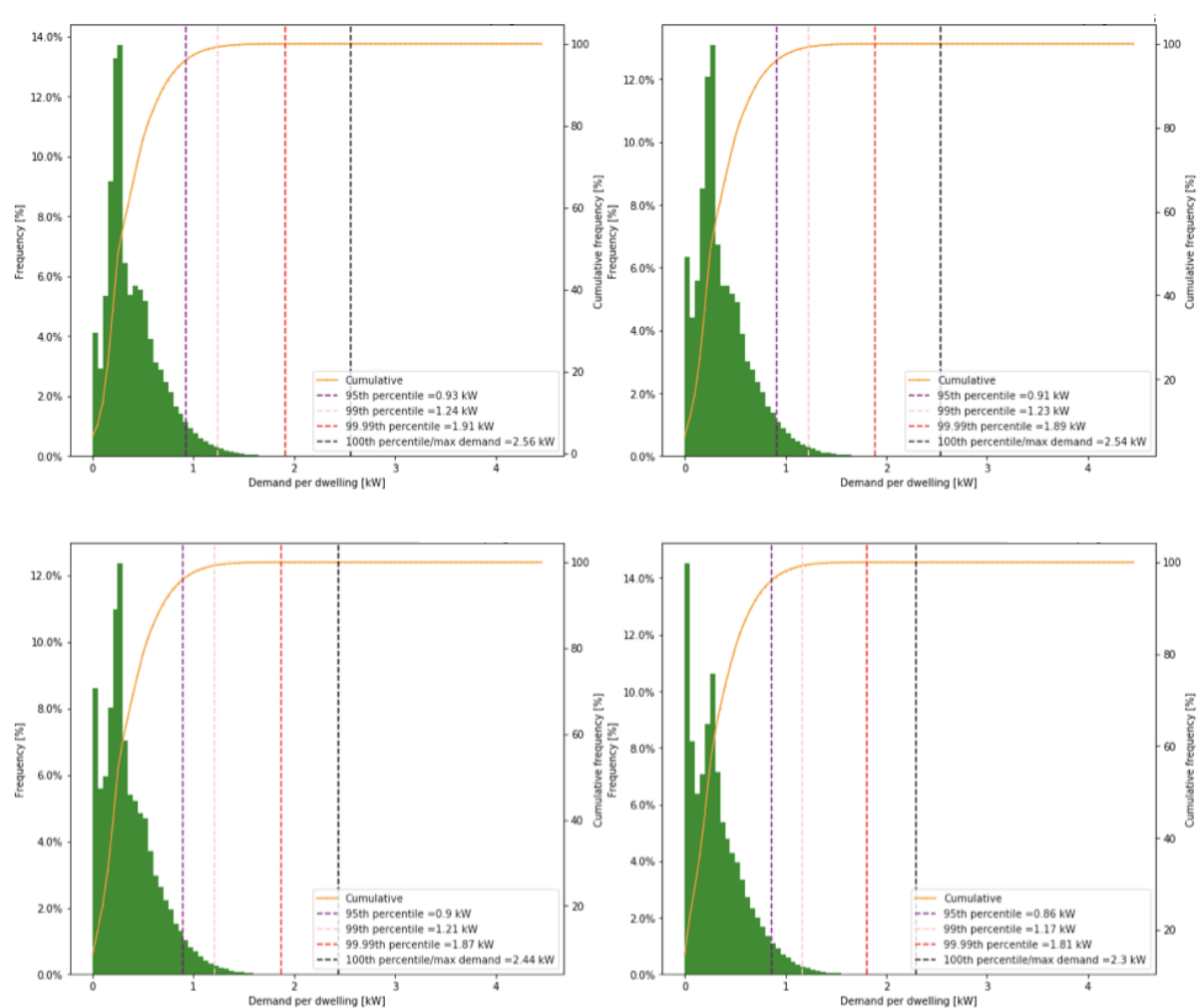


Figure 12.13: Demand distribution for the DHW demand showing the impact of increasing sampling times at an aggregation level of  $k=60$  dwellings. Top-left: 1-second; top-right: 5-second; bottom-left: 10-second; bottom-right: 30-second.

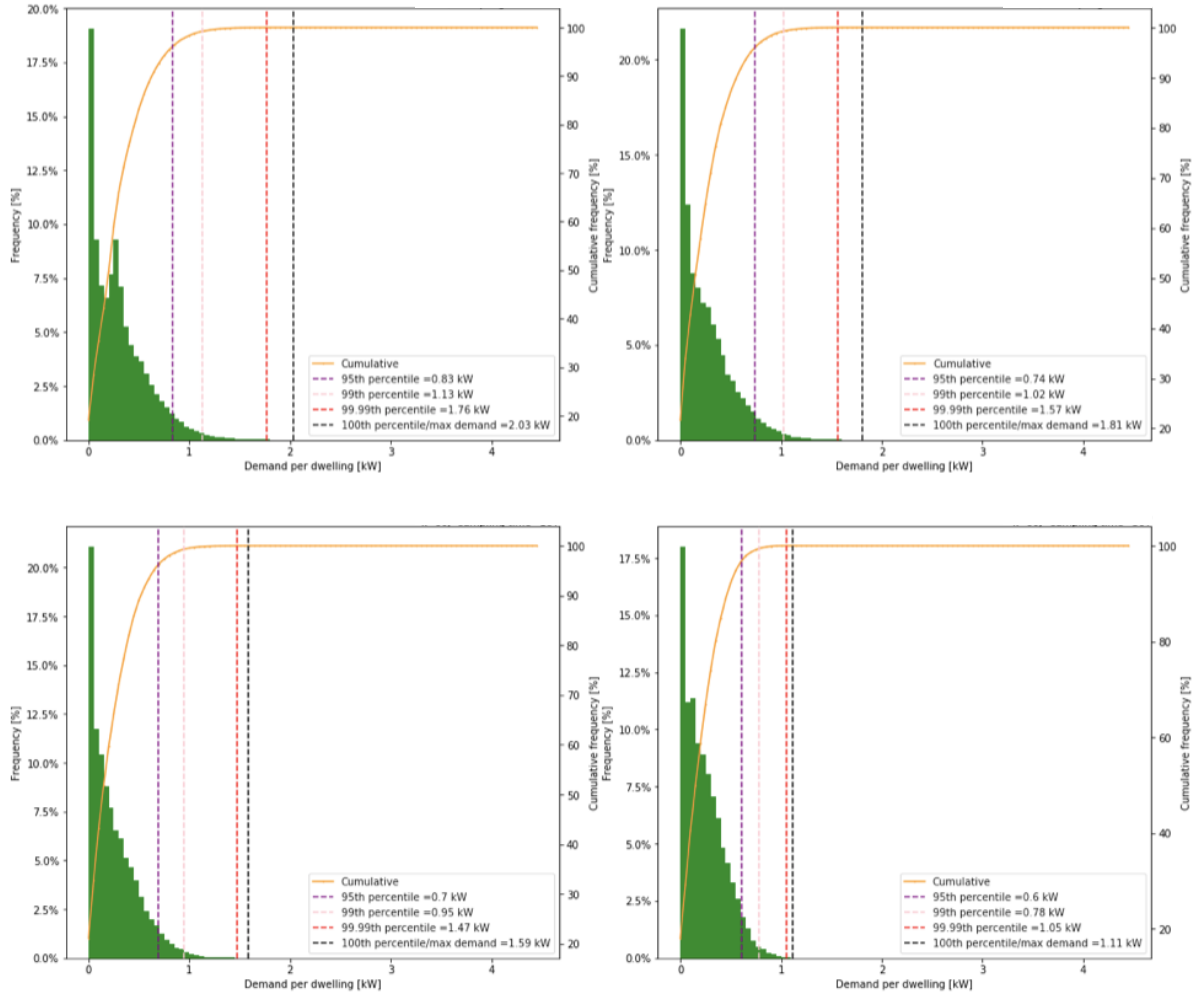


Figure 12.14: Demand distribution for the DHW demand showing the impact of increasing sampling times at an aggregation level of  $k = 60$  dwellings. Top-left: 60-second; top-right: 5-minute; bottom-left: 10-minute; bottom-right: 30-minute.

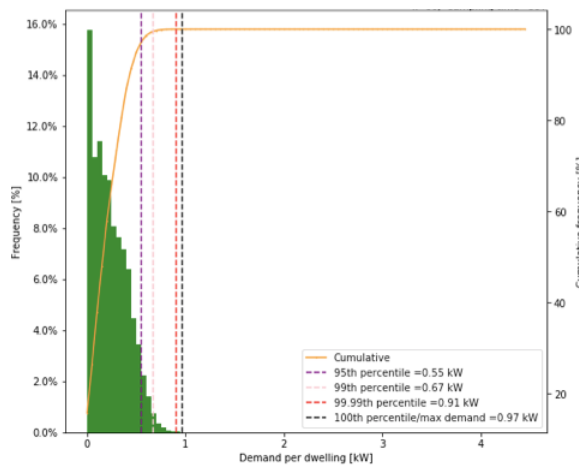


Figure 12.15: Demand distribution for the DHW demand at an aggregation level of  $k = 60$  dwellings and a sampling time of 1 hour.

Table 12.9: Summary of the demand distribution percentiles for DHW demand at an aggregation level of k=60 dwellings expressed as demand per dwelling (kW)

<b>Sampling time</b>	<b>95th</b>	<b>99th</b>	<b>99.99th</b>	<b>100<sup>th</sup></b>
<b>1 second</b>	0.93	1.24	1.91	2.56
<b>5 seconds</b>	0.91	1.23	1.89	2.54
<b>10 seconds</b>	0.9	1.21	1.87	2.44
<b>30 seconds</b>	0.86	1.17	1.81	2.3
<b>60 seconds</b>	0.83	1.13	1.76	2.03
<b>5 minutes</b>	0.74	1.02	1.57	1.81
<b>10 minutes</b>	0.7	0.95	1.47	1.59
<b>30 minutes</b>	0.6	0.78	1.05	1.11
<b>1 hour</b>	0.55	0.67	0.91	0.97

## 13 Appendix C

### 13.1 DHW and Total Demand Capacity Calculation

Equations (13-1) and (13-2) below are adapted from the diversity calculation equations in CP1.2 which are explained in detail in Sections 2.5.1 and 2.5.2. For DHW demand, the diversified flow rate is used with the temperature delta in the DHW circuit to determine the capacity required in a segment of the distribution system serving  $N$  dwellings. For the SH demand, the diversity factor is used with an assumed SH demands for a single dwelling. The values used in the calculations are given in Table 13.1 below.

$$Q_{dhw} = \left( 2q_m + \theta \left( \sum q_f - 2q_m \right) + A \sqrt{q_m \cdot \theta} \sqrt{\sum q_f - 2q_m} \right) \cdot (T_{flow}^{dhw} - T_{cold}^{dhw}) \cdot c \quad (13-1)$$

$$Q_{sh} = \left( 0.62 + \frac{0.38}{N} \right) \cdot N \cdot Q_{sh,single} \quad (13-2)$$

Table 13.1: Variables used in determining DHW and total demand capacities (CIBSE, 2020)

Demand type	Variable	Symbol	Value	Notes and source
DHW	Weighted mean water flow rate (l/s)	$q_m$	0.1	Objective 3.2 and Annex D in CP1.2 (CIBSE, 2020)
	Assumed water flow rate of randomly used outlets (l/s)	$q_f$	0.2 – 0.35	Table 9, Section 3.9.15 in CP1.2 where the minimum is given to be 0.15 l/s, however, here it was adjusted in order to keep all equation components positive (CIBSE, 2020). Measured maximum flow rates fall within this range, as shown in Figure 13.1 below.
	Safety factor	$A$	3.1	Objective 3.2 and Annex D in CP1.2 (CIBSE, 2020)
	Probability of draining $q_m$ at times of peak demand	$\theta$	0.015	Objective 3.2 and Annex D in CP1.2 (CIBSE, 2020)
	Number of dwellings	$N$	1-80	-
	Sum of assumed water flow rates (l/s)	$\sum q_f$	Equal to $N \times q_f$	-

	Flow temperature (°C)	$T_{flow}^{dhw}$	45-60	Range given in HIU specification (Heatweb Ltd, 2023b). Measured values reflect this as shown in Figure 5.13.
	Cold water temperature (°C)	$T_{cold}^{dhw}$	10	(Energy Savings Trust, 2008)
	Specific heat capacity (kJ/kg°C)	$c$	4.182	(Allison et al., 2018; Holman et al, 1992)
<b>SH</b>	Number of dwellings	$N$	1-92	
	SH demand of single dwelling (kW)	$Q_{sh,single}$	2-3	Table 11, Annex D in CP1.2 (CIBSE, 2020)

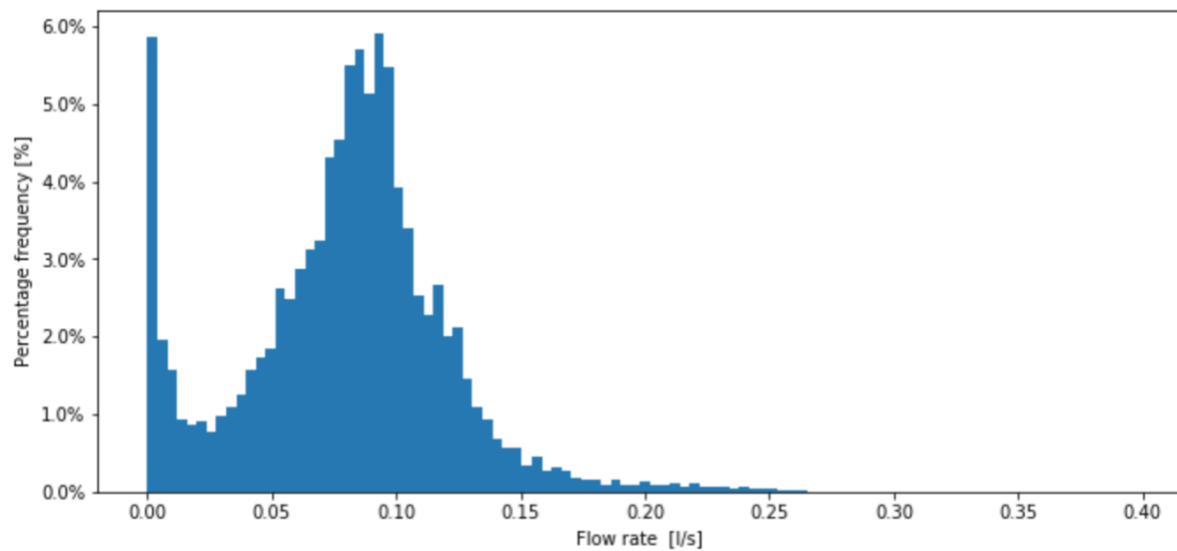


Figure 13.1: Measured DHW flow rates for the dwelling sample

## 14 Appendix D

### 14.1 Pipe Sizing

The table below gives the nominal pipe diameters and thicknesses that were used in determining thermal losses from the distribution system.

Table 14.1: Nominal pipe diameters and thickness (HardHat Engineer, 2023)

Nominal Pipe Size Chart - Nominal Pipe Dimension in Millimeter (mm)																			DN in mm
DN in mm	OD	5	5s	10	10s	20	30	40	40s	Std	60	80	80s	XS	100	120	140	160	XXS
6	10.3			1.24	1.24			1.73	1.73	1.73		2.41	2.41	2.41					
8	13.7			1.65	1.65			2.24	2.24	2.24		3.02	3.02	3.02					
10	17.1			1.65	1.65		1.85	2.31	2.31	2.31		3.20	3.20	3.20					
15	21.3	1.65	1.65	2.11	2.11		2.41	2.77	2.77	2.77		3.73	3.73	3.73				4.78	7.47
20	26.7	1.65	1.65	2.11	2.11		2.41	2.87	2.87	2.87		3.91	3.91	3.91				5.56	7.82
25	33.4	1.65	1.65	2.77	2.77		2.90	3.38	3.38	3.38		4.55	4.55	4.55				6.35	9.09
32	42.2	1.65	1.65	2.77	2.77		2.97	3.56	3.56	3.56		4.85	4.85	4.85				6.35	9.70
40	48.3	1.65	1.65	2.77	2.77		3.18	3.68	3.68	3.68		5.08	5.08	5.08				7.14	10.16
50	60.3	1.65	1.65	2.77	2.77		3.18	3.91	3.91	3.91		5.54	5.54	5.54				8.74	11.07
65	73	2.11	2.11	3.05	3.05		4.78	5.16	5.16	5.16		7.01	7.01	7.01				9.53	14.02
80	88.9	2.11	2.11	3.05	3.05		4.78	5.49	5.49	5.49		7.62	7.62	7.62				11.13	15.24
90	101.6	2.11	2.11	3.05	3.05		4.78	5.74	5.74	5.74		8.08	8.08	8.08					16.15
100	114.3	2.11	2.11	3.05	3.05		4.78	6.02	6.02	6.02		8.56	8.56	8.56		11.13		13.49	17.12
125	141.3	2.77	2.77	3.40	3.40			6.55	6.55	6.55		9.53	9.53	9.53		12.70		15.88	19.05
150	168.3	2.77	2.77	3.40	3.40			7.11	7.11	7.11		10.97	10.97	10.97		14.27		18.26	21.95
200	219.1	2.77	2.77	3.76	3.76	6.35	7.04	8.18	8.18	8.18	10.31	12.70	12.70	12.70	15.09	18.26	20.82	23.01	22.23
250	273	3.40	3.40	4.19	4.19	6.35	7.80	9.27	9.27	9.27	12.70	15.09	12.70	12.70	18.26	21.44	25.40	28.58	25.40
300	323.8	3.96	3.96	4.57	4.57	6.35	8.38	10.31	9.53	9.53	14.27	17.48	12.70	12.70	21.44	25.40	28.58	33.32	25.40
350	355.6	3.96	3.96	6.35	4.78	7.92	9.53	11.13	9.53	9.53	15.09	19.05	12.70	12.70	23.83	27.79	31.75	35.71	
400	406.4	4.19	4.19	6.35	4.78	7.92	9.53	12.70	9.53	9.53	16.66	21.44	12.70	12.70	26.19	30.96	36.53	40.49	
450	457	4.19	4.19	6.35	4.78	7.92	11.13	14.27	9.53	9.53	19.05	23.83	12.70	12.70	29.36	34.93	39.67	45.24	
500	508	4.78	4.78	6.35	5.54	9.53	12.70	15.09	9.53	9.53	20.82	26.19	12.70	12.70	32.54	38.10	44.45	50.01	
550	559	4.78	4.78	6.35	5.54	9.53	12.70		9.53	9.53	22.23	28.58		12.70	34.93	41.28	47.63	53.98	
600	610	5.54	5.54	6.35	6.35	9.53	14.27	17.48	9.53	9.53	24.61	30.96	12.70	12.70	38.89	46.02	52.37	59.54	
650	660			7.92		12.70				9.53				12.70					
700	711			7.92		12.70	15.88			9.53				12.70					
750	762	6.35	6.35	7.92	7.92	12.70	15.88			9.53				12.70					
800	813			7.92		12.70	15.88	17.48		9.53				12.70					
850	864			7.92		12.70	15.88	17.48		9.53				12.70					
900	914			7.92		12.70	15.88	19.05		9.53				12.70					
950	965									9.53				12.70					
1000	1016									9.53				12.70					
1050	1067									9.53				12.70					
1100	1118									9.53				12.70					
1150	1168									9.53				12.70					
1200	1219									9.53				12.70					
DN in mm	OD	5	5s	10	10s	20	30	40	40s	Std	60	80	80s	XS	100	120	140	160	XXS
DN in mm	OD	5	5s	10	10s	20	30	40	40s	Std	60	80	80s	XS	100	120	140	160	XXS

ASME B36.10M-2015: Welded and Seamless Wrought Steel Pipe  
ASME B36.19M-2004: Stainless Steel Pipe (For 5S, 10S, 40S and 80S)

### 14.2 Distribution System Sizing for all Scenarios

This section provides tables of the dimensions of the distribution system and related variables such as ADMD, aggregate peak demand and mass flow rates required to determine sizing across all storage scenarios.

Table 14.2: The aggregate peak demands (kW) needed to be met in the distribution system for the storage scenarios and the real demand scenario

Dwellings	SC mixed	SC stratified	CC mixed	CC stratified	Real demand
1	4.3	6	4.4	6	20.3
2	5.4	7.7	7.1	10.9	24.9
3	6.8	10.1	10.7	17.2	29.5
4	7.4	11.2	13.5	22.2	32.9
5	8.7	14.4	16.9	29.8	35.5
6	10	16.3	19.8	34.1	37.6
12	14.5	25	37.3	68.5	49.7
18	18.5	33.3	55.5	103.7	60.2
24	22.9	40.3	74.3	139.3	66.1
30	25.8	47.4	91.3	174.1	73.4
36	29.6	56	108.1	207.5	78.8
42	33	63.6	127.1	245.6	85.4
48	35.8	69.8	143.2	278.6	90.2

Table 14.3: Distribution system sizing of the real design of the case study HN

Pipe type	Pipe length (m)	No. of pipes	No. of dwellings served	Real pipe diameters (m)
Service pipes	0.36	54	1	0.022
Service pipes	0.69	18	1	0.022
Service pipes	0.32	18	1	0.022
Service pipes	0.35	6	1	0.022
Cross floor	4.5	16	1	0.022
Cross floor	4.5	16	2	0.028
Cross floor	4.5	16	3	0.028
Cross floor	4.5	16	4	0.035
Cross floor	4.5	16	5	0.035
Lateral transport	0.81	1	48	0.054
Lateral transport	3.41	1	42	0.054
Lateral transport	3.37	1	36	0.054
Lateral transport	1.44	1	30	0.054
Lateral transport	2.07	1	24	0.042
Lateral transport	4.28	1	18	0.042

<b>Lateral transport</b>	2.43	1	12	0.042
<b>Lateral transport</b>	5.98	1	6	0.035
<b>Lateral transport</b>	2.13	1	48	0.054
<b>Lateral transport</b>	2.96	1	42	0.054
<b>Lateral transport</b>	2.93	1	36	0.054
<b>Lateral transport</b>	0.16	1	30	0.054
<b>Lateral transport</b>	2.44	1	24	0.042
<b>Lateral transport</b>	0.3	1	18	0.042
<b>Lateral transport</b>	1.9	1	12	0.042
<b>Lateral transport</b>	0.82	1	6	0.035

Table 14.4: Distribution system sizing and related variables for the SC mixed scenario

<b>Pipe type</b>	<b>Pipe length (m)</b>	<b>No. of pipes</b>	<b>No. of dwellings served</b>	<b>ADMD (kW)</b>	<b>Mass flow rate (kg/s)</b>	<b>Pipe diameter (m)</b>
<b>Service pipes</b>	0.36	54	1	4.34	0.032	0.006
<b>Service pipes</b>	0.69	18	1	4.34	0.032	0.006
<b>Service pipes</b>	0.32	18	1	4.34	0.032	0.006
<b>Service pipes</b>	0.35	6	1	4.34	0.032	0.006
<b>Cross floor</b>	4.5	16	1	4.34	0.032	0.006
<b>Cross floor</b>	4.5	16	2	2.71	0.041	0.008
<b>Cross floor</b>	4.5	16	3	2.26	0.051	0.008
<b>Cross floor</b>	4.5	16	4	1.85	0.055	0.008
<b>Cross floor</b>	4.5	16	5	1.73	0.065	0.008
<b>Lateral transport</b>	0.81	1	48	0.75	0.267	0.02
<b>Lateral transport</b>	3.41	1	42	0.79	0.247	0.015
<b>Lateral transport</b>	3.37	1	36	0.82	0.222	0.015
<b>Lateral transport</b>	1.44	1	30	0.86	0.193	0.015
<b>Lateral transport</b>	2.07	1	24	0.96	0.171	0.015
<b>Lateral transport</b>	4.28	1	18	1.03	0.138	0.012

<b>Lateral transport</b>	2.43	1	12	1.21	0.109	0.01
<b>Lateral transport</b>	5.98	1	6	1.67	0.075	0.01
<b>Lateral transport</b>	2.13	1	48	0.75	0.267	0.02
<b>Lateral transport</b>	2.96	1	42	0.79	0.247	0.015
<b>Lateral transport</b>	2.93	1	36	0.82	0.222	0.015
<b>Lateral transport</b>	0.16	1	30	0.86	0.193	0.015
<b>Lateral transport</b>	2.44	1	24	0.96	0.171	0.015
<b>Lateral transport</b>	0.3	1	18	1.03	0.138	0.012
<b>Lateral transport</b>	1.9	1	12	1.21	0.109	0.01
<b>Lateral transport</b>	0.82	1	6	1.67	0.075	0.01

Table 14.5: Distribution system sizing and related variables for SC stratified scenario

<b>Pipe type</b>	<b>Pipe length (m)</b>	<b>No. of pipes</b>	<b>No. of dwellings served</b>	<b>ADMD (kW)</b>	<b>Mass flow rate (kg/s)</b>	<b>Pipe diameter (m)</b>
<b>Service pipes</b>	0.36	54	1	5.95	0.044	0.008
<b>Service pipes</b>	0.69	18	1	5.95	0.044	0.008
<b>Service pipes</b>	0.32	18	1	5.95	0.044	0.008
<b>Service pipes</b>	0.35	6	1	5.95	0.044	0.008
<b>Cross floor</b>	4.5	16	1	5.95	0.044	0.008
<b>Cross floor</b>	4.5	16	2	3.83	0.057	0.01
<b>Cross floor</b>	4.5	16	3	3.37	0.076	0.01
<b>Cross floor</b>	4.5	16	4	2.81	0.084	0.01
<b>Cross floor</b>	4.5	16	5	2.89	0.108	0.012
<b>Lateral transport</b>	0.81	1	48	1.45	0.522	0.025
<b>Lateral transport</b>	3.41	1	42	1.51	0.475	0.025
<b>Lateral transport</b>	3.37	1	36	1.56	0.419	0.02
<b>Lateral transport</b>	1.44	1	30	1.58	0.354	0.02
<b>Lateral transport</b>	2.07	1	24	1.68	0.301	0.02

<b>Lateral transport</b>	4.28	1	18	1.85	0.249	0.015
<b>Lateral transport</b>	2.43	1	12	2.08	0.187	0.015
<b>Lateral transport</b>	5.98	1	6	2.72	0.122	0.012
<b>Lateral transport</b>	2.13	1	48	1.45	0.522	0.025
<b>Lateral transport</b>	2.96	1	42	1.51	0.475	0.025
<b>Lateral transport</b>	2.93	1	36	1.56	0.419	0.02
<b>Lateral transport</b>	0.16	1	30	1.58	0.354	0.02
<b>Lateral transport</b>	2.44	1	24	1.68	0.301	0.02
<b>Lateral transport</b>	0.3	1	18	1.85	0.249	0.015
<b>Lateral transport</b>	1.9	1	12	2.08	0.187	0.015
<b>Lateral transport</b>	0.82	1	6	2.72	0.122	0.012

Table 14.6: Distribution system sizing and related variables for the CC mixed scenario

<b>Pipe type</b>	<b>Pipe length (m)</b>	<b>No. of pipes</b>	<b>No. of dwellings served</b>	<b>ADMD (kW)</b>	<b>Mass flow rate (kg/s)</b>	<b>Pipe diameter (m)</b>
<b>Service pipes</b>	0.36	54	1	4.38	0.033	0.008
<b>Service pipes</b>	0.69	18	1	4.38	0.033	0.008
<b>Service pipes</b>	0.32	18	1	4.38	0.033	0.008
<b>Service pipes</b>	0.35	6	1	4.38	0.033	0.008
<b>Cross floor</b>	4.5	16	1	4.38	0.033	0.008
<b>Cross floor</b>	4.5	16	2	3.57	0.053	0.01
<b>Cross floor</b>	4.5	16	3	3.55	0.080	0.01
<b>Cross floor</b>	4.5	16	4	3.36	0.101	0.012
<b>Cross floor</b>	4.5	16	5	3.38	0.126	0.012
<b>Lateral transport</b>	0.81	1	48	2.98	1.070	0.032
<b>Lateral transport</b>	3.41	1	42	3.03	0.949	0.032
<b>Lateral transport</b>	3.37	1	36	3.00	0.808	0.032
<b>Lateral transport</b>	1.44	1	30	3.04	0.682	0.025
<b>Lateral transport</b>	2.07	1	24	3.10	0.555	0.025

<b>Lateral transport</b>	4.28	1	18	3.08	0.415	0.02
<b>Lateral transport</b>	2.43	1	12	3.11	0.279	0.02
<b>Lateral transport</b>	5.98	1	6	3.29	0.148	0.015
<b>Lateral transport</b>	2.13	1	48	2.98	1.070	0.032
<b>Lateral transport</b>	2.96	1	42	3.03	0.949	0.032
<b>Lateral transport</b>	2.93	1	36	3.00	0.808	0.032
<b>Lateral transport</b>	0.16	1	30	3.04	0.682	0.025
<b>Lateral transport</b>	2.44	1	24	3.10	0.555	0.025
<b>Lateral transport</b>	0.3	1	18	3.08	0.415	0.02
<b>Lateral transport</b>	1.9	1	12	3.11	0.279	0.02
<b>Lateral transport</b>	0.82	1	6	3.29	0.148	0.015

Table 14.7: The distribution system sizing and related variables for CC stratified scenario

<b>Pipe type</b>	<b>Pipe length (m)</b>	<b>No. of pipes</b>	<b>No. of dwellings served</b>	<b>ADMD (kW)</b>	<b>Mass flow rate (kg/s)</b>	<b>Pipe diameter (m)</b>
<b>Service pipes</b>	0.36	54	1	5.95	0.044	0.01
<b>Service pipes</b>	0.69	18	1	5.95	0.044	0.01
<b>Service pipes</b>	0.32	18	1	5.95	0.044	0.01
<b>Service pipes</b>	0.35	6	1	5.95	0.044	0.01
<b>Cross floor</b>	4.5	16	1	5.95	0.044	0.01
<b>Cross floor</b>	4.5	16	2	5.44	0.081	0.012
<b>Cross floor</b>	4.5	16	3	5.73	0.128	0.012
<b>Cross floor</b>	4.5	16	4	5.55	0.166	0.015
<b>Cross floor</b>	4.5	16	5	5.96	0.223	0.015
<b>Lateral transport</b>	0.81	1	48	5.80	2.082	0.05
<b>Lateral transport</b>	3.41	1	42	5.85	1.835	0.04
<b>Lateral transport</b>	3.37	1	36	5.76	1.551	0.04
<b>Lateral transport</b>	1.44	1	30	5.80	1.301	0.04
<b>Lateral transport</b>	2.07	1	24	5.81	1.041	0.032

<b>Lateral transport</b>	4.28	1	18	5.76	0.775	0.032
<b>Lateral transport</b>	2.43	1	12	5.71	0.512	0.025
<b>Lateral transport</b>	5.98	1	6	5.69	0.255	0.02
<b>Lateral transport</b>	2.13	1	48	5.80	2.082	0.05
<b>Lateral transport</b>	2.96	1	42	5.85	1.835	0.04
<b>Lateral transport</b>	2.93	1	36	5.76	1.551	0.04
<b>Lateral transport</b>	0.16	1	30	5.80	1.301	0.04
<b>Lateral transport</b>	2.44	1	24	5.81	1.041	0.032
<b>Lateral transport</b>	0.3	1	18	5.76	0.775	0.032
<b>Lateral transport</b>	1.9	1	12	5.71	0.512	0.025
<b>Lateral transport</b>	0.82	1	6	5.69	0.255	0.02

Table 14.8: Distribution system sizing and related variables for the real demand scenario

<b>Pipe type</b>	<b>Pipe length (m)</b>	<b>No. of pipes</b>	<b>No. of dwellings served</b>	<b>ADMD (kW)</b>	<b>Mass flow rate (kg/s)</b>	<b>Pipe diameter (m)</b>
<b>Service pipes</b>	0.36	54	1	20.27	0.151	0.015
<b>Service pipes</b>	0.69	18	1	20.27	0.151	0.015
<b>Service pipes</b>	0.32	18	1	20.27	0.151	0.015
<b>Service pipes</b>	0.35	6	1	20.27	0.151	0.015
<b>Cross floor</b>	4.5	16	1	20.27	0.151	0.015
<b>Cross floor</b>	4.5	16	2	12.45	0.186	0.015
<b>Cross floor</b>	4.5	16	3	9.85	0.221	0.015
<b>Cross floor</b>	4.5	16	4	8.24	0.246	0.02
<b>Cross floor</b>	4.5	16	5	7.11	0.266	0.02
<b>Lateral transport</b>	0.81	1	48	1.88	0.674	0.025
<b>Lateral transport</b>	3.41	1	42	2.03	0.638	0.025
<b>Lateral transport</b>	3.37	1	36	2.19	0.589	0.025
<b>Lateral transport</b>	1.44	1	30	2.45	0.548	0.025
<b>Lateral transport</b>	2.07	1	24	2.76	0.494	0.025

<b>Lateral transport</b>	4.28	1	18	3.35	0.450	0.02
<b>Lateral transport</b>	2.43	1	12	4.14	0.371	0.02
<b>Lateral transport</b>	5.98	1	6	6.26	0.281	0.02
<b>Lateral transport</b>	2.13	1	48	1.88	0.674	0.025
<b>Lateral transport</b>	2.96	1	42	2.03	0.638	0.025
<b>Lateral transport</b>	2.93	1	36	2.19	0.589	0.025
<b>Lateral transport</b>	0.16	1	30	2.45	0.548	0.025
<b>Lateral transport</b>	2.44	1	24	2.76	0.494	0.025
<b>Lateral transport</b>	0.3	1	18	3.35	0.450	0.02
<b>Lateral transport</b>	1.9	1	12	4.14	0.371	0.02
<b>Lateral transport</b>	0.82	1	6	6.26	0.281	0.02